ISBN 5-201-09812-6

RUSSIAN ACADEMY OF SCIENCES
DORODNICYN COMPUTING CENTER

Sergey Alexandrovich Ivanenko

(1954–2003)

SELECTED CHAPTERS ON GRID GENERATION AND APPLICATIONS

DORODNICYN COMPUTING CENTER OF RAS
MOSCOW ◇ 2004

UDK 519. 63

Editor: Boris N. Azarenok

Grid generation algorithms in plane, surface, and space are considered within the frame of a general approach. The theory of the harmonic mappings is set forth in the context of using to the mesh construction problem. This theory is the basis for the numerical algorithms. The problem of constructing invertible mapping at the discrete level is considered. The conditions, being a discrete analogy of positivity of the Jacobian of a mapping, are used to provide invertibility of the grid cells in cases of meshes in plane, surface, and space. The algorithms possess the barrier property preventing cells from degenerating in the course of mesh smoothing. The problem of adaptive mesh generation is formulated by means of minimizing the energy density functional written on the surface (in the 3D case on the hyper-surface) of the graph of the adapted function. The use of the universal variational functionals allows mesh generation with any prescribed cell shape form. Results of calculations, illustrating capability of the algorithms, are presented.

Referees: V.N.Koterov,
A.Yu. Semenov

Scientific Edition

Сергей Александрович Иваненко
11 июня 1954 г. – 24 сентября 2003 г.

Предисловие

После внезапной кончины Сергея Александровича Иваненко его сын, Павел Сергеевич, передал А.А.Чарахчьяну жесткий диск от домашнего компьютера своего отца. На диске был обнаружен почти готовый к изданию курс лекций С.А.Иваненко на английском языке. Настоящая монография является отредактированным текстом этих лекций. Ранее первые две лекции, дополненные примерами конкретных алгоритмов для системы MATLAB, были опубликованы совместно с Pablo Barrera Sanches и Guilmer Gonzalez Flores в виде технического отчета Национального Автономного Университета Мексики (UNAM).

Работу по редактированию текста была выполнена Б.Н.Азаренком. Основная часть текста подверглась чисто редакторской правке: были устранены опечатки в формулах, улучшен английский, заголовок "Lecture"заменен на "Chapter и т.п. Отдельные пункты рукописи были изложены слишком конспективно. Например, п. 10.8 состоял из двух строчек, в последней главе отсутствовал текст, поясняющий рисунки с результатами расчетов. Почти во всех таких случаях Б.Н.Азаренку удалось найти соответствующие места в опубликованных работах С.А.Иваненко и вставить их в текст монографии. Исключение составляет п. 10.9, текст которого обрывается при выводе формул. Тем не менее мы решили оставить этот пункт, так как его содержание может помочь читателю довести эти выкладки до конца.

Так как в рукописи не было введения, мы сочли возможным дополнить текст настоящей монографии введением из предыдущей монографии С.А.Иваненко 1997 года, изданной в ВЦ РАН, с небольшими дополнениями о новых результатах. Кроме того Б.Н.Азаренок написал небольшое дополнение к главе 5 с описанием алгоритма расстановки граничных узлов при адаптации сетки.

При второй редакции, осуществленной в 2010г., были добавлены комментарии и ссылки, отражающие некоторые последние результаты в области построения сеток.

А.А.Чарахчьян, Б.Н.Азаренок

Preface

After a sudden death of Sergey Alexandrovich Ivanenko, his son Pavel Sergeevich Ivanenko gave a hard disk of his father's computer to Alexander Charakhchyan. On that disk, we found a nearly ready course of lectures by S.Ivanenko in English. The present monograph is an edited text of these lectures. Earlier, first two lectures, added with examples of algorithms for the system MATHLAB, were published by S.A.Ivanenko jointly with Pablo Barrera Sanches and Guilmer Gonzalez Flores as a technical report of National Autonomous University of Mexico (UNAM).

The editorial work was implemented by Boris Azarenok. A main part of the text was only slightly corrected: misprints in formulas were removed, English was corrected, title "Lecture" was substituted by "Chapter", etc. Certain sections were set forth rather briefly. For instance, Section 10.8 contained two lines, in the last Chapter there was not text with caption for figures. Nearly in all cases B.Azarenok could find corresponding text in the published papers by S.Ivanenko and inserted them into the manuscript. An exception is Section 10.9 which breaks down during derivation of formulas. Nevertheless, we decided to include this Section into the manuscript. The reader may finish derivation.

There was not an introduction and we added the text with the introduction taken from the monograph by S.A.Ivanenko, published at Computing Center of RAS in 1997 with reference to some new results. Besides, B.Azarenok wrote an Appendix to Chapter 5, where the algorithm of boundary node redistribution for adaptive meshes is described.

In the second edition, performed in 2010, it was added comments and references concerning certain new results on the subject of the monograph.

A.A.Charakhchyan, B.N.Azarenok

Contents

Introduction[1]

The grid generation methods are intensively developed within last two decades, but the first works appeared as early as 1960s. It connects with numerous applications in computational fluids dynamics and adjacent fields.

The basic purpose of grid generation is to provide such a division of the underlying domain into the cells or elements that we could obtain the most precise solution of a differential problem. In the one-dimensional case such an approach was developed by Tikhonov and Gorbunov [145], Bakvalov [16], Grebennikov [60], Emel'yanov [46], De Boor [25], Pereia and Sewel [104], Russel and Christiansen [114], Carrey and Dinh [30], and it is based on error estimate between the approximate and exact solution. It was suggested and developed the equidistribution principle based on such a mesh nodes redistribution that some positive weight function multiplied by the grid spacing was equal to a constant. As a weight function they define the modulus of a corresponding derivative of the approximate solution (White [157, 158], Anderson [2], Brackbill and Saltzman [26], etc.).

Generalization to the multidimensional case was executed in two ways. The first concerns with calculating a priory estimates. Babuska and Rheinbold [12] suggested a grid generation method to linear elliptic problems. However, generalization of this method to the nonlinear case becomes complicated because the error can be unrestricted by a residual of the equation, i.e., reducing the residual in some norm may not lead the error to reduce in the same norm. Besides these estimations are global, meanwhile they are used for local supplementary refinement of the elements.

Moving adaptive grid generation methods, based on approximation error estimate, were developed by Muller and Muller [98, 99], Dar'in and Mazhukin [36], Degtyarev and Ivanova [39].

The other approach, based on interpolation error estimate, was considered by Diaz et al. [40] and Oden et al. [101]. Conceptually it is

[1]Translated from the book [73] with additions by Editor

more simple, however, it includes calculation of derivatives of the unknown solution in the main problem. These methods are local and they can require special formulae to compute derivatives, which are known only for a very narrow class of problems. To the Poisson equation such formulae were suggested by Babuska and Miller [13] and some its generalization by Oden et al. [101]. In these works they used the governing equations to calculate the derivatives. The main difficulty in applying the error estimates is both in rather a complicate system of nonlinear equations to the grid and necessity of their regularization so as to obtain a stable numerical solution.

On the other hand the approximation error depends strongly on the minimal angle, see Thompson et al. [143]. For instance, the quantity, which is inverse to the sine of the minimal angle, is in the right part of the error estimate in the finite element method (Strang and Fix [137]). Generally among the properties, having effect upon the accuracy, we can note the following (Thompson et al. [143], Brackbill [28]): step size, cell shape and dimension, homogeneity, smoothness, angle between the grid lines, angle between the velocity vector and grid line, derivatives of the flow parameters. Obviously that it is impossible to specify only one property of the grid from the above list. Besides, some difficulties appear due to various discretization methods of the original differential formulation in the grid generation problem.

Thus, grid construction, based on the error estimate, runs into some difficulties in the multidimensional case. In addition we specify the works by Ivanenko [69, 72] where the examples of a non-uniqueness solution for the grid problem, obtained by the error minimization, are suggested.

An alternative grid generation way was developed. It was considered as the problem of constructing an information-computational medium, partially by analogy with the real continuum. For instance, in the works by Anderson and Ray [1], Nakahashi and Deiwert [100], Jaquotte [78], they use a mechanical analogy (see also the review by Thompson [142]).

This information-computational medium should possess a number of properties, such as smoothness, simplicity of computer representation, and adaptivity, i.e., the grid should condense in the subdomains where the solution undergoes sharp variations. The latter is illustrated in the work by Thompson et al. [141], when the grid nodes can be represented as a finite set of observers, placed so that to watch with maximum effectiveness for the processes in the underlying domain.

The grid generation method should possess the ellipticity property, i.e.,

determine influence of every observer upon the others, in the sense that if an observer goes to more profitable position, then his neighbours follow him. One may image such "clever"observers which can estimate the error and accumulate in the subdomains where it is great. However, formalization of this intuitive understanding is not easy and there is a large field for various assumptions. There appears a lot of difficulties and ways to overcome them, that is why the number of papers on this subject is rather great.

One of the most large difficulties is that in general the mesh is constructed in domains of a complex form. A lot of heuristic algorithms of irregular grid generation were developed. Many algorithms are based on constructing the Delaunay cells and Voronoi diagrams: Delaunay [38], Voronoi [154], Belikov [17], Sofronov et al. [129], Boender [24], George [51], [59], [130], Baker [15], etc.. Other algorithms produce an irregular mesh with refining the domain by cells: Vabishchevich [152], Baker [14], Berger and Oliger [20], Blacker [21], Blacker and Meyers [22], Dannenhoffer [35], Jiang and Carrey [80], Loehner and Parikh [96], Pyke [105], Rank and Babushka [112]; with further smoothing and adaptation: Meshcheryakov and Shapeev [97], Frey and Field [49], Kennon and Dulikravich [82], Kennon and Anderson [83], Pardhanani and Carey [102].

Consider possibilities of the regular and irregular meshes. Under the regular meshes we mean the grids where node neighbourhood is defined by numeration. The typical example of such a mesh is a curvilinear grid obtained using a mapping of the physical domain onto the parametric square. The nodes are numbered with double indexing in the 2D and triple indexing in the 3D case. On the irregular mesh, we need to define node neighbourhood. As a rule irregular grids are used in the finite element method, and often they consist of triangles in 2D and tetrahedra in the 3D case.

Since the regular mesh is a special case of the irregular grid, hence, irregular grids have wider applications, particularly in the domains with very complicated geometry. On the other hand the regular mesh describes rather well the properties of the solution or even can be a solution if, for instance, one family of the coordinate lines coincide with the stream lines (cf. Thompson et al. [140], Tolstykh [147]). Besides, the regular grid structure means regularity of the discretized problem that leads the numerical algorithms to be simplified and can be easily parallelized.

Considering a grid as an information-computational medium, one should note that there is quite a different opinion concerning practical aspects of the

adaptive meshes. In the monograph by Godunov et al. [57] the authors note that "despite of every effort and long time spent on producing curvilinear and moving meshes for numerical solving the partial differential equations, there was not elaborated a final point of view relative to principles which should lay in the basis of grid generation methods". This circumstance, specially highlighted, from authors' point of view should attract developers' attention to solving the questions formulated (see Prokopov [108]). At present, almost in twenty years, the situation is nearly the same despite a lot of effort applied to this problem.

Many formulations of objective functions for grid construction were suggested and, despite of different points of view, they come to consent that the mapping, used in grid generation, should be continuously differentiable and the Jacobian must not be equal to zero (see Godunov and Prokopov [56], Godunov et al. [57], Thompson et al. [143]). This very important property guarantees that the mapping is one-to-one. These grids are obtained when using elliptic equations (see Thompson et al. [143]) at constructing mapping of the physical domain onto the parametric square in 2D and cube in the 3D case.

However, as noted by Ivanenko and Charakhch'yan [67], not every elliptic grid generator possesses the property to be one-to-one at the discrete level. "If the boundary nodes are given so that the coordinate lines need not be too bent to provide invertibility of the cells, then all algorithms generate quite satisfactory meshes. Some grids are a bit better and the others a bit worse, some algorithms work faster and the others a bit slower, nevertheless all grids are suitable for modeling. If the coordinate lines should be strongly bent so as to yield a satisfactory mesh, then the situation changes. Most of the algorithms produce grids with folded cells, which are not fit for modeling". In papers by Ivanenko and Charakhch'yan [66, 67] they compared the suggested algorithm with others, including Winslow's method [159], on a number of domains with complex geometry. These examples have shown that in the extremal cases the most algorithms produce grids with folded cells and sometimes interior nodes even overspill the domain.

There are several approaches to overcome this difficulty. The first one is the use of the orthogonal meshes to increase the minimal angle between the coordinate lines (see Prokopov [106, 107], Sidorov et al. [126], [128], Ushakova [148], Serezhnikova et al. [119], Brackbill and Saltzman [26], Brackbill et al. [27], Ryskin and Leal [115], Steger and Shause [133], Arina and Tardity [134]). However, it is not clear how the orthogonal mesh can be

adaptive since there is insufficient number of degrees of freedom (Ryskin and Leal [115], Brackbill [28]). This is in correspondence with the statement that increase of orthogonality is achieved at the expense of adaptivity (Brackbill and Saltzman [26]).

When constructing the orthogonal grids (or close to them), lack of degrees of freedom can be compensated, for example, by refusing the fixed node position on the entire boundary or on its part. Permission to move the boundary nodes sometimes promotes to achieve desirable grids, but can complicate joining the grids of separate subdomains.

In some cases there is no such a problem. For example, when solving external problems in aerohydrodynamics, one side of the underlying domain can be bounded by the body contour, whose shape should be given precisely, and the other side by the outward shock wave, whose shape is determined during modeling, or by rather a far external boundary. On these external boundaries the requirements, imposed on the mesh nodes redistribution, can be weakened in the interest of grid generation to obtain a high accuracy first of all near the body. To this end, one may use hyperbolic and parabolic equations, which are outside of the present study.

When generating regular meshes by constructing the curvilinear coordinates (may be not orthogonal) in a complex domain one should pay attention to producing an initial mesh. To obtain it, usually one uses interpolation formulae. In a complex domain (if it is not cut into the blocks of a simple geometry), application of the interpolation formulae produces the initial mesh with folded cells. Eliminating this difficulty is the separate problem in grid generation.

As an alternative one can use the following rather an universal method. The iterative process of solving a complex system of the finite difference grid equations can be considered as solving an unsteady problem. It can include the artificial process of the domain boundary deformation. A complex domain, where one needs to produce a grid, is changes by a more simple domain, where a "good" mesh can be readily generated. Next the simple domain is gradually deformed onto the initial domain.

Another way of overcoming difficulties, caused by a complex geometry, is to apply block grids (Godunov et al. [57], Tu and Thompson [144], Thompson et al. [143], etc.). Very complicated domains are cut into parts so as to simplify grid construction in every block. The first drawback of this approach is that the mesh is not smooth in the locations of the blocks junction. The second drawback is the problem of automatical cutting the

domain into suitable subdomains even in the 2D case (Prokopov [109], Charakhch'yan [32, 33]). This way is quite realistic when generating in dialog mode in a given fixed domain (Shih et al. [122]) and is rather difficult when treating domains with deforming boundaries (as noted by Prokopov [108]). This approach is close to producing irregular (unstructured) meshes. The latter runs into difficulties in the problems with moving boundaries, when at different time levels the mesh is of different structure.

And finally the last method, where the concept of convex grids is applied (Ivanenko and Charakhch'yan [67]). The harmonic functional (Dirichlet functional), used by Brackbill and Saltzman [26], is approximated so that its minimum is attained on the grid consisting of convex quadrilateral cells. This method of approximating the functional has advantages, particularly for the mesh with not a large number of nodes, warranting that all cells are convex quadrilaterals (of course, provided that there exists at least one such a mesh). The fact is that in extremal situations, if the number of nodes is not large, due to approximation error the differential properties, including one-to-oneness, can be lost at discretization. Examples of failures were presented by Ivanenko [65], Roach and Steinberg [113].

This approach can be extended to the adaptive meshes, if to use the theory of the harmonic mappings (see Liseikin [91, 94], Ivanenko [70, 73, 74]). Here the problem of constructing harmonic coordinates on the surface of graph of the adapted function is formulated. The harmonic coordinates are generated using the harmonic mapping of the surface onto the parametric square (or cube in the 3D case). Projection of these coordinates onto the physical domain gives an adaptive-harmonic mesh (Ivanenko [71]). Similar auxiliary surfaces were also applied by Dwyer et al. [42], Eiseman [45], and Speckreijse [132].

Adaptive-harmonic meshes can be applied to the irregular grids (see Ivanenko [72]). The basic principle can be formulated as follows. The harmonic coordinates are constructed using the global mapping of the physical domain onto the parametric square. As a result we obtain the regular adaptive mesh. The irregular grid is the set of the local coordinates, and in every cell (or element) we have particular coordinates. Therefore, every cell, i.e., quadrilateral, can be mapped onto the same parametric square using the harmonic mapping, and the final irregular mesh with fixed connections should be sought by minimizing the sum of the harmonic functionals, written for every cell. It will be the smoothing stage in the method of irregular mesh generation. If the grid consists of triangles, every

triangle should be mapped onto the equilateral triangle via the harmonic mapping and the discrete functional should be fixed as a sum of the harmonic functionals written for every triangle.

[2]A variational approach of adaptive mesh generation based on minimizing the energy density functional depending on two metrics was suggested by Ivanenko [75]. One metric is responsible for adaptation to the solution, and the other, in the parametric domain, for grid lines condensing and orthogonalization near the physical domain boundary. The use of two metrics was suggested by Godunov and Prokopov [56, 111], however, they apply the direct mapping and their method does not provide the mesh from tangling in domains with complex geometry. In the approach used by Ivanenko, constructing the inverse mapping leads the Jacobian of the mapping to appear in the denominator of the functional, and this, in turn, provides the numerical method with the barrier property preventing mesh folding in the course of grid smoothing.

Simultaneously with Winslow's method [159] there appeared the papers concerning variational approaches in grid generation (see Sidorov [125], Sidorov and Shabashova [126], Sidorov and Ushakova [127], Sidorov et al. [128], Godunov and Prokopov [55], Yanenko et al. [161], Prokopov [106, 108], Belinskii et al. [18], Liseikin [93], Sakhabutdinov et al. [116], Shirokovskaya [123], Anderson [3], Bell and Shubin [19], Brackbill and Saltzman [26], Brackbill [28], Eiseman [45], Kennon and Dulikravich [82], Roach and Steinberg [113], Kennon and Anderson [83], Serezhnikova et al. [119], etc.). Direct generalization of Winslow's method was suggested by Yanenko et al. [161], Brackbill and Saltzman [26].

Dvinsky [37] was the first to suggest to apply the theory of the harmonic mappings in grid generation. Brackbill [28] derived the method of constructing the adaptive meshes from variational formulation of diffusion Winslow's method [160] (cited by [28]) and from the functional with directional control. The theory of harmonic mappings was used by Brackbill [28] to derive conditions providing the solution of elliptic equations to exist. In the works by Dvinsky [37] and Brackbill [28] adaptation is performed by introducing a special metrics in the solution domain. Liseikin [91, 93] introduced extension of the harmonic functional to the case of mapping the surface of the graph of the adapted function onto the parametric square and presented examples of adaptation by solving numerically the Euler equations.

[2]This paragraph was added by the Editor.

The algorithm of minimizing the discrete analogy of this functional was suggested by Ivanenko [70, 71, 72]. The algorithm of the boundary nodes redistribution in the course of minimizing the functional was proposed by Azarenok [6, 8].

Generalization of Winslow's method [159] in the case of surfaces was considered in number of works. The methods grid constructing on surfaces based on solving elliptic equations were considered by Thomas [139], Takagi et al. [138], Tomphson et al. [143], Warsi and Tiarn [155], Liseikin [92, 93], and based on variational approach by Saltsman [117], Jacquotte [78], Ivanenko [70].

Elliptic equations are defined via the Gauss and Beltrami formulae (Tomphson et al. [143], Warsi and Tiarn [155], Warsi [156], Steinberg and Roach [136], Khamayseh and Mastin [84] or by projecting the Poisson equations in assumption of orthogonality and zero curvature of the transverse grid lines family (Thomas [139], Takagi et al. [138]). Adaptation is performed using the source terms, but it is difficult to determine these terms on the surface and yet one-to-oneness can be lost. In the variational methods (Saltsman [117], Pearce [103]), the mesh is constructed from the condition of minimizing the linear combination of the functionals of smoothness, orthogonality, and adaptation (Brackbill and Saltzman [26]). In the papers by Liseikin [91, 93] and Ivanenko [70], the harmonic functional is used to construct the mapping of the surface onto the parametric square.

Generalization of Winslow's method [159] for the 3D case was considered by Shevelev [121], Liseikin [91], Tomphson et al. [143], Tu and Thompson [144], Eiseman [45], Brackbill et al. [27], Brackbill [28], Hegmeijer [64], Spekreijse [131], Ivanenko [73, 74], etc.).

[3]Thus, the harmonic mappings has been used for grid generation within long time. In the present study, we consider algorithms of grid construction using the harmonic mapping and its generalization, when two metrics are used, in plane, surface and space within the frame of a common approach. It allows to set forth carefully the algorithms, beginning from theoretical foundation and ending by final computational formulae. Variational methods possess one more important property: they guarantee unfolded mesh generation. It means that even in domain with complex geometry we can produce regular meshes without folded cells.

[3]This paragraph was corrected by the Editor.

Chapter 1

One-dimensional grid generation for numerical solution of partial differential equations

1.1 Transformation of independent variables

Consider the transformation of independent variables in general case.

Consider Euclidean space R^n, a bounded and connected homeomorphic domains $\Omega_0, \Omega \subset \mathrm{R}^n$, and a map $\varphi(x) : \overline{\Omega}_0 \to \overline{\Omega}$, where $x \in \overline{\Omega}_0$ and $\varphi(x) \in \overline{\Omega}$.

If we use $\varphi(x)$ as the transformation of the independent variables in the system of PDEs, describing the physical process, we need additional conditions on the transformation in order to provide the equations to be nonsingular in new variables. This is achieved by introducing additional constrains for the transformation, such as condition of smoothness and the condition guaranteeing that the transformation $\varphi(x)$ is one-to-one.

In turn, if we consider a numerical solution for the system of PDEs, we must introduce the discrete transformations $\varphi^h(x)$: $\overline{\Omega}_0^h \to \overline{\Omega}^h$ between Ω_0^h and Ω^h, approximating the domains Ω_0 and Ω correspondingly. Discretization of the domain Ω_0^h is obtained by dividing it into nonintersecting domains Ω_i^h, i=1, . . . , m, usually called finite elements or finite volumes, such that

$$\overline{\Omega}_0^h = \bigcup_{i=1}^{m} \overline{\Omega}_i^h.$$

Convergence of $\Omega_0^h \to \Omega_0$ and $\Omega^h \to \Omega$ is considered at $m \to \infty$.

In the theory of grid generation, the methods of implementing such discretizations are considered. At the same time, application of the numerical analysis will help us to find additional conditions, ensuring the convergence $\varphi^h(x) \to \varphi(x)$ of the approximate solution to the exact solution simultaneously with convergence of $\Omega_0^h \to \Omega_0$ and $\Omega^h \to \Omega$.

These questions will be considered below, first in the one-dimensional case.

We will start with the following example.

Example 1. Consider an ordinary differential equation

$$\epsilon \frac{d^2u}{dx^2} = -\frac{du}{dx}, \quad x \in (0,1) \tag{1}$$

with boundary conditions

$$u(0) = 0, \quad u(1) = 1. \tag{2}$$

An analytical solution of the equation (1) with boundary conditions (2) can be written as

$$u = \frac{1 - e^{-ax}}{1 - e^{-a}}.$$

where $a{=}1/\epsilon$. This solution has the boundary layer at the left side of the interval $(0,1)$.

Now we will look for a transformation of the independent variable $x{=}x(\xi)$, which is an invertible mapping of the unit interval $(0,1)$ onto itself, such that the equation (1) will be as simple as possible. The following relations hold

$$u_\xi = u_x x_\xi, \quad u_{\xi\xi} = u_{xx} x_\xi^2 + u_x x_{\xi\xi}.$$

Substituting these relations into (1) we obtain

$$\epsilon u_{\xi\xi} = \epsilon u_x x_{\xi\xi} - u_x x_\xi^2 = u_x(\epsilon x_{\xi\xi} - x_\xi^2). \tag{3}$$

While deriving (3), we suppose that the Jacobian of the transformation $x = x(\xi)$ does not vanish, i.e. $x_\xi \neq 0$. If the right-hand side of (3) is equal to zero, i.e.,

$$\epsilon x_{\xi\xi} - x_\xi^2 = 0. \tag{4}$$

Then the equation (1) will take the form

$$u_{\xi\xi} = 0. \tag{5}$$

The solution of the equation (5) is the linear function $u(\xi)=\xi$. We can see that in contrast to (1) the equation (4) is a nonlinear differential equation. It can be solved directly, but it is better to rewrite it as an equation with respect to $\xi(x)$. We use the following relations

$$\xi_x x_\xi = 1, \quad x_{\xi\xi}\xi_x + x_\xi^2 \xi_{xx} = 0.$$

Substituting these relations into (4) we obtain

$$\epsilon\xi_{xx} = -\xi_x.$$

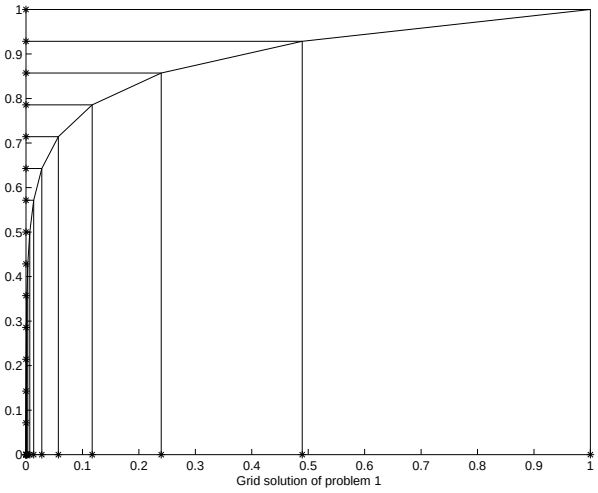

Fig. 1.1:

Geometrically, see Fig.1.1, this is the same equation as (1). Equation (5) can be rewritten also as

$$u_\xi = x_\xi u_x = const. \tag{6}$$

Theorem 1.1 *Let*

$$x(\xi) \in C^1[0,1], \; x(0) = 0, \; x(1) = 1.$$

If the Jacobian

$$x_\xi > 0, \; x \in [0,1]$$

then the mapping will be a homeomorphism (one-to-one and continuous mapping).

Proof.

Consider two points $\xi_1 < \xi_2$. It is known there exists such a point $\xi' \in (\xi_1, \xi_2)$ that

$$\int_{\xi 1}^{\xi_2} x_\xi d_\xi = x(\xi_2) - x(\xi_1) = x_\xi(\xi')(\xi_2 - \xi_1) > 0.$$

From this $x(\xi)$ is strictly monotonic, i.e. $x(\xi)$ is a homeomorphism.

l.q.q.d.

Example 2. For the ordinary differential equation

$$\frac{d^2u}{dx^2} = 0.$$

consider the transformation of independent variable $x{=}x(\xi)$. After transforming to the new independent variable ξ we obtain

$$\frac{1}{x_\xi}\ \frac{d}{d_\xi}\left(\frac{1}{x_\xi}\ \frac{du}{d_\xi}\right) = 0.$$

Boundary conditions are the following

$$u(0) = 0, \quad u(1) = 1.$$

The solution is written as

$$u = x.$$

Consider the following transformation

$$x = \begin{cases} \alpha\xi & \text{if} \quad 0 \le \xi \le 0.5 \\ 2(1 - 0.5\alpha)(\xi - 0.5) + 0.5\alpha & \text{if} \quad 0.5 \le \xi \le 1 \end{cases}.$$

The Jacobian is discontinuous in the point $\xi{=}0.5$, if $\alpha{\neq}1$

$$x_\xi = \begin{cases} \alpha & \text{if} \quad \xi < 0.5 \\ 2 - \alpha & \text{if} \quad \xi > 0.5 \end{cases}.$$

For such transformation a new problem statement is necessary

$$\frac{d^2u}{d\xi^2} = 0, \quad (\xi \in (0,1)) \bigcap (\xi \neq 0.5)$$

$$\frac{1}{\alpha} u_\xi \Big|_{0.5-0} = \frac{1}{2-\alpha} u_\xi \Big|_{0.5+0}$$

$$u(0) = 0, \; u(1) = 1.$$

We can see that the transformation of the independent variable, *which is not continuously differentiable*, leads to the new problem formulation for the equation with discontinuous coefficients. Conclusion: we need continuous differentiability.

Discrete case. As a discrete analog of the smoothness condition for the transformation, first consider the transformation of three points $\xi-h$, ξ and $\xi+h$ onto three points $x_0=x(\xi-h)$, $x_1=x(\xi)$, $x_2=x(\xi+h)$, where h is small enough.

From Taylor series the following expansions can be obtained

$$x_2 - x_1 = x_\xi h + x_{\xi\xi}\frac{h^2}{2} + O(h^3)$$

$$x_1 - x_0 = x_\xi h - x_{\xi\xi}\frac{h^2}{2} + O(h^3)$$

$$(x_2 - x_1) - (x_1 - x_0) = x_{\xi\xi}h^2 + O(h^3).$$

Consequently,

$$\begin{aligned} \frac{(x_2 - x_1)}{(x_1 - x_0)} &= 1 + \frac{x_{\xi\xi}h^2 + O(h^3)}{x_\xi h - x_{\xi\xi}h^2 + O(h^3)} \\ &= 1 + \frac{x_{\xi\xi}}{x_\xi}h + O(h^2) \end{aligned}$$

where $h=1/N$ and N is the number of intervals.

If $x_{\xi\xi}<\infty$, then in the limit we obtain the following condition on the ratio of lengths of the neighbor cells

$$\frac{(x_2 - x_1)}{(x_1 - x_0)} \longrightarrow 1 \text{ with } h \to 0.$$

From previous considerations it follows that the transformation of independent variable $x(\xi)$ must be

I. A homeomorphism ($x_\xi > 0,\ \xi \in [0,1]$).

II. Smooth ($x_\xi \in C[0,1]$) and $|x_{\xi\xi}| < \infty$.

Example 3. Consider the transformation $x = \xi^2$. The uniform grid in the ξ - axe is defined as

$$\xi_i = \frac{i}{N}, \quad i = 0, \ldots,\ N.$$

The coordinates of grid nodes in the x - axe are computed as

$$x_0 = 0,\ x_1 = \frac{1}{N^2},\ x_2 = \frac{2^2}{N^2} \ldots .$$

In this case

$$\frac{x_2 - x_1}{x_1 - x_0} = 3$$

and it does not tend to 0 for any number of grid nodes. The reason is that the Jacobian is equal to 0 if ξ=0. In this case the Taylor series for the lengths of the first and second cells contain a finite number of terms:

$$x_2 - x_1 = 2h^2 + \frac{2h^2}{2}$$

$$x_0 - x_1 = -2h^2 + h^2 = -h^2$$

and their ratio is exactly equal to 3.

1.2 Equidistribution principle

For the monotonic function $u(x)$ we can find such a transformation x=$x(\xi)$, that the function $u(x(\xi))$=$\tilde{u}(\xi)$ will be linear. In this case

$$\tilde{u}_\xi = x_\xi |u_x| = const > 0.$$

For the monotonic function $|u_x| \neq 0$ and the constant is defined from the relation

$$\text{const} = \int_0^1 |u_x| dx = |u(1) - u(0)|.$$

In the case if the derivative u_x is a linear function of ξ we obtain

$$\frac{d}{d\xi}(u_x) = x_\xi u_{xx} = \text{const}.$$

The equidistribution principle in this case takes the form,

$$x_\xi |u_{xx}| = \text{const} > 0.$$

Example 4.

Consider the boundary-value problem for the ordinary second-order differential equation

$$-\varepsilon \frac{d^2u}{dx^2} + u = 0,\ u(0) = 1,\ u(1) = 1.$$

The analytic solution can be written as

$$u = C(e^{-ax} + e^{a(x-1)}).$$

where

$$a = 1/\sqrt{\varepsilon}\ , \quad C = \frac{1 - e^{-a}}{1 - e^{-2a}}.$$

The solution has the minimum at the point x=0.5

$$u_x\,(0.5) = 0.$$

Variational formulation for the example 4

The variational statement for the problem from example 4 is to find the minimum of the functional

$$\int_0^1 \left[\left(\frac{du}{dx} \right)^2 + u^2 \right] dx \to \min\ ,$$

with boundary conditions $u(0) = 1,\ u(1) = 1.$

1.3 Nonstationary problems

1) The following nonstationary problem is considered with the solution of the problem from example 1 as its stationary solution

$$\frac{\partial u}{\partial t} + a(x)\frac{\partial u}{\partial x} = \varepsilon \frac{\partial^2 u}{\partial x^2} \ .$$

2) The following nonstationary problem is considered with the solution of the problem from example 4 as its stationary solution

$$\frac{\partial u}{\partial t} + u = \varepsilon \frac{\partial^2 u}{\partial x^2} \ .$$

3) If ε=0, we obtain the following convection equation of the first order

$$\frac{\partial u}{\partial t} + a(x)\frac{\partial u}{\partial x} = 0 \ .$$

4) The stationary solution of the problem from example 1 is obtained from the solution of the associated nonstationary problem with the following boundary and initial conditions

$$u(0,t) = 0, \ u(1,t) = 1, \ u(x,0) = u_0(x), \ a = -1, \ t \to \infty \ .$$

The stationary solution of the problem from example 4 is obtained from the solution of the appropriate nonstationary problem with the following boundary and initial conditions

$$u(0,t) = 1, \ u(1,t) = 1, \ u(x,0) = u_0(x), \ a = -1, \ t \to \infty \ .$$

Modern Numerical Methods

The following numerical methods can be used for solving these problems

- Finite difference method,
- Finite element method,
- Finite volume method.

Consider the nonuniform grid

$$0 = x_0 < x_1 < \cdots < x_{N-1} < x_N = 1.$$

We introduce the following notations

$$h = \frac{1}{N} \quad \text{and} \quad h_{i+1/2} = x_{i+1} - x_i,\ i = 0, \ldots, N-1\ .$$

1.4 Finite difference method

In the finite difference method all derivatives are replaces by finite-differences

$$u_x \approx \frac{u_{i+1} - u_i}{x_{i+1} - x_i},\ u_x \approx \frac{u_i - u_{i-1}}{x_i - x_{i-1}},\ u_x \approx \frac{u_{i+1} - u_{i-1}}{x_{i+1} - x_{i-1}}\ .$$

For the example 1, the equation

$$-\frac{du}{dx} = \varepsilon \frac{d^2u}{dx^2}$$

can be approximated as

$$-\frac{u_{i+1} - u_{i-1}}{x_{i+1} - x_{i-1}} = \varepsilon \frac{2}{x_{i+1} - x_{i-1}} \left[\frac{u_{i+1} - u_i}{x_{i+1} - x_i} - \frac{u_i - u_{i-1}}{x_i - x_{i-1}} \right]\ ,$$

or

$$-\frac{u_{i+1} - u_i}{x_{i+1} - x_i} = \varepsilon \frac{2}{x_{i+1} - x_{i-1}} \left[\frac{u_{i+1} - u_i}{x_{i+1} - x_i} - \frac{u_i - u_{i-1}}{x_i - x_{i-1}} \right]\ .$$

1.5 Finite element method

In the finite element method all unknown variables are approximated by expansions

$$u^h = \sum_{i=1}^{N-1} u_i \psi_i\ .$$

Variational formulation is used then to obtain discrete analog of the continuous problem. For the example 4 the corresponding variational formulation is as follows

$$I = \int_0^1 \left[\left(\frac{du}{dx} \right)^2 + u^2 \right] dx \to \min .$$

Substituting the expansion u^h instead of u we obtain the discrete analog of the functional

$$I^h = \int_0^1 \left[\left(\frac{du^h}{dx} \right)^2 + (u^h)^2 \right] dx \to \min_{u_i,\ i=1,\ldots,N-1} .$$

The simplest basis function ψ_i is the piecewise linear function, which is linearly increased from 0 to 1 in the interval from x_{i-1} to x_i and linearly decreased from 1 to 0 in the interval from x_i to x_{i+1}, and it is equal to 0 elsewhere.

Substituting these basis functions into the discrete functional, we obtain

$$I^h = \sum_{i=1}^{N-1} \left[\varepsilon \frac{(u_{i+1} - u_i)^2}{(x_{i+1} - x_i)} + \frac{1}{3}(u_i^2 + u_i u_{i+1} + u_{i+1}^2)(x_{i+1} - x_i) \right] .$$

If we use the simplest numerical integration formulas with quadrature nodes coinciding with the nodes of the grid, we obtain another approximation of the functional, which satisfies the maximum principle

$$\tilde{I}^h = \sum_{i=1}^{N-1} \left[\varepsilon \frac{(u_{i+1} - u_i)^2}{x_{i+1} - x_i} + \frac{1}{2}(u_i^2 + u_{i+1}^2)(x_{i+1} - x_i) \right] .$$

The necessary conditions of the minimum of the appropriate functionals can be obtained as

$$\frac{\partial I^h}{\partial u_i} = 0 \quad \text{or} \quad \frac{\partial \tilde{I}^h}{\partial u_i} = 0, \quad i = 1, \ldots, N-1 .$$

1.6 Finite Volume Method

1.6.1 Generalized formulation 1

Variational formulation for the convection equation

$$\frac{\partial u}{\partial t} + a\frac{\partial u}{\partial x} = 0,\ a = const.\ ,$$

can be expressed as

$$\int\limits_{x_1}^{x_2} \left(\frac{\partial u}{\partial t} + a\frac{\partial u}{\partial x} \right) dx = \frac{\partial}{\partial t} \int\limits_{x_1}^{x_2} u dx + a[u(x_2) - u(x_1)] = 0\ ,$$

for any $x_2 > x_1$.

This leads to the following semidiscrete approximation

$$\frac{\partial}{\partial t} u_{i+1/2} + a(u_{i+1} - u_i) = 0\ ,\ i = 1, \ldots, N-1\ .$$

In the general case $a = a(t, x)$ the upwind differences are used

$$\frac{u_{i+1/2}^{j+1} - u_{i+1/2}^{j}}{\triangle t} + a_i^j \frac{u_{i+1}^j - u_i^j}{x_{i+1} - x_i} = 0, \qquad a_i^j = a(t^j, x_i)\ ,$$

where

$$u_i^j = \begin{cases} u_{i-1/2}^j & \text{if} \quad a_i^j > 0 \\ u_{i+1/2}^j & \text{if} \quad a_i^j < 0 \end{cases} .$$

1.6.2 Generalized formulation 2

The generalized variational formulation is used for constructing numerical algorithm directly on moving grid without interpolation [57]

$$\iint\limits_D \left(\frac{\partial u}{\partial t} + a\frac{\partial u}{\partial x} \right) dxdt = \oint_{\partial D} (-udx + audt)\ ,$$

where D is an arbitrary domain in the plane (x, t) and ∂D is the domain boundary.

Integrating we obtain the following finite-difference relations

$$u_{i+1/2}^{j+1}(x_{i+1}^{j+1}-x_i^{j+1})-u_{i+1/2}^{j}(x_{i+1}^{j}-x_i^{j})+a\ u_{i+1}^{j+1/2}\triangle t$$
$$-(x_{i+1}^{j+1}-x_{i+1}^{j})u_{i+1}^{j+1/2}-a\ u_i^{j+1/2}\triangle t-(x_i^{j+1}-x_i^{j})u_i^{j+1/2}=0\ .$$

It is convenient to introduce the velocity of grid points

$$W_i^{j+1/2}=(x_i^{j+1}-x_i^{j})/\triangle t.$$

In this case the scheme can be rewritten as

$$u_{i+1/2}^{j+1}(x_{i+1}^{j+1}-x_i^{j+1})-u_{i+1/2}^{j}(x_{i+1}^{j}-x_i^{j})$$
$$+(a-W_{i+1}^{j+1/2})\triangle t\ u_{i+1}^{j+1/2}-(a-W_i^{j+1/2})\triangle t\ u_i^{j+1/2}=0\ .$$

1.6.3 Godunov's theorem

Very important Godunov's theorem [53, 54] states that even for linear convection equation and so for the hyperbolic system of equations a monotonic scheme of the second order of accuracy must be nonlinear.

Theorem 1.2 Godunov's theorem. *Two-layer linear monotonic scheme for the equation*

$$\frac{\partial u}{\partial t}+a\frac{\partial u}{\partial x}=0\ ,\quad a=const.\ ,$$

cannot be of the second-order accuracy.

Chapter 2

One-dimensional grid generation: error estimates

In the unit interval of the axis x, consider nonuniform 1D grid with node coordinates

$$x_i, \quad i = 0, \ldots, N$$

satisfying boundary conditions

$$x_0 = 0, \; x_N = 1 \; .$$

It corresponds to the uniform ξ–grid

$$\xi_i = \frac{i}{N}, \; i = 0, \ldots, N \; .$$

The mapping $x(\xi)$ is approximated by $x^h : (\xi \to x)$ constructed with the use of piecewise-linear finite element basis functions

$$x^h(\xi) = \sum_{i=0}^{N} x_i \psi_i(\xi_i)$$

$$x_i = x^h(\xi_i) \; .$$

The Jacobian of the transformation $x^h(\xi)$ for $\xi \in [i/N, (i+1)/N]$ is equal to

$$\frac{dx^h}{d\xi} = \frac{x_{i+1} - x_i}{1/N} = \frac{h_{i+1/2}}{1/N} \; .$$

The Jacobian is positive if and only if

$$h_{i+1/2} = x_{i+1} - x_i > 0,\ i = 0, \ldots, N-1 \ .$$

A posteriori error estimate

This estimate is obtained for the difference between exact and approximate solution, measured in particular norm, such as

$$||u - u^h|| \leq F(h, u^h) \ .$$

The right-hand side in the posteriori estimate is a functional dependent on approximate solution. This estimate is used in the finite element method, for the so-called h-refinement.

A priori error estimate

This estimate is obtained for the difference between the exact and approximate solution, measured in a particular norm, such as

$$||u - u^h|| \leq F(h, u) \ .$$

The right-hand side is a functional dependent on the exact solution. In the finite element method with linear elements, this estimate takes the form

$$||u - u^h||_1 \leq ch||u||_2 \ .$$

where h is a maximal diameter of the elements.

2.1 A posteriori error estimates

We will start with the following

Example 2.1

Consider the boundary-value problem (example 4) with two boundary layers in the solution:

$$\varepsilon \frac{d^2u}{dx^2} = u,\ u(0) = 1,\ u(1) = 1 \ .$$

Variational formulation is the following

$$I = \int_0^1 \left[\varepsilon \left(\frac{du}{dx} \right)^2 + u^2 \right] dx \longrightarrow \min \ . \tag{2.1}$$

The approximate solution is of the form:

$$u^h = \sum_{i=0}^{N} u_i \psi_i(x) \quad \text{with} \quad u_0 = 1,\ u_N = 1\ .$$

A discrete analog of the functional is the following

$$I^h = \sum_{i=0}^{N-1} \varepsilon \frac{(u_{i+1} - u_i)^2}{x_{i+1} - x_i} + \frac{1}{3}(u_i^2 + u_i u_{i+1} + u_{i+1}^2)(x_{i+1} - x_i)\ .$$

Now consider the functional:

$$I = a(u,u) - 2(f,u)\ ,$$

where

$$a(u,v) = \int_0^1 \left(\varepsilon \frac{du}{dx}\ \frac{dv}{dx} + uv \right) dx$$

is the scalar product and

$$||u||_E^2 = \int_0^1 (\varepsilon u_x^2 + u^2) dx\ , \quad (f,u) = \int_0^1 f u dx\ .$$

Now we can suppose that the function f is chosen so that the unknown solution u always satisfies the following boundary conditions

$$u(0) = 0\ , \quad u(1) = 0\ ,$$

for example

$$\epsilon \frac{d^2 u}{dx^2} = u - 1\ , \qquad f = u - 1$$

and we will use the following expansion for the approximate solution

$$u^h = \sum_{i=1}^{N-1} u_i \psi_i(x)\ ,$$

such that $u^h(0)=u^h(x_0)=0$, $u^h(1)=u^h(x_N)=0$. Let u be a solution to the minimization problem (2.1)

$$I = a(u,u) - 2(f,u) \longrightarrow \min\ ,$$

and let u^h be a solution to its discrete analog

$$I^h = a(u^h, u^h) - 2(f, u^h) \longrightarrow \min \ .$$

Consider an arbitrary function v such that $v(0)=0$, $v(1)=]0$. Substitution of $u+v$ instead of u into the expression for I gives

$$I = a(u+v, u+v) - 2(f, u+v) = a(u,u) + 2a(u,v) + a(v,v) - 2(f,u) - 2(f,v)$$

$$= I(u) + a(v,v) + 2[a(u,v) - (f,v)] \geq I(u) \ .$$

The inequality is always satisfied if the following necessary condition (weak formulation of the problem) holds

$$a(u,v) - (f,v) = 0 \quad \forall v, \ \text{such that } v(0) = 0, \ v(1) = 0 \ . \tag{2.2}$$

Similarly we can obtain that

$$a(u^h, v^h) - (f, v^h) = 0 \quad \forall v^h, \ \text{such that } v^h(0) = 0, \ v^h(1) = 0 \ . \tag{2.3}$$

From this it follows that at the point of minima of the functionals I and I^h the following relations hold

$$I = -(f,u) = -a(u,u) \ , \tag{2.4}$$

$$I^h = -(f,u^h) = -a(u^h, u^h) \ . \tag{2.5}$$

Note that we can substitute v^h instead of v into (2.2). As a result we obtain

$$a(u, v^h) - (f, v^h) = 0 \quad \forall v^h, \ \text{such that } v^h(0) = 0, \ v^h(1) = 0 \ . \tag{2.6}$$

Let u be the solution of the problem (2.1) and for arbitrary v^h consider the difference between u and v^h measured in the energy norm

$$||u - u^h||_E^2 = a(u - v^h, u - v^h) = a(u,u) + a(v^h, v^h) - 2a(u, v^h) \ . \tag{2.7}$$

From (2.4) and (2.6) it follows that

$$a(u - v^h, u - v^h) = a(u,u) + a(v^h, v^h) - 2a(f, v^h) = I(v^h) - I(u) \ . \tag{2.8}$$

Hence, we obtain an additional minimization property

$$a(u - u^h, u - u^h) = \min_{v^h} a(u - v^h, u - v^h) \ .$$

From (2.8) it follows that

$$a(u-u^h, u-u^h) = a(u,u) - a(u^h,u^h) = I^h - I \ ,$$

or

$$||u-u^h||_E^2 = I^h - I > 0 \ .$$

Grid adaptation can be based on minimization of the functional, obtained from the posteriori error estimate

$$\min_{x_i} \ \min_{u_i} \left(I^h(x_i,u_i) - I \right) \ .$$

Note: In the case of even number of grid nodes one half of nodes will be in the left boundary layer, another half in the right boundary layer. But if the number of nodes is odd, the central node will move to the right or to the left boundary layer, i.e., the solution is not unique. This also means that grid solution is not stable.

2.2 A priori error estimates: minimization of approximation error

2.2.1 Problem formulation

Let $u(x)$ be a smooth function and

$$u^h = \sum u_i \psi_i(x) \ .$$

Approximation error is defined as follows

$$E_A = \min_{u_i} ||u - \sum u_i \psi_i \ || \ .$$

Basis functions ψ_i can be piecewise-constant and we can use the norm

$$||u||_{L_p} = \left(\int |u|^p \, dx \right)^{1/p} \ .$$

If ψ_i are piecewise-linear, then we can use the norm

$$||u||_{W_p^1} = \left(\int (|u|^p + |u_x|^p) dx \right)^{1/p} \ .$$

Consider the problem of finding the best approximation. The solution can be obtained from the minimization of the functional

$$\min_{x_i} E_A = \min_{x_i} \min_{u_i} ||u - \sum u_i \psi_i \| \ .$$

2.2.2 Interpolation error

If the coefficients in expansion

$$\sum u_i \psi_i$$

can be computed explicitly, for example as

$$u_i = u(x_i) \ ,$$

then we can introduce the interpolation error as follows

$$E_I = ||u - \sum u_i \psi_i \| \ .$$

It is obvious that

$$E_A \leq E_I \ .$$

Consider the problem of grid generation from the minimization problem

$$\min_{x_i} E_I$$

with the following constraints

$$0 = x_0 < x_1 < x_2 < \cdots < x_N = 1 \ .$$

The following Lemma holds.

Lemma 2.1 *For any function* $u \in W_p^1$ *there is a linear combination*

$$u_I = \sum u_{i+1/2} \psi^0_{i+1/2}(x)$$

called the interpolant of the function u *such that*

$$||u - u_I \|^p_{L_p} \leq \frac{1}{N^p} \int_0^1 (x^h_\xi)^{p+1} \left(\frac{du}{dx} \right)^p d\xi \ ,$$

where

$$u_I = \sum_{i=0}^{N-1} u_{i+\frac{1}{2}} \psi^0_{i+\frac{1}{2}}(x),\ u_{i+\frac{1}{2}} = \frac{1}{h_{i+\frac{1}{2}}} \int_{x_i}^{x_{i+1}} u(x)dx\ ,$$

and

$$||f\ ||_{L_p} = \left(\int_0^1 |f|^p dx \right)^{1/p} .$$

Proof.

Let $p<\infty$, then we can write the following inequalities

$$||u-u_I\ ||^p_{L_p} = \int_0^1 |u-u_I|^p dx = \sum_{i=0}^{N-1} \int_{x_i}^{x_{i+1}} |u-u_I|^p dx$$

$$= \sum_{i=0}^{N-1} \int_{x_i}^{x_{i+1}} \left| u(x) - \frac{1}{h_{i+1/2}} \int_{x_i}^{x_{i+1}} u(x')dx' \right|^P dx$$

$$= \sum_{i=0}^{N-1} \int_{x_i}^{x_{i+1}} \left| \frac{1}{h_{i+1/2}} \int_{x_i}^{x_{i+1}} (u(x)-u(x'))dx' \right|^P dx$$

$$= \sum_{i=0}^{N-1} \int_{x_i}^{x_{i+1}} \left| \frac{1}{h_{i+1/2}} \int_{x_i}^{x_{i+1}} dx' \int_{x'}^{x} \frac{du}{dx''} dx'' \right|^P dx$$

$$\leq \sum_{i=0}^{N-1} \int_{x_i}^{x_{i+1}} \left| \frac{1}{h_{i+1/2}} \int_{x_i}^{x_{i+1}} dx' \int_{x_i}^{x_{i+1}} \left| \frac{du}{dx''} \right| dx'' \right|^P dx$$

$$= \sum_{i=0}^{N-1} h_{i+1/2} \left| \int_{x_i}^{x_{i+1}} \left| \frac{du}{dx''} \right| dx'' \right|^P .$$

Using the Hölder inequality

$$\left| \int\ u(x)v(x)dx \right| \leq \left(\int\ |u(x)|^q dx \right)^{1/q} \left(\int\ |v(x)|^p dx \right)^{1/p},$$

where

$$q \geq 1,\ 1/p + 1/q = 1,$$

we obtain

$$\int_{x_i}^{x_{i+1}} 1 \left|\frac{du}{dx''}\right| dx'' \leq \left(\int_{x_i}^{x_{i+1}} 1^q dx''\right)^{1/q} \left(\int_{x_i}^{x_{i+1}} \left|\frac{du}{dx''}\right|^p dx''\right)^{1/p},$$

$$\left(\int_{x_i}^{x_{i+1}} \left|\frac{du}{dx''}\right| dx''\right)^p \leq \int_{x_i}^{x_{i+1}} h_{i+1/2}^{p/q} \left|\frac{du}{dx''}\right|^p dx'' .$$

Consequently,

$$||u-u_I\ ||_{L_p}^p \leq \sum_{i=0}^{N-1} h_{i+1/2}^{1+p/q} \int_{x_i}^{x_{i+1}} \left|\frac{du}{dx}\right|^p dx \leq \frac{1}{N^p} \int_0^1 (x_\xi^h)^{p+1} \left|\frac{du}{dx}\right|^p d\xi .$$

l.q.q.d.

Thus, we obtain the estimate for the first-order approximation error with respect to $h = 1/N$.

Consider the functional

$$I^p = \int_0^1 (x_\xi)^{p+1} |u_x|^p d\xi$$

the Euler's equation to which is

$$x_\xi^{p+1} |u_x|^p = \text{const}.$$

From this we obtain that the asymptotic condition on the Jacobian, determining the optimal grid in norm L_p is the following:

$$x_\xi = \text{const}|u|^{-\frac{p}{p+1}} .$$

For $p \to \infty$ we obtain a condition on the Jacobian for the grid, optimal in the norm L_∞, or if the function is continuous, in the uniform norm

$$x_\xi = \text{const}|u_x|^{-1} , \qquad x_\xi |u_x| = \text{const.} ,$$

where

$$||u||_\infty = \max_{x\in[0,1]} |u| \ .$$

For the monotone function $u(x)$, the grid, obtained from the discrete analog of $u_\xi = u_x$, x_ξ=const.,

$$u(\xi_{i+1}) - u(\xi_i) = u(x_{i+1}) - u(x_i) = u(x_i) - u(x_{i-1})$$

is the exact solution not only to the best interpolation, but also for the best approximation, because

$$\epsilon_{i+1/2} = \frac{1}{2}(u(x_{i+1}) - u(x_i)) = \frac{1}{2}(u(x_i) - u(x_{i-1})) = \epsilon_{i-1/2} \ ,$$

where $\epsilon_{i+1/2}$ is the error in uniform norm in the interval $x_i \le x \le x_{i+1}$ for piecewise constant approximation.

Lemma 2.2 *For any function $u \in W_p^2$ there exists such a linear combination $u_I = \sum u(x_i)\psi_i(x)$ that*

$$||u - u_I||_{L_p}^p \le \frac{1}{N^{2p}} \int_0^1 (x_\xi^h)^{2p+1} \left|\frac{d^2u}{dx^2}\right|^p d\xi \ ,$$

$$||u - u_I||_{W_p^1}^p \le \frac{1}{N^p} \int_0^1 (x_\xi^h)^{p+1} \left|\frac{d^2u}{dx^2}\right|^p d\xi \ .$$

Conditions on the Jacobian for grids, optimal in norms L_p and W_p^1, are the following

$$x_\xi = \text{const}|u_{xx}|^{-\frac{p}{2p+1}} \text{ in the norm } L_p \ ,$$

$$x_\xi = \text{const}|u_{xx}|^{-\frac{p}{p+1}} \text{ in the norm } W_p^1 \ .$$

In the case of norms C and C^1 we have

$$x_\xi = \text{const}|u_{xx}|^{-\frac{1}{2}} \text{ in the norm of the space } C(0,1) \ ,$$

$$x_\xi = \text{const}|u_{xx}|^{-1} \text{ in the norm of the spase } C^1(0,1) \ .$$

Asymptotically the solution of the problem for the best interpolation is the same as the solution of the problem for the best approximation.

2.3 C. de Boor's algorithm

Algorithm for constructing the grid, optimal in the uniform norm, is the following

$$\xi(x)=c\int_0^x (|u_{xx}|+\varepsilon)^{1/2}dx\ ,\ c=\left[\int_0^1 (|u_{xx}|+\varepsilon)^{1/2}dx\right]^{-1}\ ,\text{where }\varepsilon\text{ is small enough,}$$

$$u^h_{xx}=\begin{cases} D^2u_1 & \text{if} \quad x_0\le x\le x_1 \\ 0.5(D^2u_{i+1}+D^2u_i) & \text{if} \quad x_i\le x\le x_{i+1} \\ D^2u_{N-1} & \text{if} \quad x_{N-1}\le x\le x_N \end{cases}\ .$$

Here

$$D^2u_i=\frac{u_{i+1}-u_i}{x_{i+1}-x_i}-\frac{u_i-u_{i-1}}{x_i-x_{i-1}}\ .$$

First $\xi(x_i)$ are computed, then new values of $\tilde{x}_i$ can be obtained from the formulas

$$\frac{k-1}{N}=\sum_{i=0}^{N}\xi_i\psi_i(\tilde{x}_k),\ k=1,\dots,N-1\ ,$$

$$\xi_i=c\int_0^{x_i}(|u^h_{xx}|+\varepsilon)^{1/2}dx,\ c=(\int_0^1(|u^h_{xx}|+\varepsilon)^{1/2}dx)^{-1}\ .$$

Repeat until convergence

$$\xi(x)=c\int_0^x(|u^h_{xx}|+\varepsilon)^{1/2}dx\ .$$

It would be good if the algorithm can be extended to the multidimensional case but seems to be quite difficult or impossible.

2.4 One-dimensional harmonic mappings

Consider the problem of constructing a harmonic mapping of a unit interval onto the graph of the function $f(x)$.

The Dirichlet functional has the form

$$I = \int_0^1 s_\xi^2 d\xi = \int_0^1 x_\xi^2 (1 + f_x^2) d\xi \ .$$

where

$$s(x) = \int_0^x \sqrt{1 + f_x^2} dx \ , \qquad s_\xi = s_x x_\xi \ .$$

For the inverse mapping we have

$$I = \int_0^1 \left(\frac{d\xi}{ds} \right)^2 ds = \int_0^1 \frac{1}{s_\xi^2} ds = \int_0^1 \frac{1}{(s_x x_\xi)^2} ds$$

$$= \int_0^1 \frac{1}{(s_x x_\xi)^2} s_\xi d\xi = \int_0^1 \frac{1}{s_x x_\xi} d\xi \ .$$

And, thus

$$I = \int_0^1 \frac{1}{x_\xi \sqrt{1 + f_x^2}} d\xi \ . \tag{2.9}$$

Euler equations are identical for both functionals

$$x_\xi \sqrt{1 + f_x^2} = \text{const.}$$

To control the number of grid points in the layer of high gradients, we introduce the scaling factor c_a and instead of f consider the scaled function

$$\tilde{f} = f \cdot c_a \ ,$$

and finally returning to the previous notation for f we obtain

$$x_\xi \sqrt{1 + c_a^2 f_x^2} = \text{const.}$$

The last expression can be rewritten as

$$x_\xi \sqrt{\frac{1}{c_a} + f_x^2} = \text{const.}$$

From this it follows that

$$x_\xi |f_x| = \text{const} \ \text{ if } c_a \to \infty \ .$$

This is also the condition on a grid, optimal in the uniform norm.

Consider the functional for the uniform grid on the curve of the vector function with the function and it first derivative as the vector components

$$I = \int_0^1 \frac{1}{x_\xi \sqrt{1 + f_x^2 + f_{xx}^2)}} \, d\xi \ .$$

Introduce two scaling factors c_1 and c_2

$$\tilde{f}_x = c_1 f_x \ , \quad \tilde{f}_{xx} = c_2 f_{xx} \ .$$

The Euler equation is the following

$$x_\xi \sqrt{1 + c_1^2 f_x^2 + c_2^2 f_{xx}^2)} = \text{const.}$$

Condition on a grid, optimal in the C^1 norm, can be then obtained if $c_2 \to \infty$, and c_1 remains fixed

$$x_\xi |f_{xx}| = \text{const.}$$

Example 2.2

Consider the piecewise linear function, see Fig.2.1

$$f(x) = \begin{cases} x/\varepsilon & \text{for} \quad 0 \le x < \varepsilon \\ 1 & \text{for} \quad \varepsilon \le x \le 1 \end{cases} \ .$$

The error on the uniform grid is the following

$$E_{eq} = \begin{cases} 1/2 & \text{for} \quad N \le \frac{1}{\varepsilon} \\ \frac{1}{2N_\varepsilon} & \text{for} \quad N > \frac{1}{\varepsilon} \end{cases} \ .$$

The error on the grid, optimal in the uniform norm

$$E_{opt} = \frac{1}{2N}$$

does not depend on ε.

The number of grid nodes in the boundary layer for adaptive-harmonic grid is the following

$$N_\varepsilon = N \frac{\sqrt{c_a^2 + \varepsilon^2}}{1 - \varepsilon + \sqrt{c_a^2 + \varepsilon^2}} \ .$$

If $\varepsilon \ll c_a$ then

$$N_\varepsilon \approx N \frac{c_a}{1 + c_a - \varepsilon} \ ,$$

if c_a=1, then

$$N_\varepsilon \approx \frac{N}{2} \ .$$

Thus, the error on adaptive-harmonic grid is the following

$$E_{harm} = \min \left(\frac{1}{2} \ , \ \frac{1 - \varepsilon + \sqrt{c_a^2 + \varepsilon^2}}{2N\sqrt{c_a^2 + \varepsilon^2}} \right) .$$

From this it follows, that

$$E_{harm} = \begin{cases} E_{eq} & \text{if} \quad c_a = 0 \\ E_{opt} & \text{if} \quad c_a \to \infty \end{cases} \ .$$

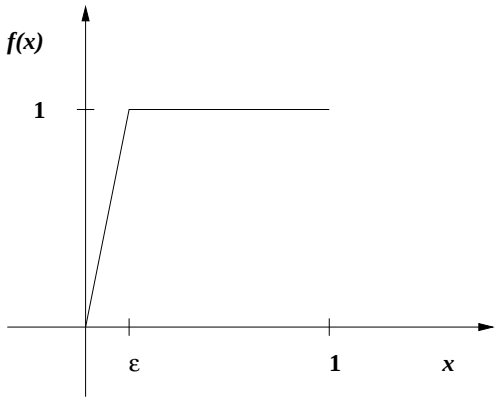

Fig. 2.1: Example of piecewise-linear function with boundary layer

Chapter 3

Nondegenerate two-dimensional grids

3.1 Topological background

Mappings defined on the closures of bounded domains will be considered. Conditions for these mappings to be one-to-one will be obtained.

Consider Euclidean space R^n, a bounded and connected domain $\Omega \subset \mathrm{R}^n$, and a map $\varphi : \overline{\Omega} \to \overline{\Omega}$ of class $\mathbb{C}^1$. The differentiability of φ at points of the boundary $\partial\Omega$ of the domain Ω is understood in the usual sense as existence of a map $\widetilde{\varphi} : \widetilde{\Omega} \to \widetilde{\Omega}$ of class $\mathbb{C}^1$ on a certain domain $\widetilde{\Omega} \supset \overline{\Omega}$ whose restriction to $\overline{\Omega}$ coincides with φ. The Jacobian matrix of φ at a point x is denoted by $\varphi'(x)$. The following theorem has been proven in [23].

Theorem 3.1 *Suppose that φ maps the boundary $\partial\Omega$ of Ω homeomorphically onto itself and*

$$\det \varphi'(x) > 0 \qquad (x \in \overline{\Omega}). \tag{3.1}$$

Then φ is a homeomorphism of $\overline{\Omega}$ onto $\overline{\Omega}$.

For simply connected domains we can avoid the condition on the map φ to be homeomorphic between boundaries.

Theorem 3.2 *Let $\Omega \subset R^N$ be a bounded, connected and simply connected domain. Suppose that $\varphi : \overline{\Omega} \to \overline{\Omega}$ of class $\mathbb{C}^1$ maps the boundary $\partial\Omega$ of Ω onto itself and satisfies the condition (3.1). Then φ is a homeomorphism of $\overline{\Omega}$ onto $\overline{\Omega}$.*

The following theorem is valid with weaker condition than (3.1).

Theorem 3.3 *Suppose that φ maps the boundary $\partial\Omega$ of Ω homeomorphically onto itself,*

$$\det \varphi'(x) > 0 \qquad (x \in \Omega),$$

and there exists such a point $x_0 \in \partial\Omega$ that $\det \varphi'(x_0) > 0$. Then φ is a homeomorphism of $\overline{\Omega}$ onto $\overline{\Omega}$.

If we have additional conditions on the boundary $\partial\Omega$ of the domain Ω we can avoid the condition that the Jacobian is positive at least at one point of the boundary.

Theorem 3.4 *Suppose that φ maps the boundary $\partial\Omega$ of the domain Ω homeomorphically onto itself, boundary $\partial\Omega$ is a $n-1$-dimensional manifold of class $\mathbb{C}^1$ and that*

$$\det \varphi'(x) > 0 \qquad (x \in \Omega),$$

Then φ is a homeomorphism of $\overline{\Omega}$ onto $\overline{\Omega}$.

Consider mappings from Ω_0 onto Ω. The following analog of the theorem 1 can be proved

Theorem 3.5 *Suppose that φ maps the boundary $\partial\Omega_0$ of the domain Ω_0 homeomorphically onto the boundary $\partial\Omega$ of Ω and*

$$\det \varphi'(x) > 0 \qquad (x \in \overline{\Omega}_0).$$

Then φ is a homeomorphism from $\overline{\Omega}_0$ onto $\overline{\Omega}$.

Analogs of theorems 3 and 4 are also valid for the mappings between bounded domains.

Consider the case when the mapping $\varphi : \overline{\Omega}_0 \to \overline{\Omega}$ is only continuous. The mapping is called a local homeomorphism if for any point $x \in \overline{\Omega}_0$ there exists such a ball $B(x, r)$ of sufficiently small radius r that $B \to \varphi(B)$ is a homeomorphism. Then the following result holds

Theorem 3.6 *Suppose that the local homeomorphism φ maps the boundary $\partial\Omega_0$ of the domain Ω_0 homeomorphically onto the boundary $\partial\Omega$ of Ω. Then φ is a homeomorphism from $\overline{\Omega}_0$ onto $\overline{\Omega}$.*

The theorems 3.1 and 3.6 can be used in the case when the mapping φ ia defined in the closure of the domain $\overline{\Omega}_0$ and its values are in the closure of the domain $\overline{\Omega}$. Let Ω_0 and Ω be two bounded connected and homeomorphic domains and let $\varphi : \overline{\Omega}_0 \to \overline{\Omega}$ be a continuous mapping. Let a domain Ω_0 is devided into nonintersecting domains Ω_i $(i{=}1, \ldots, m)$ such, that

$$\overline{\Omega}_0 = \bigcup_{i=1}^{m} \overline{\Omega}_i \ .$$

Let $\varphi : \overline{\Omega}_0 \to \overline{\Omega}$ be a continuous mapping which is C^1 smooth in the $\overline{\Omega}_i$. The restriction of φ to the $\overline{\Omega}_i$ will be denoted by φ_i $(i{=}1, \ldots, m)$.

Theorem 3.7 *Let φ be a homeomorphism between $\partial\Omega_0$ and $\partial\Omega$ and let for any number of $i{=}1, \ldots, m$, its restriction φ_i be a homeomorphism between $\partial\Omega_i$ and $\varphi_i(\partial\Omega_i)$, and let*

$$\det \varphi_i'(x) > 0 \qquad (x \in \overline{\Omega}_i), \quad i = 1, \ldots, m, \tag{3.2}$$

then φ is a homeomorphism between $\overline{\Omega}_0$ and $\overline{\Omega}$.

These theorems, particularly the theorem 3.7, can be directly used in the theory of grid generation to formulate sufficient conditions on a mesh to be nondegenerate.

3.2 Two-dimensional structured (regular) grids

Grid generation problem in two dimensions will be considered in the following formulation. In a simply connected domain Ω in the plane (x, y), a grid

$$(x, y)_{ij}, \ i = 1, \ldots, i^*, \ j = 1, \ldots, j^*, \tag{3.3}$$

must be constructed with given coordinates of boundary nodes

$$(x, y)_{i1}, \ (x, y)_{ij^*}, \ (x, y)_{1j}, \ (x, y)_{i^*j}. \tag{3.4}$$

The problem can be treated as a discrete analog of the problem of finding the functions $x(\xi, \eta)$ and $y(\xi, \eta)$ ensuring a one-to-one mapping of the parametric square

$$0 < \xi < 1, \ 0 < \eta < 1 \tag{3.5}$$

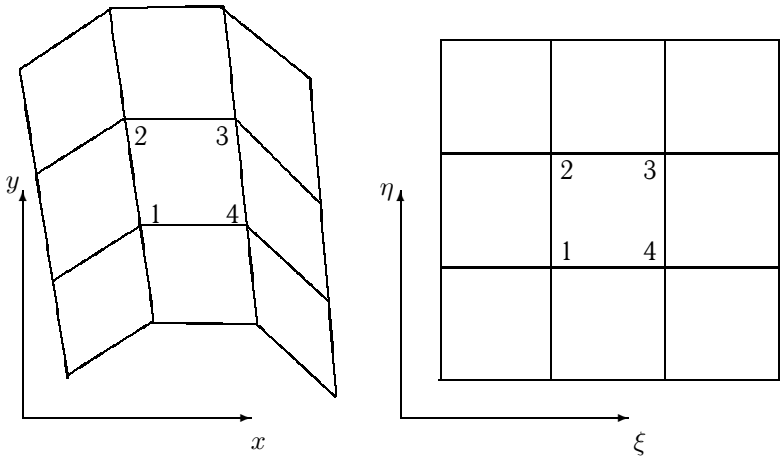

Fig. 3.1: Correspondence of node numbers for a mapping of square cell $i+1/2, j+1/2$ in plane (ξ, η) onto corresponding quadrilateral cell in plane (x, y)

onto the domain Ω, see Fig.3.1, with a given transformation of the square boundary onto the boundary of Ω, associated with the boundary conditions (3.4), i.e., on each side of the parametric square the following eight functions are specified:

$$x(\xi,0) = x_{bt}(\xi),\ x(\xi,1) = x_{top}(\xi),\ x(0,\eta) = x_{left}(\eta),\ x(1,\eta) = x_{right}(\eta),$$

$$y(\xi,0) = y_{bt}(\xi),\ y(\xi,1) = y_{top}(\xi),\ y(0,\eta) = y_{left}(\eta),\ y(1,\eta) = y_{right}(\eta).$$

Instead of the parametric square (3.5) in the plane (ξ, η) the parametric rectangle is often introduced to simplify the computational formulas

$$1 < \xi < i^*,\ 1 < \eta < j^*, \tag{3.6}$$

associated with the square grid (ξ_i, η_j) in the plane (ξ, η) such that

$$\xi_i = i,\ \eta_j = j, \quad i = 1, \ldots, i^*;\ j = 1, \ldots, j^*.$$

From the theorem 3.5 it follows that the curvilinear coordinate system, constructed in a domain Ω, is nondegenerate if the Jacobian of the mapping

$x(\xi,\eta)$, $y(\xi,\eta)$ is positive

$$J = x_\xi y_\eta - x_\eta y_\xi > 0,\ 0 \le \xi \le 1,\ 0 \le \eta \le 1\ . \tag{3.7}$$

Thus, the problem of constructing curvilinear coordinates in a domain Ω can be formulated as the problem of finding a smooth mapping of the parametric square onto the domain Ω which satisfies the condition of the Jacobian positiveness (3.7). The mapping between boundaries must be one-to-one which can be easily provided from the condition of monotonic variations of ξ and η along the appropriate parts of the boundary of the domain Ω.

Consequently, in the discrete case for the grid (3.3) a discrete analog of the Jacobian positiveness must be also applied.

3.3 Discrete analog of the Jacobian positiveness

The mapping $x(\xi,\eta)$, $y(\xi,\eta)$ will be approximated by quadrilateral finite elements [137].

Let the coordinates $(x,y)_{i,j}$ of grid nodes be given. To construct the mapping $x^h(\xi,\eta)$, $y^h(\xi,\eta)$ of the parametric rectangle (3.6) onto the domain Ω such that $x^h(i,j)=x_{i,j}$ and $y^h(i,j)=y_{ij}$ we use quadrilateral isoparametric finite elements [34, 67, 68]. The square cell numbered $i+1/2, j+1/2$ in the plane (ξ,η) is mapped onto the quadrilateral cell in the plane (x,y) formed by nodes with coordinates

$$(x,y)_{i,j},\ (x,y)_{i,j+1},\ (x,y)_{i+1,j+1},\ (x,y)_{i+1,j}.$$

The cell vertices are numbered from 1 to 4 in the clockwise manner as shown in Fig.3.1. The node (i,j) corresponds to the vertex 1, node $(i,j+1)$ to vertex 2, and so on. Each vertex is associated with a triangle: vertex 1 with $\triangle_{412}$, vertex 2 with $\triangle_{123}$ and so on. The doubled area J_k, $k=1,2,3,4$, of these triangles is introduced as follows

$$J_1 = (x_4 - x_1)(y_2 - y_1) - (y_4 - y_1)(x_2 - x_1)$$

$$= (x_{i+1,j} - x_{ij})(y_{i,j+1} - y_{ij}) - (y_{i+1,j} - x_{ij})(x_{ij+1} - x_{ij}).$$

In the first expression, the vertex indices are used and in the second the corresponding node indices are used. The functions x^h, y^h for $i \le \xi \le i+1$,

$j \le \eta \le j+1$ are represented in the form

$$x^h(\xi,\eta) = x_1+(x_4-x_1)(\xi-i)+(x_2-x_1)(\eta-j)+(x_3-x_4-x_2+x_1)(\xi-i)(\eta-j),$$

$$y^h(\xi,\eta) = y_1+(y_4-y_1)(\xi-i)+(y_2-y_1)(\eta-j)+(y_3-y_4-y_2+y_1)(\xi-i)(\eta-j). \tag{3.8}$$

Each side of the square is linearly transformed onto the appropriate side of the quadrilateral. Consequently, the global transformation x^h , y^h is continuous on the cell boundaries. To check the one-to-one property of the transformation (3.8) we write out the expression for the Jacobian

$$J^h = x^h_\xi y^h_\eta - x^h_\eta y^h_\xi = \det \begin{pmatrix} x_4 - x_1 + A(\eta - j) & x_2 - x_1 + A(\xi - i) \\ y_4 - y_1 + B(\eta - j) & y_2 - y_1 + B(\xi - i) \end{pmatrix},$$

where $A=x_3-x_4-x_2+x_1$, $B=y_3-y_4-y_2+y_1$. The Jacobian is linear, not bilinear, since the coefficient at $\xi\eta$ in this determinant is equal to zero. Consequently, if $J^h > 0$ in all corners of the square, it does not vanish inside this square. At the corner 1 ($\xi=i$, $\eta=j$) of the cell $i+1/2, j+1/2$ the Jacobian

$$J^h(i,j) = (x_4 - x_1)(y_2 - y_1) - (y_4 - y_1)(x_2 - x_1),$$

i.e., $J^h(i,j)=J_1$ is the doubled area of the triangle $\triangle_{412}$ introduced above.

From this it follows that the condition of the Jacobian positiveness for the mapping $x^h(\xi,\eta)$, $y^h(\xi,\eta)$

$$x^h_\xi y^h_\eta - x^h_\eta y^h_\xi > 0, \quad 1 \le \xi \le i^*, \ 1 \le \eta \le j^*$$

is equivalent to the system of inequalities

$$[J_k]_{i+1/2,j+1/2} > 0, \quad k = 1,2,3,4; \ i = 1,\dots,i^*-1; \ j = 1,\dots,j^*-1, \tag{3.9}$$

where

$$J_k = (x_{k-1} - x_k)(y_{k+1} - y_k) - (y_{k-1} - y_k)(x_{k+1} - x_k),$$

and in expressions for J_k one should put $k-1=4$ if $k=1$, and $k+1=1$ if $k=4$, i.e., the index k is cyclic.

From the theorem 3.7 it follows the theorem.

Theorem 3.8 *Let the piecewise-bilinear mapping $x^h(\xi,\eta)$, $y^h(\xi,\eta)$ (3.8) be a homeomorphism between the boundary of the rectangle (3.6) and its piecewise-linear image. Suppose that this mapping satisfies conditions (3.9). Then $x^h(\xi,\eta)$, $y^h(\xi,\eta)$ will be a homeomorphism.*

If conditions (3.9) are satisfied, then all grid cells are convex quadrilaterals. Hence, if the mapping $x(\xi,\eta)$, $y(\xi,\eta)$ is approximated by piecewise-bilinear functions, then the one-to-one condition is equivalent to the condition of convexity of all grid cells (3.9). Such grids were called convex grids [34, 67], and only convex grids can be used in the finite element method with conforming quadrilateral elements.

The set of grids satisfying inequalities (3.9) was called a convex grid set and denoted by $\mathcal{D}$ [34, 67]. This is a subset of Euclidean space R^N, where $N=2(i^*-2)(j^*-2)$ is the total number of degrees of freedom of the grid equal to double the number of its internal nodes. In this space $\mathcal{D}$ is an open bounded set. Its boundary $\partial\mathcal{D}$ is the set of grids for which at least one of the inequalities (3.9) becomes an equality.

3.4 Unstructured (irregular) two-dimensional meshes

While constructing irregular meshes we must define a correspondence between the local (for each element) and global node numeration. In Fig.3.2, the simplest example of an irregular mesh is shown. Element numbers are shown in circles. The local numeration is shown only for the element 1. The global numeration is shown with a bold font.

The function $n=n(N,k)$ is introduced to define a correspondence between local and global node numbers:

$$n = n(N,k),\ n = 1,\dots,N_n,\ N = 1,\dots,N_e,\ k = 1,2,3,4,$$

where n is the global node number, N_n is the total number of mesh nodes, N is an element number, N_e is the number of elements, k is a local node number in the element. This function is implemented in the computer program as a function for a regular grid and as an array for an irregular mesh. For example, for the irregular mesh shown in Fig.3.2 the correspondence between local and global numerations is defined as follows

$$n(1,1) = 1,\ n(1,2) = 3,\ n(1,3) = 4,\ n(1,4) = 2.$$

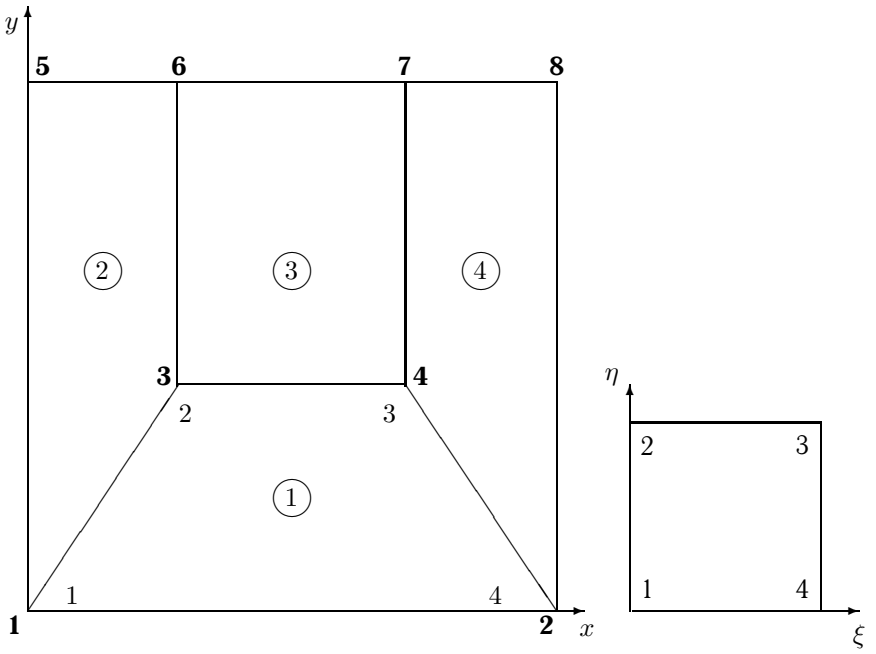

Fig. 3.2: Correspondence of node numbers for mapping of unit square in plane (ξ, η) onto quadrilateral cell 1 of irregular mesh in plane (x, y)

For unstructured grids the array $n(N, k)$ is filled in the process of grid construction, e.g., by a front method. It is often necessary to use another correspondence functions, e.g., when we must define numbers of two elements from the number of their common edge or to define the neighbor numbers for a given node. The choice of these functions depends on the type of elements used and on the solver peculiarities. We will consider below only the simplest data structure, defined by $n(N, k)$, which is enough for our purposes.

For structured grids, it is used the function with the same name instead of the array $n(N, k)$. It is convenient to use a one-dimensional numeration instead of double indices. For node numbers of a structured grid, introduced by (3.3), we have

$$N(i, j) = i + (j - 1)(i^* - 1),\ i = 1, \ldots, i^* - 1;\ j = 1, \ldots, j^* - 1,$$

$$n(i,j) = i + (j-1)i^*,\ i = 1,\dots,i^*;\ j = 1,\dots,j^*,$$

where $n(i,j)$ corresponds to the node i,j, and $N(i,j)$ corresponds to the cell number $i{+}1/2, j{+}1/2$. Then the correspondence function is defined as follows

$$n(N(i,j),1) = n(i,j),\ n(N(i,j),2) = n(i,j+1),$$
$$n(N(i,j),3) = n(i+1,j+1),\ n(N(i,j),4) = n(i+1,j).$$

Now we consider conditions for the mesh node coordinates to assure a mesh to be nondegenerate. Note that in the case of a structured grid instead of the mapping $x(\xi,\eta)$, $y(\xi,\eta)$ of the parametric rectangle (3.5) onto the domain Ω, a bilinear mapping of the same unit square onto each quadrilateral cell can be considered. All argumentation will be true in this case, since the Jacobian of the mapping $x^h(\xi,\eta)$, $y^h(\xi,\eta)$ does not change if the square cell is shifted in the plane (ξ,η). Hence, for each cell of irregular mesh a bilinear mapping of the unit square in the plane (ξ,η) onto this cell can be introduced (see Fig.3.2). The condition of the Jacobian positiveness can be written as follows

$$[J_k]_N > 0, \quad k = 1,2,3,4;\ N = 1,\dots,N_e, \tag{3.10}$$

where

$$J_k = (x_{k-1} - x_k)(y_{k+1} - y_k) - (y_{k-1} - y_k)(x_{k+1} - x_k)$$

is the area of the triangle written in local numeration. Consequently, all mesh cells, satisfying the inequalities (3.10), will be convex quadrilaterals.

As in the case of structured grids, unstructured meshes, satisfying the inequalities (3.10), will be called convex meshes.

As in the previous subsection the set of meshes, satisfying the inequalities (3.10), is called a convex mesh set and denoted by $\mathcal{D}$. This is a subset of Euclidean space $\mathrm{R}^{\mathrm{N_{in}}}$, where N_{in} is the total number of degrees of freedom on the mesh equal to double number of its internal nodes. In this space, $\mathcal{D}$ is an open bounded set. Its boundary $\partial\mathcal{D}$ is the set of meshes for which at least one of the inequalities (3.10) becomes an equality.

Chapter 4

Barrier methods in two-dimensions

4.1 Planar harmonic grid generation

The simplest and most investigated elliptic equation is the Laplace equation. That is why the following system

$$x_{\xi\xi} + x_{\eta\eta} = 0, \quad y_{\xi\xi} + y_{\eta\eta} = 0$$

or its direct extensions may be considered for grid generation.

However, these equations can not guarantee the generation of a unfolded grid. A simple example was constructed by Prokopov [110]. Let us consider the transformation

$$x(\xi,\eta) = \frac{1}{2}(\xi^2 - \eta^2) - \frac{2}{3}\xi, \quad y(\xi,\eta) = \xi\eta + \frac{1}{2}\xi - \frac{1}{3}\eta \ ,$$

defined on the unit square $0<\xi<1$, $0<\eta<1$.

Obviously, this transformation satisfies the Laplace's equation and the Jacobian is

$$J(\xi,\eta) = x_\xi y_\eta - x_\eta y_\xi = (\xi - \frac{2}{3})(\xi - \frac{1}{3}) + (\eta + \frac{1}{2})\eta \ .$$

Since

$$J(\xi,0) = (\xi - \frac{2}{3})(\xi - \frac{1}{3}) < 0$$

in the interval $\eta=0$, $\frac{1}{3}<\xi<\frac{2}{3}$, the transformation is folded near the image of the lower part of the square boundary. The example is of interest because

the image of the square has a very simple form so degeneration of the transformation and grid folding seems absolutely unexpected (see Fig.4.1).

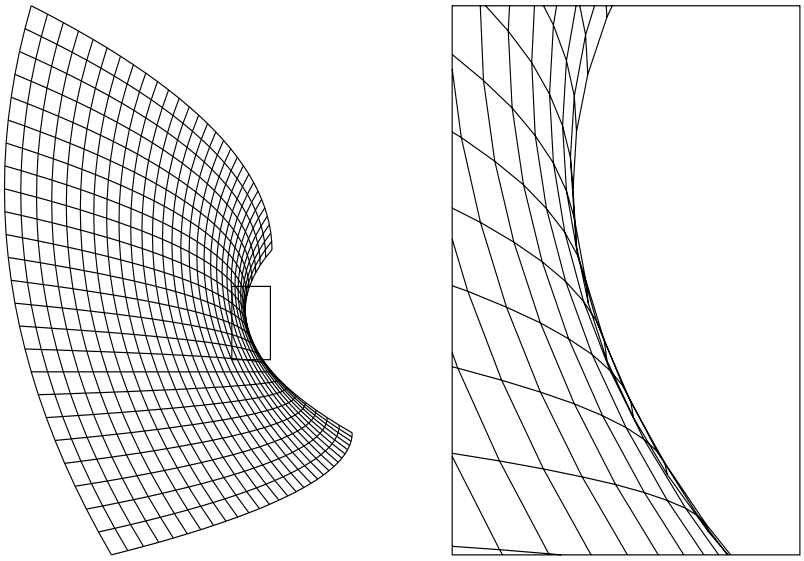

(a) (b)

Fig. 4.1:

Experience has shown the efficiency and the reliability of the method based on harmonic mapping, proposed by Winslow [159]. This is consistent with the theoretical foundation of the method, since the theory guarantees that the generated curvilinear coordinate system is nondegenerate. This property follows from the general result on the existence and uniqueness of the one-to-one harmonic mapping of an arbitrary simply connected domain onto a parametric square.

Development of the method introduced by Godunov and Prokopov [56] is based on the use of such additional parameters that there was no loss of the one-to-one property. This approach was introduced to control the grid spacing. Further developments of this approach were presented by Thompson et.al. [143].

The system of two Laplace equations is used for constructing harmonic

mappings. The natural way to extend this method is to use more common elliptic equations with right-hand sides. However, in the general case it is not clear how to obtain conditions on control parameters under which the generation of a nondegenerate curvilinear coordinate system (structured grid) is guaranteed.

4.2 Equations for harmonic grid generation

The method of grid generation guaranteeing a one-to-one mapping at the continuous level was proposed in [159]. Two families of grid lines are constructed as contours of functions $\xi(x, y)$, $\eta(x, y)$ satisfying two Laplace equations

$$\xi_{xx} + \xi_{yy} = 0, \quad \eta_{xx} + \eta_{yy} = 0 \tag{4.1}$$

with Dirichlet boundary conditions associated with the one-to-one mapping of a boundary of parametric square (3.6) onto the boundary of domain.

After transforming to the independent variables ξ, η, these equations take the form

$$\alpha x_{\xi\xi} - 2\beta x_{\xi\eta} + \gamma x_{\eta\eta} = 0, \ \alpha y_{\xi\xi} - 2\beta y_{\xi\eta} + \gamma y_{\eta\eta} = 0, \tag{4.2}$$

where

$$\begin{aligned} \alpha &= x_\eta^2 + y_\eta^2 = \frac{\xi_x^2 + \xi_y^2}{J^2}, \\ \beta &= x_\xi x_\eta + y_\xi y_\eta = \frac{\xi_x \eta_x + \xi_y \eta_y}{J^2}, \\ \gamma &= x_\xi^2 + y_\xi^2 = \frac{\eta_x^2 + \eta_y^2}{J^2}. \end{aligned} \tag{4.3}$$

The standard approximation of Eqs. (4.2) with centered differences for the first-order derivatives was used in [159, 56]. Computational formulas for the extension of the method to the case of adaptive planar grids will be described in detail below.

To extend the Winslow method, Godunov and Prokopov [56] suggested to use such additional parameters that there was no loss of the one-to-one property. This was achieved by introducing the transformation $\xi{=}\xi(\varphi, \psi)$, $\eta{=}\eta(\varphi, \psi)$. Then instead of the system (4.2) we obtain

$$\alpha' x_{\varphi\varphi} - 2\beta' x_{\varphi\psi} + \gamma' x_{\psi\psi} = a x_\varphi + b x_\psi,$$

$$\alpha' y_{\varphi\varphi} - 2\beta' y_{\varphi\psi} + \gamma' y_{\psi\psi} = a y_\varphi + b y_\psi, \tag{4.4}$$

where

$$\alpha' = x_\psi^2 + y_\psi^2,\ \beta' = x_\varphi x_\psi + y_\varphi y_\psi,\ \gamma' = x_\varphi^2 + y_\varphi^2,$$
$$a = \frac{\alpha'\xi_{\varphi\varphi} - 2\beta'\xi_{\varphi\psi} + \gamma'\xi_{\psi\psi}}{\xi_\varphi\eta_\psi - \eta_\varphi\xi_\psi}\eta_\psi - \frac{\alpha'\eta_{\varphi\varphi} - 2\beta'\eta_{\varphi\psi} + \gamma'\eta_{\psi\psi}}{\xi_\varphi\eta_\psi - \eta_\varphi\xi_\psi}\xi_\psi,$$
$$b = \frac{\alpha'\eta_{\varphi\varphi} - 2\beta'\eta_{\varphi\psi} + \gamma'\eta_{\psi\psi}}{\xi_\varphi\eta_\psi - \eta_\varphi\xi_\psi}\xi_\varphi - \frac{\alpha'\xi_{\varphi\varphi} - 2\beta'\xi_{\varphi\psi} + \gamma'\xi_{\psi\psi}}{\xi_\varphi\eta_\psi - \eta_\varphi\xi_\psi}\eta_\varphi.$$

The grid control can be achieved by specifying functions $\xi(\varphi,\psi)$, $\eta(\varphi,\psi)$, ensuring the one-to-one mapping of the parametric square in the plane (ξ,η) onto the domain in the plane (φ,ψ).

In spite of the fact that there were no concrete recommendations on the choice of control functions $\xi(\varphi,\psi)$, $\eta(\varphi,\psi)$ in [56], this paper is very important from the point of view of methodology. Indeed, we can conclude from the form of Eqs. (4.4), that if another equations, e.g., Poisson's equations, are used for grid generation instead of Laplace's equations, then for successful implementation not only right–hand sides should be specified, but also the coefficients α, β, γ. Results of a long–time research on the employment of the Poisson's equations for adaptive grid generation are presented in [143]. The absence of a considerable success in this way can be explained perhaps by the fact that the property of equations mentioned above guaranteeing the one-to-one mapping is not taken into account in such approach. We will demonstrate this on an example of the equations from [143].

4.3 The use of Poisson equations

Consider a more general system of elliptic equations instead of Laplace's equations

$$\frac{\partial}{\partial x}(D\xi_x) + \frac{\partial}{\partial y}(D\xi_y) = P,$$
$$\frac{\partial}{\partial x}(D\eta_x) + \frac{\partial}{\partial y}(D\eta_y) = Q. \tag{4.5}$$

Multiplying the first equation by x_ξ, the second by x_η, and summing we obtain

$$\left[\frac{\partial}{\partial x}(D\xi_x)+\frac{\partial}{\partial y}(D\xi_y)\right]x_\xi+\left[\frac{\partial}{\partial x}(D\eta_x)+\frac{\partial}{\partial y}(D\eta_y)\right]x_\eta = Px_\xi+Qx_\eta. \quad (4.6)$$

Left–hand side of this equation is transformed as follows

$$\left[\frac{\partial}{\partial x}(D\xi_x)+\frac{\partial}{\partial y}(D\xi_y)\right]x_\xi+\left[\frac{\partial}{\partial x}(D\eta_x)+\frac{\partial}{\partial y}(D\eta_y)\right]x_\eta$$

$$=\frac{\partial}{\partial x}(D\xi_x x_\xi)+\frac{\partial}{\partial y}(D\xi_y x_\xi)+\frac{\partial}{\partial x}(D\eta_x x_\eta)+\frac{\partial}{\partial y}(D\eta_y x_\eta)$$

$$-D\xi_x\frac{\partial}{\partial x}(x_\xi)-D\xi_y\frac{\partial}{\partial y}(x_\xi)-D\eta_x\frac{\partial}{\partial x}(x_\eta)-D\eta_y\frac{\partial}{\partial y}(x_\eta).$$

The sum of the first four terms in the right–hand side is transformed with the use of the following identity

$$\frac{\partial x}{\partial x}=1=x_\xi\xi_x+x_\eta\eta_x,$$

$$\frac{\partial x}{\partial y}=0=x_\xi\xi_y+x_\eta\eta_y,$$

and appears to be equal to D_x.

The sum of the remaining terms is transformed with the use of the following formulas

$$\frac{\partial}{\partial x}=\xi_x\frac{\partial}{\partial\xi}+\eta_x\frac{\partial}{\partial\eta},$$

$$\frac{\partial}{\partial y}=\xi_y\frac{\partial}{\partial\xi}+\eta_y\frac{\partial}{\partial\eta}.$$

As a result we obtain that the left–hand side of the equation (4.6) is equal to

$$-D(\xi_x^2+\xi_y^2)x_{\xi\xi}-2D(\xi_x\eta_x+\xi_y\eta_y)x_{\xi\eta}-D(\eta_x^2+\eta_y^2)x_{\eta\eta}+D_x.$$

Substituting (4.3) into the last expression, we finally obtain

$$\alpha x_{\xi\xi}-2\beta x_{\xi\eta}+\gamma x_{\eta\eta}=\frac{(x_\xi y_\eta-x_\eta y_\xi)^2}{D}(D_x-Px_\xi-Qx_\eta). \quad (4.7)$$

The equation for y is derived in a similar manner. Multiplying the first equation in (4.5) by y_ξ, the second by y_η, and summing we obtain

$$\left[\frac{\partial}{\partial x}(D\xi_x)+\frac{\partial}{\partial y}(D\xi_y)\right]y_\xi+\left[\frac{\partial}{\partial x}(D\eta_x)+\frac{\partial}{\partial y}(D\eta_y)\right]y_\eta=Py_\xi+Qy_\eta. \quad (4.8)$$

Left–hand side of this equation is transformed as follows

$$\begin{aligned}&\left[\frac{\partial}{\partial x}(D\xi_x)+\frac{\partial}{\partial y}(D\xi_y)\right]y_\xi+\left[\frac{\partial}{\partial x}(D\eta_x)+\frac{\partial}{\partial y}(D\eta_y)\right]y_\eta\\&=\frac{\partial}{\partial x}(D\xi_x y_\xi)+\frac{\partial}{\partial y}(D\xi_y y_\xi)+\frac{\partial}{\partial x}(D\eta_x y_\eta)+\frac{\partial}{\partial y}(D\eta_y y_\eta)\\&-D\xi_x\frac{\partial}{\partial x}(y_\xi)-D\xi_y\frac{\partial}{\partial y}(y_\xi)-D\eta_x\frac{\partial}{\partial x}(y_\eta)-D\eta_y\frac{\partial}{\partial y}(y_\eta).\end{aligned}$$

The sum of the first four terms in the left-hand side is transformed with the use of the following identity

$$\frac{\partial y}{\partial y}=1=y_\xi\xi_y+y_\eta\eta_y,$$

$$\frac{\partial y}{\partial x}=0=y_\xi\xi_x+y_\eta\eta_x,$$

and appears to be equal to D_y.

The sum of the remaining terms is transformed with the use of the above formulas for $\frac{\partial}{\partial x}$ and $\frac{\partial}{\partial y}$. As a result we obtain that the left–hand side of the equation (4.8) is equal to

$$-D(\xi_x^2+\xi_y^2)y_{\xi\xi}-2D(\xi_x\eta_x+\xi_y\eta_y)y_{\xi\eta}-D(\eta_x^2+\eta_y^2)y_{\eta\eta}+D_y.$$

Substituting (4.3) into the last expression, we finally obtain

$$\alpha y_{\xi\xi}-2\beta y_{\xi\eta}+\gamma y_{\eta\eta}=\frac{(x_\xi y_\eta-x_\eta y_\xi)^2}{D}(D_y-Py_\xi-Qy_\eta). \quad (4.9)$$

Comparing now the system (4.7),(4.9) with the system (4.4) we can see that the form of right–hand side in the last looks like this part of Eqs. (4.4), but the coefficients α,β,γ in (4.7),(4.9) are the same as in Eqs. (4.2).

Consequently, in spite of the use of a more general equation, the resulting system (4.7),(4.9) does not have such a general form as Eqs. (4.4)

and, therefore, it can be more limited in adaptive grid generation than Eqs. (4.4). In the other words, the specification of only right–hand side might be insufficient for successful adaptive grid generation and we need also to have a procedure for specificating the coefficients α, β, γ.

As it will be shown below, if a grid is generated by using a harmonic mapping between surfaces, then the resulting system of equations has the form, similar to Eqs. (4.4) with new coefficients α, β, γ.

From this viewpoint the harmonic maps approach is well substantiated and, therefore, will form the basis of all the following considerations.

4.4 Variational approach

In this section, we will consider the problem of unstructured grid smoothing with the use of harmonic functional. The method can also be used for structured grid generation, as it was described in [34, 67].

The process of unstructured grid generation usually contains two stages. The meshes produced at the first stage by automated techniques often exhibit large variations of mesh cell sizes. The smoothing techniques are used then to form better shaped cells and yield more accurate analysis.

Various approaches have been developed, but the most promising is, in our opinion, an approach based on the theory of harmonic mappings. For regular grids such algorithms were proposed [26, 34, 67, 91, 161]. In this section we will consider an extension of the method introduced in papers [34, 67], which guarantees convexity of all grid cells in the case of unstructured grids.

The Dirichlet (harmonic) functional was considered by Brackbill and Saltzman [26]

$$I = \int \frac{x_\xi^2 + y_\xi^2 + x_\eta^2 + y_\eta^2}{J} d\xi d\eta. \tag{4.10}$$

The minimum of this functional is attained on the harmonic mapping of the domain Ω onto the parametric square. This functional and its generalizations have been used in many papers for regular grid generation.

The problem of irregular mesh smoothing (or relaxation) is formulated as follows. Let the coordinates of the unstructured grid be given

$$(x, y)_n, \ n = 1, \ldots, N_n \ . \tag{4.11}$$

The mesh is formed by quadrilateral elements, i.e. the array $n(N,k)$ is also defined. The problem is to find new coordinates of the mesh nodes minimizing functional (4.10) value summed over all mesh cell when using mapping of the unit square onto each cell of the mesh.

It is clear that for a regular grid this formulation is reduced to a discrete analog of the problem of constructing harmonic coordinates ξ and η on the domain Ω. Now we will consider the approximation of the functional (4.10).

The present algorithm is based on a particular approximation of the functional (4.10) whereby the minimum ensures all mesh cells to be convex quadrilaterals and guarantees grid nondegeneracy. While implementing, it can be explicitly used peculiarity of vanishing Jacobian when the one-to-one property is lost.

The mapping $x(\xi,\eta)$, $y(\xi,\eta)$ is approximated by functions $x^h(\xi,\eta)$, $y^h(\xi,\eta)$ introduced in Section 3.3. Substituting these expressions into (4.10) and approximating the integrals over the square cell by the quadrature formulas with nodes coinciding with the square corners in the plane (ξ,η), the following discrete analog can be obtained:

$$I^h = \sum_{N=1}^{N_e} \sum_{k=1}^{4} \frac{1}{4} [F_k]_N , \tag{4.12}$$

where F_k is the integrand evaluated in the k-th grid node:

$$F_k=[(x_{k+1}-x_k)^2+(x_k-x_{k-1})^2+(y_{k+1}-y_k)^2+(y_k-y_{k-1})^2]J_k^{-1},$$

and J_k is the doubled area of a triangle introduced in Section 3.3.

Note that the approximation (4.12) of the functional (4.10) can be obtained as follows. The square cell in the plane (ξ,η) is divided into two triangles first by the diagonal 13, and then by diagonal 24. For each subdivision the mapping of the square onto a quadrilateral cell in the plane (x,y) is approximated by the function which is linear in each triangle. Denote this function as before $x^h(\xi,\eta)$, $y^h(\xi,\eta)$.

All derivatives in the integrand of the functional (4.10) are easy to compute. For example, for one of two triangles obtained by splitting the quadrilateral cell with the diagonal 13, we have

$$x_\xi^h = x_3 - x_2, \quad y_\xi^h = y_3 - y_2, \quad x_\eta^h = x_2 - x_1, \quad y_\eta^h = y_2 - y_1,$$

$$J^h = (x_1 - x_2)(y_3 - y_2) - (y_1 - y_2)(x_3 - x_2).$$

The integral (4.10) over the quadrilateral cell in the plane (ξ, η) is approximated by half of the sum of values of this integral, computed for piecewise-linear approximations on triangles, obtained for the first and the second splitting. The result is the approximation (4.12).

The function I^h has the following property, which can be formulated as a theorem:

Theorem 4.1 *The function I^h has an infinite barrier on the boundary of the set of convex meshes, i.e., if at least one of the quantities J_k tends to zero for some cell while remaining positive, then $I^h \to +\infty$.*

Proof.

In fact, suppose that $J_k \to 0$ in the function (4.12) for some cell, but I^h does not tend to $+\infty$. Then the numerator in the function (4.12) must also tend to zero, i.e., the lengths of two sides of the cell tend to zero. Consequently, the areas of all triangles that contain these sides must also tend to zero. Repeating the argument as many times as necessary, we conclude that the lengths of the sides of all grid cells, including those at the boundary of the domain, must tend to zero, i.e., the mesh compresses into a point, which is impossible. This completes the proof.

l.q.q.d.

To illustrate the theorem, consider the simplest case of 3x3 grid generation. Boundary nodes are shown in Fig.4.2*a*. The problem is to find coordinates of one internal node $(x_{2,2}, y_{2,2})$. The set of convex grids $\mathcal{D}$ is the unit square, shown in Fig.4.2*a*. The boundary of the square consists of straight lines connecting the following boundary nodes: (2,1) and (3,2), (3,2) and (2,3), (2,3) and (1,2), (1,2) and (2,1). Contours of the function (4.12) are shown also in Fig.4.2*a*. Values of the function (4.12) were computed for each position of the center grid node on the square grid 51×51 inside the unit square. An infinite barrier of the function (4.12) at the boundary of $\mathcal{D}$ is easy to determine. It is shown also in Fig.4.2*b*, where the function (4.12) is represented as a surface.

Thus, if the set $\mathcal{D}$ is not empty, the system of the algebraic equations

$$R_x = \frac{\partial I^h}{\partial x_n} = 0 \ , \quad R_y = \frac{\partial I^h}{\partial y_n} = 0 \ ,$$

has at least one solution which is a convex mesh. To find it one first must have a certain initial convex mesh, and then use a method of unconstrained minimization. Since the function (4.12) has an infinite barrier on the boundary of the set of convex meshes, each step of the method can be chosen so that the mesh remains convex always.

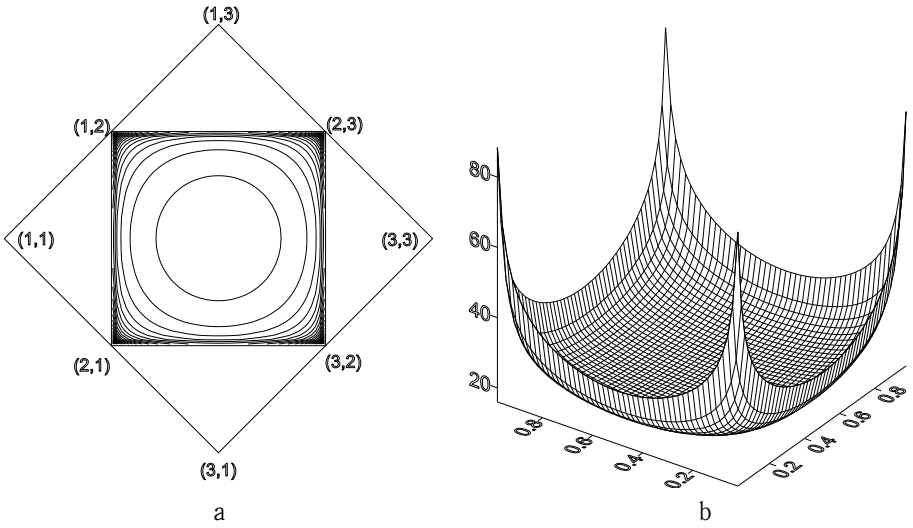

Fig. 4.2: Boundary node distribution for 3×3 mesh and contours of barrier function (4.12) in set of convex grids (a). Function (4.12) represented as surface (b).

4.5 Minimization of the functional

First we consider a method of minimizing the function (4.12) assuming that the initial convex grid has been found. Suppose the mesh at the lth step of the iterations is determined. We use the quasi-Newtonian procedure when the $(l+1)$th step is accomplished by solving two linear equations for each interior node

$$\tau R_x + \frac{\partial R_x}{\partial x_n}(x_n^{l+1} - x_n^l) + \frac{\partial R_x}{\partial y_n}(y_n^{l+1} - y_n^l) = 0 \ ,$$

$$\tau R_y + \frac{\partial R_y}{\partial x_n}(x_n^{l+1} - x_n^l) + \frac{\partial R_y}{\partial y_n}(y_n^{l+1} - y_n^l) = 0 \ . \qquad (4.13)$$

From this it follows

$$x_n^{l+1} = x_n^l - \tau \left(R_x \frac{\partial R_y}{\partial y_n} - R_y \frac{\partial R_x}{\partial y_n} \right) \left(\frac{\partial R_x}{\partial x_n} \frac{\partial R_y}{\partial y_n} - \frac{\partial R_y}{\partial x_n} \frac{\partial R_x}{\partial y_n} \right)^{-1},$$

$$y_n^{l+1} = y_n^l - \tau \left(R_y \frac{\partial R_x}{\partial x_n} - R_x \frac{\partial R_y}{\partial x_n} \right) \left(\frac{\partial R_x}{\partial x_n} \frac{\partial R_y}{\partial y_n} - \frac{\partial R_y}{\partial x_n} \frac{\partial R_x}{\partial y_n} \right)^{-1}, \quad (4.14)$$

where τ is the iteration parameter which is chosen so that the mesh remains convex. To this end, after each step the conditions (3.10) are checked and if they are not satisfied, this parameter is multiplied by 0.5. Note that (4.14) is not the Newton-Raphson iteration process, because not all the second derivatives are taken into account. The rate of convergence is slow by comparison. However, the Newton-Raphson method gives a much more complex system of linear equations.

Each derivative in the formulas (4.14) is the sum of a proper number of terms, in accordance with the number of triangles containing the given node as a vertex. For example, for the irregular mesh, shown in Fig.3.2, the number of such triangles for node 3 is equal to 9.

Rather than write out such cumbersome expressions we consider the first and second derivatives of the terms in the formulas (4.12). Arrays storing the derivatives are first cleared, and then all mesh triangles are scanned and the appropriate derivatives are added to the relevant elements of the arrays. The use of the formulas (4.14) for the boundary node (if its position on the boundary is not fixed) should be completed by the projection of this node onto the boundary.

If the initial mesh is not convex, the computational formulas should be modified so that the initial grid need not belong to the set of convex meshes [68]. To achieve this, the quantities J_k appearing in the expressions for R_x, R_y and in their derivatives are replaced with new quantities $\tilde{J}_k$:

$$\tilde{J}_k = \begin{cases} J_k & \text{if} \quad J_k > \epsilon, \\ \varepsilon & \text{if} \quad J_k \le \varepsilon, \end{cases}$$

where $\varepsilon>0$ is some sufficiently small quantity.

It is important to choose an optimal value of ε so that the convex mesh is constructed as fast as possible. The method used for specifying the value

of ε is based on computing the absolute value of the average area of triangles with negative areas

$$\varepsilon = \max[\alpha S_{neg}/(N_{neg} + 0.01), \varepsilon_1] \ ,$$

where S_{neg} is the double absolute value of the total area of triangles with negative areas, and N_{neg} is the number of these triangles. The quantity $\varepsilon_1 > 0$ defines a lower bound of ε to avoid very large values appearing in computations. The coefficient α is chosen experimentally and is in the range $0.3 \leq \alpha \leq 0.7$.

In practical implementation an arbitrary set of grid nodes can be marked as movable during iterations, while all other nodes are considered as fixed. All the terms in the function (4.12) which become independent on movable nodes are excluded from computations. Since the boundary nodes are always marked as fixed, four terms in (4.12) corresponding to "corner" triangles $\{(1,2);(1,1);(2,1)\}$, $\{(i^*-1,1);(i^*,1);(i^*,2)\}$, $\{(1,j^*-1);(1,j^*);(2,j^*)\}$, and $\{(i^*-1,j^*);(i^*,j^*);(i^*,j^*-1)\}$ are always excluded from computations. As a result the method becomes applicable to those domains for which the angle between two intersecting boundaries is greater than or equal to π, despite of the fact that the corresponding grid cell becomes non-convex independently on the interior node positions.

Computational formulas for the direct extension of the method in the case of adaptive planar grids will be described in detail below.

Chapter 5

Adaptive-harmonic grid generation

5.1 Harmonic maps between surfaces

Recall that for grid generation in a domain Ω the auxiliary problem of constructing a harmonic mapping of this domain onto the parametric square is involved. A mapping of the domain boundary onto the square boundary is given. Laplace equations for unknown functions ξ and η are "inverted" into the equations for the functions x and y, which are solved numerically then. On the other hand, the problem can be stated as a variational minimization of the harmonic functional dependent on the unknown functions $x(\xi, \eta)$ and $y(\xi, \eta)$. The variational approach is convenient for extension of the method to the case of surfaces. To do it the problem of finding the harmonic mapping of the surface onto the parametric square is formulated. The one-to-one mapping between boundaries should be specified.

In the following subsection a more general problem of constructing harmonic mapping between manifolds is considered. The emphasis is placed on the formulation of the conditions, providing the one-to-one mapping.

5.1.1 Theory of harmonic maps

Let M and N be two compact Riemannian manifolds (surfaces) of dimensions $\dim M{=}m$, $\dim N{=}n$, respectively, with metrics g and h defined in local coordinates u^i and ξ^α, $i{=}1, \ldots, m$, $\alpha{=}1, \ldots, n$. The energy density of a map $\xi(u){:}(M, g) \to (N, h)$ is called the function $e(\xi){:}M \to \mathcal{R}(\geq 0)$,

defined in local coordinates as follows

$$e(\xi)(u) = g^{ij}(u)\frac{\partial \xi^{\alpha}(u)}{\partial u^{i}}\frac{\partial \xi^{\beta}(u)}{\partial u^{j}}h_{\alpha\beta}(\xi(u)) \ , \tag{5.1}$$

where the standard summation convention is assumed, g_{ij} and h_{ij} are the elements of the metric tensors G and H of the manifolds M and N, and g^{ij} is the inverse metric

$$g^{ij}g_{jk} = \delta^{i}_{k} = \begin{cases} 1 & \text{if } \ i = k \ , \\ 0 & \text{if } i \neq k \ . \end{cases}$$

This means if g_{ij} are the elements of matrix G, then g^{ij} are the elements of the inverse matrix G^{-1}.

The generalization of the Dirichlet functional for a mapping $\xi(u)$ is called the energy of the mapping and is defined as follows

$$E(\xi) = \int\limits_{M} e(\xi)(u)dM, \qquad \text{where } \ dM = \sqrt{\det(G)}du^{1}\dots du^{m}. \tag{5.2}$$

The following definition is used to introduce the notation of harmonic mapping.

A smooth map $\xi(u)$:$(M,g) \to (N,h)$ is called harmonic if it is an extremal of the energy functional E.

The Euler-Lagrange equations, whose solution minimizes the energy (5.2), are the system of nonlinear partial differential equations and can be written in the form

$$\frac{1}{\sqrt{\det(G)}}\frac{\partial}{\partial u^{i}}\sqrt{\det(G)}g^{ij}\frac{\partial \xi^{\gamma}}{\partial u^{j}} + g^{ij}\Gamma^{\gamma}_{\alpha\beta}\frac{\partial \xi^{\alpha}}{\partial u^{i}}\frac{\partial \xi^{\beta}}{\partial u^{j}} = 0, \tag{5.3}$$

where $\Gamma^{\gamma}_{\alpha\beta}$ denote the Christoffel symbols of the second kind

$$\Gamma^{\gamma}_{\alpha\beta} = \frac{1}{2}h^{\gamma\phi}\left[\frac{\partial h_{\phi\alpha}}{\partial \xi^{\beta}} + \frac{\partial h_{\phi\beta}}{\partial \xi^{\alpha}} - \frac{\partial h_{\alpha\beta}}{\partial \xi^{\phi}}\right].$$

Partial differential equations (5.3) for a map $\xi(u)$:$(M,g) \to (N,h)$ are of considerable interest also in analysis and topology. Note, that in this context there are no linear equations, since N has no additive structure.

Harmonic mappings have been introduced by Fuller [50]. Later on, in the fundamental paper by Eells and Sampson [43] the question of existence

of solutions (5.3) has been considered for closed manifolds M and N (without boundaries) which are assumed to be smooth of class $\mathbb{C}^5$. It has been proved that in case when N has non-positive curvature, each map from M to N is homotopic to a harmonic map.

Eells and Sampson [43] approached the problem through the gradient-line technique, which amounts to replacing the equations (5.3) by a system of parabolic equations. The local equations are then replaced by global equations of essentially the same form, embedding N in Euclidean space. A stability theorem is established showing that a solution of the resulting parabolic system does in fact produce one-parameter family of mappings of M onto N. Fundamental solutions of the Laplace equation and the heat equation on compact manifolds are used to establish *a priori* derivative estimates and to construct solutions of the parabolic system. The latter is transformed into a system of integro-differential equations of the Volterra type.

Special cases of extremal mappings go back to a very beginning of differential geometry. They include geodesics, harmonic functions, and minimal submanifolds.

There are many classical examples of harmonic maps.

(a) The harmonic maps $M \to R$ are the harmonic functions.

(b) The harmonic maps $R \to M$ are the geodesics.

(c) Every isometry is harmonic.

(d) A conformal map is one which preserves angles. Every conformal map in 2D is harmonic.

(e) If N is Riemannian manifold and M is a submanifold of least volume, then the inclusion $i{:}M \to N$ is harmonic for the induced metric on M.

The theory of the energy functional and its harmonic extremals is the first-order case of a general theory of the pth order energy and its polyharmonic extremals (see [43]).

The result of Eels and Sampson [43] was extended by Hamilton [61] to the case where both M and N are allowed to have a boundary.

Theorem (Hamilton, 1975 [61]). *Let M and N be compact Riemannian manifolds with boundary,* $\dim M{=}m$, $\dim N{=}n$, *the respectively. Suppose that N has nonpositive Riemannian curvature and its boundary ∂N is convex or empty. Then there exists a harmonic map $\varphi{:}M \to N$ in every homotopy class.*

The condition that ∂N is convex is a local condition which can be expressed in terms of the Christoffel symbols. Choose a chart

$(\xi^1, \ldots, \xi^{n-1}, \xi^n)$ near ∂N such that $N=\{\xi^n \geq 0\}$. The condition that ∂N is convex is that in such a chart the matrix $\Gamma^n_{\alpha\beta}(1 \leq \alpha, \beta \leq n-1)$ is (weakly) positive definite. To see the geometric meaning consider a geodesic $\phi=\phi^\alpha(t)$ passing through a point on ∂N. The equation for a geodesic says

$$\frac{d^2\phi^n}{dt^2} + \Gamma^n_{\alpha\beta}\frac{d\phi^\alpha}{dt}\frac{d\phi^\beta}{dt} = 0.$$

If ϕ is tangent to ∂N, $d\phi^n/dt=0$, and only terms $\Gamma^n_{\alpha\beta}$ with $1 \leq \alpha, \beta \leq n-1$ appear. If $\Gamma^n_{\alpha\beta}(1 \leq \alpha, \beta \leq n-1)$ is positive definite, then $d^2\phi^n/dt^2 \leq 0$. Thus the condition that ∂N is convex is that a geodesic tangent to ∂N does not enter inside N. If $M=R$ then the harmonic maps are the geodesics, so the condition that ∂N is convex is clearly necessary.

The negative example was mentioned by Hamilton [61]. Harmonic maps of a sphere into an ellipsoid of revolution are considered, which are of degree k and axially symmetric. These exist if the ellipsoid is short and fat, but not if it is tall and thin. Thus as the ellipsoid becomes taller and thinner, at some point the harmonic map either bifurcates into a family of axially asymmetric maps, or it ceases to exist at all. Which happens is not known.

For closed manifolds Hartman [63] proved that harmonic map is unique in each homotopy class if N has strictly negative curvature.

All these resuts have been obtained without constraints on dimensions of manifolds.

In the case both M and N are two-dimensional manifolds (surfaces) with boundaries, the fundamental result on existence and uniqueness of harmonic diffeomorphism (one-to-one smooth mapping) proved independently by Sampson [118] and Shoen and Yau [124].

Theorem (Sampson 1978 [118], Shoen and Yau 1978 [124])

Let a map $\phi: M \to N$ between two-dimensional Riemannian surfaces M and N be a diffeomorphism, which is also a diffeomorphism between boundaries ∂M and ∂N. Suppose the curvature of the surface N is nonpositive and its boundary ∂N is convex, i.e., ∂N is a union of curves having nonnegative geodesic curvature with respect to N. Then there exists a unique harmonic map $\varphi: M \to N$, which is a diffeomorphism, such that φ is homotopy equivalent to ϕ and $\varphi(\partial M)=\phi(\partial M)$.

It should be noted that in case both M and N are bounded simply connected domains in the plane, the last theorem was an old theorem and was due to Rado and Choquet (see references in the paper by Shoen and Yau [124]). In this case, harmonic maps are simply pairs of harmonic functions

and the linear structure is available. For the properties of univalent harmonic maps, one should mention the result of Levy [90], who proved the Jacobian of such a map does not change sign.

In the paper by Joest and Shoen [81] it is shown that in the 2D case any diffeomorphism from M to N is homotopic to harmonic diffeomorphism if the boundary of N is locally convex without restrictions on the curvature of N. This approach gives only the existence of some diffeomorphic harmonic map homotopic to the given one. It may be possible that there are other harmonic maps in the same homotopy class which are not diffeomorphisms.

5.1.2 Examples of non-homeomorphic harmonic maps

Before considering examples of non-homeomorphic harmonic mappings, we first discuss Borel's conjecture on existence of homeomorphisms between manifolds.

Recall, that aspherical manifold is one whose universal cover is contractible. In paticular, a compact non-positively curved Riemannian manifold whose boundary is either empty or convex is an aspherical manifold. Borel made the following conjecture.

Conjecture. *Let M and N be compact Riemannian manifolds (with possibly non-empty boundaries) such that N is aspherical. Let $f{:}M \to N$ be a homotopy equivalence such that $f(\partial M) \in \partial N$ and $f|_{\partial M}{:}\partial M \to \partial N$ is a homeomorphism. Then f is homotopic to a homeomorphism via a homotopy which is fixed on ∂M.*

The results of Eells, Sampson [43] and Hamilton [61] would verify Borel's conjecture in the important case where N is non-positively curved with either empty or convex boundary and M is a Riemannian manifold, provided that the harmonic map they produce is always a homeomorphism. Although both Sampson [118], and Shoen and Yau [124], have shown that this is always true when $\dim N{=}2$, the examples, constructed by Farrell and Jones [48] show that it is sometimes *not* true when $\dim N{>}2$. On the other hand, Borel's conjecture has been verified by a different method in [47] in a large subclass of the above cases, namely, when N is closed (that is, ∂N is empty), nonpositively curved and $\dim N{\neq}3, 4$. The following Theorem has been proved in [48].

Theorem (Farrell and Jones 1996 [48]). *For each integer $m{>}11$, there exists a pair of compact (connected) m-dimensional Riemmaniam*

manifolds (M,g) *and* (N,h) *with both boundaries convex, and a harmonic map* $\varphi{:}(M,g)\to(N,h)$ *with the following properties.*

1. The sectional curvatures of (M,g) *are all equal to -1, and the sectional curvatures of* (N,h) *are all non-positive. Also* ∂M *is strictly convex, that is, its second fundamental form is definite.*

2. φ *is homotopic to a diffeomorphism via a homotopy which is fixed on* ∂M*. In particular,* φ *is homotopy equivalence, and its restriction* $\varphi|_{\partial M}{:}\partial M\to\partial N$ *is a diffeomorphism.*

3. φ *is not a diffeomorphism; that is, there are points* $x\neq y$ *in* M *with* $\varphi(x)=\varphi(y)$.

It is still an open problem to find additional conditions for such harmonic map to be a homeomorphism. Note, that in the 3D case it is still unknown whether a harmonic map of an arbitrary domain $\Omega\subset R^3$ onto a convex domain (unit cube) with a given homeomorphic mapping between boundaries is always a homeomorphism.

From this it follows that the theory of harmonic maps is incomplete in 3D case, most important for applications. This is the reason for additional investigations directed to the development of variational approaches to grid generation and optimization.

5.1.3 Derivation of governing equations

We denote by S^{rn} a n-dimensional surface in $\mathcal{R}^{n+k}$ with a local coordinate system

$$(u^1,\dots,u^n)=u\in S^n\subset\mathcal{R}^n\ .$$

The surface is defined by a nondegenerate transformation

$$r(u):S^n\to S^{rn},\qquad r=(r^1,\dots,r^{n+k}). \tag{5.4}$$

The new parameterizations of the surface S^{rn} is defined by a mapping of a unit cube $Q^n:\{0<\xi^i<1,\ i=1,\dots,n\}$ in $\mathcal{R}^n$ onto a surface S^{rn}

$$r(u(\xi)):Q^n\to S^{rn},\qquad \xi=(\xi^1,\dots,\xi^n)\in Q^n, \tag{5.5}$$

which is the composition of $r(u)$ and some nondegenerate transformation

$$u(\xi):Q^n\to S^n. \tag{5.6}$$

The problem of finding a new parameterizations of the surface is stated as the problem of constructing this transformation $u(\xi)$. The mapping $r(u(\xi))$

defines on a surface S^{rn} a new coordinate system $(\xi^1 \dots \xi^n)=\xi$, which generates a local metric tensor

$$G^{r\xi} = \{g_{ij}^{r\xi}\}, \qquad i,j = 1,2\dots,n,$$

whose elements are scalar products of the vectors $r_i=\partial r/\partial\xi^i$ and $r_j=\partial r/\partial\xi^j$:

$$g_{ij}^{r\xi} = r_i r_j = \sum_{m=1}^{n+k} \frac{\partial r^m}{\partial \xi^i}\frac{\partial r^m}{\partial \xi^j}.$$

The elements of the metric tensor defined by the transformation $r(u)$ are given by

$$G^{ru} = \{g_{ij}^{ru}\}, \qquad i,j = 1,2\dots,n.$$

These elements are the scalar products of the vectors $\partial r/\partial u^i$ and $\partial r/\partial u^j$:

$$g_{ij}^{ru} = \sum_{m=1}^{n+k} \frac{\partial r^m}{\partial u^i}\frac{\partial r^m}{\partial u^j}.$$

Consider the contravariant metric tensors whose elements form the symmetric matrices $G_{\xi r}$ and G_{ur}, inverse to the matrices $G^{r\xi}$ and G^{ru}:

$$g_{\xi r}^{ij} = (-1)^{i+j} d_{\xi r}^{ji}/\det(G^{r\xi}),\ g_{ur}^{ij} = (-1)^{i+j} d_{ur}^{ji}/\det(G^{ru}),$$

where $d_{\xi r}^{ji}$ and d_{ur}^{ji} are the determinants of cofactors of the elements $g_{ij}^{r\xi}$ and g_{ij}^{ru} in the matrices $G^{r\xi}$ and G^{ru} correspondingly.

Let prove the following relation

$$g_{\xi r}^{ij} = \sum_{m,l}^{n} g_{ur}^{ml}\frac{\partial \xi^i}{\partial u^m}\frac{\partial \xi^j}{\partial u^l}. \tag{5.7}$$

Indeed, substituting in the following identity the right-hand side of (5.7) instead of $g_{\xi r}^{lp}$ we obtain

$$\delta_i^p = g_{il}^{r\xi} g_{\xi r}^{lp} = \frac{\partial r^\alpha}{\partial \xi^i}\frac{\partial r^\alpha}{\partial \xi^l} g_{\xi r}^{lp} = \frac{\partial r^\alpha}{\partial u^t}\frac{\partial r^\alpha}{\partial u^h}\frac{\partial u^t}{\partial \xi^i}\frac{\partial u^h}{\partial \xi^l} g_{\xi r}^{lp} = g_{th}^{ru} g_{ur}^{mj}\frac{\partial u^t}{\partial \xi^i}\frac{\partial u^h}{\partial \xi^l}\frac{\partial \xi^l}{\partial u^m}\frac{\partial \xi^p}{\partial u^j}$$

$$= g_{th}^{ru} g_{ur}^{mj}\delta_m^h\frac{\partial u^t}{\partial \xi^i}\frac{\partial \xi^p}{\partial u^j} = g_{th}^{ru} g_{ur}^{hj}\frac{\partial u^t}{\partial \xi^i}\frac{\partial \xi^p}{\partial u^j} = \delta_t^j\frac{\partial u^t}{\partial \xi^i}\frac{\partial \xi^p}{\partial u^j} = \delta_i^p.$$

The summation is performed on repeated indices, here $\alpha = 1, 2, \ldots, n + k$; $i, j, l, p, t, h, m = 1, \ldots, n$. Now taking (5.7) into account, the functional (5.2) takes the form

$$I = \int\limits_{S^{rn}} g^{ii}_{\xi^r} dS^{rn} = \int\limits_{S^{rn}} \sum_{i,m,l}^{n} g^{ml}_{ur} \frac{\partial \xi^i}{\partial u^m} \frac{\partial \xi^i}{\partial u^l} dS^{rn}. \tag{5.8}$$

In the derivation of the Euler equations the integration domain in (5.8) will be replaced by S^n, and the surface element is transformed as follows

$$dS^{rn} = \sqrt{\det(G^{ru})} dS^n = \sqrt{\det(G^{ru})} du^1 \ldots du^n.$$

Consequently the functional (5.8) can be written as:

$$I = \int\limits_{S^n} \sqrt{\det(G^{ru})} \left(\sum_{i,m,l}^{n} g^{ml}_{ur} \frac{\partial \xi^i}{\partial u^m} \frac{\partial \xi^i}{\partial u^l} \right) du^1 \ldots du^n. \tag{5.9}$$

The quantities $\sqrt{\det(G^{ru})}$ and g^{ml}_{ur} in the functional (5.9) are independent of the functions $\xi^i(u)$ and their derivatives, and hence remain unchanged when $\xi(u)$ is varied. Therefore the Euler equations for the functions $\xi^i(u)$, minimizing (5.9) are of the form

$$L(\xi^i) = \sum_{m=1}^{n} \frac{\partial}{\partial u^m} \left(\sqrt{\det(G^{ru})} \sum_{l=1}^{n} g^{ml}_{ur} \frac{\partial \xi^i}{\partial u^l} \right) = 0, i = 1, \ldots, n. \tag{5.10}$$

The equations which each component $u^i(\xi)$ of the function $u(\xi)$ satisfies, can be derived from (5.10). To achieve this, the ith equation of the system (5.10) is multiplied by $\partial u^j / \partial \xi^i$ and summed over i. As a result, we have

$$\sum_{i=1}^{n} L(\xi^i) \frac{\partial u^j}{\partial \xi^i} = \sum_{i,m=1}^{n} \frac{\partial}{\partial u^m} \left(\sum_{p=1}^{n} \sqrt{\det(G^{ru})} g^{mp}_{ur} \frac{\partial \xi^i}{\partial u^p} \right) \frac{\partial u^j}{\partial \xi^i} = \sum_{m=1}^{n} \frac{\partial}{\partial u^m} \Big(\sum_{i,p=1}^{n} \sqrt{\det(G^{ru})} g^{mp}_{ur} \frac{\partial \xi^i}{\partial u^p} \frac{\partial u^j}{\partial \xi^i} \Big) - \sum_{i,m,p,t=1}^{n} \sqrt{\det(G^{ru})} g^{mp}_{ur} \frac{\partial \xi^i}{\partial u^p} \frac{\partial \xi^t}{\partial u^m} \frac{\partial^2 u^j}{\partial \xi^i \partial \xi^t} = 0.$$

Here j=1, …, n.

Now, multiplying each equation by $1/\sqrt{\det(G^{ru})}$ and taking into account (5.7) and the relation $\sum_{i=1}^{n} \frac{\partial \xi^i}{\partial u^p} \frac{\partial u^j}{\partial \xi^i} = \delta_p^j$, we finally obtain

$$g_{\xi r}^{it} \frac{\partial^2 u^j}{\partial \xi^i \partial \xi^t} = \frac{1}{\sqrt{\det(G^{ru})}} \sum_{m=1}^{n} \frac{\partial}{\partial u^m} \left(\sqrt{\det(G^{ru})} g_{ur}^{mj} \right), \quad j = 1, \ldots, n. \tag{5.11}$$

This is a quasilinear system of elliptic equations which is a direct extension of the system (4.2). It can be considered as a basis of the algorithms for structured two-dimensional and three-dimensional adaptive grids, and also grids on surfaces. For derivation of governing equations in all these cases we need only to express the contravariant components $g_{\xi r}^{ij}$ and g_{ur}^{ij} as functions on the covariant components $g_{ij}^{\xi r}$ and g_{ij}^{ur} and substitute the associate expressions into (5.11) for n=2 and n=3.

5.2 Construction of two-dimensional adaptive-harmonic structured grids by solving Euler equations

5.2.1 Derivation of equations

Let Ω be a two-dimensional domain in $\mathcal{R}^2$ and let in an Euclidean space $\mathcal{R}^3$ the surface S^{r2} be given as $z = f(x, y)$. We introduce new notations

$$r = (r^1, r^2, r^3) = (x, y, z) = (x, y, f(x, y)) \in S^{r2} \subset \mathcal{R}^3 \ ,$$

$$u = (u^1, u^2) = (x, y) \in \Omega \subset \mathcal{R}^2,$$

$$\xi = (\xi^1, \xi^2) = (\xi, \eta) \in Q^2 \subset \mathcal{R}^2, \ r_\xi = (x_\xi, y_\xi, z_\xi), \ r_\eta = (x_\eta, y_\eta, z_\eta) \ .$$

The problem formulation is the following. Suppose we are given a simply connected domain Ω with a smooth boundary in the plane (x, y). Consider the surface z=$f(x, y)$ of the graph of the function $f \in C^2(\Omega)$. It is required to find a mapping of the parametric square Q^2 onto the domain Ω under a given mapping between the boundaries such that the mapping of the surface onto the parametric square be harmonic (see Fig.5.1). Thus, the problem is to minimize the Dirichlet functional written for a surface

$$I = \int \left(g_{\xi r}^{11} + g_{\xi r}^{22} \right) dS^{r2}, \tag{5.12}$$

where $g^{11}_{\xi r}$, $g^{12}_{\xi r}$ $g^{22}_{\xi r}$ are the elements of the contravariant metric tensor $G_{\xi r}$ dependent on the elements of the covariant metric tensor $G^{r\xi}$ as follows

$$g^{11}_{\xi r} = g^{r\xi}_{22}/\det(G^{r\xi}), \quad g^{22}_{\xi r} = g^{r\xi}_{11}/\det(G^{r\xi}), \quad g^{12}_{\xi r} = g^{21}_{\xi r} = -g^{r\xi}_{12}/\det(G^{r\xi}),$$

where

$$g^{r\xi}_{11} = r^2_\xi = x^2_\xi + y^2_\xi + z^2_\xi \ , \ g^{r\xi}_{12} = g^{r\xi}_{21} = (r_\xi \cdot r_\eta) = x_\xi x_\eta + y_\xi y_\eta + z_\xi z_\eta \ ,$$

$$g^{r\xi}_{22} = r^2_\eta = x^2_\eta + y^2_\eta + z^2_\eta \ ,$$

$$\det(G^{r\xi}) = g^{r\xi}_{11} g^{r\xi}_{22} - (g^{r\xi}_{12})^2, \ z_\xi = f_x x_\xi + f_y y_\xi, z_\eta = f_x x_\eta + f_y y_\eta. \quad (5.13)$$

Inverting dependent and independent variables in (5.12) and noting that

$$dS^{r2} = \sqrt{g^{r\xi}_{11} g^{r\xi}_{22} - (g^{r\xi}_{12})^2} d\xi d\eta,$$

we obtain

$$I = \int \frac{g^{r\xi}_{11} + g^{r\xi}_{22}}{\sqrt{g^{r\xi}_{11} g^{r\xi}_{22} - (g^{r\xi}_{12})^2}} d\xi d\eta \ . \quad (5.14)$$

The Euler equation for the functional (5.14) follows from (5.11) for n=2, k=1. We need only to compute the elements of the covariant metric tensor $G^{r\xi}$ and contravariant metric tensor $G_{\xi r}$ of the transform $r(u)$=$r(x,y)$:$\Omega \to S^{r2}$

$$r = (x, y, f(x,y)), r_x = (1, 0, f_x), r_y = (0, 1, f_y),$$

$$g^{ru}_{11} = r^2_x = 1 + f^2_x, \ g^{ru}_{12} = g^{ru}_{21} = r_x \cdot r_y = f_x f_y, \ g^{ru}_{22} = r^2_y = 1 + f^2_y,$$

$$\det(G^{ru}) = g^{ru}_{11} g^{ru}_{22} - (g^{ru}_{12})^2 = 1 + f^2_x + f^2_y, \ \det(G^{r\xi}) = \det(G^{ru})(x_\xi y_\eta - x_\eta y_\xi)^2$$

$$g^{11}_{ur} = g^{ru}_{22}/\det(G^{ru}) = (1 + f^2_y)/(1 + f^2_x + f^2_y).$$

$$g^{12}_{ur} = -g^{ru}_{21}/\det(G^{ru}) = -f_x f_y/(1 + f^2_x + f^2_y),$$

$$g^{22}_{ur} = g^{ru}_{11}/\det(G^{ru}) = (1 + f^2_x)/(1 + f^2_x + f^2_y).$$

Substituting these expressions into (5.11) we obtain equations written in the form convenient for the practical use

$$L(x) = \alpha x_{\xi\xi} - 2\beta x_{\xi\eta} + \gamma x_{\eta\eta} - J^2 D \left[\frac{\partial}{\partial x} \frac{1 + f^2_y}{D} - \frac{\partial}{\partial y} \frac{f_x f_y}{D} \right] = 0,$$

$$L(y) = \alpha y_{\xi\xi} - 2\beta y_{\xi\eta} + \gamma y_{\eta\eta} - J^2 D \left[\frac{\partial}{\partial x} \frac{-f_x f_y}{D} + \frac{\partial}{\partial y} \frac{1 + f_x^2}{D} \right] = 0, \quad (5.15)$$

where

$$D = \sqrt{1 + f_x^2 + f_y^2} \ , \quad J = x_\xi y_\eta - x_\eta y_\xi \ , \quad \alpha = x_\eta^2 + y_\eta^2 + f_\eta^2 \ ,$$

$$\beta = x_\xi x_\eta + y_\xi y_\eta + f_\xi f_\eta \ , \quad \gamma = x_\xi^2 + y_\xi^2 + f_\xi^2 \ .$$

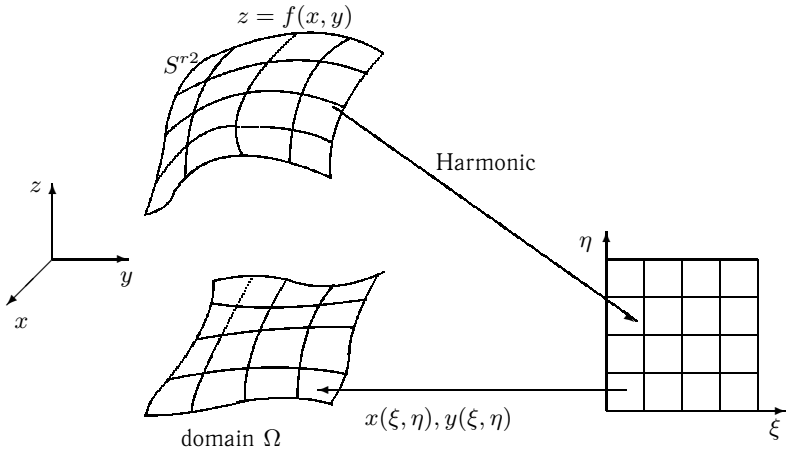

Fig. 5.1: Harmonic coordinates on surface of graph of function $z{=}f(x, y)$.

5.2.2 Numerical implementation

Equations (5.15) are approximated on the square grid of unit size with the simplest difference relations

$$x_\xi \approx [x_\xi]_{ij} = 0.5(x_{i+1,j} - x_{i-1,j}), \ x_\eta \approx [x_\eta]_{ij} = 0.5(x_{i,j+1} - x_{i,j-1}),$$

$$y_\xi \approx [y_\xi]_{ij} = 0.5(y_{i+1,j} - y_{i-1,j}), \ y_\eta \approx [y_\eta]_{ij} = 0.5(y_{i,j+1} - y_{i,j-1}),$$

$$f_\xi \approx [f_\xi]_{ij} = 0.5(f_{i+1,j} - f_{i-1,j}), \ f_\eta \approx [f_\eta]_{ij} = 0.5(f_{i,j+1} - f_{i,j-1}),$$

$$x_{\xi\xi} \approx [x_{\xi\xi}]_{ij} = x_{i+1,j} - 2x_{ij} + x_{i-1,j},$$

$$x_{\xi\eta} \approx [x_{\xi\eta}]_{ij} = 0.25(x_{i+1,j+1} - x_{i+1,j-1} - x_{i-1,j+1} + x_{i-1,j-1}),$$

$$x_{\eta\eta} \approx [x_{\eta\eta}]_{ij} = x_{i,j+1} - 2x_{ij} + x_{i,j-1},\ y_{\xi\xi} \approx [y_{\xi\xi}]_{ij} = y_{i+1,j} - 2y_{ij} + y_{i-1,j},$$

$$y_{\xi\eta} \approx [y_{\xi\eta}]_{ij} = 0.25(y_{i+1,j+1} - y_{i+1,j-1} - y_{i-1,j+1} + y_{i-1,j-1}),$$

$$y_{\eta\eta} \approx [y_{\eta\eta}]_{ij} = y_{i,j+1} - 2y_{ij} + y_{i,j-1},$$

$$\alpha \approx [x_\eta]_{ij}^2 + [y_\eta]_{ij}^2 + [f_\eta]_{ij}^2,\ \beta \approx [x_\xi]_{ij}[x_\eta]_{ij} + [y_\xi]_{ij}[y_\eta]_{ij} + [f_\xi]_{ij}[f_\eta]_{ij},$$

$$\gamma \approx [x_\xi]_{ij}^2 + [y_\xi]_{ij}^2 + [f_\xi]_{ij}^2. \tag{5.16}$$

Substitute these expressions into (5.15) and denote the difference approximations of $L(x)$ and $L(y)$ as $[L(x)]_{ij}$ and $[L(y)]_{ij}$, respectively. Suppose that the coordinates of the grid nodes $(x,y)_{ij}$ at the lth step of iterations are determined. Then the $(l+1)$th step is accomplished as follows

$$x_{ij}^{l+1} = x_{ij}^l + \tau\frac{[L(x)]_{ij}}{2[\alpha]_{ij} + 2[\gamma]_{ij}},\ y_{ij}^{l+1} = y_{ij}^l + \tau\frac{[L(y)]_{ij}}{2[\alpha]_{ij} + 2[\gamma]_{ij}}. \tag{5.17}$$

The expressions in square brackets denote the corresponding approximations of expressions in the grid node (i,j) at the lth iteration step. The value of iteration parameter τ is chosen within limits $0<\tau<1$, and usually $\tau=0.5$.

Derivatives $[f_x]_{ij}$ and $[f_y]_{ij}$ in the ijth grid node are evaluated with the centered differences

$$[f_x]_{ij} = \frac{(f_{i+1,j} - f_{i-1,j})(y_{i,j+1} - y_{i,j-1}) - (f_{i,j+1} - f_{i,j-1})(y_{i+1,j} - y_{i-1,j})}{(x_{i+1,j} - x_{i-1,j})(y_{i,j+1} - y_{i,j-1}) - (x_{i,j+1} - x_{i,j-1})(y_{i+1,j} - y_{i-1,j})},$$

$$[f_y]_{ij} = -\frac{(f_{i+1,j} - f_{i-1,j})(x_{i,j+1} - x_{i,j-1}) - (f_{i,j+1} - f_{i,j-1})(x_{i+1,j} - x_{i-1,j})}{(x_{i+1,j} - x_{i-1,j})(y_{i,j+1} - y_{i,j-1}) - (x_{i,j+1} - x_{i,j-1})(y_{i+1,j} - y_{i-1,j})}.$$

These formulas must be modified for the boundary nodes. Indices, "leaving" the computational domain must be replaced by the nearest boundary indices. For example, if $j=1$, then $(i,j-1)$ must be replaced by (i,j).

Note, that if $[f_\xi]_{ij}=0$ and $[f_\eta]_{ij}=0$, then $[f_x]_{ij}=0$ and $[f_y]_{ij}=0$ and the method (5.17) reduces to the Winslow method [159].

The adaptive-harmonic grid generation algorithm is formulated as follows:

1. Compute the values of the control function at each grid node. The result is f_{ij}.

2. Evaluate derivatives $(f_x)_{ij}$ and $(f_y)_{ij}$ and other expressions in (5.17) using the above formulas.

3. Make one iteration step and compute new values of x_{ij} and y_{ij}.

4. Repeat starting with Step 1 to convergency.

The resulting algorithm can be used in the numerical solution of the partial differential equations. In this case at the first step of the algorithm the values f_{ij} in each grid node are taken from the finite-difference or finite element solution of the host equations.

Note, that to control the grid nodes number in the layers of high gradients it is convenient to use $c_a f$ instead of $f(x, y)$. The larger the coefficient c_a, the greater the number of nodes in the layer of high gradients of the function f.

5.3 Variational barrier method for two-dimensional adaptive-harmonic grid generation

5.3.1 Problem formulation

In notations of the previous section the problem is formulated as follows. Suppose a simply connected domain Ω with a smooth boundary in the plane (x, y) is given. Consider the surface $z{=}f(x, y)$ of the graph of the function $f{\in}C^1(\Omega)$. It is required to find a mapping of the parametric square Q^2 onto a domain Ω under a given mapping between the boundaries so that the mapping of the surface onto the parametric square be harmonic (see Fig.5.1). Thus, the problem is to minimize the harmonic functional (5.14).

Substituting the expressions (5.13) for z_ξ and z_η into (5.14) we obtain the functional from [70] to define an adaptive-harmonic grid, clustered in regions of high gradients of the function $f(x, y)$

$$I = \int \frac{(x_\xi^2 + x_\eta^2)(1 + f_x^2) + (y_\xi^2 + y_\eta^2)(1 + f_y^2) + 2f_x f_y(x_\xi y_\xi + x_\eta y_\eta)}{(x_\xi y_\eta - x_\eta y_\xi)\sqrt{1 + f_x^2 + f_y^2}} d\xi d\eta. \tag{5.18}$$

The problem of irregular mesh smoothing and adaption is formulated as follows. Let the coordinates of an irregular mesh be given. The mesh is formed by quadrilateral elements, i.e. the array $n(N, k)$ is also defined. The problem is to find new coordinates of the mesh nodes, minimizing the sum

of the functional (5.18) values, computed for a mapping of the unit square onto an each cell of the mesh.

5.3.2 Approximation of the functional

The functional (5.18) possesses the same properties as the functional (4.10), and it can be also approximated in such a way that its minimum is attained on a mesh of convex quadrilaterals

$$I^h = \sum_{N=1}^{N_e} \sum_{k=1}^{4} \frac{1}{4} \left[F_k\right]_N , \tag{5.19}$$

where

$$F_k = \frac{D_1[1+(f_x)_k^2] + D_2[1+(f_y)_k^2] + 2D_3(f_x)_k(f_y)_k}{J_k[1+(f_x)_k^2+(f_y)_k^2]^{1/2}},$$

$$D_1 = (x_{k-1}-x_k)^2 + (x_{k+1}-x_k)^2, \quad D_2 = (y_{k-1}-y_k)^2 + (y_{k+1}-y_k)^2,$$

$$D_3 = (x_{k-1}-x_k)(y_{k-1}-y_k) + (x_{k+1}-x_k)(y_{k+1}-y_k) \ ,$$

$$J_k = (x_{k-1}-x_k)(y_{k+1}-y_k) - (x_{k+1}-x_k)(y_{k-1}-y_k) \ .$$

Here $(f_x)_k$ and $(f_y)_k$ are the values of derivatives at the kth node of the Nth cell.

If the set of convex meshes D is not empty, the system of the algebraic equations

$$R_x = \frac{\partial I^h}{\partial x_n} = 0, \ R_y = \frac{\partial I^h}{\partial y_n} = 0,$$

has at least one solution which is a convex mesh. To find it, one must first find a certain initial convex mesh, and then use some method of unconstrained minimization of the function I^h. Since this function has an infinite barrier on the boundary of the set D, each step of the method can be chosen so that the mesh always remains convex.

5.3.3 Minimization of the functional

Suppose the mesh at the lth step of the iterations is determined. We use the quasi-Newtonian procedure when the $(l+1)$th step is accomplished as

follows

$$x_n^{l+1} = x_n^l - \tau \left(R_x \frac{\partial R_y}{\partial y_n} - R_y \frac{\partial R_x}{\partial y_n} \right) \left(\frac{\partial R_x}{\partial x_n} \frac{\partial R_y}{\partial y_n} - \frac{\partial R_y}{\partial x_n} \frac{\partial R_x}{\partial y_n} \right)^{-1},$$

$$y_n^{l+1} = y_n^l - \tau \left(R_y \frac{\partial R_x}{\partial x_n} - R_x \frac{\partial R_y}{\partial x_n} \right) \left(\frac{\partial R_x}{\partial x_n} \frac{\partial R_y}{\partial y_n} - \frac{\partial R_y}{\partial x_n} \frac{\partial R_x}{\partial y_n} \right)^{-1}, \quad (5.20)$$

where τ is the iteration parameter, which is chosen so that the mesh remains convex. With this purpose after each step conditions (3.10) are checked and if they are not satisfied, this parameter is multiplied by 0.5. Then conditions (3.10) are checked for the grid, computed with a new value of τ and if they are not satisfied, this parameter is multiplied by 0.25, etc.

The adaptive-harmonic algorithm for r-refinement is formulated as follows:

1. Generate an initial mesh by the use of a marching method.
2. Compute the values of the control function f_n at every mesh node.
3. Evaluate the derivatives $(f_x)_n$, $(f_y)_n$ and other expressions in (5.20).
4. Make one iteration step and compute new values of x_n and y_n.
5. Repeat starting with Step 2 to convergency.

Computational formulas for $[f_x]_n$ and $[f_y]_n$ will be presented below.

5.3.4 Derivation of computational formulas

Four triangles, introduced above, are considered for the quadrilateral cell with number N. Each of these triangles corresponds to a corner with number k and gives a proper contribution to the functional and also to the value of its derivatives. Since the integrand in (5.18) does not depend on the rotation of the coordinate system ξ, η, then all the computational formulas will be the same for all triangles. We enumerate nodes of the triangle which corresponds to the corner with local number k from 1 to 3 as follows:
node 1 corresponds to the local node number $k-1$ of the Nth cell,
node 2 corresponds to the local node number k of the Nth cell,
node 3 corresponds to the local node number $k+1$ of the Nth cell.

Then in new numeration the expression for F_k will be

$$F_k = \frac{D_1[1 + (f_x)_k^2] + D_2[1 + (f_y)_k^2] + 2D_3(f_x)_k(f_y)_k}{J_2[1 + (f_x)_k^2 + (f_y)_k^2]^{1/2}}, \quad (5.21)$$

where

$$D_1 = (x_1 - x_2)^2 + (x_3 - x_2)^2, \quad D_2 = (y_1 - y_2)^2 + (y_3 - y_2)^2,$$

$$D_3 = (x_1 - x_2)(y_1 - y_2) + (x_3 - x_2)(y_3 - y_2),$$

$$J_2 = (x_1 - x_2)(y_3 - y_2) - (x_3 - x_2)(y_1 - y_2).$$

We introduce notations

$$U = \frac{D_1[1 + (f_x)_k^2] + D_2[1 + (f_y)_k^2] + 2D_3(f_x)_k(f_y)_k}{[1 + (f_x)_k^2 + (f_y)_k^2]^{1/2}} \ ,$$

$$V = (x_1 - x_2)(y_3 - y_2) - (x_3 - x_2)(y_1 - y_2) \ .$$

We use the formulas for the derivatives of two functions ratio (chain rule). Differentiating, we obtain

$$F = \frac{U}{V} \ ,$$

$$F_x = \frac{U_x - FV_x}{V}, \quad F_y = \frac{U_y - FV_y}{V} \quad F_{xx} = \frac{U_{xx} - 2F_xV_x - FV_{xx}}{V}, \quad (5.22)$$

$$F_{yy} = \frac{U_{yy} - 2F_yV_y - FV_{yy}}{V} \ , \quad F_{xy} = F_{yx} = \frac{U_{xy} - F_xV_y - F_yV_x - FV_{xy}}{V}.$$

For the triangle vertex with number 1 we should substitute appropriate expressions instead of U and V, U_x and V_x, etc. into (5.21) and replace x and y by x_1 and y_1.

For vertex 1 we have

$$V_x = y_3 - y_2 \ , \quad V_y = x_2 - x_3 \ ,$$

$$V_{xx} = 0 \ , \quad V_{xy} = 0 \ , \quad V_{yy} = 0 \ .$$

$$U_x = 2\frac{[1 + (f_x)_k^2](x_1 - x_2) + (f_x)_k(f_y)_k(y_1 - y_2)}{[1 + (f_x)_k^2 + (f_y)_k^2]^{1/2}} \ ,$$

$$U_y = 2\frac{[1 + (f_y)_k^2](y_1 - y_2) + (f_x)_k(f_y)_k(x_1 - x_2)}{[1 + (f_x)_k^2 + (f_y)_k^2]^{1/2}} \ ,$$

$$U_{xx} = 2\frac{1 + (f_x)_k^2}{[1 + (f_x)_k^2 + (f_y)_k^2]^{1/2}} \ , \quad U_{xy} = 2\frac{(f_x)_k(f_y)_k}{[1 + (f_x)_k^2 + (f_y)_k^2]^{1/2}} \ ,$$

$$U_{yy} = 2\frac{1+(f_y)_k^2}{[1+(f_x)_k^2+(f_y)_k^2]^{1/2}} \ .$$

For vertex 2 we have

$$V_x = y_1 - y_3 \ , \quad V_y = x_3 - x_1 \ ,$$

$$V_{xx} = 0 \ , \quad V_{xy} = 0 \ , \quad V_{yy} = 0 \ .$$

$$U_x = 2\frac{[1+(f_x)_k^2](2x_2 - x_1 - x_3) + (f_x)_k(f_y)_k(2y_2 - y_1 - y_3)}{[1+(f_x)_k^2+(f_y)_k^2]^{1/2}} \ ,$$

$$U_y = 2\frac{[1+(f_y)_k^2](2y_2 - y_1 - y_3) + (f_x)_k(f_y)_k(2x_2 - x_1 - x_3)}{[1+(f_x)_k^2+(f_y)_k^2]^{1/2}} \ ,$$

$$U_{xx} = 4\frac{1+(f_x)_k^2}{[1+(f_x)_k^2+(f_y)_k^2]^{1/2}} \ , \quad U_{xy} = 4\frac{(f_x)_k(f_y)_k}{[1+(f_x)_k^2+(f_y)_k^2]^{1/2}} \ ,$$

$$U_{yy} = 4\frac{1+(f_y)_k^2}{[1+(f_x)_k^2+(f_y)_k^2]^{1/2}} \ .$$

For vertex 3 we have

$$V_x = y_2 - y_1 \ , \quad V_y = x_1 - x_2 \ ,$$

$$V_{xx} = 0 \ , \quad V_{xy} = 0 \ , \quad V_{yy} = 0 \ .$$

$$U_x = 2\frac{[1+(f_x)_k^2](x_3 - x_2) + (f_x)_k(f_y)_k(y_3 - y_2)}{[1+(f_x)_k^2+(f_y)_k^2]^{1/2}} \ ,$$

$$U_y = 2\frac{[1+(f_y)_k^2](y_3 - y_2) + (f_x)_k(f_y)_k(x_3 - x_2)}{[1+(f_x)_k^2+(f_y)_k^2]^{1/2}} \ ,$$

$$U_{xx} = 2\frac{1+(f_x)_k^2}{[1+(f_x)_k^2+(f_y)_k^2]^{1/2}} \ , \quad U_{xy} = 2\frac{(f_x)_k(f_y)_k}{[1+(f_x)_k^2+(f_y)_k^2]^{1/2}} \ ,$$

$$U_{yy} = 2\frac{1+(f_y)_k^2}{[1+(f_x)_k^2+(f_y)_k^2]^{1/2}} \ .$$

Computations are performed as follows. Let F and its derivatives with respect to x_1 and y_1 be computed via the formulas (5.22) for the Nth cell and kth triangle number. Then the computed values are added to the appropriate array elements

$$I^h += F, \quad [R_x]_n += F_x, \quad [R_y]_n += F_y,$$

$$[R_{xx}]_n+ = F_{xx}, \quad [R_{xy}]_n+ = F_{xy}, \quad [R_{yy}]_n+ = F_{yy},$$

where $n{=}n(N,k{-}1)$.

Similarly for vertex 2, the correspondence between local and global number is $n{=}n(N,k)$.

Similarly for vertex 3, the correspondence between local and global number is $n{=}n(N,k{+}1)$.

Derivatives $[f_x]_n$ and $[f_y]_n$ are computed as follow. All triangles of the mesh are scanned and for the kth triangle of the Nth cell the following values are computed

$$fx = (f_1 - f_2)(y_3 - y_2) - (f_3 - f_2)(y_1 - y_2) \ ,$$

$$fy = (x_1 - x_2)(f_3 - f_2) - (x_3 - x_2)(f_1 - f_2) \ ,$$

$$J_2 = (x_1 - x_2)(y_3 - y_2) - (x_3 - x_2)(y_1 - y_2) \ .$$

Where f_1, f_2 and f_3 are the values of the function f at the triangle vertices, numbered as 1, 2 and 3, corresponding to the local numbers of corners $k-1$, k, and $k+1$ of a quadrilateral cell. Computed values are added to the corresponding array elements (which were first cleared)

$$[f_x]_n+ = fx, \quad [f_y]_n+ = fy, \quad [J]_n+ = J_2, \quad n = n(N,k) \ .$$

New values of derivatives are computed as follows

$$[f_x]_n/ = [J]_n, \quad [f_y]_n/ = [J]_n.$$

Here, according to C-language notation, $a+ = b$ means, that the new value of a becomes equal to $a + b$, and $a/ = b$ means, that the new value of a becomes equal to a/b.

[1]It is of importance the matter of boundary nodes redistributing, since a proper algorithm to the boundary nodes allows for performing more robust adaptive grid generation and modelling of the flow problems. This matter is considered in the Appendix.

[1]This paragraph was added by the Editor.

Chapter 6

Adaptive-harmonic surface grid generation

6.1 Finite-difference adaptive-harmonic surface grid generator

6.1.1 Derivation of equations

Introduce the following notations

$$r = (r^1, r^2, r^3, r^4) = (x, y, z, f) \in S^{r2} \subset \mathcal{R}^4,$$

$$u = (u^1, u^2) = (u, v) \in Q^2 \subset \mathcal{R}^2,$$

$$\xi = (\xi^1, \xi^2) = (\xi, \eta) \in Q^2 \subset \mathcal{R}^2.$$

$$r_\xi = (x_\xi, y_\xi, z_\xi, f_\xi), r_\eta = (x_\eta, y_\eta, z_\eta, f_\eta) \ ,$$

$$r_u = (x_u, y_u, z_u, f_u), r_v = (x_v, y_v, z_v, f_v) \ .$$

Thus, consider a two-dimensional surface in a four-dimensional space, defined as $x{=}x(u,v)$, $y{=}y(u,v)$, $z{=}z(u,v)$, $f{=}f(u,v)$. Let the functions $\xi = \xi(u,v)$, $\eta = \eta(u,v)$ be used to define a new parametrization of a surface.

Note that a harmonic mapping of a surface onto a parametric square can be defined with the use of the first differential Beltrami's parameter

$$(\nabla_s \xi \nabla_s \eta) = \frac{g_{11}^{ru} \xi_v \eta_v - g_{12}^{ru} (\xi_u \eta_v + \xi_v \eta_u) + g_{22}^{ru} \xi_u \eta_u}{g_{11}^{ru} g_{22}^{ru} - (g_{12}^{ru})^2} \ ,$$

Then the general harmonic functional can be written in the form

$$I = \int [(\nabla_s \xi \nabla_s \xi) + (\nabla_s \eta \nabla_s \eta)] dS^{r2} \ , \tag{6.1}$$

where dS^{r2} is the element of a surface S^{r2}.

The problem of constructing the quasiuniform harmonic grid on the surface is stated as the problem of finding the new parametrization of a surface $u{=}u(\xi,\eta)$, $v{=}v(\xi,\eta)$, minimizing the functional (6.1), when $f(u,v){=}0$. Inverting dependent and independent variables in (6.1), we have

$$I = \int \frac{g_{11}^{ru}(u_\xi^2 + u_\eta^2) + 2g_{12}^{ru}(u_\xi v_\xi + u_\eta v_\eta) + g_{22}^{ru}(v_\xi^2 + v_\eta^2)}{\sqrt{g_{11}^{ru} g_{22}^{ru} - (g_{12}^{ru})^2}(u_\xi v_\eta - u_\eta v_\xi)} d\xi d\eta \ , \tag{6.2}$$

$$g_{11}^{ru} = x_u^2 + y_u^2 + z_u^2, \ g_{12}^{ru} = x_u x_v + y_u y_v + z_u z_v, \ g_{22}^{ru} = x_v^2 + y_v^2 + z_v^2.$$

The result of minimization will be a new parametrization $u{=}u(\xi,\eta)$, $v{=}v(\xi,\eta)$ defining the quasiuniform grid on a surface. Difficulties encountered in this problem are concerned with uniqueness of the solution to its discrete analog. This is in spite of the result from the harmonic map theory that the continuous problem has a unique solution.

To construct an adaptive grid on a surface we introduce a control function $f(u,v)$ which will define clustering in regions where its gradient is large. In this case the functional (6.2) is to be minimized with the metric tensor elements g_{ij}^{ru} defined as follows

$$\begin{aligned} g_{11}^{ru} &= x_u^2 + y_u^2 + z_u^2 + f_u^2 \ , \\ g_{12}^{ru} &= x_u x_v + y_u y_v + z_u z_v + f_u f_v \ , \\ g_{22}^{ru} &= x_v^2 + y_v^2 + z_v^2 + f_v^2 \ . \end{aligned} \tag{6.3}$$

We write out the Euler equations for the functional (6.2) in the case of adaption. These equations follow from the general equations if $n{=}2$, $k{=}2$

$$\begin{aligned} L(u) &= \alpha u_{\xi\xi} - 2\beta u_{\xi\eta} + \gamma u_{\eta\eta} - J^2 D \left[\frac{\partial}{\partial u} \frac{g_{22}^{ru}}{D} - \frac{\partial}{\partial v} \frac{g_{12}^{ru}}{D} \right] = 0 \ , \\ L(v) &= \alpha v_{\xi\xi} - 2\beta v_{\xi\eta} + \gamma v_{\eta\eta} - J^2 D \left[\frac{\partial}{\partial u} \frac{-g_{12}^{ru}}{D} + \frac{\partial}{\partial v} \frac{g_{11}^{ru}}{D} \right] = 0 \ , \end{aligned} \tag{6.4}$$

where

$$D = \sqrt{g_{11}^{ru} g_{22}^{ru} - (g_{12}^{ru})^2} \ ,$$

$$J = u_\xi v_\eta - u_\eta v_\xi \ ,$$

$$\alpha = g_{22}^{r\xi} D^2 J^2 = x_\eta^2 + y_\eta^2 + z_\eta^2 + f_\eta^2 \ ,$$

$$\beta = g_{12}^{r\xi} D^2 J^2 = x_\xi x_\eta + y_\xi y_\eta + z_\xi z_\eta + f_\xi f_\eta \ ,$$

$$\gamma = g_{11}^{r\xi} D^2 J^2 = x_\xi^2 + y_\xi^2 + z_\xi^2 + f_\xi^2 \ .$$

6.1.2 Numerical implementation

The algorithm similar to the method used for planar harmonic grid generation is applied for numerical solution of (6.4), where x and y are replaced by u and v, and $[L(u)]_{ij}$ and $[L(v)]_{ij}$ are the approximations of the equations (6.4) at the grid node (i, j).

All derivatives with respect to u and v are computed via the formulas

$$[f_u]_{ij} = \frac{(f_{i+1,j} - f_{i-1,j})(v_{i,j+1} - v_{i,j-1}) - (f_{i,j+1} - f_{i,j-1})(v_{i+1,j} - v_{i-1,j})}{(u_{i+1,j} - u_{i-1,j})(v_{i,j+1} - v_{i,j-1}) - (u_{i,j+1} - u_{i,j-1})(v_{i+1,j} - v_{i-1,j})} \ ,$$

$$[f_v]_{ij} = \frac{(f_{i+1,j} - f_{i-1,j})(u_{i,j+1} - u_{i,j-1}) - (f_{i,j+1} - f_{i,j-1})(u_{i+1,j} - u_{i-1,j})}{(u_{i+1,j} - u_{i-1,j})(v_{i,j+1} - v_{i,j-1}) - (u_{i,j+1} - u_{i,j-1})(v_{i+1,j} - v_{i-1,j})} \ .$$

The adaptive-harmonic surface grid generation algorithm is formulated as follows:

1. Generate a quasi-uniform harmonic surface grid using the same algorithm as for adaption, but with f=0.

2. Compute the values of the control function at each grid node. The result is f_{ij}.

3. Evaluate derivatives $(f_u)_{ij}$ and $(f_v)_{ij}$ and other expressions in (6.4) using the above formulas.

4. Make one iteration step and compute new values of u_{ij} and v_{ij}.

5. Repeat starting with Step 2 to convergency.

The resulting algorithm is simple in implementation but can demand a special procedure for the choice of the parameter τ to achieve the numerical stability.

6.2 Variational barrier method

6.2.1 Problem formulation

We introduce the following notations

$$r = (r^1, r^2, r^3, r^4, \ldots, r^{3+p}) = (x, y, z, f_1, \ldots, f_p) \in S^{r2} \subset \mathcal{R}^{3+p},$$

$$u = (u^1, u^2) = (u, v) \in Q^2 \subset \mathcal{R}^2,$$

$$\xi = (\xi^1, \xi^2) = (\xi, \eta) \in Q^2 \subset \mathcal{R}^2.$$

$$r_\xi = (x_\xi, y_\xi, z_\xi, f_{1,\xi}, \ldots, f_{p,\xi}) \ , \quad r_\eta = (x_\eta, y_\eta, z_\eta, f_{1,\eta}, \ldots, f_{p,\eta} \ ,$$

$$r_u = (x_u, y_u, z_u, f_{1,u}, \ldots, f_{p,u}) \ , \quad r_v = (x_v, y_v, z_v, f_{1,v}, \ldots, f_{p,v}) \ .$$

Thus, consider a two-dimensional surface in a $(3+p)$-dimensional space, defined as $x{=}x(u,v)$, $y{=}y(u,v)$, $z{=}z(u,v)$, $f_1{=}f_1(u,v)$,. . . ,$f_p{=}f_p(u,v)$. Let the functions $\xi{=}\xi(u,v)$, $\eta{=}\eta(u,v)$ be used to define a new parametrization of a surface.

Harmonic mapping of a surface onto a parametric square can be defined with the use of the first differential Beltrami's parameter

$$(\nabla_s \xi \nabla_s \eta) = \frac{g_{11}^{ru} \xi_v \eta_v - g_{12}^{ru}(\xi_u \eta_v + \xi_v \eta_u) + g_{22}^{ru} \xi_u \eta_u}{g_{11}^{ru} g_{22}^{ru} - (g_{12}^{ru})^2} \ ,$$

Then the harmonic functional can be written in the form

$$I = \int [(\nabla_s \xi \nabla_s \xi) + (\nabla_s \eta \nabla_s \eta)] dS^{r2} \ , \tag{6.5}$$

where dS^{r2} is the element of a surface S^{r2}.

The problem of construction the quasiuniform harmonic grid on the surface of control vector-function is stated as the problem of finding a new parametrization of a surface $u{=}u(\xi,\eta)$, $v{=}v(\xi,\eta)$, minimizing the functional (6.5).

Inverting dependent and independent variables in (6.5), we have

$$I = \int \frac{g_{11}^{ru}(u_\xi^2 + u_\eta^2) + 2 g_{12}^{ru}(u_\xi v_\xi + u_\eta v_\eta) + g_{22}^{ru}(v_\xi^2 + v_\eta^2)}{\sqrt{g_{11}^{ru} g_{22}^{ru} - (g_{12}^{ru})^2}(u_\xi v_\eta - u_\eta v_\xi)} d\xi d\eta \ . \tag{6.6}$$

To construct an adaptive grid on a surface $x{=}x(u,v)$, $y{=}y(u,v)$, $z{=}z(u,v)$, a control vector-function with components $f_1{=}f_1(u,v),\ldots,$

$f_p{=}f_p(u,v)$ is introduced which will define clustering in the regions where its gradient is large. In this case the functional (6.6) is to be minimized with the metric tensor elements g_{ij}^{ru} defined as follows

$$g_{11}^{ru} = x_u^2 + y_u^2 + z_u^2 + f_{1,u}^2 + \cdots + f_{p,u}^2) \ ,$$
$$g_{12}^{ru} = x_u x_v + y_u y_v + z_u z_v + f_{1,u} f_{1,v} + \cdots + f_{p,u} f_{p,v} \ , \qquad (6.7)$$
$$g_{22}^{ru} = x_v^2 + y_v^2 + z_v^2 + f_{1,v}^2 + \cdots + f_{p,v}^2) \ .$$

The problem of irregular surface mesh smoothing and adaption is formulated as follows. Let the coordinates of the irregular mesh in the plane (u,v) be given

$$(u,v)_n, \ n = 1, \ldots, N_n \ .$$

The mesh is formed by quadrilateral elements,i.e., the array $n(N,k)$ is also defined. The functions $x{=}x(u,v)$, $y{=}y(u,v)$, $z{=}z(u,v)$, $f_1{=}f_1(u,v)$, $\ldots, f_p{=}f_p(u,v)$ are assumed to be known. For example, they can be computed by analytic formulas.

The problem is to find new coordinates of the mesh nodes, minimizing the sum of the functional (6.6) values, computed for a mapping of the unit square in the plane (ξ,η) onto each a cell of the mesh in the plane (x,y).

6.2.2 Approximation of functional

The functional (6.6) possesses all the properties of the functional used for adaptive-harmonic grid generation and also can be approximated in such a way that the minimum of its discrete analog is attained on a non-degenerate grid of convex quadrilaterals in the plane (u,v). The same algorithm can be used for its approximation and minimization

$$I^h = \sum_{N=1}^{N_e} \sum_{k=1}^{4} \frac{1}{4} \left[F_k\right]_N \ , \qquad (6.8)$$

where

$$F_k = \frac{D_1 g_{11}^{ru} + D_2 g_{22}^{ru} + 2 D_3 g_{12}^{ru}}{J_k \sqrt{g_{11}^{ru} g_{22}^{ru} - (g_{12}^{ru})^2}} \ ,$$
$$D_1 = (u_{k-1} - u_k)^2 + (u_{k+1} - u_k)^2 \ , \quad D_2 = (v_{k-1} - v_k)^2 + (v_{k+1} - v_k)^2,$$
$$D_3 = (u_{k-1} - u_k)(v_{k-1} - v_k) + (u_{k+1} - u_k)(v_{k+1} - v_k) \ ,$$

$$J_k = (u_{k-1} - u_k)(v_{k+1} - v_k) - (u_{k+1} - u_k)(v_{k-1} - v_k) \ .$$

Here the values g_{ij}^{ru} are computed at the kth node of the Nth cell. Note that to control the mesh nodes number in the layers of high gradient it is convenient to use $c_i f_i$ instead of $f_i(u, v)$, where c_i is the coefficient of adaptation for the ith component. The larger the coefficient c_i, the greater the number of nodes in the layer of high gradients of the function f_i.

If the set of convex meshes D is not empty, the system of the algebraic equations

$$R_u = \frac{\partial I^h}{\partial u_n} = 0 \ , \quad R_v = \frac{\partial I^h}{\partial v_n} = 0$$

has at least one solution which is a convex mesh. To find it, first one must find a certain initial convex mesh, and then use some method of unconstrained minimization of the function I^h. Since this function has the infinite barrier on the boundary of the set of convex meshes, each step of the method can be chosen so that the mesh always remains convex.

6.2.3 Minimization of functional

Suppose the mesh at the lth step of the iterations is determined. We use the quasi-Newtonian procedure when the $(l+1)$th step is accomplished by solving two linear equations for each interior node

$$\tau R_u + \frac{\partial R_u}{\partial u_n}(u_n^{l+1} - u_n^l) + \frac{\partial R_u}{\partial v_n}(v_n^{l+1} - v_n^l) = 0 \ ,$$

$$\tau R_v + \frac{\partial R_v}{\partial u_n}(u_n^{l+1} - u_n^l) + \frac{\partial R_v}{\partial v_n}(v_n^{l+1} - v_n^l) = 0 \ .$$

From this it follows

$$u_n^{l+1} = u_n^l - \tau \left(R_u \frac{\partial R_v}{\partial v_n} - R_v \frac{\partial R_u}{\partial v_n} \right) \left(\frac{\partial R_u}{\partial u_n}\frac{\partial R_v}{\partial v_n} - \frac{\partial R_v}{\partial u_n}\frac{\partial R_u}{\partial v_n} \right)^{-1} ,$$

$$v_n^{l+1} = v_n^l - \tau \left(R_v \frac{\partial R_u}{\partial u_n} - R_u \frac{\partial R_v}{\partial u_n} \right) \left(\frac{\partial R_u}{\partial u_n}\frac{\partial R_v}{\partial v_n} - \frac{\partial R_v}{\partial u_n}\frac{\partial R_u}{\partial v_n} \right)^{-1} , \quad (6.9)$$

where τ is the iteration parameter, which is chosen so that the mesh remains convex. With this purpose after each step the conditions of convexity are checked and, if they are not satisfied, this parameter is multiplied by 0.5.

The adaptive-harmonic algorithm for the mesh relaxation on a surface is formulated as follows:

1. Generate an initial mesh using a marching method.
2. Compute new values x_n, y_n, z_n, and $(f_i)_n$ at each mesh node.
3. Evaluate derivatives $[x_u]_n$ and $[x_v]_n$, $[y_u]_n$ and $[y_v]_n$, $[z_u]_n$ and $[z_v]_n$, $[(f_{i,u}]_n$ and $[(f_{i,v}]_n$ used in (6.9).
4. Make one iteration step (6.9) and compute new values of u_n and v_n.
5. Repeat starting with Step 2 to convergency.

Computational formulas for $[(f_{i,u}]_n$ and $[(f_{i,v}]_n$ will be presented below.

6.2.4 Derivation of computational formulas

Note, that the approximation (6.8) of the functional (6.6) can be obtained also as follows. The square cell in the plane (ξ, η) is divided into two triangles, first by the diagonal 13, and then by 24. The mapping of the square onto a quadrilateral cell in the plane (u, v) is approximated by a function which is linear in each triangle. Denote these functions as $u^h(\xi, \eta)$, $v^h(\xi, \eta)$. All derivatives in the integrand of (6.6) is easy to compute as it was done in the planar case. Then the integral (6.6) over the square cell in the plane (ξ, η) is approximated by a half of the sum of this integral values, computed for piecewise-linear approximation on the triangles, obtained for the first and the second splitting. The result is the approximation (6.8).

Four triangles, introduced above, are considered to the quadrilateral cell with number N. Each of this triangles corresponds to a corner with number k and gives a proper contribution to the functional and also to the value of its derivatives. Since the integrand in (6.6) does not depend on the rotation of the coordinate system ξ,η, then all the computational formulas will be the same for all triangles. We enumerate the triangle nodes corresponding to the corner with local number k from 1 to 3 as follows:
node 1 corresponds to local node number $k-1$ of the Nth cell,
node 2 corresponds to local node number k of the Nth cell,
node 3 corresponds to local node number $k+1$ of the Nth cell.

Then in new numeration the expression for F_k will be

$$F = \frac{D_1 g_{11}^{ru} + D_2 g_{22}^{ru} + 2D_3 g_{11}^{ru}}{J_k \sqrt{g_{11}^{ru} g_{22}^{ru} - (g_{12}^{ru})^2}} \ ,$$

$$D_1 = (u_1 - u_2)^2 + (u_3 - u_2)^2 \ , \quad D_2 = (v_1 - v_2)^2 + (v_3 - v_3)^2,$$

$$D_3 = (u_1 - u_2)(v_1 - v_2) + (u_3 - u_2)(v_3 - v_2) \ ,$$

$$J_k = (u_1 - u_2)(v_3 - v_2) - (u_3 - u_2)(v_1 - v_2) \ .$$

We introduce notations

$$U = \frac{D_1 g_{11}^{ru} + D_2 g_{22}^{ru} + 2D_3 g_{11}^{ru}}{\sqrt{g_{11}^{ru} g_{22}^{ru} - (g_{12}^{ru})^2}} \ ,$$

$$V = (u_1 - u_2)(v_3 - v_2) - (u_3 - u_2)(v_1 - v_2) \ .$$

For vertex 1 we have

$$V_u = v_3 - v_2 \ , \quad V_v = u_2 - u_3 \ ,$$

$$U_u = 2\frac{g_{11}^{ru}(u_1 - u_2) + g_{12}^{ru}(v_1 - v_2)}{\sqrt{g_{11}^{ru} g_{22}^{ru} - (g_{12}^{ru})^2}}, \ U_v = 2\frac{g_{11}^{ru}(v_1 - v_2) + g_{12}^{ru}(u_1 - u_2)}{\sqrt{g_{11}^{ru} g_{22}^{ru} - (g_{12}^{ru})^2}},$$

$$U_{uu} = 2\frac{g_{11}^{ru}}{\sqrt{g_{11}^{ru} g_{22}^{ru} - (g_{12}^{ru})^2}} \ , \quad U_{uv} = 2\frac{g_{12}^{ru}}{\sqrt{g_{11}^{ru} g_{22}^{ru} - (g_{12}^{ru})^2}} \ ,$$

$$U_{vv} = 2\frac{g_{22}^{ru}}{\sqrt{g_{11}^{ru} g_{22}^{ru} - (g_{12}^{ru})^2}} \ ,$$

$$V_{uv} = 0 \ , \quad V_{uv} = 0 \ , \quad V_{uv} = 0 \ .$$

For vertex 2 we have

$$V_u = v_1 - v_3 \ , \quad V_v = u_3 - u_1 \ ,$$

$$U_u = 2\frac{g_{11}^{ru}(2u_2 - u_1 - u_3) + g_{12}^{ru}(2v_2 - v_1 - v_3)}{\sqrt{g_{11}^{ru} g_{22}^{ru} - (g_{12}^{ru})^2}} \ ,$$

$$U_v = 2\frac{g_{22}^{ru}(2v_2 - v_1 - v_3) + g_{12}^{ru}(2u_2 - u_1 - u_3)}{\sqrt{g_{11}^{ru} g_{22}^{ru} - (g_{12}^{ru})^2}} \ ,$$

$$U_{uu} = 4\frac{g_{11}^{ru}}{\sqrt{g_{11}^{ru} g_{22}^{ru} - (g_{12}^{ru})^2}} \ , \quad U_{uv} = 4\frac{g_{12}^{ru}}{\sqrt{g_{11}^{ru} g_{22}^{ru} - (g_{12}^{ru})^2}} \ ,$$

$$U_{vv} = 4\frac{g_{22}^{ru}}{\sqrt{g_{11}^{ru} g_{22}^{ru} - (g_{12}^{ru})^2}} \ ,$$

$$V_{uu} = 0 \ , \quad V_{uu} = 0 \ , \quad V_{uu} = 0 \ .$$

For vertex 3 we have

$$V_u = v_2 - v_1 \ , \quad V_v = u_1 - u_2 \ ,$$

$$U_u = 2\frac{g_{11}^{ru}(u_3 - u_2) + g_{12}^{ru}(v_3 - v_2)}{\sqrt{g_{11}^{ru} g_{22}^{ru} - (g_{12}^{ru})^2}} \ , \quad U_v = 2\frac{g_{22}^{ru}(v_3 - v_2) + g_{12}^{ru}(u_3 - u_2)}{\sqrt{g_{11}^{ru} g_{22}^{ru} - (g_{12}^{ru})^2}} \ ,$$

$$U_{uu} = 2\frac{g_{11}^{ru}}{\sqrt{g_{11}^{ru} g_{22}^{ru} - (g_{12}^{ru})^2}} \ , \quad U_{uv} = 2\frac{g_{12}^{ru}}{\sqrt{g_{11}^{ru} g_{22}^{ru} - (g_{12}^{ru})^2}} \ ,$$

$$U_{vv} = 2\frac{g_{22}^{ru}}{\sqrt{g_{11}^{ru} g_{22}^{ru} - (g_{12}^{ru})^2}} \ , \quad V_{uv} = 0 \ , \quad V_{uv} = 0 \ , \quad V_{uv} = 0 \ .$$

Computations are performed as follows. Let F and its derivatives on u_1 and v_1 be computed for the Nth cell and kth triangle. Then the computed values are added to the appropriate array elements

$$I^h += F, \quad [R_u]_n += F_u \ , \quad [R_v]_n += F_v \ ,$$

$$[R_{uu}]_n += F_{uu} \ , \quad [R_{uv}]_n += F_{uv} \ , \quad [R_{vv}]_n += F_{vv},$$

where $n{=}n(N, k{-}1)$.

Analogous for vertex 2, correspondence between local and global number is $n{=}n(N, k)$.

Analogous for vertex 3, correspondence between local and global number is $n{=}n(N, k{+}1)$.

The algorithm for evaluating the derivatives $[f_u]_n$ and $[f_v]_n$ is formulated as follows. All triangles of the mesh are scanned and for the kth triangle of the Nth cell the following values are computed

$$fu = (f_1 - f_2)(v_3 - v_2) - (f_3 - f_2)(v_1 - v_2) \ ,$$

$$fv = (u_1 - u_2)(f_3 - f_2) - (u_3 - u_2)(f_1 - f_2) \ ,$$

$$J_2 = (x_1 - x_2)(y_3 - y_2) - (x_3 - x_2)(y_1 - y_2) \ .$$

Where f_1, f_2 and f_3 are the values of the function f at the vertices 1,2, and 3 of the triangle corresponding to local numbers $k{-}1$, k, $k{+}1$ of the corners in the quadrilateral cell. Computed values are added to the corresponding array elements (which were first cleared)

$$[f_u]_n += fu, \quad [f_v]_n += fv, \quad [J]_n += J_2, \quad n = n(N, k).$$

New values of the derivatives are computed as follows

$$[f_u]_n/ = [J]_n, \quad [f_v]_n/ = [J]_n.$$

Here, $a/=b$ means that the new value of a becomes equal to a/b.

The derivatives $[x_u]_n$ and $[x_v]_n$, $[y_u]_n$ and $[y_v]_n$, $[z_u]_n$ and $[z_v]_n$ are computed in a similar manner.

Thus, the iteration method for irregular surface mesh relaxation and adaptation is described in detail.

6.3 Adaptation to curvature of surface

Consider a two-dimensional surface in the 6-dimensional space

$$r(u,v) = (r^1, r^2, r^3, r^4, r^5, r^6)(u,v) = (x, y, z, n_x, n_y, n_z)(u,v) \in S^{r2} \subset R^6,$$

where n_x, n_y, n_z are the component of the unit normal to the surface S^{r2}, computed by formulas

$$n_x = \frac{y_u z_v - z_u y_v}{\sqrt{(y_u z_v - z_u y_v)^2 + (x_u z_v - z_u x_v)^2 + (x_u y_v - y_u x_v)^2}} \ ,$$

$$n_y = -\frac{x_u z_v - z_u x_v}{\sqrt{(y_u z_v - z_u y_v)^2 + (x_u z_v - z_u x_v)^2 + (x_u y_v - y_u x_v)^2}} \ ,$$

$$n_z = \frac{x_u y_v - y_u x_v}{\sqrt{(y_u z_v - z_u y_v)^2 + (x_u z_v - z_u x_v)^2 + (x_u y_v - y_u x_v)^2}} \ .$$

The elements of the metric tensor g_{ij}^{ru} are

$$g_{11}^{ru} = x_u^2 + y_u^2 + z_u^2 + n_{x,u}^2 + n_{y,u}^2 + n_{z,u}^2 \ ,$$

$$g_{12}^{ru} = x_u x_v + y_u y_v + z_u z_v + n_{x,u} n_{x,v} + n_{y,u} n_{y,v} + n_{z,u} n_{z,v} \ ,$$

$$g_{22}^{ru} = x_v^2 + y_v^2 + z_v^2 + n_{x,v}^2 + n_{y,v}^2 + n_{z,v}^2 \ .$$

One-dimensional case is

$$r(s) = (r^1, r^2, r^3, r^4)(s) = (x, y, n_x, n_y)(s) \in S^{r1} \subset R^4,$$

where s is the length of the flat curve, i.e $x_s^2 + y_s^2 = 1$. Components of the unit normal are computed as

$$n_x = -y_s, \qquad n_y = x_s.$$

The harmonic functional takes the form

$$\int \frac{d\xi}{s_\xi |r_s|} \ ,$$

where $r_s = x_s^2 + y_s^2 + x_{ss}^2 + y_{ss}^2$. The Euler equation for the functional is

$$s_\xi \sqrt{x_s^2 + y_s^2 + x_{ss}^2 + y_{ss}^2} = const.$$

From this it follows that if $x_{ss}^2 + y_{ss}^2 \gg x_s^2 + y_s^2$, then $s_\xi K = const$, where K is the curvature of the flat curve, equal to $K = \sqrt{x_{ss}^2 + y_{ss}^2}$.

On the other hand, it is the asymptotic condition on a grid, being optimal in the norm C^1. Consider the element of the curve which can be approximated by the arc of the circle of the radius $R{=}1/K$. Let the grid size along the curve will be equal to h. Then, to obtain the error in the norm C^1 on the small part of the curve, corresponding to the small angle $\alpha{=}h/R$, it is necessary to find the difference between the length of the arc and length of the line segment connecting its ends. From the equidistribution principle we obtain that this value is the constant along the curve

$$\frac{\alpha R - \sin \alpha R}{\alpha R} = const.$$

From this it follows that

$$\alpha = h/R = s_\xi K = const.$$

6.4 Example of nonuniqueness in grid generation on surface

Consider the flat curve $x{=}x(s)$, $y{=}y(s)$, $0{\le}s{\le}L$, where s is the curve length.

The harmonic functional is

$$\int s_\xi^2 d\xi \ , \quad \text{where} \ \ s_\xi = x_\xi^2 + y_\xi^2 \ .$$

The functional for the mapping, inverse to harmonic, is

$$\int s_\xi^{-2} du = \int s_\xi^{-1} d\xi \ .$$

The Euler equations are the same

$$s_\xi = const \ .$$

The example of nonuniqueness is drawn in [135]. Let the curve

$$(x-0.5)^2 + y^2 = 0.25 \ , \quad y = \sqrt{x(1-x)} \ , \quad 0 \le x \le 1 \ ,$$

be given. Consider the one-point grid generation problem

$$(x_2 - x_1)^2 + (y_2 - y_1)^2 + (x_2 - x_3)^2 + (y_2 - y_3)^2 \to \min \ .$$

In our example $x_1{=}y_1{=}y_3{=}0$, $x_3{=}1$. Introduce notation $x_2{=}x$ and substitute $y{=}\sqrt{x(x-1)}$ instead of y_2. We have

$$x^2 + (1-x)^2 + 2x(1-x) = 1.$$

Consequently, this problem has infinitely many solutions. If we use the functional

$$\int s_\xi^{-1} d\xi \ ,$$

the approximation takes the form

$$x^{-1/2} + (1-x)^{-1/2}.$$

After minimization we obtain the unique solution

$$x = \frac{1}{2} \ .$$

Chapter 7

Adaptive-harmonic three-dimensional grid generation

7.1 Three-dimensional regular grids

In the 3D case for constructing a harmonic grid the system of equations, defining a harmonic mapping of the domain Ω onto a parametric cube, is considered

$$\xi_{xx} + \xi_{yy} + \xi_{zz} = 0 \ , \quad \eta_{xx} + \eta_{yy} + \eta_{zz} = 0 \ , \quad \mu_{xx} + \mu_{yy} + \mu_{zz} = 0 \ . \quad (7.1)$$

These equations are usually inverted to the equations for the functions $x{=}x(\xi,\eta,\mu)$, $y{=}y(\xi,\eta,\mu)$, $z{=}z(\xi,\eta,\mu)$ which define one-to-one mapping of the parametric cube onto the domain Ω. Instead of the Laplace equations the Poisson equations have been also considered

$$\xi_{xx} + \xi_{yy} + \xi_{zz} = P_1 \ , \quad \eta_{xx} + \eta_{yy} + \eta_{zz} = P_2 \ , \quad \mu_{xx} + \mu_{yy} + \mu_{zz} = P_3 \ ,$$

and adaptation is achieved by a proper choice of functions P_1, P_2 and P_3.

7.1.1 Derivation of equations

We will derive equations for the case of adaptation. Introduce notations

$$r = (r^1, r^2, r^3, r^4) = (x, y, z, f) \in S^{r3} \subset \mathcal{R}^4,$$

$$u = (u^1, u^2, u^3) = (x, y, z) \in \Omega \subset \mathcal{R}^3,$$
$$\xi = (\xi^1, \xi^2, \xi^3) = (\xi, \eta, \mu) \in Q^3 \subset \mathcal{R}^3.$$
$$r_\xi = (x_\xi, y_\xi, z_\xi, f_\xi),$$
$$r_\eta = (x_\eta, y_\eta, z_\eta, f_\eta),$$
$$r_\mu = (x_\mu, y_\mu, z_\mu, f_\mu),$$
$$r_x = (1, 0, 0, f_x),\ r_y = (0, 1, 0, f_y),\ r_z = (0, 0, 1, f_z).$$

The general harmonic functional in the 3D case has the form

$$I = \int \left(g^{11}_{\xi r} + g^{22}_{\xi r} + g^{33}_{\xi r}\right) dS^{r3},$$

where dS^{r3} is the element of the surface S^{r3}.

Let the adapted/control function $f(x, y, z)$ defines a three-dimensional surface in four-dimensional space. Then this functional can be written as follows

$$I = \int \frac{g^{r\xi}_{11} g^{r\xi}_{22} - (g^{r\xi}_{12})^2 + g^{r\xi}_{11} g^{r\xi}_{33} - (g^{r\xi}_{13})^2 + g^{r\xi}_{22} g^{r\xi}_{33} - (g^{r\xi}_{23})^2}{\sqrt{g^{r\xi}_{11}[g^{r\xi}_{22} g^{r\xi}_{33} - (g^{r\xi}_{23})^2] - g^{r\xi}_{12}(g^{r\xi}_{12} g^{r\xi}_{33} - g^{r\xi}_{13} g^{r\xi}_{23}) + g^{r\xi}_{13}(g^{r\xi}_{12} g^{r\xi}_{23} - g^{r\xi}_{22} g^{r\xi}_{13})}} d\xi d\eta d\mu, \tag{7.2}$$

where

$$g^{r\xi}_{11} = r^2_\xi,\ g^{r\xi}_{22} = r^2_\eta\ ,\quad g^{r\xi}_{33} = r^2_\mu\ ,\quad g^{r\xi}_{12} = g^{r\xi}_{21} = (r_\xi \cdot r_\eta)\ ,$$

$$g^{r\xi}_{13} = g^{r\xi}_{31} = (r_\xi \cdot r_\mu)\ ,\quad g^{r\xi}_{23} = g^{r\xi}_{32} = (r_\eta \cdot r_\mu)\ ,$$

here

$$f_\xi = f_x x_\xi + f_y y_\xi + f_z z_\xi,\ f_\eta = f_x x_\eta + f_y y_\eta + f_z z_\eta,\ f_\mu = f_x x_\mu + f_y y_\mu + f_z z_\mu\ .$$

The functional (7.2) can be used for harmonic coordinate generation on the surface of the graph of the control function $f(x, y, z)$ dependent on three variables. Projection of these coordinates onto the physical domain gives an adaptive-harmonic grid, clustered in the regions of high gradients of the control function $f(x, y, z)$.

The Euler equations of the functional (7.2) follow from the general equations for n=3, k=1. We need only to compute the elements of the covariant metric tensor G^{ru} and contravariant tensor G_{ur} of the transformation $r(u)$=$r(x,y,z)$:$\Omega \to S^{r3}$

$$g_{11}^{ru} = r_x^2 = 1 + f_x^2,$$

$$g_{22}^{ru} = r_y^2 = 1 + f_y^2,$$

$$g_{33}^{ru} = r_z^2 = 1 + f_z^2,$$

$$g_{12}^{ru} = g_{21}^{ru} = r_x \cdot r_y = f_x f_y,$$

$$g_{13}^{ru} = g_{31}^{ru} = r_x \cdot r_z = f_x f_z,$$

$$g_{23}^{ru} = g_{32}^{ru} = r_y \cdot r_z = f_y f_z,$$

$$\det(G^{ru}) = g_{11}^{ru}[g_{22}^{ru}g_{33}^{ru} - (g_{23}^{ru})^2)] - g_{12}^{ru}(g_{12}^{ru}g_{33}^{ru} - g_{13}^{ru}g_{23}^{ru}) + g_{13}^{ru}(g_{12}^{ru}g_{23}^{ru} - g_{22}^{ru}g_{13}^{ru}) =$$

$$(1 + f_x^2)(1 + f_y^2 + f_z^2) - f_x^2 f_y^2 - f_x^2 f_z^2 = 1 + f_x^2 + f_y^2 + f_z^2,$$

$$\det(G^{r\xi}) = g_{11}^{r\xi}[g_{22}^{r\xi}g_{33}^{r\xi} - (g_{23}^{r\xi})^2] - g_{12}^{r\xi}(g_{12}^{r\xi}g_{33}^{r\xi} - g_{13}^{r\xi}g_{23}^{r\xi}) + g_{13}^{r\xi}(g_{12}^{r\xi}g_{23}^{r\xi} - g_{22}^{r\xi}g_{13}^{r\xi}) =$$

$$\det(G^{ru})[x_\xi(y_\eta z_\mu - y_\mu z_\eta) - y_\xi(x_\eta z_\mu - x_\mu z_\eta) + z_\xi(x_\xi y_\eta - x_\eta y_\xi)],$$

$$g_{\xi r}^{11} = [g_{22}^{r\xi}g_{33}^{r\xi} - (g_{23}^{r\xi})^2]/\det(G^{r\xi}),$$

$$g_{\xi r}^{12} = -(g_{12}^{r\xi}g_{33}^{r\xi} - g_{13}^{r\xi}g_{23}^{r\xi})/\det(G^{r\xi}),$$

$$g_{\xi r}^{13} = (g_{12}^{r\xi}g_{23}^{r\xi} - g_{13}^{r\xi}g_{22}^{r\xi})/\det(G^{r\xi}),$$

$$g_{\xi r}^{22} = [g_{11}^{r\xi}g_{33}^{r\xi} - (g_{12}^{r\xi})^2]/\det(G^{r\xi}),$$

$$g_{\xi r}^{23} = -(g_{11}^{r\xi}g_{23}^{r\xi} - g_{13}^{r\xi}g_{12}^{r\xi})/\det(G^{r\xi}),$$

$$g_{\xi r}^{33} = [g_{11}^{r\xi}g_{22}^{r\xi} - (g_{12}^{r\xi})^2]/\det(G^{r\xi}),$$

$$g_{ur}^{11} = (1 + f_y^2 + f_z^2)/(1 + f_x^2 + f_y^2 + f_z^2),$$

$$g_{ur}^{12} = -f_x f_y/(1 + f_x^2 + f_y^2 + f_z^2),$$

$$g_{ur}^{13} = -f_x f_z/(1 + f_x^2 + f_y^2 + f_z^2),$$

$$g_{ur}^{22} = (1 + f_x^2 + f_z^2)/(1 + f_x^2 + f_y^2 + f_z^2),$$

$$g_{ur}^{23} = -f_y f_z/(1 + f_x^2 + f_y^2 + f_z^2),$$

$$g^{33}_{ur} = (1 + f_x^2 + f_y^2)/(1 + f_x^2 + f_y^2 + f_z^2).$$

Substituting these expressions into the general equations, we obtain

$$L(x) = g^{11}_{\xi r} x_{\xi\xi} + 2g^{12}_{\xi r} x_{\xi\eta} + 2g^{13}_{\xi r} x_{\xi\mu} + g^{22}_{\xi r} x_{\eta\eta} + 2g^{23}_{\xi r} x_{\eta\mu} + g^{33}_{\xi r} x_{\mu\mu} -$$
$$\frac{1}{D}\left[\frac{\partial}{\partial x}\frac{1 + f_y^2 + f_z^2}{D} + \frac{\partial}{\partial y}\frac{-f_x f_y}{D} + \frac{\partial}{\partial z}\frac{-f_x f_z}{D}\right] = 0,$$
$$L(y) = g^{11}_{\xi r} y_{\xi\xi} + 2g^{12}_{\xi r} y_{\xi\eta} + 2g^{13}_{\xi r} y_{\xi\mu} + g^{22}_{\xi r} y_{\eta\eta} + 2g^{23}_{\xi r} y_{\eta\mu} + g^{33}_{\xi r} y_{\mu\mu} -$$
$$\frac{1}{D}\left[\frac{\partial}{\partial x}\frac{-f_x f_y}{D} + \frac{\partial}{\partial y}\frac{1 + f_x^2 + f_z^2}{D} + \frac{\partial}{\partial z}\frac{-f_y f_z}{D}\right] = 0, \qquad (7.3)$$
$$L(z) = g^{11}_{\xi r} z_{\xi\xi} + 2g^{12}_{\xi r} z_{\xi\eta} + 2g^{13}_{\xi r} z_{\xi\mu} + g^{22}_{\xi r} z_{\eta\eta} + 2g^{23}_{\xi r} z_{\eta\mu} + g^{33}_{\xi r} z_{\mu\mu} -$$
$$\frac{1}{D}\left[\frac{\partial}{\partial x}\frac{-f_x f_z}{D} + \frac{\partial}{\partial y}\frac{-f_y f_z}{D} + \frac{\partial}{\partial z}\frac{1 + f_x^2 + f_y^2}{D}\right] = 0\ ,$$

where

$$D = \sqrt{1 + f_x^2 + f_y^2 + f_z^2}\ .$$

7.1.2 Numerical implementation

The problem of grid generation in three dimensions will be considered in the following formulation. In a simply connected domain Ω in space x, y, z, a grid

$$(x, y, z)_{ijm},\ i = 1, \ldots, i^*;\ j = 1, \ldots, j^*\ , m = 1, \ldots, m^*,$$

must be constructed with given coordinates of the boundary nodes

$$(x, y, z)_{ij1},\ (x, y, z)_{ijm^*},\ (x, y, z)_{i1m},\ (x, y, z)_{ij^*m},\ (x, y, z)_{1jm},\ (x, y, z)_{i^*jm}.$$

Instead of the parametric cube the following parametric domain can be introduced to simplify the computational formulas

$$1 < \xi < i^*,\ 1 < \eta < j^*,\ 1 < \mu < m^*,$$

associated with the cube grid (ξ_i, η_j, μ_m) such that

$$\xi_i = i,\ \eta_j = j\ , \mu_m = m,\ i = 1, \ldots, i^*;\ j = 1, \ldots, j^*;\ m = 1, \ldots, m^*.$$

Equations (7.3) are approximated on this grid with the use of a simplest finite-difference relations for derivatives with respect to ξ, η, μ. For example, derivatives of $f(\xi, \eta, \mu)$ are approximated as follows

$$f_\xi \approx [f_\xi]_{ijm} = \frac{1}{2}(f_{i+1,j,m} - f_{i-1,j,m}),$$

$$f_\eta \approx [f_\eta]_{ijm} = \frac{1}{2}(f_{i,j+1,m} - f_{i,j-1,m}),$$

$$f_\mu \approx [f_\mu]_{ijm} = \frac{1}{2}(f_{i,j,m+1} - f_{i,j,m-1}),$$

$$f_{\xi\xi} \approx [f_{\xi\xi}]_{ijm} = f_{i+1,j,m} - 2f_{ijm} + f_{i-1,j,m},$$

$$f_{\xi\eta} \approx [f_{\xi\eta}]_{ijm} = \frac{1}{4}(f_{i+1,j+1,m} - f_{i+1,j-1,m} - f_{i+1,j-1,m} + f_{i-1,j-1,m}),$$

$$f_{\xi\mu} \approx [f_{\xi\mu}]_{ijm} = \frac{1}{4}(f_{i+1,j,m+1} - f_{i+1,j,m-1} - f_{i-1,j,m+1} + f_{i-1,j,m-1}),$$

$$f_{\eta\eta} \approx [f_{\eta\eta}]_{ijm} = f_{i,j+1,m} - 2f_{ijm} + f_{i,j-1,m},$$

$$f_{\eta\mu} \approx [f_{\eta\mu}]_{ijm} = \frac{1}{4}(f_{i,j+1,m+1} - f_{i,j+1,m-1} - f_{i,j-1,m+1} + f_{i,j-1,m-1}),$$

$$f_{\mu\mu} \approx [f_{\mu\mu}]_{ijm} = f_{i,j,m+1} - 2f_{ijm} + f_{i,j,m-1}.$$

The explicit method is used to numerical solution of the resulting difference equations

$$x_{ijm}^{l+1} = x_{ijm}^{l} + \tau \frac{[L(x)]_{ijm}}{2[g_{\xi r}^{11}]_{ijm} + 2[g_{\xi r}^{22}]_{ijm} + 2[g_{\xi r}^{33}]_{ijm}} ,$$

$$y_{ijm}^{l+1} = y_{ijm}^{l} + \tau \frac{[L(y)]_{ijm}}{2[g_{\xi r}^{11}]_{ijm} + 2[g_{\xi r}^{22}]_{ijm} + 2[g_{\xi r}^{33}]_{ijm}} , \qquad (7.4)$$

$$z_{ijm}^{l+1} = z_{ijm}^{l} + \tau \frac{[L(z)]_{ijm}}{2[g_{\xi r}^{11}]_{ijm} + 2[g_{\xi r}^{22}]_{ijm} + 2[g_{\xi r}^{33}]_{ijm}} .$$

Consider the formulas for the derivatives transformation in the 3D case

$$x_\xi f_x + y_\xi f_y + z_\xi f_z = f_\xi ,$$

$$x_\eta f_x + y_\eta f_y + z_\eta f_z = f_\eta ,$$

$$x_\mu f_x + y_\mu f_y + z_\mu f_z = f_\mu \ ,$$

from this it follows

$$f_x = f_\xi(y_\eta z_\mu - y_\mu z_\eta)/J - f_\eta(y_\xi z_\mu - y_\mu z_\xi)/J + f_\mu(y_\xi z_\eta - y_\eta z_\mu)/J \ ,$$

$$f_y = -f_\xi(x_\eta z_\mu - x_\mu z_\eta)/J + f_\eta(x_\xi z_\mu - x_\mu z_\xi)/J - f_\mu(x_\xi z_\eta - x_\eta z_\mu)/J \ ,$$

$$f_z = f_\xi(x_\eta y_\mu - x_\mu y_\eta)/J - f_\eta(x_\xi y_\mu - x_\mu y_\xi)/J + f_\mu(x_\xi y_\eta - x_\eta y_\mu)/J \ ,$$

where

$$J = x_\xi(y_\eta z_\mu - y_\mu z_\eta) - x_\eta(y_\xi z_\mu - y_\mu z_\xi) + x_\mu(y_\xi z_\eta - y_\eta z_\mu) \ .$$

Approximating all the derivatives ξ, η, μ in these expressions with the use of the above formulas, we obtain the approximation of the derivatives $[f_x]_{ijm}$, $[f_y]_{ijm}$ and $[f_z]_{ijm}$, used in (7.4).

The adaptive-harmonic grid generation algorithm in three dimensions is formulated as follows:

1. Generate a quasi-uniform harmonic grid using the same algorithm as for adaptation, but with f=0.

2. Compute the values of the control function f_{ijm} at every grid node.

3. Evaluate derivatives $[f_x]_{ijm}$, $[f_y]_{ijm}$, $[f_z]_{ijm}$ and substitute them into (7.4).

4. Make one iteration step and compute new values of x_{ijm}, y_{ijm} , z_{ijm}.

5. Repeat starting with Step 2 to convergence.

The resulting algorithm is simple in implementation and can be used for meshing 3D domains until the increased complexity of domain or boundary layers produce the appearance of self-intersecting cells. Then the special algorithm should be employed, based on a variational formulation and guaranteeing nondegenerate grid generation.

7.2 Variational barrier method in 3D

7.2.1 Discrete analog of Jacobian positiveness

The 3D case is much more complicated then 2D case, because simple conditions of Jacobian positiveness cannot be obtained for the trilinear mapping of the unit cube onto the hexahedral cell, cf. [149]. The notation of convexity also cannot be used, since faces of hexahedron are not plane.

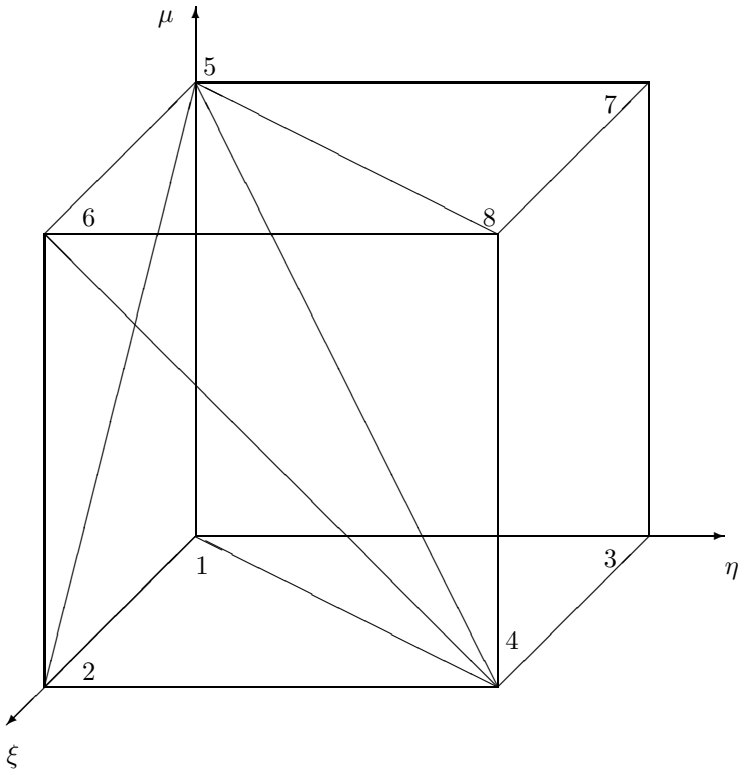

Fig. 7.1: Vertex numeration and decomposition of cube to tetrahedra

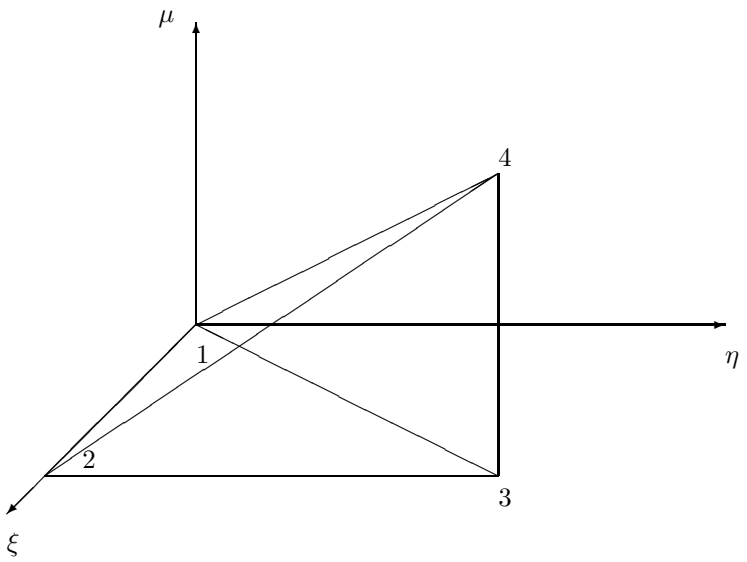

Fig. 7.2: Vertex numeration for basis tetrahedron

That is why the approach developed for the 2D meshes cannot be extended to the 3D case.

Nevertheless, the discrete analog of the Jacobian positiveness for the mapping of the unit cube onto a hexahedral cell can be obtained. We use the decomposition of the parametric cube to tetrahedra, which are mapped onto the corresponding tetrahedra of the decomposed hexahedral cell. The mapping of every tetrahedra is one-to-one. This approach is analogous to the technique used in the 2D case for approximation of the harmonic functional in such a way that it has an infinite barrier at the boundary of the set of unfolded meshes. Remind that in the 2D case the quadrilateral cell is divided into two triangles first by the one diagonal and then by the other. In the first and second decomposition, the mapping is approximated by the functions which are linear in each triangle. All conditions of Jacobian positiveness for every such mapping coincide with the condition providing that all the mesh cells to be convex quadrilaterals.

Consider a unit cube in $\mathcal{R}^3$ space of variables ξ, η, μ shown in Fig.7.1. We decompose it into two prisms by the plane 1584. Then we decompose the prism shown in Fig.7.1 into three tetrahedra drawing the planes through the diagonals 14, 25, 58, 45, 46. Denote T^{ξ}_{5124}, T^{ξ}_{5684}, T^{ξ}_{5624} the obtained tetrahedra. Note that all these tetrahedra are equal to each other (up to rotation and reflection) and one of the cube edges corresponds to one of them. For example, the tetrahedron T^{ξ}_{5124} can be referred to the edge 12. Only one extra tetrahedron is referred to this edge namely T^{ξ}_{3126}. What is the difference between the tetrahedra T^{ξ}_{5124} and T^{ξ}_{3126} ? The answer is that each of them corresponds to a proper type of the coordinate system, right-hand or left-hand. It is easy to compute the total number of such tetrahedra. It is equal to double number of the cube edges, i.e., 24. For the unit cube the volume of one tetrahedron is equal to 1/6, and the total volume of all such tetrahedra is equal to 4.

Consider the basis tetrahedron shown in Fig.7.2. Vertices are enumerated from 1 to 4 as shown in Fig.7.2. Each of this vertex corresponds to a radius-vector r_1, r_2, r_3, r_4, respectively, in space x, y, z. All these vectors define the tetrahedron in space x, y, z. We introduce the basis vectors

$$e_1 = r_2 - r_1, \quad e_2 = r_3 - r_2, \quad e_3 = r_4 - r_3.$$

Note that the coordinate system e_1, e_2, e_3 is a right-hand system what is easy to see from the orientation of the basis tetrahedron in Fig.7.2. Hence, the volume of the "right" tetrahedron is equal to

$$J_{Tright} = (e_1 \times e_2) \cdot e_3$$

At the same time, the volume of the "left" tetrahedron is equal to

$$J_{Tleft} = -(e_1 \times e_2) \cdot e_3$$

Now, by analogy with the 2D case, the condition for the mesh to be nondegenerate for the 3D hexahedral mesh can be expressed as follows

$$[(J_{Tleft})_m]_N > 0, \ [(J_{Tright})_m]_N > 0, \ m = 1, \ldots, 12; \ N = 1, \ldots, N_e, \quad (7.5)$$

where $(J_{Tleft})_m$ is a volume of the tetrahedron corresponding to the edge number m and defining the left-hand coordinate system, $(J_{Tright})_m$ is a volume of the tetrahedron corresponding to the edge number m and defining the right-hand coordinate system (every cube has 12 edges), N is the cell

number, N_e is the total number of cells. Conditions (7.5) define the discrete analog of the Jacobian positiveness in the 3D case. Meshes, satisfying inequalities (7.5), we will call nondegenerate hexahedral meshes.[1]

As in the 2D case, we must introduce the correspondence between local and global node numbers

$$n = n(N,k),\ n = 1,\dots,N_n,\ N = 1,\dots,N_e,\ k = 1,\dots,8\ ,$$

where n is the global node number, N_n is the total number of mesh nodes, N is the element number, N_e is the number of elements, k is the local node number in the element.

Remark. Fig. 7.3 presents the mesh consisting of one degenerated cell with positive volume of the corner tetrahedra. This cell is obtained from the cell, depicted in Fig. 7.1, by rotating top face 5678 through 180 degrees about its center, directed parallel to x_3-axis and passing through the center of this face. One can see that the volume of all the corner tetrahedra are positive (e.g. see the tetrahedron with vertices 1235). Consequently, as a discrete analog of the condition of positiveness to the Jacobian one uses the condition of positiveness to the corner tetrahedra, and then the cases, like depicted in Fig. 7.3, are admitted.

That is why we have to use above described division into 24 tetrahedra and introduce rather a complicated construction of the set of unfolded grids, defined by the inequalities (7.5). It provides the discrete analog of the harmonic functional with an infinite barrier on the boundary of the set of unfolded meshes, see the next subsection for description.

7.2.2 Problem formulation

We use notations

$$r = (r^1, r^2, r^3, r^4) = (x, y, z, f) \in S^{r3} \subset \mathcal{R}^4,$$

$$u = (u^1, u^2, u^3) = (x, y, z) \in \Omega \subset \mathcal{R}^3,$$

$$\xi = (\xi^1, \xi^2, \xi^3) = (\xi, \eta, \mu) \in Q^3 \subset \mathcal{R}^3.$$

[1] In [10], it was suggested another, more effective, approximate conditions of hex cell and mesh nondegeneracy. It implies the use of a set of 10 basis tetrahedra for every hex cell. Comparison of effectiveness of the present nondegeneracy conditions and those of [10] was performed in [151] (Editor).

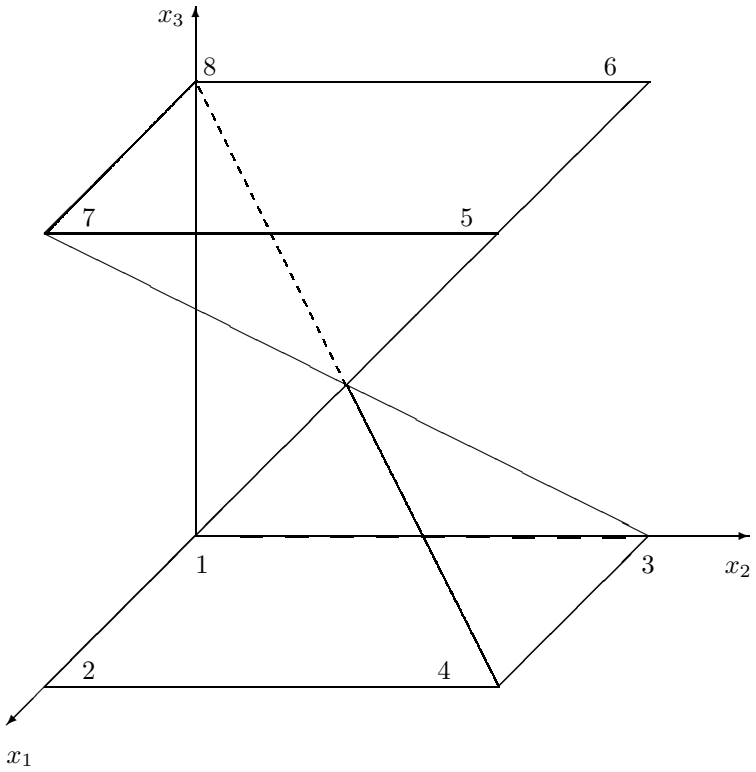

Fig. 7.3: Example of hex cell with positive corner Jacobians and zero Jacobian in the center

$$r_\xi = (x_\xi, y_\xi, z_\xi, f_\xi),$$

$$r_\eta = (x_\eta, y_\eta, z_\eta, f_\eta),$$

$$r_\mu = (x_\mu, y_\mu, z_\mu, f_\mu),$$

$$r_x = (1, 0, 0, f_x),\ r_y = (0, 1, 0, f_y),\ r_z = (0, 0, 1, f_z).$$

The harmonic functional in the 3D case has the form

$$I = \int \left(g^{11}_{\xi r} + g^{22}_{\xi r} + g^{33}_{\xi r}\right) dS^{r3},$$

where dS^{r3} is the element of the surface S^{r3}.

Let the adapted/control function $f(x, y, z)$ defines a three-dimensional surface in four-dimensional space. Then this functional can be written as follows

$$I = \int \frac{g_{11}g_{22} - (g_{12})^2 + g_{11}g_{33} - (g_{13})^2 + g_{22}g_{33} - (g_{23})^2}{\sqrt{g_{11}[g_{22}g_{33} - (g_{23})^2] - g_{12}(g_{12}g_{33} - g_{13}g_{23}) + g_{13}(g_{12}g_{23} - g_{22}g_{13})}} d\xi d\eta d\mu, \tag{7.6}$$

where

$$g_{11} = r_\xi^2,\ g_{22} = r_\eta^2,\ g_{33} = r_\mu^2\ ,\quad g_{12} = g_{21} = (r_\xi \cdot r_\eta)\ ,$$

$$g_{13} = g_{31} = (r_\xi \cdot r_\mu)\ ,\quad g_{23} = g_{32} = (r_\eta \cdot r_\mu)\ .$$

The functional (7.6) can be used for harmonic coordinate generation on the surface of the graph of the control function dependent on three variables. Projection of these coordinates onto the physical domain gives an adaptive-harmonic grid, clustered in regions of high gradients of the adapted function $f(x, y, z)$.

The problem of irregular 3D mesh smoothing and adaption is formulated as follows. Let the coordinates of the irregular mesh in space x, y, z be given

$$(x, y, z)_n,\ n = 1, \ldots, N_n\ , \tag{7.7}$$

The mesh is formed by hexahedral elements, i.e., the correspondence $n{=}n(N, k)$ is also defined. The problem is to find new nodal coordinates, minimizing the sum of the functional (7.6) values, computed for a mapping of the unit cube onto every cell of the mesh.

7.2.3 Approximation of the functional

First consider the case when $f(x,y,z)$=0. The functional (7.6) in this case can be written in a more simple form

$$I = \int \frac{(r_\xi \times r_\eta)^2 + (r_\xi \times r_\mu)^2 + (r_\eta \times r_\mu)^2}{(r_\xi \times r_\eta) \cdot r_\mu} d\xi d\eta d\mu, \tag{7.8}$$

where "×" is a vector product, and "·" is a scalar product,

$$r_\xi = (x_\xi, y_\xi, z_\xi, f_\xi), \quad r_\eta = (x_\eta, y_\eta, z_\eta, f_\eta), \quad r_\mu = (x_\mu, y_\mu, z_\mu, f_\mu).$$

Let the linear transformation $x^h(\xi,\eta,\mu)$,$y^h(\xi,\eta,\mu)$,$z^h(\xi,\eta,\mu)$ maps the basis tetrahedron T^ξ_{1234} in space ξ,η,μ onto a tetrahedron T_{1234} in space x,y,z. The value of the functional with the linear functions $x^h(\xi,\eta,\mu)$, $y^h(\xi,\eta,\mu)$, $z^h(\xi,\eta,\mu)$ can be computed precisely. Consequently, the approximation of this functional can be written as

$$I^h = \sum_{N=1}^{N_e} \sum_{m=1}^{12} \frac{1}{24} \left[(F_m)_{left} + (F_m)_{right} \right]_N , \tag{7.9}$$

where

$$(F_m)_{left} = \frac{(r^h_\xi \times r^h_\eta)^2 + (r^h_\xi \times r^h_\mu)^2 + (r^h_\eta \times r^h_\mu)^2}{(J_m)_{left}},$$

$$(F_m)_{right} = \frac{(r^h_\xi \times r^h_\eta)^2 + (r^h_\xi \times r^h_\mu)^2 + (r^h_\eta \times r^h_\mu)^2}{(J_m)_{right}},$$

$$(J_m)_{left} = -(r^h_\xi \times r^h_\eta) \cdot r^h_\mu,$$

$$(J_m)_{right} = (r^h_\xi \times r^h_\eta) \cdot r^h_\mu.$$

Consider one term in (7.9), for example $(F_m)_{left}$, and suppose that the Jacobian $(J_m)_{left}$ tends to zero, remaining positive. So as I^h does not tend to infinity in this situation it is necessary that the numerator in $(F_m)_{left}$ must also tend to zero. From the form of the numerator it follows that the vectors e_1=r_2−r_1, e_2=r_3−r_2, e_3=r_4−r_3 are parallel and, hence, all points r_1, r_2, r_3, r_4 lie on a straight line. Consequently, the volumes of all tetrahedra that contain corresponding faces must also tend to zero, including tetrahedron defined by the edge 34 containing edge 23. Repeating argument as many

times as necessary, we conclude that all mesh nodes, including those at the boundary of the domain, must lie on a straight line, which is impossible.

From this it follows that the function (7.9) has the infinite barrier at the boundary of nondegenerate 3D hexahedral meshes, satisfying inequalities (7.5). Hence, if this set is not empty, the system of the algebraic equations

$$R_x = \frac{\partial I^h}{\partial x_n} = 0 \ , \quad R_y = \frac{\partial I^h}{\partial y_n} = 0 \ , \quad R_z = \frac{\partial I^h}{\partial z_n} = 0 \ ,$$

has at least one solution which is a nondegenerate mesh. To find it, one must first find a certain initial nondegenerate mesh and then use some method of unconstrained minimization of the function I^h. Since this function has the infinite barrier on the boundary of the set of nondegenerate meshes, each step of the method can be chosen so that the mesh always satisfies the inequalities (7.5).

For adaptive mesh generation with employing functional (7.2) we use the same approach. Consider cell decomposition into the 24 tetrahedra, described above. Then the mapping of the basis tetrahedron onto every of these tetrahedra is approximated by the linear functions, with assumption that f is also approximated by a linear function defined by its values at the tetrahedron vertices. Then the integrand in (7.2) will be equal to constant. Note that the integrand in (7.2) differs from (7.6). The first one is invariant relative to orthogonal transformations of the basis tetrahedron. It means that we need not use two terms in the approximation of (7.2) corresponding to the right-hand and left-hand coordinate systems. The value of this functional depends only on nodes numeration in the basis tetrahedron and does not on its type.

7.2.4 Minimization of functional

Suppose the mesh at the lth step of the iterations is determined. We use the quasi-Newtonian procedure when the $(l+1)$th step is accomplished by solving two linear equations for every interior node

$$\tau R_x + \frac{\partial R_x}{\partial x_n}(x_n^{l+1} - x_n^l) + \frac{\partial R_x}{\partial y_n}(y_n^{l+1} - y_n^l) + \frac{\partial R_x}{\partial z_n}(z_n^{l+1} - z_n^l) = 0 \ ,$$

$$\tau R_y + \frac{\partial R_y}{\partial x_n}(x_n^{l+1} - x_n^l) + \frac{\partial R_y}{\partial y_n}(y_n^{l+1} - y_n^l) + \frac{\partial R_y}{\partial z_n}(z_n^{l+1} - z_n^l) = 0 \ ,$$

$$\tau R_z + \frac{\partial R_z}{\partial x_n}(x_n^{l+1} - x_n^l) + \frac{\partial R_z}{\partial y_n}(y_n^{l+1} - y_n^l) + \frac{\partial R_z}{\partial z_n}(z_n^{l+1} - z_n^l) = 0 \ ,$$

From this it follows

$$x_n^{l+1} = x_n^l - \tau$$

$$\frac{R_x\left(\frac{\partial R_y}{\partial y_n}\frac{\partial R_z}{\partial z_n} - \frac{\partial R_z}{\partial y_n}\frac{\partial R_y}{\partial z_n}\right) - R_y\left(\frac{\partial R_x}{\partial y_n}\frac{\partial R_z}{\partial z_n} - \frac{\partial R_z}{\partial y_n}\frac{\partial R_x}{\partial z_n}\right) + R_z\left(\frac{\partial R_x}{\partial y_n}\frac{\partial R_y}{\partial z_n} - \frac{\partial R_y}{\partial y_n}\frac{\partial R_x}{\partial z_n}\right)}{det(R)},$$

$$y_n^{l+1} = y_n^l - \tau$$

$$\frac{-R_x\left(\frac{\partial R_y}{\partial x_n}\frac{\partial R_z}{\partial z_n} - \frac{\partial R_z}{\partial x_n}\frac{\partial R_y}{\partial z_n}\right) + R_y\left(\frac{\partial R_x}{\partial x_n}\frac{\partial R_z}{\partial z_n} - \frac{\partial R_z}{\partial x_n}\frac{\partial R_x}{\partial z_n}\right) - R_z\left(\frac{\partial R_x}{\partial x_n}\frac{\partial R_y}{\partial z_n} - \frac{\partial R_y}{\partial x_n}\frac{\partial R_x}{\partial z_n}\right)}{det(R)},$$

$$z_n^{l+1} = z_n^l - \tau$$

$$\frac{R_x\left(\frac{\partial R_y}{\partial x_n}\frac{\partial R_z}{\partial y_n} - \frac{\partial R_z}{\partial x_n}\frac{\partial R_y}{\partial y_n}\right) - R_y\left(\frac{\partial R_x}{\partial x_n}\frac{\partial R_z}{\partial y_n} - \frac{\partial R_z}{\partial x_n}\frac{\partial R_x}{\partial y_n}\right) + R_z\left(\frac{\partial R_x}{\partial x_n}\frac{\partial R_y}{\partial y_n} - \frac{\partial R_y}{\partial x_n}\frac{\partial R_x}{\partial y_n}\right)}{det(R)}, \tag{7.10}$$

$$det(R) = \frac{\partial R_x}{\partial x_n}\left(\frac{\partial R_y}{\partial y_n}\frac{\partial R_z}{\partial z_n} - \frac{\partial R_z}{\partial y_n}\frac{\partial R_y}{\partial z_n}\right) - \frac{\partial R_x}{\partial y_n}\left(\frac{\partial R_y}{\partial x_n}\frac{\partial R_z}{\partial z_n} - \frac{\partial R_z}{\partial x_n}\frac{\partial R_y}{\partial z_n}\right) +$$

$$\frac{\partial R_x}{\partial z_n}\left(\frac{\partial R_y}{\partial x_n}\frac{\partial R_z}{\partial y_n} - \frac{\partial R_z}{\partial x_n}\frac{\partial R_y}{\partial y_n}\right).$$

where τ is the iteration parameter which is chosen so that the mesh remains nondegenerate. With this purpose after every step the conditions (7.5) are checked and if they are not satisfied, this parameter is multiplied by 0.5.

The adaptive-harmonic algorithm for the 3D mesh relaxation and adaption is formulated as follows:

1. Generate an initial mesh using a marching method.
2. Compute new values f_n at every mesh node.
3. Make one iteration step (7.10) and compute new values of x_n,y_n,z_n.
4. Repeat starting with Step 2 to convergency.

Note that the entire algorithm contains computational formulas for $[f_x]_n$, $[f_y]_n$, $[f_z]_n$ which will be presented below.

7.2.5 Derivation of computational formulas

We will obtain computational formulas in the case of adaptation, i.e., we approximate the functional (7.2). The used approach is similar to the method in 2D.

Consider the linear transformation $x^h(\xi,\eta,\mu),\ y^h(\xi,\eta,\mu),\ z^h(\xi,\eta,\mu)$ of the basis tetrahedron shown in Fig.7.2 onto a tetrahedra of the cell decomposition. The function f will be approximated by the linear function $f^h(\xi,\eta,\mu)$. Derivatives of these functions can be easily computed taking into account the enumeration of the vertices in the basis tetrahedron

$$r^h_\xi = (x^h_\xi, y^h_\xi, z^h_\xi, f^h_\xi) = r_2 - r_1 = (x_2 - x_1, y_2 - y_1, z_2 - z_1, f_2 - f_1)\ ,$$

$$r^h_\eta = (x^h_\eta, y^h_\eta, z^h_\eta, f^h_\eta) = r_3 - r_2 = (x_3 - x_2, y_3 - y_2, z_3 - z_2, f_3 - f_2)\ ,$$

$$r^h_\mu = (x^h_\mu, y^h_\mu, z^h_\mu, f^h_\mu) = r_4 - r_3 = (x_4 - x_3, y_4 - y_3, z_4 - z_3, f_4 - f_3)\ .$$

From this it follows

$$g_{ij} = (r_{i+1} - r_i)\cdot(r_{j+1} - r_j),$$

that is,

$$g_{11} = (r_2 - r_1)^2,\ g_{22} = (r_3 - r_2)^2,\ g_{33} = (r_4 - r_3)^2\ ,$$

$$g_{12} = g_{21} = ((r_3 - r_2)\cdot(r_2 - r_1))\ ,$$

$$g_{13} = g_{31} = ((r_4 - r_3)\cdot(r_2 - r_1))\ ,$$

$$g_{23} = g_{32} = ((r_4 - r_3)\cdot(r_3 - r_2))\ . \qquad (7.11)$$

Substituting these expressions into the integrand of (7.2) we obtain

$$F = U/V\ ,$$

where

$$U = g_{11}g_{22} - (g_{12})^2 + g_{11}g_{33} - (g_{13})^2 + g_{22}g_{33} - (g_{23})^2\ , \qquad (7.12)$$

$$V = \sqrt{g_{11}[g_{22}g_{33} - (g_{23})^2] - g_{12}(g_{12}g_{33} - g_{13}g_{23}) + g_{13}(g_{12}g_{23} - g_{22}g_{13})}\ . \qquad (7.13)$$

We use the chain rule to differentiate the ratio of two functions. After differentiating we obtain

$$F_x = \frac{U_x - FV_x}{V}, \quad F_y = \frac{U_y - FV_y}{V}, \quad F_z = \frac{U_z - FV_z}{V},$$

$$F_{xx} = \frac{U_{xx} - 2F_xV_x - FV_{xx}}{V},$$

$$F_{yy} = \frac{U_{yy} - 2F_yV_y - FV_{yy}}{V},$$

$$F_{zz} = \frac{U_{zz} - 2F_zV_z - FV_{zz}}{V}, \tag{7.14}$$

$$F_{xy} = F_{yx} = \frac{U_{xy} - F_xV_y - F_yV_x - FV_{xy}}{V},$$

$$F_{xz} = F_{zx} = \frac{U_{xz} - F_xV_z - F_zV_x - FV_{xz}}{V},$$

$$F_{yz} = F_{zy} = \frac{U_{yz} - F_zV_y - F_yV_z - FV_{yz}}{V}.$$

For vertex 1 of the tetrahedron we should substitute the expressions (7.11), (7.12),(7.13) into (7.14) instead of U, V, and also replace x, y, z by x_1, y_1, z_1 in the resulting formulas.

For vertex 2 x, y, z in (7.14) are replaced by x_2, y_2, z_2.

For vertex 3 x, y, z in (7.14) are replaced by x_3, y_3, z_3.

For vertex 4 x, y, z in (7.14) are replaced by x_4, y_4, z_4.

When computing derivatives of f_i on x_j, y_j, z_j, i=1, . . . , 4, j=1, . . . , 4 we use the formulas for the transformation of derivatives in the 3D space

$$x_\xi f_x + y_\xi f_y + z_\xi f_z = f_\xi \ ,$$

$$x_\eta f_x + y_\eta f_y + z_\eta f_z = f_\eta \ ,$$

$$x_\mu f_x + y_\mu f_y + z_\mu f_z = f_\mu \ .$$

From this it follows

$$f_x = f_\xi(y_\eta z_\mu - y_\mu z_\eta)/J - f_\eta(y_\xi z_\mu - y_\mu z_\xi)/J + f_\mu(y_\xi z_\eta - y_\eta z_\xi)/J \ ,$$

$$f_y = -f_\xi(x_\eta z_\mu - x_\mu z_\eta)/J + f_\eta(x_\xi z_\mu - x_\mu z_\xi)/J - f_\mu(x_\xi z_\eta - x_\eta z_\xi)/J \ ,$$

$$f_z = f_\xi(x_\eta y_\mu - x_\mu y_\eta)/J - f_\eta(x_\xi y_\mu - x_\mu y_\xi)/J + f_\mu(x_\xi y_\eta - x_\eta y_\xi)/J \ , \tag{7.15}$$

where

$$J = x_\xi(y_\eta z_\mu - y_\mu z_\eta) - x_\eta(y_\xi z_\mu - y_\mu z_\xi) + x_\mu(y_\xi z_\eta - y_\eta z_\xi) \ .$$

Note that the derivatives with respect to x, y, z are independent on what a system of coordinates, right-hand or left-hand, is used. Substituting expressions for the derivatives of x^h, y^h, z^h with respect to ξ, η, μ into (7.15) we obtain the formulas for computation of the derivatives f^h_x, f^h_y, f^h_z. We use the following formulas in computations

$$\frac{\partial f_i}{\partial x_j} = \begin{cases} f^h_x & \text{if } \ i{=}j, \\ 0 & \text{if } \ i{\neq}j, \end{cases}$$

$$\frac{\partial f_i}{\partial y_j} = \begin{cases} f^h_y & \text{if } \ i{=}j, \\ 0 & \text{if } \ i{\neq}j, \end{cases}$$

$$\frac{\partial f_i}{\partial z_j} = \begin{cases} f^h_z & \text{if } \ i{=}j, \\ 0 & \text{if } \ i{\neq}j, \end{cases}$$

Computations are performed as follows. Let F and its derivatives with respect to x_1,y_1, and z_1 in the numeration of the basis tetrahedron be computed using formulas to the Nth cell and the local node number k. Then the computed values are added to the appropriate array elements (which were first cleared)

$$I^h{+}{=}F, \quad [R_x]_n{+}{=}F_x, \quad [R_y]_n{+}{=}F_y, \quad [R_z]_n{+}{=}F_z,$$

$$[R_{xx}]_n{+}{=}F_{xx}, \quad [R_{yy}]_n{+}{=}F_{yy}, \quad [R_{zz}]_n{+}{=}F_{zz},$$

$$[R_{xy}]_n{+}{=}F_{xy}, \quad [R_{xz}]_n{+}{=}F_{xz}, \quad [R_{yz}]_n{+}{=}F_{yz},$$

where $n{=}n(N,k_1)$. Here $a{+}{=}b$ means that the new value of a becomes equal to $a{+}b$.

Analogous for vertex 2, correspondence between local and global number is $n{=}n(N,k_2)$.

Analogous for vertex 3, correspondence between local and global number is $n{=}n(N,k_3)$.

Analogous for vertex 4, correspondence between local and global number is $n{=}n(N,k_4)$.

Thus, the iteration method for irregular 3D mesh relaxation and adaptation is described in detail.

Chapter 8

Grid-quality measures

Relevant quality measures for unstructured meshes is still an open problem. Recent progress is presented in [41, 88, 95].

8.1 Tetrahedron shape measures

First we present the definition of a tetrahedron shape measure [41, 95]

Definition 1.

A tetrahedron shape measure is a continuous function that evaluates the quality of a tetrahedron. It must be invariant to the translation, rotation, reflection, and uniform scaling of the tetrahedron, i.e., to a linear conformal mapping. There is no local maximum other than the global maximum for a regular tetrahedron and there is no local minimum other than the global minimum for a degenerate tetrahedron. For easy comparison it should be scaled in the interval $[0, 1]$. *Value 1 corresponds to the regular tetrahedron and 0 corresponds to a degenerate tetrahedron.*

Degenerate tetrahedron is a tetrahedron whose volume vanishes and some of the edges do not vanish. When the volume of the tetrahedron is negative, the tetrahedron is more than degenerate, it is inverted. If the mesh contains negative tetrahedra, at the first stage the shape optimizer should try to untangle them.

We use the following notations. $T(r_0, r_1, r_2, r_3)$ stands for a non-degenerate tetrahedron T with the vertices r_0, r_2, r_3, r_4, V denotes the volume of T; $s_0{=}area(\triangle r_1, r_2, r_3)$, $s_1{=}area(\triangle r_0, r_2, r_3)$, $s_2{=}area(\triangle r_0, r_1, r_3)$, and $s_3{=}area(\triangle r_0, r_1, r_2)$ are the areas of the tetrahedron faces, $l_{ij}{=}|r_i - r_j|$, $0{\leq}i{<}j{\leq}3$, denotes the length of the six edges of T.

8.1.1 Radius ratio

The radius ratio RR of a tetrahedron T is defined as $RR = N\rho_{in}/\rho_{out}$, where ρ_{in} and ρ_{out} are the inradius and circumradius of T, respectively, and N is dimension of the spase. In [95] an easy way to compute this tetrahedron shape measure in 3D is given

$$\rho_{in} = 3V \Big/ \sum_{i=0}^{3} s_i \ ,$$

$$\rho_{out} = \frac{\sqrt{(a+b+c)(a+b-c)(a+c-b)(b+c-a)}}{24V} \ ,$$

$$RR = 3\frac{\rho_{in}}{\rho_{out}} = \frac{216V^2}{\sqrt{(a+b+c)(a+b-c)(a+c-b)(b+c-a)}\sum_{i=0}^{3} s_i} \ ,$$

where a, b, c are the products of the lengths of opposite edges of T.

8.1.2 Mean ratio

Let R be an equilateral tetrahedron and M be the matrix involved in an affine transformation from R to T. The mean ratio MR of the tetrahedron T is the ratio of the geometric mean over the algebraic mean of the eigenvalues λ_1, λ_2, λ_3 of the matrix M^TM. For positive numbers the geometric mean is less or equal to the algebraic mean. A simple expression involving only the volume and the edge lengths can be obtained (see [41])

$$MR = \frac{3(\det(M^TM))^{1/3}}{tr(M^TM)} = \frac{3(\lambda_1\lambda_2\lambda_3)^{1/3}}{\lambda_1+\lambda_2+\lambda_3} = \frac{12(9V^2)^{1/3}}{\sum\limits_{0\le i<j\le 3} l_{ij}^2} \ .$$

Similarly, for the inverse transformation the mean ratio can be defined as (see the chapter of Weatherill in [62])

$$MR_{-} = \frac{3(\det((M^{-1})^TM^{-1}))^{1/3}}{tr(M^{-1})^TM^{-1})} = \frac{3(\lambda_1^{-1}\lambda_2^{-1}\lambda_3^{-1})^{1/3}}{\lambda_1^{-1}+\lambda_2^{-1}+\lambda_3^{-1}} = \frac{4(3V)^{4/3}}{\sum\limits_{i=0}^{3} s_i^2} \ .$$

8.1.3 Solid angle

The solid angle θ_i at the vertex r_i of the tetrahedron T is defined to be the surface area formed by projecting each point of the face not containing r_i to the unit sphere centered at r_i. The area of the unit sphere is 4π, the maximum solid angle for a positive tetrahedron is 2π in the case of a flat tetrahedron. The solid angle at the corner of rectangular tetrahedron is $\pi/2$. The solid angle tetrahedron measure $SA = \sigma_{min}$ can be computed as follows [41]:

$$SA = \sigma_{min} = \alpha \min_{0 \leq ß \leq 3} \sin(\theta_i/2) \ ,$$

$$\sin(\theta_i/2) = 12V \left(\prod_{i,k \neq i} \left((l_{ij} + l_{ik})^2 - l_{jk}^2 \right) \right)^{-1/2} \ ,$$

where

$$\alpha^{-1} = \sqrt{6}/9 = 0.2721655$$

is the value of $\sin(\theta_i/2)$ for four solid angles of the regular tetrahedron.

8.1.4 Dihedral angle

Each of six edges of a tetrahedron is surrounded by two triangular faces. At a given edge, the dihedral angle between two faces is the angle between the intersection of these faces and a plane perpendicular to the edge. For a positive tetrahedron, the dihedral angle is bounded between zero and π. It is equal to π minus the angle between the normals of the faces. The minimum dihedral angle DA can be computed as

$$DA = \varphi_{min} = \alpha \min_{0 \leq ß < j \leq 3} (\pi - arccos(n_{ij1} \cdot n_{ij2})),$$

where n_{ij1} and n_{ij2} are normals of the two triangular faces adjacent to the edge ij and

$$\alpha_{-1} = \pi - arccos(-1/3) = 1.230959$$

is the value of the six dihedral angles of the regular tetrahedron.

According to *Def. 1* of a tetrahedron shape measure the minimum of dihedral angles DM is not a tetrahedron shape measure.

8.1.5 Edge ratio

The edge ratio ER of a tetrahedron T is the ratio of the smallest edge to the largest edge

$$ER = \frac{\min\limits_{0 \le ß < j \le 3} l_{ij}}{\max\limits_{0 \le ß < j \le 3} l_{ij}} \ .$$

According to *Def. 1* of a tetrahedron shape measure the edge ratio ER is not a tetrahedron shape measure.

8.1.6 Aspect ratio

Tetrahedron shape measures that are the ratio of two characteristic sizes of the tetrahedron can be called aspect ratio. They are usually some quantity vanishing with the volume normalized by something that does not vanish when the volume vanishes. The aspect ratio can be proportional to the volume of the tetrahedron, radius, area or volume of the insphere, or minimum of four solid angles. It can not be a function of the circumsphere, smallest edge, and minimum dihedral angle because a degenerate tetrahedron may have non-null circumsphere, smallest edge or minimum dihedral angle. The aspect ratio may be normalized by the longest edge, average of edges, sum of edges, sum of area of the faces, radius, area or volume of the circumsphere, etc. One of such aspect ratio is used at INRIA, France

$$AR = \frac{12}{\sqrt{6}} \frac{\rho_{in}}{\max\limits_{0 \le ß < j \le 3} l_{ij}} \ .$$

8.1.7 Equivalence of tetrahedron shape measures

One of the deepest analysis of tetrahedron shape measures is available from Liu and Joe [95]. They define a notion of tetrahedron shape measure equivalence.

Definition 2. (see [95])

Let p and q be two different tetrahedron shape measures with values from $[0, 1]$. They are called equivalent if there exists positive constants c_0, c_1, e_0, e_1 such that

$$c_0 p^{e_0} \le q \le c_1 p^{e_1} \ .$$

Liu and Joe [95] proved the equivalence of the tetrahedron shape measures: radius ratio RR, mean ratio MR, and solid angle SA. It implies that if one of these tetrahedron shape measures approaches zero, which indicates poor shaped tetrahedron, then the others do so. Conversely, if one of these tetrahedron shape measures approaches unity, then the others do so.

Liu and Joe [95] made a conjecture about how the tetrahedron shape measures should be equivalent. Another conjecture is proposed in [41].

Conjecture (see [41])

All tetrahedron shape measures that satisfy Definition 1 are equivalent in the sense of Definition 2.

But it is obvious that this conjecture is false. Two tetrahedron shape measures can be constructed such that one approaches zero as $V^\alpha, \alpha > 0$, when $V \to 0$, another approaches zero as $\exp(-1/V)$, where V is the volume of a tetrahedron. These measures will satisfy Def.1 but obviously will not satisfy Def.2.

As it was mentioned in [41] "the more a mesh is optimized with a given tetrahedron shape measure, the closer to the optimal mesh it is for any other tetrahedron shape measure. At the limit, if it were possible to mesh a domain with only equilateral tetrahedra, as it is in 2D, all mesh optimizers should converge to that mesh, whichever shape measure is used in the mesh optimizer. The problem is that the optimal mesh does not exist in 3D. It is impossible to fill the space with regular tetrahedra. So, the converged state is unknown and depends slightly of the tetrahedron shape measure used".

8.2 Trilinear mapping

Consider a trilinear mapping of a unit cube in space of variables u, v, w onto a hexahedral cell in space of variables x, y, z with vertices $\mathbf{r}^{ijk}=\mathbf{r}(i,j,k)$, $i,j,k \in \{0,1\}$

$$\begin{aligned}\mathbf{r}(\xi_1,\xi_2,\xi_3) = (1-\xi_1)(1-\xi_2)(1-\xi_3)\mathbf{r}^{000} + \xi_1(1-\xi_2)(1-\xi_3)\mathbf{r}^{100} + \\ (1-\xi_1)\xi_2(1-\xi_3)\mathbf{r}^{010} + (1-\xi_1)(1-\xi_2)\xi_3\mathbf{r}^{001} + \\ \xi_1\xi_2(1-\xi_3)\mathbf{r}^{110} + \xi_1(1-\xi_2)\xi_3\mathbf{r}^{101} + \\ (1-\xi_1)\xi_2\xi_3\mathbf{r}^{011} + \xi_1\xi_2\xi_3\mathbf{r}^{111}\ .\end{aligned} \tag{8.1}$$

Here $\mathbf{r}=(x_1,x_2,x_3)^T=(x,y,z)^T$ is a spatial position vector.

Curvilinear coordinates are $(\xi_1, \xi_2, \xi_3)=(u, v, w)$, where $u, v, w \in [0, 1]$. Cell vertices are enumerated with triple indices (see fig.8.1)

$$\mathbf{r}^{000}, \mathbf{r}^{100}, \mathbf{r}^{010}, \mathbf{r}^{110}, \mathbf{r}^{001}, \mathbf{r}^{101}, \mathbf{r}^{011}, \mathbf{r}^{111} \ .$$

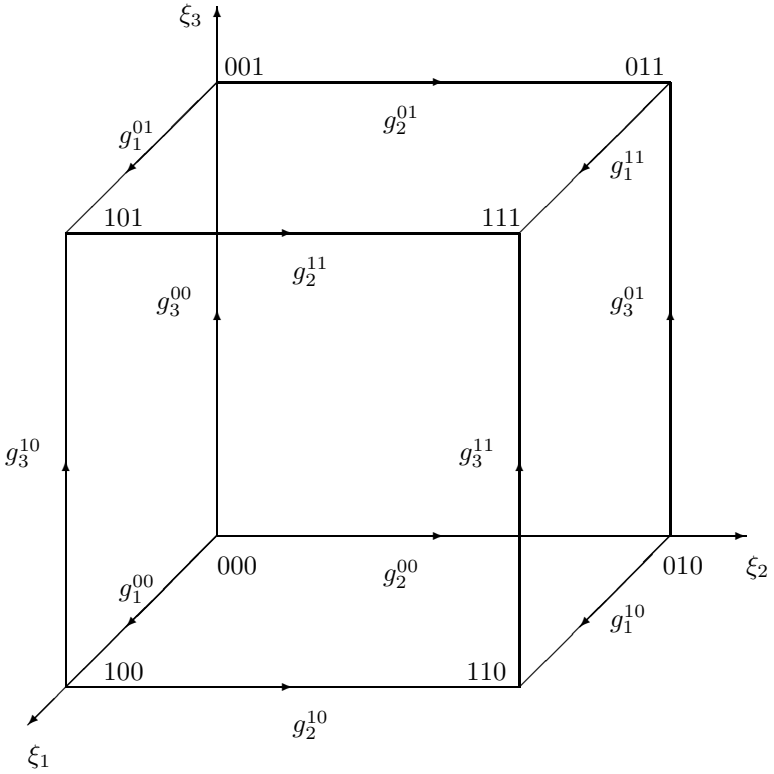

Fig. 8.1: Numeration of vertices in hexahedral cell

Covariant basis vectors are the following

$$g_i = \frac{\partial r}{\partial \xi_i} \ .$$

Covariant basis vectors for trilinear mapping are equal to

$$g_i(\xi_j, \xi_k) = (1-\xi_j)(1-\xi_k)g_i^{00} + \xi_j(1-\xi_k)g_i^{10} + (1-\xi_j)\xi_k g_i^{01} + \xi_j\xi_k g_i^{11} \ ,$$

where $\{i,j,k\}$ is the cyclic permutation from $\{1,2,3\}$ and

$$g_1^{mn} = \mathbf{r}^{1mn} - \mathbf{r}^{0mn}, \quad m,n \in \{0,1\} ,$$
$$g_2^{mn} = \mathbf{r}^{m1n} - \mathbf{r}^{m0n}, \quad m,n \in \{0,1\} ,$$
$$g_3^{mn} = \mathbf{r}^{mn1} - \mathbf{r}^{mn0}, \quad m,n \in \{0,1\} .$$

The Jacobian of the trilinear mapping is equal to $J{=}g_1{\cdot}(g_2{\times}g_3)$. Obviously that

$$J = \sum_{i,j,k,l,m,n=0}^{1} \alpha_{ijklmn}\ g_1^{ij} \cdot (g_2^{kl} \times g_3^{mn}) ,$$

where

$$\alpha_{ijklmn} = (1-\xi_2)^{1-i}\xi_2^i(1-\xi_3)^{1-j}\xi_3^j(1-\xi_1)^{1-k}\xi_1^k(1-\xi_3)^{1-l}$$
$$\times\xi_3^l(1-\xi_1)^{1-m}\xi_1^m(1-\xi_2)^{1-n}\xi_3^n \geq 0,$$

and the coefficients α_{ijklmn} are strictly positive for the interior points of the trilinear cell. It means that that if

$$g_1^{ij} \cdot (g_2^{kl} \times g_3^{mn}) > 0, \quad i,j,k,l,m,n \in \{0,1\} ,$$

then it follows that the Jacobian of the trilinear mapping is positive in the interior of the cell. Since on the boundary of cell some of the coefficients α_{ijklmn} are always positive we obtain that J will be positive on the cell boundary as well. There are additional conditions on g_i (see fig.1)

$$g_1^{00} + g_2^{10} = g_2^{00} + g_1^{10}, \quad g_1^{00} + g_3^{10} = g_3^{00} + g_1^{01}, \quad g_2^{00} + g_3^{01} = g_3^{00} + g_2^{01},$$

$$g_2^{01} + g_1^{11} = g_1^{01} + g_2^{11}, \quad g_1^{10} + g_3^{11} = g_3^{01} + g_1^{11}, \quad g_2^{10} + g_3^{11} = g_3^{10} + g_2^{11}.$$

Each condition is associated with the corresponding face.

Necessary conditions of nondegeneracy of the trilinear mapping (8.1) were considered in [10, 85, 86, 149, 150] and sufficient conditions in [149, 150, 153]. The most detailed analysis was performed in [149, 150] and it was suggested the necessary and sufficient conditions of nondegeneracy which do not coincide.[1]

[1]This paragraph was added by the Editor.

8.3 Metric coefficients

Coefficients of the metric tensor are computed as follows

$$g_{ij} = g_i g_j = \frac{\partial \mathbf{r}}{\partial \xi_i} \frac{\partial \mathbf{r}}{\partial \xi_j} \ .$$

For the trilinear mapping (8.1) it follows that

$$\begin{aligned}
\frac{\partial \mathbf{r}}{\partial u} &= (1-v)(1-w)(\mathbf{r}^{100} - \mathbf{r}^{000}) + v(1-w)(\mathbf{r}^{110} - \mathbf{r}^{010}) \\
&\quad + vw(\mathbf{r}^{111} - \mathbf{r}^{011}) + (1-v)w(\mathbf{r}^{101} - \mathbf{r}^{001}), \\
\frac{\partial \mathbf{r}}{\partial v} &= (1-u)(1-w)(\mathbf{r}^{010} - \mathbf{r}^{000}) + u(1-w)(\mathbf{r}^{110} - \mathbf{r}^{100}) \\
&\quad + uw(\mathbf{r}^{111} - \mathbf{r}^{101}) + (1-u)w(\mathbf{r}^{011} - \mathbf{r}^{001}), \\
\frac{\partial \mathbf{r}}{\partial w} &= (1-u)(1-v)(\mathbf{r}^{001} - \mathbf{r}^{000}) + u(1-v)(\mathbf{r}^{101} - \mathbf{r}^{100}) \\
&\quad + uv(\mathbf{r}^{111} - \mathbf{r}^{110}) + (1-u)v(\mathbf{r}^{011} - \mathbf{r}^{010}).
\end{aligned}$$

Components of the metric tensor are computes as follows

$$g_{11} = \frac{\partial \mathbf{r}}{\partial u}\frac{\partial \mathbf{r}}{\partial u}, \quad g_{12} = \frac{\partial \mathbf{r}}{\partial u}\frac{\partial \mathbf{r}}{\partial v}, \quad g_{13} = \frac{\partial \mathbf{r}}{\partial u}\frac{\partial \mathbf{r}}{\partial w}, \quad g_{23} = \frac{\partial \mathbf{r}}{\partial v}\frac{\partial \mathbf{r}}{\partial w} \ ,$$
$$g_{22} = \frac{\partial \mathbf{r}}{\partial v}\frac{\partial \mathbf{r}}{\partial v}, \quad g_{33} = \frac{\partial \mathbf{r}}{\partial w}\frac{\partial \mathbf{r}}{\partial w}.$$

The Jacobian is equal to

$$J = \frac{\partial \mathbf{r}}{\partial u}\Big(\frac{\partial \mathbf{r}}{\partial v} \times \frac{\partial \mathbf{r}}{\partial w}\Big) = x_u(y_v z_w - z_v y_w) - x_v(y_u z_w - z_u y_w) + x_w(y_u z_v - z_u y_v).$$

The Determinant of the metric tensor

$$g = g_{11}(g_{22}g_{33} - g_{23}g_{23}) - g_{12}(g_{12}g_{33} - g_{13}g_{23}) + g_{13}(g_{12}g_{23} - g_{13}g_{22}).$$

can be computed also as $g = J^2$.

Components of the contravariant metric tensor are computes as follows

$$g^{11} = g^{-1}(g_{22}g_{33} - g_{23}^2), \ g^{12} = -g^{-1}(g_{12}g_{33} - g_{13}g_{23}), \ g^{13} = g^{-1}(g_{12}g_{23} - g_{13}g_{22}),$$
$$g^{23} = -g^{-1}(g_{11}g_{23} - g_{13}g_{12}), \ g^{22} = g^{-1}(g_{11}g_{33} - g_{13}^2), \ g^{33} = g^{-1}(g_{11}g_{22} - g_{12}^2).$$

8.4 Quality measures of curvilinear coordinate systems

In this section we present quality measures for curvilinear coordinate system from [94]

8.4.1 Aspect ratio

In the 2D case the aspect ratio is the measure of the departure of the cell from a rhombus. In the 3D case the aspect ratio in the point u, v, w is computed as follows

$$Q_{sk} = \frac{g_{11}}{g_{22}} + \frac{g_{22}}{g_{11}} + \frac{g_{11}}{g_{33}} + \frac{g_{33}}{g_{11}} + \frac{g_{22}}{g_{33}} + \frac{g_{33}}{g_{22}} \ .$$

The normalized aspect ratio

$$\tilde{Q}_{sk} = \frac{6}{Q_{sk}} \ .$$

8.4.2 Skewness

There are four measures of skewness

$$Q_{sk,1} = \frac{g_{12}^2}{g_{11}g_{22}} + \frac{g_{13}^2}{g_{11}g_{33}} + \frac{g_{23}^2}{g_{22}g_{33}} \ ,$$

$$Q_{sk,2} = \frac{g_{12}^2}{g_{11}g_{22} - g_{12}^2} + \frac{g_{13}^2}{g_{11}g_{33} - g_{13}^2} + \frac{g_{23}^2}{g_{22}g_{33} - g_{23}^2} \ ,$$

$$Q_{sk,3} = \frac{(g^{12})^2}{g^{11}g^{22}} + \frac{(g^{13})^2}{g^{11}g^{33}} + \frac{(g^{23})^2}{g^{22}g^{33}} \ ,$$

$$Q_{sk,4} = \frac{(g^{12})^2}{g^{11}g^{22} - (g^{12})^2} + \frac{(g^{13})^2}{g^{11}g^{33} - (g^{13})^2} + \frac{(g^{23})^2}{g^{22}g^{33} - (g^{23})^2} \ ,$$

Normalized measures are the following

$$\tilde{Q}_{sk,1} = 1 - Q_{sk,1}/3 \ , \quad \tilde{Q}_{sk,2} = 1/(Q_{sk,2} + 1) \ ,$$

$$\tilde{Q}_{sk,3} = 1 - Q_{sk,3}/3 \ , \quad \tilde{Q}_{sk,4} = 1/(Q_{sk,4} + 1) \ .$$

8.4.3 Orthogonality

Another quantities, characterizing departure from orthogonality, are as follows

$$Q_{o,1} = g_{11}g_{22}g_{33}/g \ , \quad Q_{o,2} = g^{11}g^{22}g^{33}g \ ,$$
$$Q_{o,3} = g_{12}^2 + g_{13}^2 + g_{23}^2 \ , \quad Q_{o,4} = (g^{12})^2 + (g^{13})^2 + (g^{23})^2 \ .$$

Normalized quantities are

$$\tilde{Q}_{o,1} = 1/Q_{o,1} \ , \quad \tilde{Q}_{o,2} = 1/Q_{o,2} \ ,$$
$$\tilde{Q}_{o,3} = 1/(Q_{o,3}+1) \ , \quad \tilde{Q}_{o,4} = 1/(Q_{o,4}+1) \ .$$

8.4.4 Conformality

Deviation of the trilinear mapping from conformal can be measured by

$$Q_{cf,1} = g^{1/3}(g^{11} + g^{22} + g^{33}) \ , \quad Q_{cf,2} = g^{-2/3}(g_{11} + g_{22} + g_{33}) \ .$$

Normalized quantities are

$$\tilde{Q}_{cf,1} = 1/Q_{cf,1} \ , \quad \tilde{Q}_{cf,2} = 1/Q_{cf,2} \ .$$

8.4.5 Warping

Computational formulas for the second derivatives are the following

$$\begin{aligned}
\frac{\partial^2 \mathbf{r}}{\partial u \partial v} &= -v(1-w)(\mathbf{r}^{100} - \mathbf{r}^{000}) + (1-w)(\mathbf{r}^{110} - \mathbf{r}^{010}) \\
&\quad + w(\mathbf{r}^{111} - \mathbf{r}^{011}) - vw(\mathbf{r}^{101} - \mathbf{r}^{001}), \\
\frac{\partial^2 \mathbf{r}}{\partial v \partial w} &= -(1-u)(\mathbf{r}^{010} - \mathbf{r}^{000}) - u(\mathbf{r}^{110} - \mathbf{r}^{100}) \\
&\quad + u(\mathbf{r}^{111} - \mathbf{r}^{101}) + (1-u)(\mathbf{r}^{011} - \mathbf{r}^{001}), \\
\frac{\partial^2 \mathbf{r}}{\partial u \partial w} &= -(1-v)(\mathbf{r}^{100} - \mathbf{r}^{000}) - w(\mathbf{r}^{110} - \mathbf{r}^{010}) \\
&\quad + v(\mathbf{r}^{111} - \mathbf{r}^{011}) + (1-v)(\mathbf{r}^{101} - \mathbf{r}^{001}).
\end{aligned}$$

It is easy to see that

$$\partial^2 r/\partial u^2 = 0, \quad \partial^2 r/\partial v^2 = 0, \quad \partial^2 r/\partial w^2 = 0 \ .$$

Components of the vector product for the u, v surface are the following

$$s_x = y_u z_v - y_v z_u \ , \quad s_y = -(x_u z_v - x_v z_u) \ , \quad s_z = x_u y_v - x_v y_u \ .$$

Elements of the second fundamental form are

$$b_{11} = 0 \ , \quad b_{12} = \frac{x_{uv} s_x + y_{uv} s_y + z_{uv} s_z}{\sqrt{s_x^2 + s_y^2 + s_z^2}} \ , \quad b_{22} = 0 \ .$$

Determinant of the metric tensor on the u, v surface is

$$g^{uv} = g_{11} g_{22} - g_{12}^2 \ .$$

Mean curvature squared on the u, v surface is

$$Q_1^{uv} = \left(\frac{g_{22}^{uv} b_{11} - 2 g_{12}^{uv} b_{12} + g_{11}^{uv} b_{22}}{2 g^{uv}} \right)^2 \ .$$

Gaussian curvature squared is

$$Q_2^{uv} = \left(\frac{b_{11} b_{22} - b_{12}^2}{g^{uv}} \right)^2 \ .$$

Torsion is

$$Q_3^{uu} = \alpha |\partial^2 r/\partial u^2| = 0 \ .$$

Eccentricity is

$$Q_4^{uu} = \alpha_1 |\partial^2 r/\partial u^2| = 0 \ .$$

Quality measures are

$$Q_{w,1} = Q_1^{uv} + Q_1^{uw} + Q_1^{vv} \ , \quad Q_{w,2} = Q_2^{uv} + Q_2^{uw} + Q_2^{vw} \ ,$$

$$Q_{w,3} = Q_3^{uu} + Q_3^{vv} + Q_3^{ww} \ , \quad Q_{w,4} = Q_4^{uu} + Q_4^{vv} + Q_4^{ww} \ .$$

Normalized quantities are

$$\tilde{Q}_{w,1} = 1/Q_{w,1} \ , \quad \tilde{Q}_{w,2} = 1/Q_{w,2} \ ,$$

$$\tilde{Q}_{w,3} = 1/(Q_{w,3} + 1) \ , \quad \tilde{Q}_{w,4} = 1/(Q_{w,4} + 1) \ .$$

8.5 Hexahedron shape measures

In the case of a hexahedron we can measure the quality of all corner tetrahedrons. But in some cases it is not enough. There is an example of a hexahedron which possesses positive corner Jacobians (volumes of the corner tetrahedrons), but zero Jacobian at the center.

Not all shape measures, developed for measuring the deviation of the shape of a tetrahedron from the shape of equilateral tetrahedron, presented in the previous section, can be used in this case.

The mean ratio and condition number, introduced by Knupp [88], can be used for these purposes. Let R be a tetrahedron (R_0, R_1, R_2, R_3) formed by three orthogonal vectors $(R_1 - R_0)$, $(R_2 - R_0)$, and $(R_3 - R_0)$, each of unit length, and M be the matrix involved in an affine transformation from R to T. The mean ratio MR of the tetrahedron T is the ratio of the geometric mean to the algebraic mean of the eigenvalues λ_1, λ_2, λ_3 of the matrix $M^T M$. For positive numbers the geometric mean is less or equal to the algebraic mean. A simple expression involving only the volume and the edge lengths can be obtained

$$MR = \frac{3(\det(M^T M))^{1/3}}{tr(M^T M)} = \frac{3(\lambda_1 \lambda_2 \lambda_3)^{1/3}}{\lambda_1 + \lambda_2 + \lambda_3} = \frac{3(3V)^{2/3}}{\sum\limits_{i=1}^{3} l_{0i}^2} \ .$$

Similarly, for the inverse transformation the mean ratio can be defined as

$$MR_- = \frac{3(\det((M^{-1})^T M^{-1}))^{1/3}}{tr(M^{-1})^T M^{-1})} = \frac{3(\lambda_1^{-1} \lambda_2^{-1} \lambda_3^{-1})^{1/3}}{\lambda_1^{-1} + \lambda_2^{-1} + \lambda_3^{-1}} = \frac{3(3V)^{4/3}}{4 \sum\limits_{i=1}^{3} s_i^2} \ .$$

The condition number CN can be introduced as follows (see [88])

$$\frac{1}{(CN)^2} = (MR)(MR_-)$$

$$= \frac{9}{(\lambda_1 + \lambda_2 + \lambda_3)(\lambda_1^{-1} + \lambda_2^{-1} + \lambda_3^{-1})} = \frac{9(3V)^2}{4 \sum\limits_{i=1}^{3} l_{0i}^2 \sum\limits_{i=1}^{3} s_i^2} \ .$$

Using the inequality

$$3(\lambda_1 \lambda_2 + \lambda_1 \lambda_3 + \lambda_2 \lambda_3) \leq (\lambda_1 + \lambda_2 + \lambda_3)^2$$

we can obtain the following estimates for the condition number

$$(MR_{-})^{3/2} = \frac{9\lambda_1\lambda_2\lambda_3}{\sqrt{3}(\lambda_1\lambda_2 + \lambda_1\lambda_3 + \lambda_2\lambda_3)^{3/2}} \geq \frac{1}{(CN)^2}$$

$$\geq \frac{27\lambda_1\lambda_2\lambda_3}{(\lambda_1 + \lambda_2 + \lambda_3)^3} = (MR)^3 \ .$$

Chapter 9

Grid optimization

An approach, presented herein, is based on the principle of the minimal energy density of a mapping. This also leads to the variational formulation of an elliptic grid generator.

The main idea is the following. A local shape measure is formulated for every cell or element. With this purpose a linear mapping, which transforms points in the simplex element with prescribed objective shape to points in an arbitrary physical element, is considered. The energy density of a linear mapping is defined as an averaged energy stored in the right-angled parallelepiped of the unit volume in the physical space, provided that the parallelepiped is the image of a cube in computational space. The shape measure is a quantity inverse to the energy density. Maximum of such a shape measure corresponds to the minimum of the energy density and it is attained if and only if the shape of the element is the same as the corresponding objective shape. For example, only two parameters define the shape of a triangle: the lengths ratio of two sides and the angle between them. Two triangles are of the same shape if these two parameters are identical for the both triangles, which is equivalent to the minimum of the energy density of the linear transformation between these triangles.

The sum of local energy densities forms the global energy density of the grid deformation from prescribed objective shapes. This user-defined grid quality measure is implemented in the optimization-based method for grid generation and improvement. The approach can be considered as a generalization of methods, based on constructing a mapping, which are a composition of the algebraic map and inverse to harmonic mapping [56, 131] and give a guarantee that the composite mapping is invertible at the continuous level. The present approach gives such a guarantee at the discrete

level.

The energy density of grid deformation is a discrete functional with an infinite barrier on the boundary of the set of unfolded grids. This discrete functional is an extension of the barrier function from [34]. Barrier functions for grid generation and optimization have been considered also in [89, 146]. The barrier property is very important in problems with moving boundaries and in moving adaptive grid technology because such methods ensure generation of unfolded grids at every time step. Direct control of cell shape is used to provide mesh orthogonality with prescribed width of cells near the boundary. Adaptation to the solution of the host equations can be realized as in the adaptive-harmonic grid generator. In the 3D case the well known tetrahedron shape measure, such as the mean ratio, can be obtained from the energy density of the deformation of the equilateral tetrahedron. The condition number of the Jacobian matrix of [88], measured in the Frobenius norm, can be obtained as well.

9.1 Energy density of linear transformation in 2D

Consider a linear mapping between two planes $(X,Y)\rightarrow(x,y)$, where $X(\xi,\eta), Y(\xi,\eta)$ and $x(\xi,\eta), y(\xi,\eta)$ are the linear transformations $(\xi,\eta)\rightarrow(X,Y)$ and $(\xi,\eta)\rightarrow(x,y)$ with matrices C and c, respectively (see fig. 9.1). Squared lengths of vectors with coordinates (X,Y) and (x,y) are the positive-definite quadratic forms

$$X^2+Y^2=G_{11}\xi^2+2G_{12}\xi\eta+G_{22}\eta^2,$$
$$x^2+y^2=g_{11}\xi^2+2g_{12}\xi\eta+g_{22}\eta^2,$$

with matrices

$$G=(G_{ij})=C^TC \quad \text{and} \quad g=(g_{ij})=c^Tc,$$

respectively. A quadratic form, corresponding to the mapping $(X,Y)\rightarrow(x,y)$, is defined with the matrix $(C^{-1})^Tc^TcC^{-1}$. The characteristic equation is of the form

$$\det((C^{-1})^Tc^TcC^{-1}-\lambda E)=\det(C)^{-2}\det(c^Tc-\lambda C^TC)=0,$$

where E is the identity matrix. Consequently, if the matrix C is non-singular, the characteristic equation for the matrix $(C^{-1})^T c^T c C^{-1}$ has the same solutions $\lambda_{1,2}$ as the characteristic equation for the pair of the quadratic forms

$$det(g - \lambda G) = \det(G)\det(G^{-1}g - \lambda E) = 0.$$

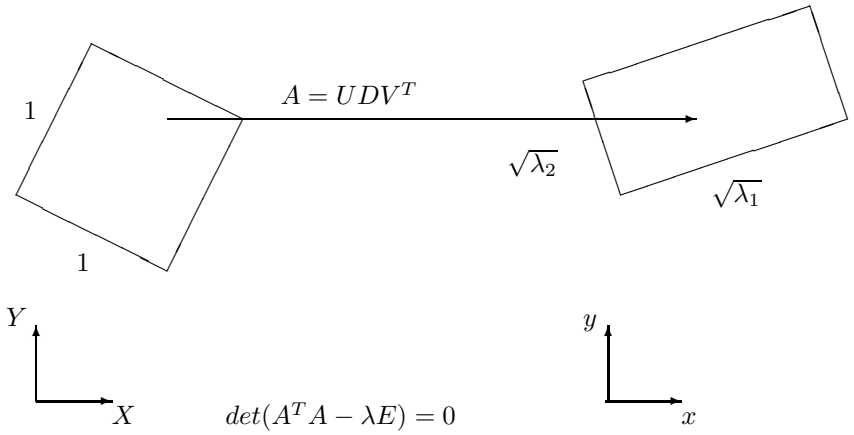

Fig. 9.1: Linear transformation of unit square to rectangle

The orthogonal invariants d_1, d_2 of a mapping $(X, Y) \to (x, y)$ depend upon eigenvalues $\lambda_{1,2}$ of the matrix $G^{-1}g$

$$\begin{aligned} d_1 = \lambda_1 + \lambda_2 = tr(G^{-1}g) = \frac{g_{11}G_{22} - 2g_{12}G_{12} + g_{22}G_{11}}{\det(G)}, \\ d_2 = \lambda_1\lambda_2 = \det(G^{-1}g) = \frac{\det(g)}{\det(G)}. \end{aligned} \tag{9.1}$$

The energy density is defined as an averaged energy stored in the rectangle of a unit area, provided that the rectangle is the image of a square [75]. In linear, algebra it is known that any matrix A can be represented in the form $A = UDV^T$, where U and V are the orthogonal matrices, D

is a diagonal matrix with diagonal elements equal to singular eigenvalues of the matrix A. From this it follows that for any linear transformation there exists such a unit square which is transformed into a rectangle with sides length equal to $\sqrt{\lambda_1}$ and $\sqrt{\lambda_2}$ (singular eigenvalues of the matrix cC^{-1} in our case). The averaged energy, stored in this rectangle, is equal to $0.5d_1 = 0.5(\lambda_1 + \lambda_2)$. Area of the rectangle is equal to $\sqrt{d_2} = \sqrt{\lambda_1\lambda_2}$. Consequently, the energy density can be expressed as

$$e(x,y)(X,Y) = \frac{1}{2}\frac{d_1}{\sqrt{d_2}} = \frac{1}{2}\frac{\lambda_1+\lambda_2}{\sqrt{\lambda_1\lambda_2}} \geq 1. \tag{9.2}$$

Substituting expressions (9.1) for d_1 and d_2 into (9.2) we obtain the final expression to the energy density of a mapping $(X,Y)\rightarrow(x,y)$

$$e(x,y)(X,Y) = \frac{1}{2}\frac{tr(G^{-1}g)}{\sqrt{\det(G^{-1}g)}} = \frac{1}{2}\frac{g_{11}G_{22} - 2g_{12}G_{12} + g_{22}G_{11}}{\sqrt{\det(g)}\sqrt{\det(G)}}. \tag{9.3}$$

The properties of the energy density of a linear mapping are the following:

1. The energy density is an orthogonal invariant, which remains unchanged for orthogonal transformations of planes (X,Y) and (x,y). Moreover, it is also a conformal invariant, since $e(x,y)(X,Y) = e(\alpha x,\alpha y)(\beta X,\beta Y)$ for any $\alpha,\beta > 0$. In the 2D case the energy density is identical for direct and inverse linear transformations, i.e., $e(x,y)(X,Y) = e(X,Y)(x,y)$.

2. If a mapping $x(X,Y), y(X,Y)$ becomes singular, i.e., $J\rightarrow 0$, and if at least one of the quantities λ_1 or λ_2 does not tend to 0, then the energy density $e\rightarrow\infty$. If the energy density does not tend to ∞ while $J\rightarrow 0$, the transformation degenerates into a point: $(X,Y)\rightarrow(0,0)$, and in this case $\lambda_1 \rightarrow 0$ and $\lambda_2 \rightarrow 0$ simultaneously.

3. Optimality principle. Minimum of the energy density $e(x,y)(X,Y)$ of a linear transformation $(X,Y)\rightarrow(x,y)$ is equal to 1 and is attained if and only if $\lambda_1{=}\lambda_2$, i.e., the transformation is conformal.

9.2 Shape measures of triangular and quadrilateral cells

Consider a linear transformation of a given triangle in the plane (X,Y) to an arbitrary triangle in the plane (x,y). The sides L_1, L_2, l_1, l_2 and angles Φ, φ

of the triangles are shown in fig. 9.2. Correspondence between the vertices of the triangles defines a unique linear transformation $(X,Y)\rightarrow(x,y)$. The Jacobian of the transformation is equal to the areas ratio

$$J = \frac{l_1 l_2 \sin\varphi}{L_1 L_2 \sin\Phi} > 0 \ .$$

Note that the conditions of the transformation to be conformal are the following

$$l_1/l_2 = L_1/L_2, \quad \varphi = \Phi \ . \tag{9.4}$$

This also means that triangles are of the same shape. Our purpose is to construct such a function $e^t(l_1, l_2, \varphi, L_1, L_2, \Phi)$ that its minimum ensures (9.4).

Consider auxiliary linear transformations $(\xi,\eta) \rightarrow (x,y)$ and $(\xi,\eta) \rightarrow (X,Y)$ with matrices c and C of the right-angled triangle (half of the unit square) in the plane (ξ,η), shown in fig.9.1, such that

$$g_{11} = l_1^2,\ g_{22} = l_2^2,\ g_{12} = l_1 l_2 \cos\varphi,\ G_{11} = L_1^2,\ G_{22} = L_2^2,\ G_{12} = L_1 L_2 \cos\Phi.$$

In this notations the energy density (9.3) takes the form

$$e^t = \frac{1}{2}\frac{l_1^2 L_2^2 + l_2^2 L_1^2 - 2 l_1 l_2 L_1 L_2 \cos\varphi\cos\Phi}{l_1 l_2 \sin\varphi L_1 L_2 \sin\Phi}. \tag{9.5}$$

Note that conditions $l_1, l_2, L_1, L_2 \neq 0$; $\varphi, \Phi \neq 0$ and $\varphi, \Phi \neq \pi$ have been used in derivation of (9.5).

To check the property of the function (9.5) to have the minimum in the case when the triangles are of the same shape we introduce notations from [58].

$$l_1^2 = \rho\exp(\beta), \quad L_1^2 = R\exp(B), \quad l_2^2 = \rho\exp(-\beta), \quad L_2^2 = R\exp(-B) \ .$$

In these notations the expression (9.5) takes the form independent of ρ and R

$$e^t = 2\frac{sh^2\frac{\beta-B}{2} + \sin^2\frac{\varphi-\Phi}{2}}{\sin\varphi\sin\Phi} + 1 \ . \tag{9.6}$$

It is clear that the minimum of (9.6) is attained if $\beta{=}B$ and $\varphi{=}\Phi$, i.e., the conditions (9.4) are satisfied. Note that $1/e^t$ is a triangular shape measure according to the definition given in [41] and being applied to triangles.

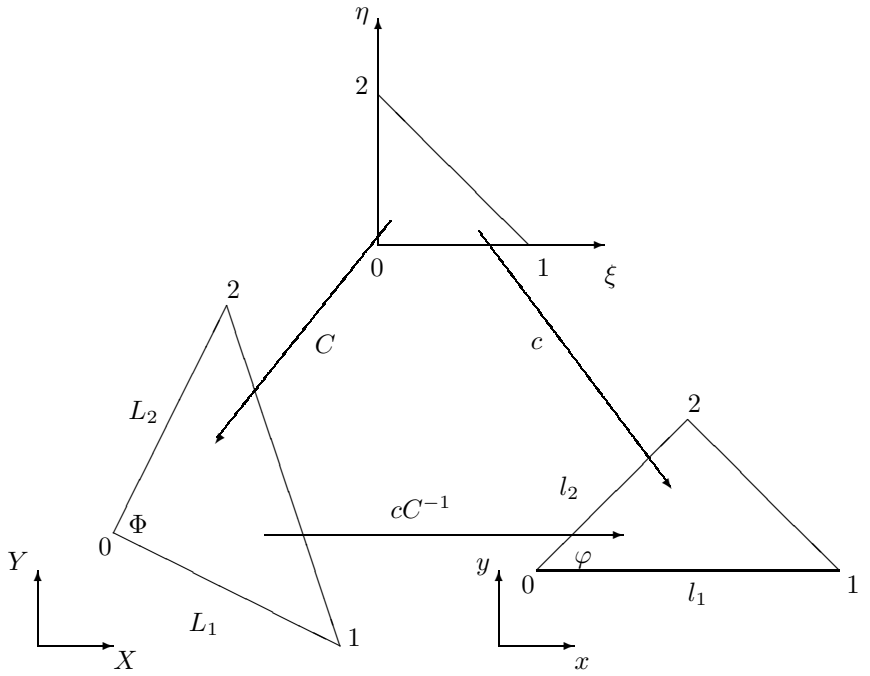

Fig. 9.2: Linear transformation of triangle

Properties of the function (9.5) follow from the properties of the energy density, formulated in Section 9.1.

The energy density of a quadrilateral element can be expressed as

$$e^q = \frac{1}{4}(e_0^t + e_1^t + e_2^t + e_3^t),$$

where e_k^t is the function (9.5) for the triangle corresponding to the kth vertex of the quadrilateral element.

9.3 Energy density of grid deformation

Consider an unstructured grid, formed by quadrilateral elements. In this case the correspondence between local and global enumerations is defined

as

$$n = n(N,k),\ n = 1,2,\ldots,N_n,\ N = 1,2,\ldots,N_e,\ k = 0,1,2,3,$$

where n is the global node number, N_n is the total number of grid nodes, N is an element number, N_e is the number of elements, k is the local node number in the element.

The energy density of grid deformation can be obtained as an averaged value

$$e^h = \frac{1}{N_e}\sum_{N=1}^{N_e}\left[e_k^q\right]_N = \frac{1}{N_e}\sum_{N=1}^{N_e}\sum_{k=0}^{3}\frac{1}{4}\left[e_k^t\right]_N\ , \tag{9.7}$$

where e_k^t is defined via (9.5). For a given grid in the plane (x,y) the optimization problem to find the minimum of e^h is formulated. Parameters, defining the objective shapes of the quadrilaterals, expressed in (9.5) with capital letters, must be specified for every grid cell. The procedure from [74] is applied for minimization of e^h. Note that if the objective shape is a square for every cell, e^h reduces to the barrier approximation of the harmonic functional, described in detail in [34, 74].

There is an interesting property of the function (9.7). Consider a hypothetical case when the structure of the grid and objective shapes for every cell, identical to shapes of an existing grid, are known. If we specify positions of two arbitrary neighboring nodes of the grid, then the positions of all other nodes can be obtained sequentially from the condition $e^h = 1$. Similarly, if the positions of internal boundary nodes are specified, then all other nodes can be obtained layer by layer as it can be done by a hyperbolic method. At the same time the present method is elliptic [75].

Function (9.7) possesses a barrier property, i.e., $e^h \to \infty$ if the area of any triangle tends to zero.

9.4 Specification of objective shape near boundary

To achieve grid orthogonality near the boundary we must specify corresponding objective shape of cells. First, an "orthogonal" direction has to be specified to every boundary node. To this end, a point of intersection

of two lines, parallel to the corresponding parts of the boundary line, is determined (see fig.9.3a). The vector r_1, orthogonal to the interval $(i-1,i)$ of the boundary (see fig.9.3a), is obtained as

$$x_1 = d_0(-y_i + y_{i-1})/\sqrt{(x_{i-1}-x_i)^2 + (y_{i-1}-y_i)^2}\ ,$$
$$y_1 = d_0(x_i - x_{i-1})/\sqrt{(x_{i-1}-x_i)^2 + (y_{i-1}-y_i)^2}\ .$$

Here d_0 is the width of the layer of cells adjacent to the boundary. Coordinates of the vector r_2 are computed similarly. The vector r is determined from the conditions

$$r_1(r-r_1) = 0\ , \qquad r_2(r-r_2) = 0.$$

Solving this system of linear equations, we obtain

$$x = \frac{y_2|r_1|^2 - y_1|r_2|^2}{x_1y_2 - x_2y_1}\ , \qquad y = -\frac{x_2|r_1|^2 - x_1|r_2|^2}{x_1y_2 - x_2y_1}\ .$$

Cell shape in the next layer can be obtained similarly. For the smooth transformation of cell shape from the boundary to the internal field a linear interpolation of the objective shape is used along the corresponding curvilinear coordinate lines. Shape of two cells at the ends of the layer of interpolation are known. These cells are scaled and rotated in such a way that their bottom sides coincide and interpolation is performed along lines, connecting two top vertices of the cells (see fig.9.3b)

$$\tilde{r}_2(j) = (1-s)r_2 + sr_{2'}, \qquad \tilde{r}_3(j) = (1-s)r_3 + sr_{3'}\ . \tag{9.8}$$

Interpolation coefficient s is determined from the position of the cell in the interpolation layer: $s{=}(j{-}1)/(N_j{-}1)$, where N_j is the total number of cells in the interpolation layer along j-direction, j is the number of the cell in the layer.

Coordinates of the objective cell vertices (X_k, Y_k), $k{=}0,1,2,3$ are specified as follows

$$(X_0,Y_0) = (0,0),\ (X_1,Y_1) = (1,0),\ (X_2,Y_2) = (\tilde{x}_2,\tilde{y}_2),\ (X_3,Y_3) = (\tilde{x}_3,\tilde{y}_3).$$

Note that many other algorithms can be formulated for specification of objective shapes. The notation “orthogonality near the boundary” can be introduced by the user.

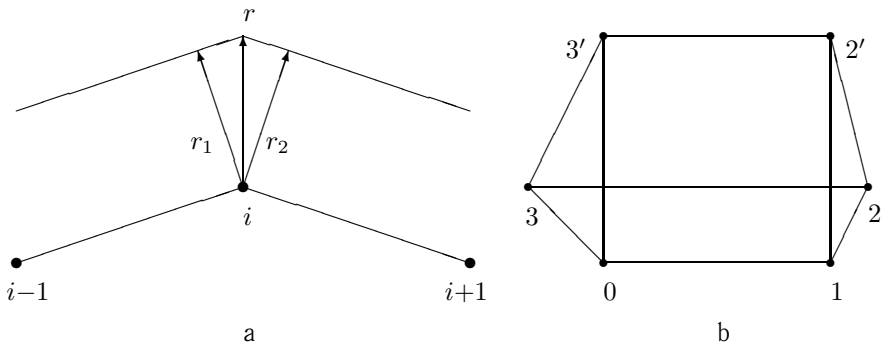

Fig. 9.3: Cell shape specification for obtaining orthogonality near boundary (a). Transformation of one cell shape to another by linear interpolation (9.8) (b).

9.5 Energy density functional

In the continuous level the energy density functional can be written as follows

$$I = \frac{1}{2}\int\int \frac{tr(G^{-1}g)}{\sqrt{\det(G^{-1}g)}}d\xi d\eta = \frac{1}{2}\int\int \frac{tr(g^{-1}G)}{\sqrt{\det(g^{-1}G)}}d\xi d\eta$$
$$= \frac{1}{2}\int\int \frac{g_{11}G_{22} - 2g_{12}G_{12} + g_{22}G_{11}}{\sqrt{\det(g)}\sqrt{\det(G)}}d\xi d\eta \ .$$

Note that the harmonic functional can be written as

$$\tilde{I} = \frac{1}{2}\int\int \frac{g_{11}G_{22} - 2g_{12}G_{12} + g_{22}G_{11}}{\sqrt{\det(g)}}d\xi d\eta.$$

Consequently, the mapping delivering minimum to the functional I will be harmonic if instead of the metric G_{ij} the "scaled" metric $\tilde{G}_{ij}{=}G_{ij}/\sqrt{det(G)}$ is used. In this case
$det(\tilde{G}){=}1$.

Consider adaptation to the function $f(x, y)$. In this case

$$g_{11} = x_\xi^2 + y_\xi^2 + (f_x x_\xi + f_y y_\xi)^2,$$

$$g_{12} = x_\xi x_\eta + y_\xi y_\eta + (f_x x_\xi + f_y y_\xi)(f_x x_\eta + f_y y_\eta) \ ,$$

$$g_{22} = x_\eta^2 + y_\eta^2 + (f_x x_\eta + f_y y_\eta)^2 \ .$$

Substituting these expressions into I, we finally obtain

$$I = \frac{1}{2} \int\int \frac{\alpha(1+f_x^2) + 2\beta f_x f_y + \gamma(1+f_y^2)}{(x_\xi y_\eta - x_\eta y_\xi)\sqrt{1+f_x^2+f_y^2}\sqrt{G_{11}G_{22} - G_{12}^2}} d\xi d\eta,$$

where

$$\alpha = x_\xi^2 G_{22} - 2x_\xi x_\eta G_{12} + x_\eta^2 G_{11} = \det(G)[(x_\xi, x_\eta)G^{-1}(x_\xi, x_\eta)^T],$$

$$\beta = x_\xi y_\xi G_{22} - (x_\xi y_\eta + x_\eta y_\xi)G_{12} + x_\eta y_\eta G_{11} = \det(G)[(x_\xi, x_\eta)G^{-1}(y_\xi, y_\eta)^T],$$

$$\gamma = y_\xi^2 G_{22} - 2y_\xi y_\eta G_{12} + y_\eta^2 G_{11} = \det(G)[(y_\xi, y_\eta)G^{-1}(y_\xi, y_\eta)^T].$$

Here G^{-1} is the matrix inverse to the matrix G.

The minimization problem for the functional is equivalent to the problem of constructing such a curvilinear coordinate system (structured grid) on the surface $z{=}f(x,y)$ that the averaged energy density for the mapping $(X,Y){\rightarrow}(x,y,f(x,y))$ is minimized. The mapping $(\xi,\eta){\rightarrow}(X,Y)$ is assumed to be known, and the metric tensor components G_{ij} are calculated as

$$G_{11} = X_\xi^2 + Y_\xi^2, \ G_{12} = X_\xi X_\eta + Y_\xi Y_\eta, \ G_{22} = X_\eta^2 + Y_\eta^2 \ .$$

In the case of an unstructured grid, the problem is posed for the energy density of the mapping of a target cell in the plane (X,Y) to the corresponding surface cell. In summary, a minimization problem is posed for the sum of functionals written for every cell, i.e., for the averaged energy density. To control the number of cells contained in a region of steep gradient, it was previously proposed to replace the function $f(x,y)$ (e.g., see [74]) by the function $c_a f(x,y)$. Here, $f(x,y)$ is scaled so that the difference of the maximal and minimal values of f equals the diagonal of the rectangle circumscribed about the domain in the plane x,y:

$$f_{max} - f_{min} = \sqrt{(x_{max} - x_{min})^2 + (y_{max} - y_{min})^2} \ .$$

The relative number of grid points, contained in a steep-gradient layer, increases with rise of the adaptation factor c_a, whose value is usually set between 0.1 and 0.5. In the case of an elliptic problem, the relative number of grid points contained in the layer is approximately equal to $c_a/(c_a{+}1)$;

that is about one-third of the points belongs to the steep-gradient layer when c_a=0.5.

Practical computations show that when a grid is adapted to a smooth function, increase of c_a makes the resulting grid "sensitive" to a larger domain of sufficiently steep gradient. Furthermore, as $c_a \to \infty$, the grid adapted to a continuously differentiable function f of one variable is optimal in the $\mathbb{C}$ norm in the sense that the $\mathbb{C}$-norm error of piecewise constant interpolation is minimized. Indeed, with f replaced by $c_a f(x)$, the one-dimensional functional (in which $G_{ij}=\delta_{ij}$) has the form

$$I = \int \frac{1}{x_\xi \sqrt{1 + c_a^2 f_x^2}} d\xi \ ,$$

and the corresponding Euler-Lagrange equation, which determines the asymptotic behavior of the Jacobian of an adaptive harmonic grid, can be written as

$$x_\xi = const(1/c_a^2 + f_x^2)^{-1/2} \ .$$

At the same time, a grid that is optimal in the $\mathbb{C}$ norm under a piecewise constant interpolation is characterized by a Jacobian asymptotically expressed as

$$x_\xi = const|f_x|^{-1} \ .$$

Therefore, the adaptive harmonic grid is optimal in the $\mathbb{C}$ norm as $c_a \to \infty$.

When an adaptive grid is to be generated for a vector function with components $f_i(x, y)$, rather than for a scalar $f(x, y)$, one can write the functional I in the following generalized form:

$$I = \frac{1}{2} \int \int \frac{\alpha \tilde{g}_{11} + 2\beta \tilde{g}_{12} + \gamma \tilde{g}_{22}}{(x_\xi y_\eta - x_\eta y_\xi) \sqrt{\tilde{g}_{11}\tilde{g}_{22} - \tilde{g}_{12}^2} \sqrt{G_{11}G_{22} - G_{12}^2}} d\xi d\eta,$$

where

$$\tilde{g}_{11} = 1 + \sum_i c_i^2 (f_i)_x^2, \quad \tilde{g}_{12} = \sum_i c_i^2 (f_i)_x (f_i)_y, \quad \tilde{g}_{22} = 1 + \sum_i c_i^2 (f_i)_y^2.$$

The minimization problem for this functional is equivalent to the problem of constructing such a coordinate system on the surface described by the vector function

$$r(x, y) = (c_1 f_1, c_2 f_2 ...)(x, y) \ ,$$

that the averaged energy density for the mapping $(X,Y)\rightarrow(x,y,r(x,y))$ is minimized. As a result one obtains a surface parametrization in the form $(x,y,c_1f_1,c_2f_2...)(\xi,\eta)$, which corresponds to a structured grid. In the case of an unstructured grid, the problem is posed for the energy density for the mapping of a given cell in the plane (X,Y) to the corresponding surface cell. When a problem in computational fluid dynamics is to be solved, $f_i(x,y)$ denote either the flow variables u,v,p,ρ or their functions (e.g., $|V|=\sqrt{u^2+v^2}$), cf. [5].

A finite-difference analogue of the functional I can be derived as follows. A square cell in the plane (ξ,η) is split into triangles by diagonals 02 and 13. The mapping of the square to a quadrilateral cell in the plane (x,y) is approximated by the half-sum of two functions that are linear on the triangles resulting from the two partitions. Denote the half-sums of these functions by $x^h(\xi,\eta)$ and $y^h(\xi,\eta)$, respectively. They define a piecewise linear mapping of a parametric square onto a quadrilateral cell. Unlike a bilinear mapping, the inverse mapping of the quadrilateral to the parametric square will then have derivatives that are discontinuous across the diagonals. Furthermore, the mapping of a square to a quadrilateral cell in the plane (X,Y) with vertices having coordinates $X_0,Y_0,\ X_1,Y_1,\ X_2,Y_2,\ X_3,Y_3$ is also approximated by the half-sum of two functions that are linear on the triangles resulting from similar partitions. All derivatives in the integrand of I are easy to calculate, and the integral over the square cell in the plane (ξ,η) is approximated by the half-sum of the integrals of the piecewise linear approximations of desired functions corresponding to the triangular partitions of the square. As a result one obtains an approximation of the integral I in the form

$$I^h=\frac{1}{2}\sum_{N=1}^{N_e}\sum_{k=0}^{3}\frac{1}{4}\left[F_k\right]_N\ ,$$

where

$$F_k=\frac{\alpha_k[1+(f_x)_k^2]+2\beta_k(f_x)_k(f_y)_k+\gamma_k[1+(f_y)_k^2]}{J_kD_k[1+(f_x)_k^2+(f_y)_k^2]^{1/2}}\ ,$$

$$\alpha_k=(x_{k+1}-x_k)^2(G_{22})_k-2(x_{k+1}-x_k)(x_{k-1}-x_k)(G_{12})_k+(x_{k-1}-x_k)^2(G_{11})_k,$$

$$\beta_k=(x_{k+1}-x_k)(y_{k+1}-y_k)(G_{22})_k-[(x_{k+1}-x_k)(y_{k-1}-y_k)$$

$$+(x_{k-1}-x_k)(y_{k+1}-y_k)](G_{12})_k+(x_{k-1}-x_k)(y_{k-1}-y_k)(G_{11})_k\ ,$$

$$\gamma_k = (y_{k+1}-y_k)^2(G_{22})_k - 2(y_{k+1}-y_k)(y_{k-1}-y_k)(G_{12})_k + (y_{k-1}-y_k)^2(G_{11})_k \ ,$$

$$J_k = (x_{k+1}-x_k)(y_{k-1}-y_k) - (x_{k-1}-x_k)(y_{k+1}-y_k) \ ,$$

$$G_{11} = (X_{k+1}-X_k)^2 + (Y_{k+1}-Y_k)^2,$$

$$G_{12} = (X_{k+1}-X_k)(X_{k-1}-X_k) + (Y_{k+1}-Y_k)(Y_{k-1}-Y_k),$$

$$G_{22} = (X_{k-1}-X_k)^2 + (Y_{k-1}-Y_k)^2,$$

$$D_k = (X_{k+1}-X_k)(Y_{k-1}-Y_k) - (X_{k-1}-X_k)(Y_{k+1}-Y_k)$$

$$= \sqrt{(G_{11})_k(G_{22})_k - (G_{12})_k^2} \ .$$

The expressions for $(f_x)_k$ and $(f_y)_k$ are the derivatives of f at the grid point locally indexed by k in the Nth cell. Approximation I^h is minimized by applying the method described in detail in [74].

9.6 Derivation of computational formulas

Four triangles are considered for the quadrilateral cell with number N. Each of these triangles corresponds to a corner with number k and gives a proper contribution to the functional and also to the values of its derivatives. Since the integrand in the functional does not depend on the rotation of the coordinate system ξ, η, then all the computational formulas will be the same for all triangles. We enumerate nodes of the triangle which corresponds to the corner with the local number k from 0 to 2 as follows:

node 2 corresponds to the local node number $k-1$ of the Nth cell,
node 0 corresponds to the local node number k of the Nth cell,
node 1 corresponds to the local node number $k+1$ of the Nth cell.
Then in the new numeration the expression for F_k will be

$$F = \frac{\alpha[1+(f_x)_k^2] + 2\beta(f_x)_k(f_y)_k + \gamma[1+(f_y)_k^2]}{2J_0D_0[1+(f_x)_k^2+(f_y)_k^2]^{1/2}},$$

where

$$\alpha = (x_1-x_0)^2G_{22} - 2(x_1-x_0)(x_2-x_0)G_{12} + (x_2-x_0)^2G_{11},$$

$$\beta = (x_1-x_0)(y_1-y_0)G_{22} - [(x_1-x_0)(y_2-y_0) + (x_2-x_0)(y_1-y_0)]G_{12}$$
$$+(x_2-x_0)(y_2-y_0)G_{11},$$

$$\gamma = (y_1-y_0)^2G_{22} - 2(y_1-y_0)(y_2-y_0)G_{12} + (y_2-y_0)^2G_{11},$$

$$J_0 = (x_1 - x_0)(y_2 - y_0) - (x_2 - x_0)(y_1 - y_0),$$
$$G_{11} = (X_1 - X_0)^2 + (Y_1 - Y_0)^2,$$
$$G_{12} = (X_1 - X_0)(X_2 - X_0) + (Y_1 - Y_0)(Y_2 - Y_0),$$
$$G_{22} = (X_2 - X_0)^2 + (Y_2 - Y_0)^2,$$
$$D_0 = (X_1 - X_0)(Y_2 - Y_0) - (X_2 - X_0)(Y_1 - Y_0)\ .$$

Introduce notations

$$U = \frac{\alpha[1 + (f_x)_k^2] + 2\beta(f_x)_k(f_y)_k + \gamma_k[1 + (f_y)_k^2]}{2D_0[1 + (f_x)_k^2 + (f_y)_k^2]^{1/2}}\ ,$$
$$V = (x_1 - x_0)(y_2 - y_0) - (x_2 - x_0)(y_1 - y_0)\ .$$

We use the chain rule for the derivatives of two functions ratio

$$F = \frac{U}{V},$$
$$F_x = \frac{U_x - FV_x}{V}, \quad F_y = \frac{U_y - FV_y}{V},$$
$$F_{xx} = \frac{U_{xx} - 2F_xV_x - FV_{xx}}{V},$$
$$F_{yy} = \frac{U_{yy} - 2F_yV_y - FV_{yy}}{V},$$
$$F_{xy} = F_{yx} = \frac{U_{xy} - F_xV_y - F_yV_x - FV_{xy}}{V}.$$

For the triangle vertex with number 1 we should substitute appropriate expressions instead of U and V, U_x and V_x, etc. and replace x and y by x_1 and y_1.

$$V_x = y_2 - y_0, \quad V_y = x_0 - x_2,$$
$$U_x = \Big([1 + (f_x)_k^2][(x_1 - x_0)G_{22} - (x_2 - x_0)G_{12}] + (f_x)_k(f_y)_k\times$$
$$[(y_1 - y_0)G_{22} - (y_2 - y_0)G_{12}]\Big)\Big/\Big(D_0[1 + (f_x)_k^2 + (f_y)_k^2]^{1/2}\Big)\ ,$$
$$U_y = \Big([1 + (f_y)_k^2][(y_1 - y_0)G_{22} - (y_2 - y_0)G_{12}] + (f_x)_k(f_y)_k\times$$
$$[(x_1 - x_0)G_{22} - (x_2 - x_0)G_{12}]\Big)\Big/\Big(D_0[1 + (f_x)_k^2 + (f_y)_k^2]^{1/2}\Big)\ ,$$

$$U_{xx} = \frac{[1+(f_x)_k^2]G_{22}}{D_0[1+(f_x)_k^2+(f_y)_k^2]^{1/2}}\ , \quad U_{xy} = \frac{(f_x)_k(f_y)_k G_{22}}{D_0[1+(f_x)_k^2+(f_y)_k^2]^{1/2}}\ ,$$

$$U_{yy} = \frac{[1+(f_y)_k^2]G_{22}}{D_0[1+(f_x)_k^2+(f_y)_k^2]^{1/2}},$$

$$V_{xx} = 0, \quad V_{xy} = 0, \quad V_{yy} = 0.$$

For vertex 0 we have

$$V_x = y_1 - y_2, \quad V_y = x_2 - x_1,$$

$$U_x = \frac{[1+(f_x)_k^2][(x_0-x_1)G_{22} - (2x_0 - x_1 - x_2)G_{12} + (x_0 - x_2)G_{11}]}{D_2[1+(f_x)_k^2+(f_y)_k^2]^{1/2}} +$$

$$\frac{(f_x)_k(f_y)_k[(y_0-y_1)G_{22} - (2y_0 - y_1 - y_2)G_{12} + (y_0 - y_2)G_{11}]}{D_0[1+(f_x)_k^2+(f_y)_k^2]^{1/2}},$$

$$U_y = \frac{[1+(f_y)_k^2][(y_0-y_1)G_{22} - (2y_0 - y_1 - y_2)G_{12} + (y_0 - y_2)G_{11}]}{D_0[1+(f_x)_k^2+(f_y)_k^2]^{1/2}} +$$

$$\frac{(f_x)_k(f_y)_k[(x_0-x_1)G_{22} - (2x_0 - x_1 - x_2)G_{12} + (x_0 - x_2)G_{11}]}{D_0[1+(f_x)_k^2+(f_y)_k^2]^{1/2}},$$

$$U_{xx} = \frac{[1+(f_x)_k^2](G_{11} - 2G_{12} + G_{22})}{D_0[1+(f_x)_k^2+(f_y)_k^2]^{1/2}},$$

$$U_{xy} = \frac{(f_x)_k(f_y)_k(G_{11} - 2G_{12} + G_{22})}{D_0[1+(f_x)_k^2+(f_y)_k^2]^{1/2}},$$

$$U_{yy} = \frac{[1+(f_y)_k^2](G_{11} - 2G_{12} + G_{22})}{D_0[1+(f_x)_k^2+(f_y)_k^2]^{1/2}},$$

$$V_{xx} = 0, \quad V_{xy} = 0, \quad V_{yy} = 0.$$

For vertex 2 we have

$$V_x = y_0 - y_1, \quad V_y = x_1 - x_0,$$

$$U_x = \Big([1+(f_x)_k^2][(x_2-x_0)G_{11} - (x_1-x_0)G_{12}] + (f_x)_k(f_y)_k \times$$

$$[(y_2-y_0)G_{11} - (y_1-y_0)G_{12}] \Big/ \Big(D_0[1+(f_x)_k^2+(f_y)_k^2]^{1/2}\Big)\ ,$$

$$U_y = \Big(1 + (f_y)_k^2][(y_2 - y_0)G_{11} - (y_1 - y_0)G_{12}] + (f_x)_k(f_y)_k \times$$

$$[(x_2 - x_0)G_{11} - (x_1 - x_0)G_{12}]\Big/\Big(D_0[1 + (f_x)_k^2 + (f_y)_k^2]^{1/2}\Big) \ ,$$

$$U_{xx} = \frac{[1 + (f_x)_k^2]G_{11}}{D_0[1 + (f_x)_k^2 + (f_y)_k^2]^{1/2}} \ , \quad U_{xy} = \frac{(f_x)_k(f_y)_k G_{11}}{D_0[1 + (f_x)_k^2 + (f_y)_k^2]^{1/2}} \ ,$$

$$U_{yy} = \frac{[1 + (f_y)_k^2]G_{11}}{D_0[1 + (f_x)_k^2 + (f_y)_k^2]^{1/2}},$$

$$V_{xx} = 0, \quad V_{xy} = 0, \quad V_{yy} = 0.$$

Computations are performed as follows. Let F and its derivatives with respect to x_1 and y_1 be computed using the formulas for the Nth cell and kth triangle. Then the computed values are added to the appropriate array elements

$$I^h += F, \quad [R_x]_n += F_x, \quad [R_y]_n += F_y,$$
$$[R_{xx}]_n += F_{xx}, \quad [R_{xy}]_n += F_{xy}, \quad [R_{yy}]_n += F_{yy},$$

where $n{=}n(N, k{+}1)$.

Similarly to vertex 0, correspondence between the local and global number is $n{=}n(N, k)$.

Similarly to vertex 2, correspondence between the local and global number is $n = n(N, k{-}1)$.

Derivatives $[f_x]_n$ and $[f_y]_n$ are computed as follow. All triangles of the mesh are scanned and for the triangle number k of the Nth cell the following values are computed

$$f_x = (f_1 - f_0)(y_2 - y_0) - (f_2 - f_0)(y_1 - y_0),$$
$$f_y = (x_1 - x_0)(f_2 - f_0) - (x_2 - x_0)(f_1 - f_0),$$
$$J_0 = (x_1 - x_0)(y_2 - y_0) - (x_2 - x_0)(y_1 - y_0).$$

Here f_0, f_1, f_2 are the values of the function f at the triangle vertices, numbered as 2,0,1, with respect to local numbers of corners $k{-}1$, k, $k{+}1$ of a quadrilateral cell. Computed values are added to the corresponding array elements (which were first cleared)

$$[f_x]_n += f_x \ , \quad [f_y]_n += f_y \ , \quad [J]_n += J_0 \ , \quad n = n(N, k) \ .$$

New values of derivatives are computed as follows

$$[f_x]_n/ = [J]_n \ , \quad [f_y]_n/ = [J]_n \ .$$

Here $a{+}{=}b$ means that the new value of a becomes equal to $a{+}b$, and $a/{=}b$ means that the new value of a becomes equal to a/b.

In the case of adaptation to the vector-function we replace

$$[1+(f_x)_k^2] \ \text{ by } \ \tilde{g}_{11}, \quad [(f_x)_k(f_y)_k] \ \text{ by } \ \tilde{g}_{12}, \quad [1+(f_y)_k^2] \ \text{ by } \ \tilde{g}_{22},$$

$$\text{and } \ \sqrt{1+(f_x)_k^2+(f_y)_k^2} \ \text{ by } \ \sqrt{\tilde{g}_{11}\tilde{g}_{22}-\tilde{g}_{12}^2}.$$

Here $\tilde{g}_{11}$, $\tilde{g}_{12}$, and $\tilde{g}_{22}$ are computed by using the formulas from Section 9.5.

9.7 Three-dimensional case

Similarly to the 2D case consider a linear mapping $(X,Y,Z){\to}(x,y,z)$, where $(\xi,\eta,\mu){\to}(X,Y,Z)$ and $(\xi,\eta,\mu){\to}(x,y,z)$ are two linear transformations with matrices C and c. The characteristic equation for the matrix $(C^{-1})^T c^T c C^{-1}$ has the same solutions $\lambda_{1,2,3}$ as the characteristic equation for the pair of quadratic forms

$$\det(g-\lambda G) = \det(G)\det(G^{-1}g-\lambda E) = 0,$$

where $g{=}c^T c$, $G{=}C^T C$.

The energy density of a linear transformation is defined as an averaged energy stored in the right-angled parallelepiped of a unit volume, provided that the parallelepiped is the image of a cube. Similarly to the 2D case it can be shown that for any linear transformation there exists such a unit cube, which is transformed to a right-angled parallelepiped with lengths of sides equal to $\sqrt{\lambda_1}$, $\sqrt{\lambda_2}$, and $\sqrt{\lambda_3}$. In contrast to the 2D case, the energy densities are different for the direct and inverse transformations

$$e^+ = e(x,y,z)(X,Y,Z) = \frac{1}{3}\frac{\lambda_1+\lambda_2+\lambda_3}{(\lambda_1\lambda_2\lambda_3)^{1/3}} = \frac{1}{3}\frac{tr(G^{-1}g)}{(\det(G^{-1}g))^{1/3}} \ ,$$

$$e^- = e(X,Y,Z)(x,y,z) = \frac{1}{3}\frac{\lambda_1\lambda_2+\lambda_1\lambda_3+\lambda_2\lambda_3}{(\lambda_1\lambda_2\lambda_3)^{2/3}} = \frac{1}{3}\frac{tr(g^{-1}G)}{(\det(g^{-1}G))^{1/3}} \ .$$

It is easy to see that the inverse quantities $1/e^+$ and $1/e^-$ are tetrahedron shape measures according to the definition from [41, 95].

The condition number k of the matrix cC^{-1}

$$k^2 = \|cC^{-1}\|^2\|Cc^{-1}\|^2 = tr(G^{-1}g)tr(g^{-1}G)$$
$$= (\lambda_1+\lambda_2+\lambda_3)\left(\lambda_1^{-1}+\lambda_2^{-1}+\lambda_3^{-1}\right) ,$$

was introduces in [88]. It is easy to see that the condition number k is proportional to the geometric mean of energy densities of direct and inverse transformations, i.e., $k^2{=}9e^+e^-$. Using the inequality

$$3(\lambda_1\lambda_2+\lambda_1\lambda_3+\lambda_2\lambda_3) \le (\lambda_1+\lambda_2+\lambda_3)^2$$

we can obtain the following estimates for the condition number

$$9(e^-)^{3/2} = \frac{\sqrt{3}(\lambda_1\lambda_2+\lambda_1\lambda_3+\lambda_2\lambda_3)^{3/2}}{\lambda_1\lambda_2\lambda_3} \le k^2 \le \frac{(\lambda_1+\lambda_2+\lambda_3)^3}{3\lambda_1\lambda_2\lambda_3} = 9(e^+)^3 .$$

Consider energy densities for tetrahedra. Let a tetrahedron in space (x,y,z) be defined such that one of vertices $r_0{=}0$, the other vertices be defined by three vectors r_1, r_2, and r_3. Similarly a tetrahedron in space (X,Y,Z) is defined by $R_0{=}0$, R_1, R_2, and R_3. If the tetrahedron in space (X,Y,Z) is formed by orthogonal vectors of the unit length, then the energy densities for the direct and inverse transformations are the following

$$e^+ = \frac{1}{3}\frac{r_1^2+r_2^2+r_3^2}{V^{2/3}}, \qquad e^- = \frac{1}{3}\frac{(r_1\times r_2)^2+(r_2\times r_3)^2+(r_3\times r_1)^2}{V^{4/3}},$$

where

$$V = r_3\cdot(r_1\times r_2)$$

is the triple tetrahedron volume. For the equilateral objective tetrahedron in space (X,Y,Z) it is easy to obtain that the energy density of the direct transformation is inverse to the mean ratio, defined in [41]

$$e^+ = \frac{(r_1-r_2)^2+(r_2-r_3)^2+(r_1-r_3)^2+r_1^2+r_2^2+r_3^2}{12V^{2/3}} .$$

The energy density of the inverse transformation e^- is proportional to the ratio of the sum of squared areas of all faces to the corresponding degree of the volume.

The energy density of a hexahedron can be defined similarly to the 2D case as a sum of 8 energy densities e^+ of the corner tetrahedrons. In this case the procedure of minimization of the corresponding functional is also the same as in 2D, only expressions are more cumbersome. This functional possesses a barrier property, associated with conditions of positive volumes of all corner tetrahedrons for all hexahedral grid cells.

Chapter 10

Optimality principle for nondegenerate grids

10.1 Equidistribution principle

In one space dimension for grid generation it was developed the equidistribution principle, cf. [143]. The idea is that the Jacobian of the mapping multiplied by some positive weight function is set equal to a positive constant

$$\omega x_\xi = const > 0 \ , \quad \omega(\xi) > 0 \ , \quad \xi \in (0,1) \ , \tag{10.1a}$$

and the mapping $x(\xi)$ satisfies the boundary conditions

$$x(0) = 0 \ , \quad x(1) = 1 \ . \tag{10.1b}$$

Instead of (10.1a) we may consider the minimization problem for the functional

$$F = \int_0^1 \omega x_\xi^2 d\xi \ , \tag{10.2}$$

on the class of the functions $x(\xi)$ satisfying the boundary conditions (10.1b). By differentiating (10.1a) with respect to ξ we get the Euler equation to the functional

$$(\omega x_\xi)_\xi = 0 \ . \tag{10.3}$$

In practice all the adaptive methods are reduced to the equidistribution principle. This is due to the function $x(\xi)$, being the solution of (10.3) with

the boundary conditions (10.1*b*), is one-to-one mapping $\xi \to x$, since from (10.1*a*) it follows that the Jacobian is positive. On the other hand, for any smooth one-to-one mapping $x^*(\xi)$ with the positive Jacobian we can define the weight function $w = const(x^*_\xi)^{-1}$ and then $x^*(\xi)$ will satisfy the equation (10.3). Therefore, both the variation formulation of minimizing the functional (10.2) and the Euler equation (10.3) include as solutions all smooth one-to-one mappings with positive Jacobian. A mapping, being not one-to-one, can not satisfy the equation (10.3) with a positive weight function.

There are many attempts to extend the equidistribution principle to the two-dimensional case. As one of many possible approaches the following system may be considered as the 2D extension

$$(\omega_1 x_\xi)_\xi + (\omega_2 x_\eta)_\eta = 0 \ ,$$

$$(\omega_1 y_\xi)_\xi + (\omega_2 y_\eta)_\eta = 0 \ .$$

However, the class of all solutions of these equations with positive ω_1 and ω_2 contains functions $x(\xi,\eta)$, $y(\xi,\eta)$ which cannot ensure that the mapping to be a homeomorphism.

10.2 Formulation of variational principle

Consider the problem of constructing a smooth mapping of the parametric square

$$Q = \{(\xi,\eta): \quad 0 < \xi < 1, \ 0 < \eta < 1\}$$

onto an arbitrary domain Ω with the given transformation between the boundaries

$$(x_\Gamma, y_\Gamma) : \partial Q \to \partial\Omega \ ,$$

where x_Γ, y_Γ are given functions such that the resulting mapping $x(\xi,\eta)$, $y(\xi,\eta)$ is invertible.

The energy density functional is given by

$$F = \frac{1}{2}\int_0^1\int_0^1 \frac{(x_\xi^2 + y_\xi^2)G_{22} - 2(x_\xi x_\eta + y_\xi y_\eta)G_{12} + (x_\eta^2 + y_\eta^2)G_{11}}{(x_\xi y_\eta - x_\eta y_\xi)\sqrt{G_{11}G_{22} - G_{12}^2}} d\xi d\eta \ .$$

Here $\{G_{lm},\, l,m{=}1,2\}$ are the elements of the symmetric and positive definite matrix $G(\xi,\eta){=}G^T{>}0$.

Consider the metric $g=(g_{lm})$ of the transformation $x(\xi,\eta)$, $y(\xi,\eta)$ with the elements

$$g_{11}=x_\xi^2+y_\xi^2\ ,\quad g_{12}=g_{21}=x_\xi x_\eta+y_\xi y_\eta\ ,\quad g_{22}=x_\eta^2+y_\eta^2\ .$$

The integrand in the above integral can be written as

$$\frac{1}{2}\frac{tr(G^{-1}g)}{\sqrt{\det(G^{-1}g)}}=\frac{1}{2}\frac{\lambda_1+\lambda_2}{\sqrt{\lambda_1\lambda_2}}\geq 1\ ,$$

where λ_1 and λ_2 are the eigenvalues of the matrix $G^{-1}g$. The equality is attained if and only if $\lambda_1=\lambda_2$. Then it follows that $F\geq 1$ and $F=1$ if and only if

$$G_{lm}=\alpha(\xi,\eta)g_{lm}\ ,$$

where $\alpha(\xi,\eta)$ is an arbitrary smooth function defined in the unit square.

Instead of G it is convenient to introduce the matrix $\tilde{G}$ with the elements $\tilde{G}_{lm}=G_{lm}/\sqrt{\det(G)}$, such that $\det(\tilde{G})=1$. The functional takes the form

$$F=\frac{1}{2}\int_0^1\int_0^1\frac{(x_\xi^2+y_\xi^2)\tilde{G}_{22}-2(x_\xi x_\eta+y_\xi y_\eta)\tilde{G}_{12}+(x_\eta^2+y_\eta^2)\tilde{G}_{11}}{x_\xi y_\eta-x_\eta y_\xi}d\xi d\eta. \quad (10.4)$$

The corresponding Euler equations for this functional can be written as[1]

$$\alpha x_{\xi\xi}-2\beta x_{\xi\eta}+\gamma x_{\eta\eta}=x_\xi(-P\tilde{G}_{22}+Q\tilde{G}_{12})+x_\eta(P\tilde{G}_{12}-Q\tilde{G}_{11})\ ,$$

$$\alpha y_{\xi\xi}-2\beta y_{\xi\eta}+\gamma y_{\eta\eta}=y_\xi(-P\tilde{G}_{22}+Q\tilde{G}_{12})+y_\eta(P\tilde{G}_{12}-Q\tilde{G}_{11})\ ,$$

where

$$\alpha=x_\eta^2+y_\eta^2\ ,\quad \beta=x_\xi x_\eta+y_\xi y_\eta\ ,\quad \gamma=x_\xi^2+y_\xi^2\ ,$$

$$P=\frac{1}{2}\left(\alpha\frac{\partial\tilde{G}_{11}}{\partial\xi}-2\beta\frac{\partial\tilde{G}_{12}}{\partial\xi}+\gamma\frac{\partial\tilde{G}_{22}}{\partial\xi}\right),\ Q=\frac{1}{2}\left(\alpha\frac{\partial\tilde{G}_{11}}{\partial\eta}-2\beta\frac{\partial\tilde{G}_{12}}{\partial\eta}+\gamma\frac{\partial\tilde{G}_{22}}{\partial\eta}\right).$$

Consider the class of all homeomorphisms from the unit square onto a domain Ω, satisfying the same boundary conditions as $(x_\Gamma,y_\Gamma):\to\partial\Omega$.

[1]This form of the Euler equations is incorrect. Correct Euler equations are given in [11] (Editor).

Recall that $(x_\Gamma, y_\Gamma) : \partial Q \to \partial\Omega$ is a homeomorphism between the boundaries. We formulate the conjecture in the form of the

Optimality principle. *A smooth mapping from the unit square Q onto a domain Ω is a homeomorphism if and only if it is the minimum of the functional (10.4) for some symmetric and positive definite matrix-function G.*

10.3 Discrete case

On a simply connected domain Ω in the plane x, y a grid $\{(x,y)_{ij}, i{=}1,\dots,i^*;\ j{=}1,\dots,j^*\}$ must be constructed with given coordinates of boundary nodes $(x,y)_{i1}$, $(x,y)_{ij^*}$, $(x,y)_{1j}$, $(x,y)_{i^*j}$.

Discrete analog of Jacobian positiveness may be written as inequalities

$$[J_k]_{i+1/2,j+1/2} > 0,\ k = 0,1,2,3;\ i = 1,\dots,i^*-1;\ j = 1,\dots,j^*-1\ ,$$

where

$$J_k = (x_{k+1} - x_k)(y_{k-1} - y_k) - (y_{k+1} - y_k)(x_{k-1} - x_k),$$

index k is cyclic.

The class of unfolded grids, with convex quadrilateral cells, satisfying the conditions for the Jacobian we denote as W_D.

Discrete analog of the functional (10.4) is

$$F^h = \frac{1}{(i^*-1)(j^*-1)} \sum_{i=1}^{i^*-1} \sum_{j=1}^{j^*-1} \sum_{k=0}^{3} \frac{1}{4} [F_k]_{i+1/2,j+1/2}\ , \qquad (10.5a)$$

$$F_k = \frac{(r_{k+1}-r_k)^2(\tilde{G}_{22})_k - 2(r_{k+1}-r_k)(r_{k-1}-r_k)(\tilde{G}_{12})_k + (r_{k-1}-r_k)^2(\tilde{G}_{11})_k}{2[(x_{k+1} - x_k)(y_{k-1} - y_k) - (y_{k+1} - y_k)(x_{k-1} - x_k)]}, \qquad (10.5b)$$

where

$$r_k = (x_k, y_k)^T,\ (r_{k+1} - r_k)^2 = (x_{k+1} - x_k)^2 + (y_{k+1} - y_k)^2,$$
$$(r_{k+1} - r_k)(r_{k-1} - r_k) = (x_{k+1} - x_k)(x_{k-1} - x_k) + (y_{k+1} - y_k)(y_{k-1} - y_k),$$
$$(r_{k-1} - r_k)^2 = (x_{k-1} - x_k)^2 + (y_{k-1} - y_k)^2\ ,$$

$(\tilde{G}_{lm})_k$ are the elements of the matrix $\tilde{G}_k=\tilde{G}_k^T>0$, $\det(\tilde{G}_k)=1$, referred to as a triangle with number k of the cell $i+1/2, j+1/2$.

Consider the set of symmetric positive definite matrices g_k with the elements

$$(g_{11})_k = (r_{k+1} - r_k)^2 \ , \quad (g_{12})_k = (g_{21})_k = (r_{k+1} - r_k)(r_{k-1} - r_k) \ ,$$

$$(g_{22})_k = (r_{k-1} - r_k)^2 \ . \tag{10.6}$$

Substituting (10.6) into (10.5) we obtain

$$F_k = \frac{tr(\tilde{G}_k^{-1} g_k)}{2\sqrt{\det(\tilde{G}_k^{-1} g_k)}} = \frac{\lambda_1 + \lambda_2}{2\sqrt{\lambda_1 \lambda_2}} \geq 1,$$

where λ_1 and λ_2 are the eigenvalues of the matrix $\tilde{G}_k^{-1} g_k$. The strict equality is attained if and only if $\lambda_1 = \lambda_2$. From this it follows that $F_k \geq 1$ and $F_k = 1$ if and only if

$$(\tilde{G}_{lm})_k = (g_{lm})_k / \sqrt{\det(g_k)}.$$

The function F^h possesses the barrier property.

Lemma *For any set of symmetric and positive definite matrices at every cell* $\{\tilde{G}_k(ij),\ k=0,1,2,3;\ i=1,\ldots,i^*-1;\ j=1,\ldots,j^*-1\}$ *such that* $\det(\tilde{G}_k)=1$, *the function* F^h *has an infinite barrier on the boundary of the class of unfolded grids* W_D, *i.e., if in a cell the area of one of the triangles tends to zero, at the same time remaining positive, then* $F^h \to +\infty$.

Proof. Assume that $J_k \to 0$ in some cell while F^h does not tend to $+\infty$. Then the numerator in (10.5b) must tend to zero as well. From this and inequality

$$(r_{k+1} - r_k)^2 (\tilde{G}_{22})_k - 2(r_{k+1} - r_k)(r_{k-1} - r_k)(\tilde{G}_{12})_k + (r_{k-1} - r_k)^2 (\tilde{G}_{11})_k \geq$$
$$\lambda_{min}(\tilde{G}_k) \left[(r_{k+1} - r_k)^2 + (r_{k-1} - r_k)^2\right]$$

it follows that the lengths of two corresponding sides of the cell tend to zero, and, consequently, the areas of all triangles, including these sides, tend to zero as well. Reiterating this argumentation as many as necessary one finds that the lengths of all sides of all cells must tend to zero. In other words the grid will shrink to a point, and this contradicts the boundary conditions (the boundary grid nodes belong to the domain boundary).

10.4 Discrete form of optimality principle

The discrete counterpart of the optimality principle is given by the following theorem.

Theorem. *A structured grid, constructed on a domain Ω for the given coordinates of the boundary nodes is an element of the class of unfolded grids W_D if and only if it is the minimum of the functional F^h for some set of symmetric and positive definite matrices $\tilde{G}_k(ij)$, such that* $\det(\tilde{G}_k)$=1.

Proof of the necessity. Let a grid satisfying inequalities

$$[J_k]_{i+1/2,j+1/2} > 0,\ k = 0,1,2,3;\ i = 1,\ldots,i^*-1;\ j = 1,\ldots,j^*-1\ ,$$

be given. Let in every cell four matrices $\tilde{G}_k$, k=0, 1, 2, 3 be introduced as

$$(\tilde{G}_{11})_k = (r_{k+1}-r_k)^2,\ (\tilde{G}_{12})_k = (g_{21})_k = (r_{k+1}-r_k)(r_{k-1}-r_k)\ ,$$
$$(\tilde{G}_{22})_k = (r_{k-1}-r_k)^2\ .$$

It is easy to see that

$$F_k = \frac{tr(\tilde{G}_k^{-1}g_k)}{2\sqrt{\tilde{G}_k^{-1}\det(g_k)}} = \frac{tr(g_k^{-1}g_k)}{2\sqrt{\det(g_k^{-1}g_k)}} = 1\ .$$

Consequently, for every grid from W_D there exists such a set of matrices $\tilde{G}_k(ij)$ that F^h takes a minimal value equal 1. Let us show that the grid, which corresponds to a minimum F^h=1, is unique.

Indeed, if F^h=1, then each term takes the minimal possible value equal to F_k=1. Considering the sum of four terms for one cell we can see that if coordinates of two adjacent vertices are specified, the last two are determined uniquely from the conditions

$$F_k = 1,\quad k = 0,1,2,3.$$

Hence, in this case the grid can be constructed sequentially, starting from the boundary. The constructed grid is unique.

Proof of the sufficiency. The function F^h is bounded from below and has a barrier on the boundary of the set of unfolded grids according to the Lemma of the barrier property. Since it is a continuous function, there exists at least one grid which is the minimum of F^h and the equations (the necessary conditions of minimum)

$$\partial F^h/\partial x_{ij} = 0\ ,\quad \partial F^h/\partial y_{ij} = 0\ ,$$

have at least one solution which is an unfolded grid. This completes the proof.

10.5 Conformal invariants

Consider a smooth one-to-one mapping

$$x(\xi) : \mathcal{R}^n \to \mathcal{R}^n \ , \quad x = (x^1, \ldots, x^n)^T \ , \quad \xi = (\xi^1, \ldots, \xi^n)^T \ .$$

The elements of the Jacobi matrix a are

$$a_j^i = \frac{\partial x^i}{\partial \xi^j} \ .$$

The metric tensor g corresponding to the mapping $x(\xi)$ is

$$g_{ij}(\xi) = \sum_{m=1}^{n} \frac{\partial x^m}{\partial \xi^i} \frac{\partial x^m}{\partial \xi^j} = \sum_{m=1}^{n} a_i^m a_j^m,$$

or in matrix form

$$g = a^T a \ .$$

If $\det a \neq 0$, the symmetric matrix g will be positive definite. The element of the length $(dx)^2=(dx^1)^2 + \cdots + (dx^n)^2$ is defined with the use of $d\xi=(d\xi^1, \ldots, d\xi^n)^T$ as follows

$$(dx)^2 = \sum_{i=1}^{n} (dx^i)^2 = g_{ij}(\xi) d\xi^i d\xi^j \ . \tag{10.7}$$

After the change of variables $\xi=\xi(\eta)$ it is transformed to

$$(dx)^2 = \tilde{g}_{ij}(\eta) d\eta^i d\eta^j \ ,$$

where

$$\tilde{g}_{ij}(\eta) = g_{km}(\xi(\eta)) \frac{\partial \xi^k}{\partial \eta^i} \frac{\partial \xi^m}{\partial \eta^j} \ .$$

It is known that

$$(dx)^2 = \sum_{i=1}^{n} \lambda_i (d\eta^i)^2,$$

where $\lambda_i>0$ are the eigenvalues of the matrix g. For the change of variables $\xi=\xi(\eta)$ such that at every point the Jacobi matrix $b = (b^i_j)=(\partial\xi^i/\partial\eta^j)$ is continuous and orthogonal, this change $\xi=\xi(\eta)$ is linear orthogonal transformation $b=const$. The condition of orthogonality is $b^Tb=I$, where I is the identity matrix.

The eigenvalues of the matrix g are determined from the characteristic equation

$$\det(g-\lambda I)=0\ ,$$

which can be rewritten in the form

$$\lambda^n+O_1\lambda^{n-1}+\cdots+O_n=0\ . \tag{10.8}$$

Since the matrix g is symmetric and positive definite, the algebraic equation (10.8) has n real roots $\lambda_i>0$, $i=1,2,\ldots,n$. The coefficients of (10.8) are called orthogonal invariants O_k of the metric g or quadric form (10.7). Invariant O_k is a sum of the determinants of the major minors obtained from the matrix g by deleting of $n-k$ strings and columns. In particular we have that

$$O_1=tr(g)=\sum_{i=1}^n g_{ii}=\sum_{i=1}^n\lambda_i\ ,\quad O_n=\det g=(\det a)^2=\lambda_1\ldots\lambda_n.$$

Consider the "normalized" characteristic equation to $\tilde\lambda$

$$\tilde\lambda=\lambda/(\det g)^{1/n}=\lambda/(\lambda_1\ldots\lambda_n)^{1/n}\ ,$$

which can be written as

$$\det\left(\frac{g}{(\det g)^{1/n}}-\tilde\lambda I\right)=0\ ,$$

or in the equivalent form

$$\tilde\lambda^n+C_1\tilde\lambda^{n-1}+C_2\tilde\lambda^{n-2}+\cdots+1=0\ .$$

The value $C_k=O_k/O_n^{k/n}$ is called a conformal invariant of the metric g because it does not change under invertible conformal transforms $\xi=\xi(\eta)$, being the superposition of the orthogonal transformation and dilatation of the coordinate system by factor of α. Since for the inverse mapping $\xi=\xi(x)$

the eigenvalues $\lambda_i(g^{-}1)=1/\lambda_i(g)$, then C_k are invariant under the invertible conformal transforms $y=y(x)$ as well. Obviously, that any smooth functions of the conformal invariants are the conformal invariants. Similar is true for the orthogonal invariants.

The following relations between the conformal and orthogonal invariants are valid

$$O_{n-k}(g^{-1}) = \frac{O_k(g)}{O_n(g)} \ ,$$

$$C_{n-k}(g^{-1}) = \frac{O_{n-k}(g^{-1})}{O_n(g^{-1})^{(n-k)/n}} = \frac{O_k(g)}{O_n(g)O_n(g)^{(k-n)/n}} = C_k(g) \ .$$

Therefore, all invariants of the inverse mapping can be expressed in the explicit form through the invariants of the direct mapping and, consequently, through the elements of the matrix g. Further we will use only the invariants $O_k(g)$ and $C_k(g)$.

Number of independent conformal invariants is equal $n-1$. Therefore, in the 2D case there is one conformal invariant and two conformal invariants in the 3D case. In the 1D case any transformation is conformal, therefore, the concept of conformal invariant is senseless.

The conformal invariant C_k is equal to n multiplied by a ratio of the arithmetic mean of all possible products of k different λ_i to their geometric mean, consequently,

$$C_k/n \geq 1, \qquad k = 1, \ldots, n-1 \ .$$

Hence, if the mapping $x=x(\xi)$ is conformal (i.e. if all λ_i are equal to each other), then C_k takes the least possible value equal n.

At present the values $O_k(g)$ and $C_k(g)$ at $n=3$ are applied to grid quality estimate. Moreover, functionals depending on these quantities are used for grid deformation.

10.6 Dirichlet type functionals

The problem of regular grid generation is considered as a discrete analog of the problem on finding a homeomorphic mapping of come canonical domain (e.g. a unit cube) onto a countable domain when the mapping between the boundaries is defined. The general form of the functionals, invariant under

orthogonal transformations for the direct $x(\xi)$ and inverse $\xi(x)$ mapping, is

$$F_o(x(\xi)) = \int f_1(O_1, \ldots, O_n) d\xi^1 \ldots d\xi^n,$$

$$F_o(\xi(x)) = \int f_2(O_1, \ldots, O_n) (\det g)^{1/2} d\xi^1 \ldots d\xi^n = \int f_2(O_1, \ldots, O_n) dx^1 \ldots dx^n.$$

Here f_1, f_2 are some given functions of invariants. Note that these functionals do not change at orthogonal transformations of the both coordinates ξ and x. This is due to the Jacobian of transformation is the orthogonal invariant.

The general form of the functionals, invariant under conformal transformations for the direct $x(\xi)$ and inverse $\xi(x)$ mapping, is

$$F_c(x(\xi)) = \int f_1(C_1, \ldots, C_n) d\xi^1 \ldots d\xi^n, \tag{10.9}$$

$$F_c(\xi(x)) = \int f_2(C_1, \ldots, C_n) (\det g)^{1/2} d\xi^1 \ldots d\xi^n$$

$$= \int f_2(C_1, \ldots, C_n) dx^1 \ldots dx^n \ . \tag{10.10}$$

It is easy to see that the functional (10.9) is invariant under conformal transformations of the coordinates x and (10.10) is invariant under conformal transformations of the coordinates ξ. The integrands in these functionals differ by a factor of $(\det\ g)^{1/2}$, the Jacobian of the transformation $x(\xi)$ is not the conformal invariant. Consequently, there are no functionals invariant under conformal transformations of the coordinates x and ξ simultaneously.

If the functional is invariant under some class of transformations of the coordinates ξ, consequently, the Euler equations to this functional are invariant under this class of transformations. Therefore, if $x(\xi)$ is an extremal of the functional and $y(\eta)$ is an extremal of the same functional, written in new coordinates in the case of the transformation $\xi = \xi(\eta)$ from this class, then a new solution is obtained by a simple change of variables $y(\eta) = x(\xi(\eta))$. The same is valid for the functionals invariant under some class of transformations of the coordinates x. If $x(\xi)$ is an extremal of a functional of the same kind upon the coordinate transformation $\tilde{y} = \tilde{y}(x)$, under which the functional is invariant, then a new solution is obtained by change of the variables $y(\xi) = \tilde{y}(x(\xi))$.

Examples.

1. Dirichlet functionals in the case $n = 2$.

$$F(x(\xi,\eta), y(\xi,\eta)) = \int (x_\xi^2 + y_\xi^2 + x_\eta^2 + y_\eta^2) d\xi d\eta \ , \tag{10.11}$$

where $x_\xi = \partial x/\partial\xi$, etc.

The conformal invariant is equal to the integrand in (10.11) divided by the Jacobian

$$C = \frac{x_\xi^2 + y_\xi^2 + x_\eta^2 + y_\eta^2}{x_\xi y_\eta - x_\xi y_\eta} \ .$$

Consequently, the integral (10.11) is the functional of kind (10.10) and, therefore, it is invariant under conformal transformations of the plane (ξ, η).

For the inverse mapping $\xi(x, y)$, $\eta(x, y)$, the Dirichlet functional is

$$F(\xi(x,y), \eta(x,y)) = \int (\xi_x^2 + \eta_x^2 + \xi_y^2 + \eta_y^2) dx dy$$

$$= \int \frac{x_\xi^2 + y_\xi^2 + x_\eta^2 + y_\eta^2}{x_\xi y_\eta - x_\xi y_\eta} d\xi d\eta \ , \tag{10.12}$$

The integrand in (10.12) is the conformal invariant, therefore, the Dirichlet functional for the inverse mapping is the functional of kind (10.9) and, therefore, it is invariant under conformal transformations of the plane (x, y).

2. Dirichlet functionals in the case $n > 2$. For n-dimensional mappings $x = x(\xi)$ the Dirichlet functional is expressed in terms of the first orthogonal invariant

$$F(x(\xi)) = \int O_1 d\xi^1 \dots d\xi^n = \int \sum_{i,j=1}^{n} \left(\frac{\partial x^i}{\partial \xi^j} \right)^2 d\xi^1 \dots d\xi^n \ .$$

It is easy to see that this functional can be represented neither in form of (10.9) nor (10.10); therefore it is not invariant under conformal transformations of both the coordinates x and ξ. To derive the functional invariant under conformal transformations of the coordinates ξ, we use the relation $O_1^{n/2} = C_1^{n/2} O_n^{1/2}$. Functional of kind (10.10), possessing the required

property, is of the form

$$F(x(\xi)) = \int O_1^{n/2} d\xi^1 \dots d\xi^n = \int C_1^{n/2} dx^1 \dots dx^n$$
$$= \int \left(\sum_{i,j=1}^{n} \left(\frac{\partial x^i}{\partial \xi^j} \right)^2 \right)^{n/2} d\xi^1 \dots d\xi^n \ .$$

The integral with $C_1^{n/2}$ is of kind (10.9) and, therefore, it is invariant under conformal transformations of the coordinates x

$$F(x(\xi)) = \int C_1^{n/2} d\xi^1 \dots d\xi^n$$
$$= \int \left(\sum_{i,j=1}^{n} \left(\frac{\partial x^i}{\partial \xi^j} \right)^2 \right)^{n/2} (\det g)^{-1} dx^1 \dots dx^n \ .$$

For the inverse transformation we have

$$F(\xi(x)) = \int O_{n-1} O_n^{-1} dx^1 \dots dx^n = \int O_{n-1} O_n^{-1/2} d\xi^1 \dots d\xi^n,$$

which is not also invariant. The following functional possesses this property

$$F(\xi(x)) = \int C_{n-1}^{p} dx^1 \dots dx^n = \int O_{n-1}^{p} d\xi^1 \dots d\xi^n,$$

where

$$p = \frac{n}{2(n-1)},$$

is invariant under conformal transformations of ξ.

The functional

$$F(\xi(x)) = \int C_{n-1}^{p} d\xi^1 \dots d\xi^n$$

is invariant under conformal transformations of x.

3. Euler equations in the case $n = 3$.

The system of the Laplace equations are the Euler equations for the Dirichlet functional

$$\triangle x = 0, \quad \triangle y = 0, \quad \triangle z = 0,$$

where

$$\triangle = \frac{\partial^2}{\partial \xi^2} + \frac{\partial^2}{\partial \eta^2} + \frac{\partial^2}{\partial \mu^2}$$

are not invariant under conformal transformations of ξ, η, μ.

The Euler equations

$$\frac{\partial}{\partial \xi}\left(D\frac{\partial x}{\partial \xi}\right) + \frac{\partial}{\partial \eta}\left(D\frac{\partial x}{\partial \eta}\right) + \frac{\partial}{\partial \mu}\left(D\frac{\partial x}{\partial \mu}\right) = 0,$$

$$\frac{\partial}{\partial \xi}\left(D\frac{\partial y}{\partial \xi}\right) + \frac{\partial}{\partial \eta}\left(D\frac{\partial y}{\partial \eta}\right) + \frac{\partial}{\partial \mu}\left(D\frac{\partial y}{\partial \mu}\right) = 0,$$

$$\frac{\partial}{\partial \xi}\left(D\frac{\partial z}{\partial \xi}\right) + \frac{\partial}{\partial \eta}\left(D\frac{\partial z}{\partial \eta}\right) + \frac{\partial}{\partial \mu}\left(D\frac{\partial z}{\partial \mu}\right) = 0,$$

where

$$D = (x_\xi^2 + y_\xi^2 + z_\xi^2 + x_\eta^2 + y_\eta^2 + z_\eta^2 + x_\mu^2 + y_\mu^2 + z_\mu^2)^{1/2},$$

are invariant under conformal transformations of ξ, η, μ.

In the 2D case any conformal transformation is harmonic but this is not the case in $n \geq 3$. Consider the transformation

$$x^i(\xi) = \frac{\xi^i - \xi_0^i}{\sum_{i=1}^n (\xi^i - \xi_0^i)^2}.$$

This is a conformal transformation but it does not satisfy the system of Laplace equations.

10.7 Extension to case of manifolds

Consider the smooth invertible transformation

$$X(\xi) : \mathcal{R}^n \to \mathcal{R}^n, \quad X = (X^1, \ldots, X^n)^T, \quad \xi = (\xi^1, \ldots, \xi^n)^T.$$

Elements of the Jacobi matrix for the mappings $x(\xi)$, $x(X)$, and $X(\xi)$ are written as

$$a_j^i = \frac{\partial x^i}{\partial \xi^j}\ , \quad A_j^i = \frac{\partial x^i}{\partial X^j}\ , \quad B_j^i = \frac{\partial X^i}{\partial \xi^j}\ .$$

The metric tensors are

$$g = a^T a\ , \quad \tilde{g} = A^T A\ , \quad G = B^T\ .$$

We have $a{=}AB$, and $A{=}aB^{-1}$. From this it follows

$$\tilde{g} = A^T A = (B^{-1})^T a^T a B^{-1} \ .$$

The characteristic equation for the metric $\tilde{g}$ can be written as

$$\det(\tilde{g} - \lambda I) = (\det B)^2 \det(a^T a - \lambda B^T B) = (\det B)^2 \det(g - \lambda G) = 0 \ .$$

The mapping $X(\xi)$ is invertible, therefore, $\det B{\neq}0$. We can use the following characteristic equation for the pair of quadratic forms with the matrices g and G

$$\det(g - \lambda G) = \det G \det(gG^{-1} - \lambda I) = 0 \ .$$

A conformal invariant C_1 of the metric $\tilde{g}{=}A^T A$ can be written as

$$C_1 = tr(gG^{-1}) \det G^{1/n} \det g^{-1/n} \ ,$$

and the functional takes the form

$$F(x(\xi)) = \int C_1^{n/2} d\xi^1 \dots d\xi^n$$
$$= \int \left(g_{ij} G^{ji}\right)^{n/2} (\det G)^{1/2} (\det g)^{-1/2} d\xi^1 \dots d\xi^n .$$

Here G^{ji} are the elements of the matrix inverse to the matrix G. This functional is called the energy density functional of the mapping $x(X)$. It is invariant under conformal transformations of the coordinates x and X simultaneously.

Consider a mapping between manifolds $(M, G){\to}(N, \bar{g})$ with local coordinates ξ and x. Instead of g_{ij} we use the following expression

$$\bar{g}_{km} \frac{\partial x^k}{\partial \xi^i} \frac{\partial x^m}{\partial \xi^j},$$

and obtain the functional of the energy density of the mapping $(M, G){\to}(N, \bar{g})$

$$F(x(\xi)) = \int \left(\bar{g}_{km} \frac{\partial x^k}{\partial \xi^i} \frac{\partial x^m}{\partial \xi^j} G^{ij} \right)^{n/2} (\det \bar{g})^{-1/2} (\det g)^{-1/2} dM \ , \quad (10.13)$$

where $dM=(\det G)^{1/2}d\xi^1\dots d\xi^n$ is the element of volume of the manifold M. This functional is invariant under conformal transformations of the manifolds M and N simultaneously.

More simple form has the functional of the energy, used in the theory of harmonic mappings

$$F_e(x(\xi)) = \int \left(\bar{g}_{km}\frac{\partial x^k}{\partial \xi^i}\frac{\partial x^m}{\partial \xi^j}G^{ij}\right)(\det G)^{1/2}d\xi^1\dots d\xi^n \ . \qquad (10.14)$$

The functional (10.14) is called the mapping energy and its extremal is the harmonic mapping. At present the theory of the harmonic mappings is well developed and applied in various fields, cf. [44].

10.8 Curvilinear coordinates on manifold

Application of the theory of harmonic mappings for grid generation in the 3D case runs into some problems, since there is no theoretical base for developing numerical algorithms. This is confirmed by numerical results of [73]. Meanwhile 2D adaptive harmonic grids were successfully applied in some applied problems, cf. [4, 5, 6, 7, 9, 73, 76].

Possibly, the energy density mapping functional (10.13) will help to overcome this "dimensionality crisis". Consider the problem of curvilinear coordinate construction on the manifold $(N,\bar{g})$. Assume that $x(\xi)$: $(M,G)\to(N,\bar{g})$ is the mapping of manifolds with the local coordinates ξ and x, respectively. The manifold M is a unit cube $0\le\xi^i\le1$ with the defined metric G; and $x\in\Omega$, where $\Omega\subset\mathbb{R}^3$ is a simply connected domain. Suppose that a homeomorphic mapping between the boundaries $\partial M\to\partial N$ is defined. It is necessary to construct a homeomorphic mapping $x(\xi):(M,G)\to(N,\bar{g})$ at the given mapping between the boundaries; meanwhile the latter is written as a Dirichlet boundary condition. The mapping constructed in such a way generates curvilinear coordinates on the manifold $(N,\bar{g})$. At the same time $x(\xi)$ is a curvilinear coordinate system in the domain Ω.

We formulate a hypothesis that represents the variational principle allowing to distinguish a class of homeomorphic mappings among all possible smooth mappings of a unit cube onto the manifold $(N,\bar{g})$.

Optimality principle. *A smooth mapping $x(\xi):(M,G)\to(N,\bar{g})$ is a homeomorphism if and only if it minimizes the energy density functional F (see (10.13)) with certain "control" metric M.*

In the 2D case a discrete analog of this principle was proved in [77], see Section 9.4.

The functional (10.13) depends on two metrics. The metric $\bar{g}$ can be defined depending on numerical solutions of a physical problem, for instance, as the metric of the surface of a vector-function graph analogously as it is executed when generating adaptive-harmonic meshes [73]. The metric G can be defined so as to provide gride refining and orthogonalization near the boundary. Realization of this approach in the 2D case is considered in sec.9.4.

10.9 Approximation of energy density functional in 3D case

Consider the transformation between two manifolds $x(\xi) : (Q^3, \tilde{G}) \to (\Omega, \bar{g})$, where

$$r = (r^1, r^2, r^3, r^4) = (x, y, z, f) \in S^{r3} \subset \mathcal{R}^4,$$
$$x = (x^1, x^2, x^3) = (x, y, z) \in \Omega \subset \mathcal{R}^3,$$
$$\xi = (\xi^1, \xi^2, \xi^3) = (\xi, \eta, \mu) \in Q^3 \subset \mathcal{R}^3,$$
$$r_x = (1, 0, 0, f_x),\ r_y = (0, 1, 0, f_y),\ r_z = (0, 0, 1, f_z).$$

The functional of the energy density in the 3D case can be written as

$$F_\rho(x(\xi)) = \int \left(\bar{g}_{km} \frac{\partial x^k}{\partial \xi^i} \frac{\partial x^m}{\partial \xi^j} \tilde{G}^{ij} \right)^{3/2} (\det \bar{g})^{-1/2} (\det g)^{-1/2} \dot{\mathrm{M}},$$

where $\dot{\mathrm{M}} = (\det \tilde{G})^{1/2} d\xi^1 \dots d\xi^n$ is the element of volume of the manifold $(Q^3, \tilde{G})$.

Let adapted function $f(x, y, z)$ define a three-dimensional surface in four-dimensional space. In this case the metric defined by the transformation $\Omega \to S^{r3}$ can be computed as follows

$$\bar{g}_{11} = r_x^2 = 1 + f_x^2\ ,\quad \bar{g}_{22} = r_y^2 = 1 + f_y^2\ ,\quad \bar{g}_{33} = r_z^2 = 1 + f_z^2\ ,$$
$$\bar{g}_{12} = \bar{g}_{21} = r_x \cdot r_y = f_x f_y\ ,\quad \bar{g}_{13} = \bar{g}_{31} = r_x \cdot r_z = f_x f_z\ ,$$
$$\bar{g}_{23} = \bar{g}_{32} = r_y \cdot r_z = f_y f_z\ ,$$

$$\bar{g} = \begin{pmatrix} 1+f_x^2 & f_x f_y & f_x f_z \\ f_x f_y & 1+f_y^2 & f_y f_z \\ f_x f_z & f_y f_z & 1+f_z^2 \end{pmatrix}, \quad \det \bar{g} = 1 + f_x^2 + f_y^2 + f_z^2.$$

The metric g, defined by the transformation $Q^3 \to S^{r3}$, is

$$g = \begin{pmatrix} r_\xi^2 & (r_\xi \cdot r_\eta) & (r_\xi \cdot r_\mu) \\ (r_\xi \cdot r_\eta) & r_\eta^2 & (r_\eta \cdot r_\mu) \\ (r_\xi \cdot r_\mu) & (r_\eta \cdot r_\mu) & r_\mu^2 \end{pmatrix}.$$

The control metric $\tilde{G} = \tilde{G}^T > 0$ is the following

$$\tilde{G}^{-1} = \begin{pmatrix} \tilde{G}^{11} & \tilde{G}^{12} & \tilde{G}^{13} \\ \tilde{G}^{12} & \tilde{G}^{22} & \tilde{G}^{23} \\ \tilde{G}^{13} & \tilde{G}^{23} & \tilde{G}^{33} \end{pmatrix}.$$

The energy density of the transformation $(Q^3, \tilde{G}) \to S^{r3}$ in one point can be expressed as

$$\rho = \frac{\left(\frac{1}{3} tr(\tilde{G}^{-1} g)\right)^{3/2}}{\sqrt{\tilde{G}^{-1} g}}.$$

Here the manifold $(Q^3, \tilde{G})$ is defined as as the unit cube Q^3 with the metric $\tilde{G}$. Instead of the metric it is convenient to introduce a normalized metric

$$G = \frac{\tilde{G}}{\left(\det \tilde{G}\right)^{1/3}},$$

such that $\det G = 1$. In this case $G^{ij} = \left(\det \tilde{G}\right)^{1/3} \tilde{G}^{ij}$.

Then the energy density can be written as

$$\rho = \left(\frac{1}{3} \bar{g}_{ij} \frac{\partial x^i}{\partial \xi^k} \frac{\partial x^j}{\partial \xi^l} G^{kl}\right)^{3/2} (\det g)^{-1/2} (\det \bar{g})^{-1/2} = \frac{\alpha^{3/2}}{3\sqrt{3} J \sqrt{\det \bar{g}}},$$

where $J = \sqrt{\det g}$ is the determinant of the Jacobi matrix

$$J = \det \begin{pmatrix} x_\xi & x_\eta & x_\mu \\ y_\xi & y_\eta & y_\mu \\ z_\xi & z_\eta & z_\mu \end{pmatrix} = \det \left(\frac{\partial x^i}{\partial \xi^k} \right) .$$

It is easy to see that the expression for ρ contains 3x3x3x3=81 terms, some of them are the same because the matrices $\bar{g}$ and G are symmetric.

The expression for α is rather cumbersome. The expression, containing only terms with $\bar{g}_{11}$ and $\bar{g}_{12}$ can be written as

$$\alpha = \bar{g}_{11} \left(\frac{\partial x^1}{\partial \xi^1} \frac{\partial x^1}{\partial \xi^l} G^{11} + \frac{\partial x^1}{\partial \xi^2} \frac{\partial x^1}{\partial \xi^2} G^{22} + \frac{\partial x^1}{\partial \xi^3} \frac{\partial x^1}{\partial \xi^3} G^{33} \right) +$$

$$\bar{g}_{11} \left(+2 \frac{\partial x^1}{\partial \xi^1} \frac{\partial x^1}{\partial \xi^2} G^{12} + 2 \frac{\partial x^1}{\partial \xi^1} \frac{\partial x^1}{\partial \xi^3} G^{13} + 2 \frac{\partial x^1}{\partial \xi^2} \frac{\partial x^1}{\partial \xi^3} G^{23} \right) + 2\bar{g}_{12} \times$$

$$\left(\frac{\partial x^1}{\partial \xi^1} \frac{\partial x^2}{\partial \xi^1} G^{11} + \frac{\partial x^1}{\partial \xi^2} \frac{\partial x^2}{\partial \xi^2} G^{22} + \frac{\partial x^1}{\partial \xi^3} \frac{\partial x^2}{\partial \xi^3} G^{33} \right) + 2\bar{g}_{12} \left(\frac{\partial x^1}{\partial \xi^1} \frac{\partial x^2}{\partial \xi^2} + \frac{\partial x^1}{\partial \xi^2} \frac{\partial x^2}{\partial \xi^1} \right) G^{12}$$

$$+ 2\bar{g}_{12} \left(\frac{\partial x^1}{\partial \xi^1} \frac{\partial x^2}{\partial \xi^3} + \frac{\partial x^1}{\partial \xi^3} \frac{\partial x^2}{\partial \xi^1} \right) G^{13} + 2\bar{g}_{12} \left(\frac{\partial x^1}{\partial \xi^2} \frac{\partial x^2}{\partial \xi^3} + \frac{\partial x^1}{\partial \xi^3} \frac{\partial x^2}{\partial \xi^2} \right) G^{23} + \dots .$$

Note that in the discretization we will obtain more complicated expressions. Moreover, wee need also to compute derivatives such, as

$$U_x = \frac{\partial \alpha^{3/2}}{\partial x} = \frac{3}{2} \alpha^{1/2} \frac{\partial \alpha}{\partial x},$$

$$U_{xy} = \frac{\partial^2 \alpha^{3/2}}{\partial x \partial y} = \frac{3}{4} \alpha^{-1/2} \frac{\partial \alpha}{\partial x} \frac{\partial \alpha}{\partial x} + \frac{3}{2} \alpha^{1/2} \frac{\partial^2 \alpha}{\partial x \partial y}.$$

In general, these expressions after discretization will be extremely complicated, that produces additional difficulties in writing and debugging the computer code.

To simplify these expressions it is necessary to use tensor notations. Consider the tetrahedron, shown in Fig.10.1. Coordinates of 4 vertices of the tetrahedron can be denoted as following

$$x_k^i, \quad i = 1, 2, 3, \quad k = 0, 1, 2, 3.$$

Here i is the coordinate and k is the vertex number.

Consider the linear transformation of the coordinate tetrahedron in space ξ^1, ξ^2, ξ^3 onto the tetrahedron in space $(x^1, x^2\, x^3)$. In this case

$$\frac{\partial x^i}{\partial \xi^k} = x^i_k - x^i_0 = \triangle x^i_k \ .$$

Expression for α in new notations will be the following

$$\alpha = \bar{g}_{ij} \triangle x^i_k \triangle x^j_l G^{kl}.$$

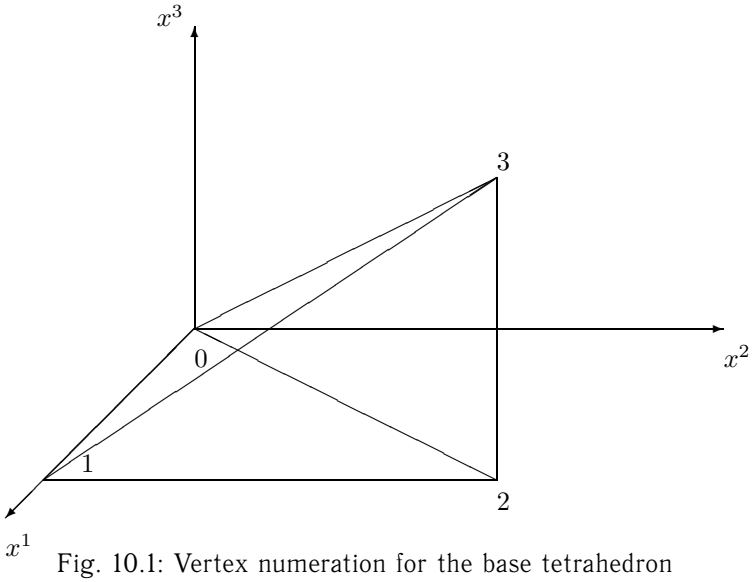

Fig. 10.1: Vertex numeration for the base tetrahedron

We readily obtain the following relations. For $n \neq 0$

$$\frac{\partial \triangle x^i_k}{\partial x^m_n} = \delta^i_m \delta^n_k, \quad i, k, m = 1, 2, 3.$$

If $n = 0$, we obtain

$$\frac{\partial \triangle x^i_k}{\partial x^m_n} = \delta^i_m \delta^0_k, \quad \text{where} \quad \delta^0_k = -1 \quad \text{for} \quad k = 1, 2, 3.$$

In derivation of computational formulas first we consider the case $n \neq 0$

$$\frac{\partial \alpha}{\partial x_n^m} = \bar{g}_{ij}\delta_m^i \delta_k^n \triangle x_l^i G^{kl} + \bar{g}_{ij}\delta_m^j \delta_l^n \triangle x_k^i G^{kl} =$$

$$\bar{g}_{mj} \triangle x_l^j G^{nl} + \bar{g}_{im} \triangle x_k^i G^{kn} = 2g_{mj} \triangle x_l^j G^{nl}.$$

$$\frac{\partial^2 \alpha}{\partial x_n^m \partial x_k^i} = 2\bar{g}_{mi} G^{nk}.$$

Note, that we need only the derivatives, corresponding to $n = k$. From this we obtain

$$\frac{\partial^2 \alpha}{\partial x_n^m \partial x_k^i} = 2\bar{g}_{mi} G^{nn}, \quad m, i, n = 1, 2, 3.$$

Now consider the case $n = 0$

$$\frac{\partial \alpha}{\partial x_0^m} = 2\bar{g}_{ij}\delta_m^i \delta_k^0 \triangle x_l^i G^{kl} = -2\bar{g}_{mj} \triangle x_l^j (G^{1l} + G^{2l} + G^{3l}).$$

$$\frac{\partial^2 \alpha}{\partial x_0^m \partial x_0^i} = -2\bar{g}_{mj}\delta_n^j \delta_l^0 (G^{1l} + G^{2l} + G^{3l}) =$$

$$2\bar{g}_{mj}(G^{11} + 2G^{12} + 2G^{13} + G^{22} + 2G^{23} + G^{33}) =$$

$$2\bar{g}_{mi}\delta_k^0 \delta_l^0 G^{kl}, \quad m, n, k, l = 1, 2, 3.$$

.....

At this place the chapter breaks down (Editor).

Chapter 11

Curvilinear grids in finite element method

Consider an elliptic equation in a simply connected domain Ω with the boundary Γ

$$-\frac{\partial}{\partial y}(p\frac{\partial u}{\partial x})+\frac{\partial}{\partial x}(p\frac{\partial u}{\partial y})-\frac{\partial}{\partial x}(r\frac{\partial u}{\partial x})-\frac{\partial}{\partial y}(r\frac{\partial u}{\partial y})=f\ , \qquad (11.1a)$$

with the boundary condition

$$u\mid_{\Gamma}=0. \qquad (11.1b)$$

We will assume that the input data of the problem is such that the solution u is smooth enough for the validity all the following transformations.

To obtain an integral identity, multiply (11.1a) by v, which is equal to 0 on Γ, integrate over the domain Ω and use the Gauss formula. As a result we obtain

$$a(u,v)=(f,v), \qquad (11.2)$$

where

$$a(u,v)=\int_{\Omega}[r(\frac{\partial u}{\partial x}\frac{\partial v}{\partial x}+\frac{\partial u}{\partial y}\frac{\partial v}{\partial y})+p(\frac{\partial u}{\partial x}\frac{\partial v}{\partial y}-\frac{\partial u}{\partial y}\frac{\partial v}{\partial x})]d\Omega\ ,$$

$$(f,v)=\int_{\Omega}fvd\Omega\ .$$

11.1 Standard finite element method

Suppose that a structured grid is constructed on a domain Ω. Every interior node (i,j) is associated with the basis function $\psi_{ij}(x,y)$, constructed using

isoparametric quadrilateral finite elements. An approximate solution of the problem is represented in the form

$$u^h = \sum_{i=2}^{i^*-1} \sum_{j=2}^{j^*-1} u_{ij} \psi_{ij}(x,y) \ . \tag{11.3}$$

Note that the function u^h satisfies the boundary condition (11.1b). Here h denotes the longest side of the grid cells. Substituting the expression (11.3) to u^h instead of u and the analogous expansion to v^h instead of v into (11.2) and equating the expressions at the coefficients in the series for v^h to zero, we obtain the system of the linear equations for the coefficients u_{ij} in (11.3) which can be written in the form

$$(\mathbf{A}^h + \mathbf{B}^h)\mathbf{u} = \mathbf{f}. \tag{11.4}$$

Elements of matrices $\mathbf{A}^h$ and $\mathbf{B}^h$ are calculated as

$$a_{ij}^{kl} = \int_\Omega r^h \left(\frac{\partial \psi_{ij}}{\partial x}\frac{\partial \psi_{kl}}{\partial x} + \frac{\partial \psi_{ij}}{\partial y}\frac{\partial \psi_{kl}}{\partial y}\right) d\Omega \ , \tag{11.5}$$

$$b_{ij}^{kl} = \int_\Omega p^h \left(\frac{\partial \psi_{kl}}{\partial x}\frac{\partial \psi_{ij}}{\partial y} - \frac{\partial \psi_{kl}}{\partial y}\frac{\partial \psi_{ij}}{\partial x}\right) d\Omega \ . \tag{11.6}$$

The components of the vector $\mathbf{f}$ are equal to

$$f_{ij} = \int_\Omega f(x,y)\psi_{ij}(x,y)d\Omega. \tag{11.7}$$

The quantities r^h and p^h approximate r and p and are expansions in terms of piecewise-constant basis functions $\psi^0_{i+1/2,j+1/2}(x,y)$, which are equal to one inside the grid cell $(i{+}1/2, j{+}1/2)$ and zero elsewhere

$$r^h = \sum_{i=1}^{i^*-1} \sum_{j=1}^{j^*-1} r_{i+1/2,j+1/2} \psi^0_{i+1/2,j+1/2}(x,y) \ ,$$

$$p^h = \sum_{i=1}^{i^*-1} \sum_{j=1}^{j^*-1} p_{i+1/2,j+1/2} \psi^0_{i+1/2,j+1/2}(x,y) \ ,$$

where

$$r_{i+1/2,j+1/2} = (r_{ij} + r_{i,j+1} + r_{i+1,j+1} + r_{i+1,j})/4 \ ,$$
$$p_{i+1/2,j+1/2} = (p_{ij} + p_{i,j+1} + p_{i+1,j+1} + p_{i+1,j})/4 \ .$$

Now consider the structure of non-zero element distribution for the matrices $\mathbf{A}^h$ and $\mathbf{B}^h$. Since the basis functions $\psi_{ij}(x,y)$ are non-zero only inside quadrilaterals with a common vertex at grid node (i,j), it is easy to see that these matrices will be block-tridiagonal matrices and each block will be a tridiagonal matrix of order (i^*-2).

Thus, the structure of the matrix of the system of the linear equations (11.4) corresponds to a finite-difference approximation of the operator of the problem (11.1) on the nine-point stencil. Because this matrix has a regular structure, it is required to store in the computer memory only its non-zero elements. On the other hand, the elements of this matrix can be calculated at every step of the iteration for its inversion, as it is usual for finite-difference methods, achieving an even greater saving of computer memory, although at the expense of increasing the computer time.

The successive over relaxation method is used for the numerical solution of the system (11.4).

Consider computational formulas. In isoparametric finite elements the mapping x^h, y^h of the unit square cell in the plane (ξ,η) onto the cell $Q_{i+1/2,j+1/2}$ in the plane (x,y) is used. Computational formulas for these elements are valid if all grid cells are convex quadrilaterals.

Inside a square cell in the plane (ξ,η) the derivatives of the function u^h are computed from the formulas

$$\frac{\partial u^h}{\partial x} = \frac{1}{J}\left(\frac{\partial u^h}{\partial \xi}\frac{\partial y^h}{\partial \eta} - \frac{\partial u^h}{\partial \eta}\frac{\partial y^h}{\partial \xi}\right) \ , \quad \frac{\partial u^h}{\partial y} = \frac{1}{J}\left(-\frac{\partial u^h}{\partial \xi}\frac{\partial x^h}{\partial \eta} + \frac{\partial u^h}{\partial \eta}\frac{\partial x^h}{\partial \xi}\right) \ .$$

If these expressions are substituted into the formula (11.5) for the elements of the matrix $\mathbf{A}^h$, the integrand in (11.5) will be a polynomial divided by a linear function of ξ,η. This integral can be evaluated exactly, but the expressions obtained are too cumbersome. It is better to use the simple quadrature formulas.

To evaluate the integral (11.5) over the cell $Q_{i+1/2,j+1/2}$ in the plane (x,y), consider the bilinear form

$$I_A = \int\limits_{Q_{i+1/2,j+1/2}} \left(\frac{\partial u^h}{\partial x}\frac{\partial v^h}{\partial x} + \frac{\partial u^h}{\partial y}\frac{\partial v^h}{\partial y}\right) dxdy \ .$$

The integral is approximated by a quadrature formula with nodes coincident with the vertices of the parametric square

$$I_A^h = \frac{1}{4}(\nabla u^h \nabla v^h J\mid_1 + \nabla u^h \nabla v^h J\mid_2 + \nabla u^h \nabla v^h J\mid_3 + \nabla u^h \nabla v^h J\mid_4) \ .$$

Then the elements of the local matrix corresponding to $\mathbf{A}^h$ are computed as follows

$$a_{ij} = a_{ji} = \frac{\partial^2 I_A^h}{\partial u_i \partial v_j}, \quad i,j = 1,2,3,4.$$

To obtain the elements of the matrix $\mathbf{B}^h$ consider the bilinear form

$$I_B = \int\limits_{Q_{i+1/2,j+1/2}} (\frac{\partial u^h}{\partial x}\frac{\partial v^h}{\partial y} - \frac{\partial u^h}{\partial y}\frac{\partial v^h}{\partial x})dxdy = \int\limits_{\partial Q_{i+1/2,j+1/2}} u^h \frac{\partial v^h}{\partial s} ds.$$

The integral can be calculated exactly

$$I_B = \frac{u_1+u_4}{2}(v_4-v_1)+\frac{u_4+u_3}{2}(v_3-v_4)+\frac{u_3+u_2}{2}(v_2-v_3)+\frac{u_1+u_2}{2}(v_2-v_1).$$

Introducing the notation

$$b_{ij} = -b_{ji} = \frac{\partial^2 I_B}{\partial u_i \partial v_j}, \quad i,j = 1,2,3,4,$$

finally we obtain

$$b_{11} = 0, \quad b_{12} = 1/2, \quad b_{13} = 0, \quad b_{14} = -1/2, \quad b_{22} = 0,$$

$$b_{23} = 1/2, \quad b_{24} = 0, \quad b_{33} = 0, \quad b_{34} = 1/2, \quad b_{44} = 0.$$

It is well known, that the expansion with coefficients u_{ij}, defined by the solution of the linear system (11.4) converges to the exact solution u of the problem (11.1), and the following estimate holds

$$\|u - u^h\|_1 \le ch,$$

with a constant c independent on h. Here the norm $\|u\|_1$ is defined as

$$\|u\|_1 = \int (u^2 + u_x^2 + u_y^2) d\Omega \ .$$

11.2 Upstream finite element method

Note that the first two terms in (11.1a) are expressions dependent only on u_x and u_y, and p can be considered as an analog of the stream function. Indeed, (11.1a) can be rewritten in the form

$$q_x\frac{\partial u}{\partial x}+q_y\frac{\partial u}{\partial y}-\frac{\partial}{\partial x}(r\frac{\partial u}{\partial x})-\frac{\partial}{\partial y}(r\frac{\partial u}{\partial y})=f\ ,$$

where $q_x=-\partial p/\partial y$ and $q_y=\partial p/\partial x$ satisfy the continuity equation

$$\frac{\partial q_x}{\partial x}+\frac{\partial q_y}{\partial y}=0\ .$$

This fact can be used to construct such an approximation, which is similar to the finite-difference scheme with upwind differences. It can be done if the first two terms in (11.1a) are approximated by a box method, and the second two terms are approximated by the standard finite element method described in the previous subsection. These approximations must be conformal in a sense that the approximate solution to the problem (11.1) converges to the exact one.

Consider approximations of first two terms in (11.1a). Every grid cell is divided into four quadrilaterals, joining the mid-point of the opposite sides by the straight-line sections, as shown in Fig.11.1. Equation (11.1a) is integrated over the octogonal cell with vertices $(11'22'33'44)$, consisting of the quadrilaterals obtained at subdivision and containing the node (ij) as a vertex. Denote this octagon by E_{ij}. Integrating, we obtain

$$\int\limits_{\partial E_{ij}}(-\frac{\partial p}{\partial s}u-r\frac{\partial u}{\partial n})ds=\int\limits_{E_{ij}}f dxdy\ , \tag{11.8}$$

where $\partial/\partial n$ and $\partial/\partial s$ are the derivatives in the normal and tangential directions to the boundary ∂E_{ij} of the octagon E_{ij}. The first term in the left-hand side of (11.4) is approximated as follows

$$\left[\int\limits_{\partial E_{ij}}-\frac{\partial p}{\partial s}uds\right]_{ij}=[p_1-p_2]_{ij}\widetilde{u}_{i,j+1/2}$$

$$+[p_4 - p_1]_{ij}\widetilde{u}_{i+1/2,j} + [p_3 - p_4]_{ij}\widetilde{u}_{i,j-1/2} + [p_2 - p_3]_{ij}\widetilde{u}_{i-1/2,j}, \qquad (11.9)$$

where

$$\widetilde{u}_{i,j+1} = \begin{cases} u_{ij} & \text{if } [p_1 - p_2]_{ij} \geq 0, \\ u_{i,j+1} & \text{if } [p_1 - p_2]_{ij} < 0. \end{cases} \qquad (11.10)$$

Here $\widetilde{u}_{i+1/2,j}$, $\widetilde{u}_{i-1/2,j}$, and $\widetilde{u}_{i,j-1/2}$ are calculated similarly. According to the notation in Fig.11.1

$$\begin{aligned} [p_1 - p_2]_{ij} &= q_{i,j+1/2} = p_{i+1/2,j+1/2} - p_{i-1/2,j+1/2} \ , \\ [p_2 - p_3]_{ij} &= q_{i-1/2,j} = p_{i-1/2,j+1/2} - p_{i-1/2,j-1/2} \ , \\ [p_3 - p_4]_{ij} &= q_{i,j-1/2} = p_{i-1/2,j-1/2} - p_{i+1/2,j-1/2} \ , \\ [p_4 - p_1]_{ij} &= q_{i+1/2,j} = p_{i+1/2,j-1/2} - p_{i+1/2,j+1/2} \ . \end{aligned}$$

Now, instead of (11.4) consider the system of the linear equations

$$(\mathbf{A}^h + \mathbf{B}^h + \mathbf{C}^h)\mathbf{u} = \mathbf{f} \ . \qquad (11.11)$$

The sum of the second and the third terms in (11.11) corresponds to the approximation (11.9), (11.10) of the first two terms in (11.1a). Matrix $\mathbf{B}^h$ is the same as in (11.4) and its elements are computed by formulas introduced in previous subsection. The matrix $\mathbf{C}^h$ is symmetric and positive definite. To show this, we will rewrite (11.9) in the form

$$\left[\int\limits_{\partial E_{ij}} -\frac{\partial p}{\partial s} u ds\right]_{ij} = q_{i,j+1/2}u_{i,j+1/2}$$

$$\begin{aligned} &+q_{i+1/2,j}u_{i+1/2,j} + q_{i,j-1/2}u_{i,j-1/2} + q_{i-1/2,j}u_{i-1/2,j} \ , \qquad (11.12) \\ &+\frac{1}{2}|q_{i,j+1/2}|(u_{ij} - u_{i,j+1}) + \frac{1}{2}|q_{i+1/2,j}|(u_{ij} - u_{i+1,j}) \ , \\ &+\frac{1}{2}|q_{i,j-1/2}|(u_{ij} - u_{i,j-1}) + \frac{1}{2}|q_{i-1/2,j}|(u_{ij} - u_{i-1,j}) \ , \end{aligned}$$

where

$$\begin{aligned} u_{i,j+1/2} &= \frac{1}{2}(u_{ij} + u_{i,j+1}), \qquad u_{i,j-1/2} = \frac{1}{2}(u_{ij} + u_{i,j-1}), \\ u_{i+1/2} &= \frac{1}{2}(u_{ij} + u_{i+1,j}), \qquad u_{i-1/2} = \frac{1}{2}(u_{ij} + u_{i-1,j}). \end{aligned}$$

The first four terms in the right-hand side of (11.12) correspond to $\mathbf{B}^h\mathbf{u}$ and can be obtained by the standard procedure of the finite-element method. The matrix $\mathbf{B}^h$ is skew-symmetric

$$(\mathbf{B}^h\mathbf{u}, \mathbf{u}) = 0 \ .$$

The last four terms in the right-hand side of (11.12) correspond to $\mathbf{C}^h$. Multiplying (11.12) by u_{ij} and summing over all internal nodes, we obtain

$$(\mathbf{C}^h\mathbf{u}, \mathbf{u}) = \sum [\frac{1}{4}|q_{i,j+1/2}|(u_{ij} - u_{i,j+1})^2 + \frac{1}{4}|q_{i+1/2,j}|(u_{ij} - u_{i+1,j})^2$$
$$+\frac{1}{4}|q_{i,j-1/2}|(u_{ij} - u_{i,j-1})^2 + \frac{1}{4}|q_{i-1/2,j}|(u_{ij} - u_{i-1,j})^2] \geq 0.$$

It can be shown that the expansion (11.4) with the coefficients u_{ij}, defined by the solution of the linear system (11.11), converges to the exact solution u of the problem (11.1) and the following estimate holds

$$\|u - u^h\|_1 \leq ch \ ,$$

with a constant c independent on h. This means that approximations by the standard procedure of the finite element method and by upstream method are conformal. This method is used for the numerical solution of the shallow water equations, described in the next section.

The use of the upstream finite element method with a standard approximation of the second derivatives on the square grid with the grid size h for the equation

$$-\triangle u + u_x = 0 \ ,$$

gives a system of finite-difference equations

$$(8u_{ij} - u_{i-1,j-1} - u_{i,j-1} - u_{i+1,j-1} - u_{i-1,j} - u_{i+1,j}$$
$$- u_{i-1,j+1} - u_{i+1,j+1} - u_{i,j+1})/3 + h(u_{ij} - u_{i-1,j}) = 0 \ ,$$

of first order approximation, satisfying the maximum principle.

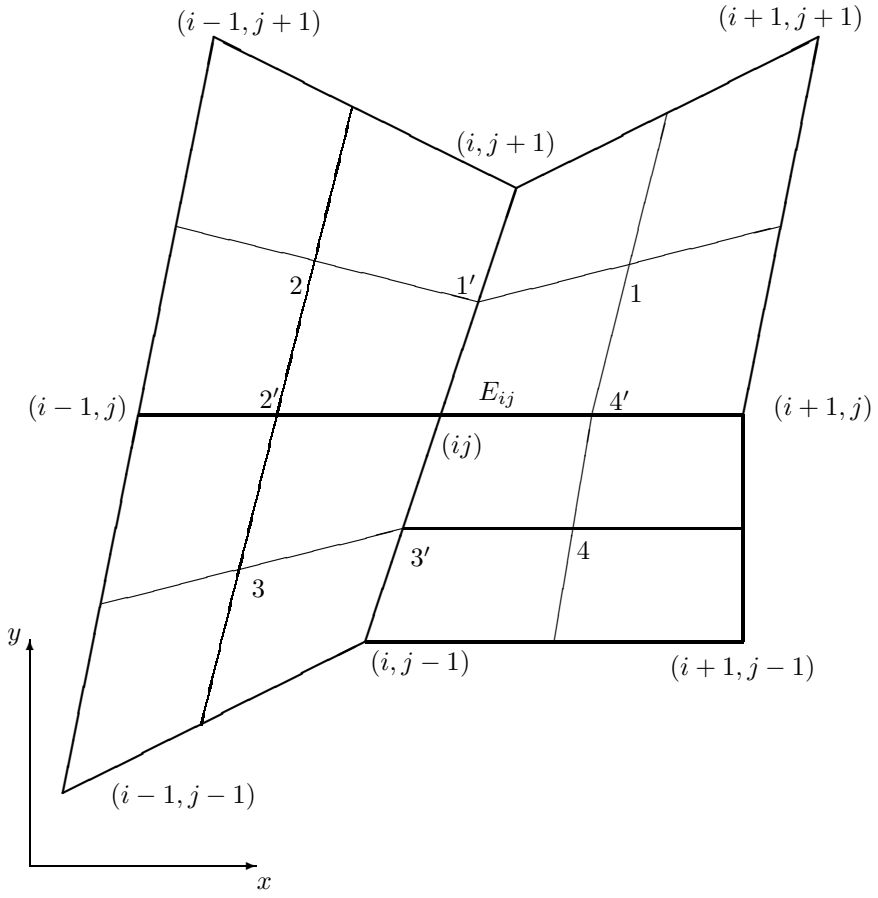

Fig. 11.1: Nine-point stencil and domain of integration E_{ij} in box method

Chapter 12

Test computations

The methods of constructing adaptive-harmonic grids involve computation of the adapted function at the grid nodes. But if that function is obtained by numerical solution of a boundary-value problem, the nodal values differ from the exact ones by a quantity $O(h^k)$, where k is the order of convergence. This gives rise to the following contradiction. If the unknown function is approximated by means of an expansion in terms of piecewise-constant basis functions, the function

$$u_0^h = \sum u_i \varphi_i^0(x)$$

obtained by numerical solution cannot be used to construct a uniform grid over its graph. Moreover, if the values of the function u_0^h at cell centers differ from exact value by $O(h)$, in general case the derivative might be computed with accuracy $O(1)$, so there might be no convergence for the grid.

The same is true for approximation by piecewise-linear functions. In this case a scheme of not higher than second-order approximation is obtained for a second-order equation, and again convergence of the finite difference approximation to the second derivative cannot be guaranteed, since it can be computed only with the accuracy $O(1)$. In order to calculate this derivative with sufficient accuracy, we must use additional information provided by the hosted equation. This approach has been developed for the Poisson's equation, and formulas can be given to calculate the second derivatives at grid nodes with the second order accuracy. These formulas contain the function which approximates the control function with the second order in the norm L_2.

One possible way of constructing a universal algorithm which does not suffer of this contradiction is the following. The solution is sought in the

form of an expansion in terms of piecewise-linear basis functions in the 1D case and piecewise-linear to triangular and piecewise-bilinear functions and quadrilateral elements. The grid is generated by projection of the harmonic coordinates constructed on the curve/surface of the approximate solution. In this case it is not the error of the piecewise-linear approximation $\|u-u^h\|_{\mathbb{C}}$ or $\|u-u^h\|_{\mathbb{C}^1}$, but the approximation error of the piecewise-constant functions $\|u-u_0^h\|_{\mathbb{C}}$, which is minimized. And although the resulting grid will be not optimal for the piecewise-linear approximation, it does help to improve the accuracy and is quite suitable for calculations. It should be mentioned that we usually start with the grid with spacings being clearly larger than the width of the boundary layer. On this initial grid the error for the function is of $O(1)$ and for the derivative is of $O(1/h)$. In such a situation such "loss of the order"at adaptation seems natural. Perhaps it is the only way to perform adaptation in real-world simulations.

Consider the equation

$$\epsilon\left(\frac{\partial^2 u}{\partial x^2}+\frac{\partial^2 u}{\partial y^2}\right)+\frac{\partial u}{\partial x}=\pi\sin(\pi y), \qquad 0<x<1, \quad 0<y<1, \tag{12.1a}$$

with the boundary conditions

$$u\,|_{\Gamma}=0\ . \tag{12.1b}$$

The analytic solution of the problem (12.1) has the form

$$u=\frac{1}{\pi\epsilon}\sin(\pi y)[(1-c)\exp(ax)+c\exp(bx)-1]\ , \tag{12.2}$$

where

$$a=\frac{1}{2\epsilon}(-1+\sqrt{1+4\pi^2\epsilon^2}), \quad b=\frac{1}{2\epsilon}(-1-\sqrt{1+4\pi^2\epsilon^2}),$$

$$c=(\exp a-1)/(\exp a-\exp b).$$

Fig.12.1a shows the function (12.2) plots. The grid in Fig.12.1b was constructed by the adaptive-harmonic grid generation method with ϵ=0.05. This function has a boundary layer on the left-hand side of the square.

The calculations were carried out with four values of the parameter ϵ=0.2, 0.05, 0.01, 0.001 on four embedded grids of 9×9, 17×17, 33×33, 65×65 nodes. The corresponding mesh spacing h=1/N was equal to h=1/8, 1/16, 1/32, 1/64.

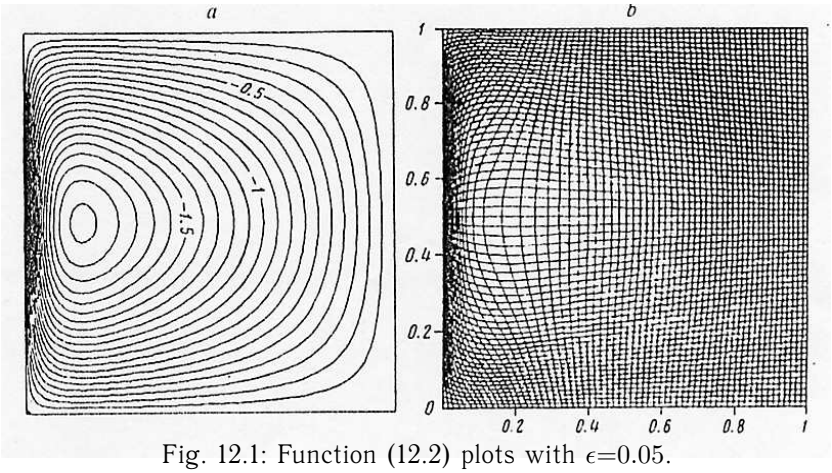

Fig. 12.1: Function (12.2) plots with ϵ=0.05.

Every step of the iterative method of adaptive harmonic grid generation consists of two stages. At the first stage, we compute the adapted function values at the grid nodes. At the second stage, the new grid nodes coordinates are determined. Once the convergence has been obtained, we estimate four quantity characterizing the error. The first quantity, referred to as E_0, is equal to the approximation error in the $\mathbb{C}$ norm when approximating by piece-wise constant functions

$$E_0 = \frac{\max\limits_{x,y} |u - u_0^h|}{u_{max} - u_{min}} \ ,$$

where

$$u_0^h = \sum_{i=1}^{i^*-1} \sum_{j=1}^{j^*-1} u_{i+1/2,j+1/2} \phi^o_{i+1/2,j+1/2}(x,y) \ ,$$

$$u_{i+1/2,j+1/2} = \frac{1}{4}(u_{ij} + u_{i,j+1} + u_{i+1,j+1} + u_{i+1,j} \ .$$

The basis function $\phi^o_{i+1/2,j+1/2}(x,y)$ is equal to 1 inside the cell (i+1/2, j+1/2) and 0 outside this cell. u_{max} and u_{min} is the maximal and minimal function value.

The second quantity is the approximation error in the $\mathbb{C}$ norm when approximating by the quadrilateral finite elements

$$E_1 = \frac{\max\limits_{x,y} |u - u^h|}{u_{max} - u_{min}} \ ,$$

where

$$u^h = \sum_{i=2}^{i^*-1} \sum_{j=2}^{j^*-1} u_{ij} \phi_{i,j}(x,y) \ ,$$

u_{ij} is the function value in the node (i,j), and $\phi_{i,j}(x,y)$ is the basis function of the quadrilateral isoparametric finite elements.

The quantity

$$E_2 = \frac{\max\limits_{i,j} |u(x_{ij}, y_{ij}) - u_{ij}|}{u_{max} - u_{min}}$$

is the maximal difference of the approximate and exact solutions in the grid nodes.

The error in the $\mathbb{C}^1$ norm

$$E_3 = \frac{\max\limits_{x,y} (|u_x - u_x^h|, |u_y - u_y^h|)}{\max\limits_{x,y} \sqrt{u_x^2 + u_y^2}}$$

is the maximal error of derivatives, normalized with respect to the maximal modulus of the function $u(x,y)$ gradient.

We will now analyze the experimental results. In the first series of calculations, we used the values of u_{ij} obtained for the analytic solution, i.e. u_{ij}=$u(x_{ij}, y_{ij})$, where $u(x,y)$ is the analytic solution of the problem (12.1). The curves of the error E_0 as the function of the spacing h=$1/N$ are shown for the uniform square grid in Fig.12.2a and for the adaptive grid in Fig.12.2b. Here and below the labels on the curves correspond to the following values of the parameter ϵ: curve 1 was obtained with ϵ=0.2, 2 with ϵ=0.05, 3 with ϵ=0.01, and 4 with ϵ=0.001. Obviously, on the uniform grids when ϵ is small, the error E_0 behaves like the approximation error in the $\mathbb{C}$ norm on a uniform grid in the 1D case. On the adaptive grid the error E_0 decreases linearly with h as that of on the adaptive grid in the 1D case. Hence, adaptive grids help to preserve the correct convergence rate to u_0^h with practically any number of nodes.

The dependence of E_1 on h for the uniform and adaptive grids are shown in Figs.12.2c,d. Now we have a different situation. The adaptive grid is highly accurate for small numbers of ϵ, as that of in the above calculations, but does not give the correct convergence rate, especially with large values of ϵ. In fact, the error decreases as $O(h^2)$ on the uniform grid with ϵ=0.2, but decreases as $O(h)$ on the adaptive grid for the same value of ϵ. Moreover, the error E_1 is less on the uniform grid than that of on the adaptive grid. This is because the method minimizes E_0, and does not E_1. The results of the next series of calculations are shown in Fig.12.3. The standard finite element method, using a scheme with centered differences to approximate the first derivatives, is used here to obtain the values of u_{ij} in the grid nodes. The solution is distorted by oscillations for small values of ϵ, and the iteration does not converge at all with ϵ=0.001. That is why the Fig.12.3 does not show any curves corresponding to this value of ϵ.

Graphs of the error E_0 as a function of h are shown for the uniform grid in Fig.12.3a, and for the adaptive grid in Fig.12.3b. As in the case of the analytic solution, the error E_0 decreases as $O(h)$ on the adaptive grid, and with ϵ=0.001 and $h>1/32$ it is larger than 0.6 on the uniform grid due to the presence of spurious oscillations. The behavior of the error E_0 on the adaptive grid with ϵ=0.01 demonstrates that oscillations are slightly suppressed. The graphs of the error E_1 for the uniform and adaptive grids are shown in Fig.12.3c and Fig.12.3d, respectively. They are similar to the respective graphs of the analytic solution. Here with ϵ=0.2 the convergence rate is also higher on the uniform grid than on the adaptive grid and the error E_1 is less on the uniform grid than that of on the adaptive grid.

The graphs of the E_2 error in the grid nodes are shown for the structured and adaptive grids in Fig.12.3e and Fig.13.3f, respectively. On the uniform grid a superconvergence is observed when ϵ=0.2, that is E_2 decreases as $O(h^{2+\alpha})$, where $\alpha>0$. At the same time, on the adaptive grid the error E_2 changes as $O(h)$. Note that on the uniform grid with ϵ=0.01 and $h=1/8$ we have $E_2>0.8$ due to the fact that the scheme is not-monotone.

The next series of computations was carried out with the upstream finite element method. The graphs of the errors E_0, E_1 and E_2 against h for the uniform and adaptive grids are shown in Fig. 12.4. The uniform grid corresponds to the cases a, c, e, and the adaptive grid to b, d, f. Even though the scheme is only of the first-order approximation, the algorithm for constructing a grid operates stably for any ϵ. In fact, the approximation of the derivatives of the function $u(x, y)$ is fairly accurate, since the corresponding

estimate shows that they converge with first order with respect to h in the norm L_2. The fact that the scheme is of the first order is quite clear from Fig.12.4c for the dependence of E_1 on h with ϵ=0.2 and ϵ=0.05. We also note that when ϵ=0.001 the values of E_2 (the error in grid nodes) obtained on the uniform grid are very small. Hence, with small ϵ and large h the error in grid nodes does not reflect the accuracy of the method.

We are primarily interested in E_1, the error of approximation by the finite element method. As we have seen, the adaptive-harmonic grid generator does not minimize E_1 and, as a result, the correct rate of convergence of the error E_1 is not achieved for large h and ϵ. It turns out that the correct convergence rate of the error E_1 can be obtained if the grid is constructed as the projection of the harmonic grid constructed on the graph of the vector-function whose components are the partial derivatives u_x and u_y, rather than on the surface of the graph of the function $u(x, y)$. However, this means that the values of the derivatives at grid nodes must be computed with sufficient accuracy.

Figure 12.5a,b shows the graphs of E_3 (the error in norm $\mathbb{C}^1$) against h for the uniform and adaptive grids, respectively. The adaptive grid was generated by a harmonic grid on the surface of the graph of the derivatives. The values of the derivatives at the nodes are computed analytically. First-order convergence is obtained for the derivatives. Figure 12.5c shows the graphs of E_0 against h and Fig.12.5d shows graphs of E_1 against h. Note that E_0 behaves again as $O(h)$, but correct second-order convergence was obtained to E_1, at least with values ϵ between 0.01 and 0.2. However, this method could not be used for the approximate solution for the problem (12.1), because the derivatives were not calculated with sufficient accuracy of the function in grid nodes. Moreover, we were not able to obtain a good adaptive grid, even by computing the derivatives using exact values of the function in grid nodes using the analytic solution. Clearly, additional information about the solution must be used to compute the second derivatives with sufficient accuracy.

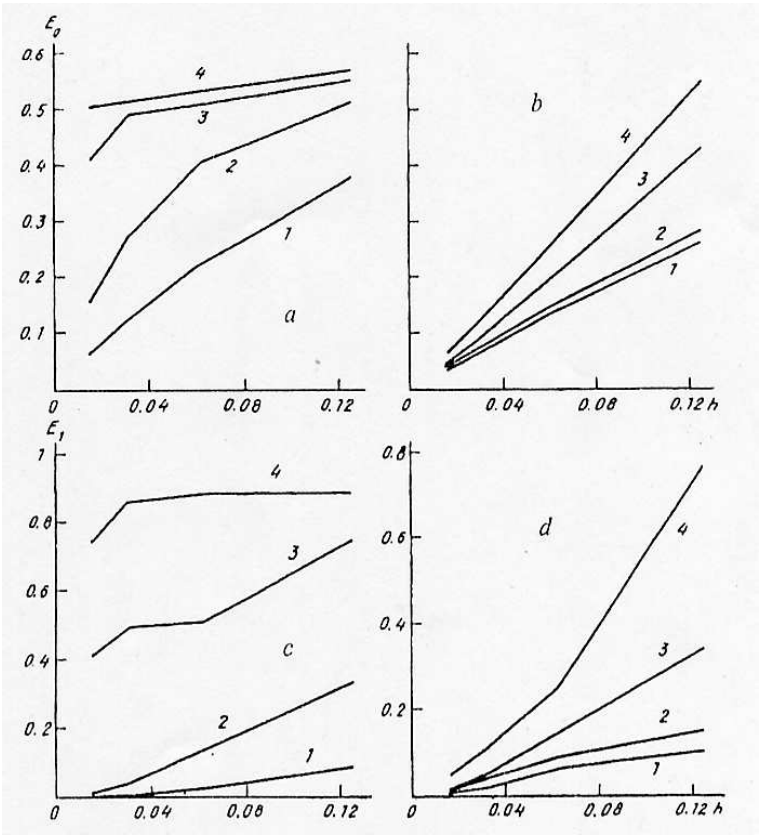

Fig. 12.2: Curves of errors E_0 and E_1.

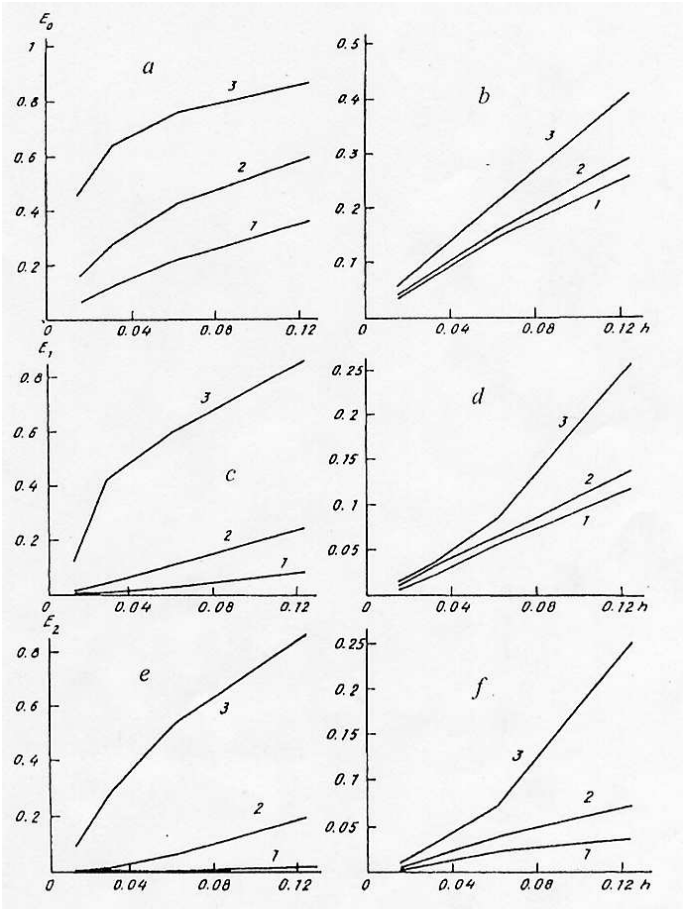

Fig. 12.3: Graphs of E_2, E_1 and E_0.

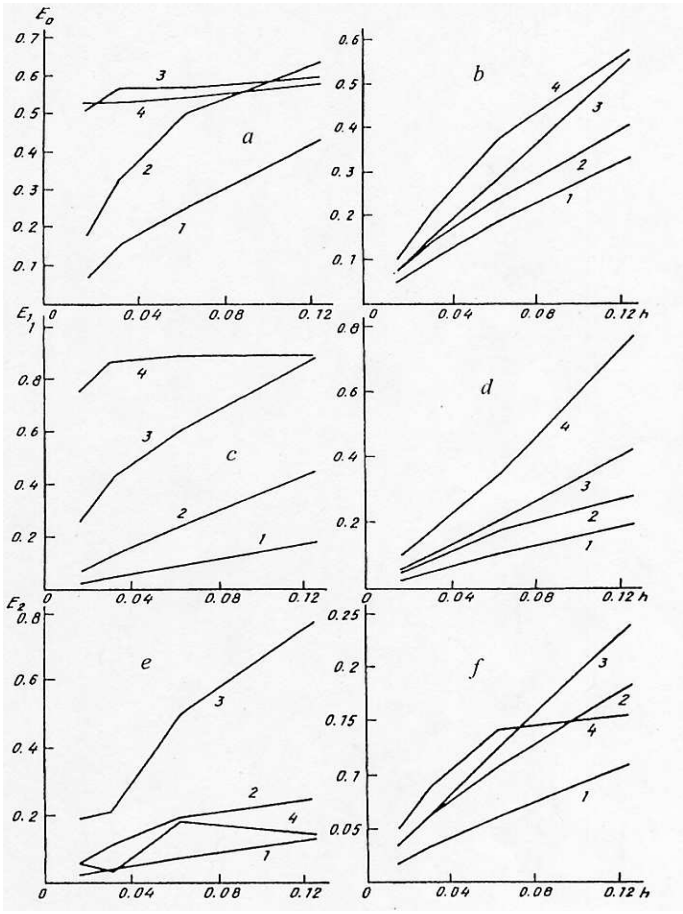

Fig. 12.4: Graphs of errors E_0, E_1 and E_2

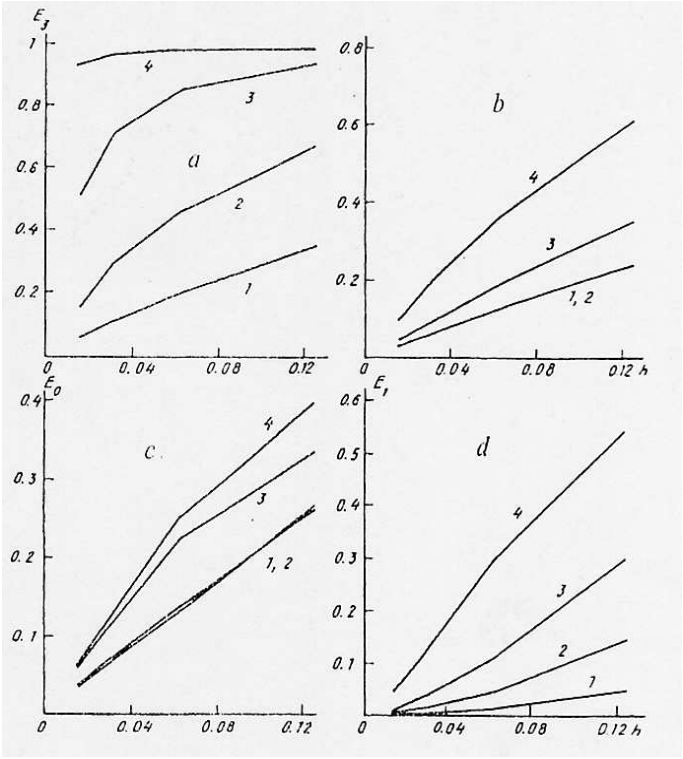

Fig. 12.5: Graphs of E_3 and E_0.

Chapter 13

Model of wind-induced circulation in shallow water

13.1 Three-dimensional shallow water equations

The system of three-dimensional Navier-Stokes equations can be written as

$$\frac{\partial \tilde{u}}{\partial t} + \tilde{u}\frac{\partial \tilde{u}}{\partial x} + \tilde{v}\frac{\partial \tilde{u}}{\partial y} + \tilde{w}\frac{\partial \tilde{u}}{\partial z} = -\frac{1}{\rho}\frac{\partial p}{\partial x} + f_x, \tag{13.1a}$$

$$\frac{\partial \tilde{v}}{\partial t} + \tilde{u}\frac{\partial \tilde{v}}{\partial x} + \tilde{v}\frac{\partial \tilde{v}}{\partial y} + \tilde{w}\frac{\partial \tilde{v}}{\partial z} = -\frac{1}{\rho}\frac{\partial p}{\partial y} + f_y, \tag{13.1b}$$

$$\frac{\partial \tilde{w}}{\partial t} + \tilde{u}\frac{\partial \tilde{w}}{\partial x} + \tilde{v}\frac{\partial \tilde{w}}{\partial y} + \tilde{w}\frac{\partial \tilde{w}}{\partial z} = -\frac{1}{\rho}\frac{\partial p}{\partial z} + f_z, \tag{13.1c}$$

$$\frac{\partial \tilde{u}}{\partial x} + \frac{\partial \tilde{v}}{\partial y} + \frac{\partial \tilde{w}}{\partial z} = 0. \tag{13.1d}$$

Here $\tilde{u}$, $\tilde{v}$ and $\tilde{w}$ are the velocity components in the x, y, z directions respectively, ρ is the density, p is the pressure, f_x, f_y, and f_z represent components of mass force per unit volume. They can be written in the form

$$f_x = l_C\tilde{v} + k_z\frac{\partial^2 \tilde{u}}{\partial z^2},$$

$$f_y = -l_C\tilde{u} + k_z\frac{\partial^2 \tilde{v}}{\partial z^2},$$

$$f_z = -g,$$

where k_z is the coefficient of vertical viscosity, g is the acceleration due to gravity, l_C is the Coriolis parameter, defined as

$$l_C = 2\omega \sin\theta,$$

where ω is the angular speed of the Earth and θ is the latitude.

If we consider that the characteristic horizontal length scale is much larger than the characteristic vertical length scale, then the equation (13.1c) can be written as

$$\frac{1}{\rho}\frac{\partial p}{\partial z} = -g. \tag{13.2}$$

This equation is called the hydrostatic equation. Consider the function $\varsigma(x, y, t)$ defining the free surface level against the reference plane z=0. Integrating the equation (13.2) from z to ς results in

$$p(x, y, z, t) = g\int_z^{\varsigma} \rho dz + p_a. \tag{13.3}$$

Here p_a is the atmospheric pressure. Suppose that ρ and p_a are constants. Then the pressure term in equations (13.1a) and (13.1b) can be written as

$$\frac{1}{\rho}\frac{\partial p}{\partial x} = g\frac{\partial \varsigma}{\partial x}, \quad \frac{1}{\rho}\frac{\partial p}{\partial y} = g\frac{\partial \varsigma}{\partial y}. \tag{13.4}$$

To obtain additional equation for the unknown free surface $\varsigma(x, y, t)$, we integrate the continuity equation (13.1d) along the vertical axis

$$\tilde{w}(x, y, \varsigma, t) - \tilde{w}(x, y, h(x, y), t) = -\int_{-h}^{\varsigma} \frac{\partial \tilde{u}}{\partial x} dz - \int_{-h}^{\varsigma} \frac{\partial \tilde{v}}{\partial y} dz, \tag{13.5}$$

where $h(x, y)$ is water depth below the reference plane $z = 0$. Changes of the bed are considered to be small and they are therefore neglected. Thus, h does not depend on time. Equation (13.5) can be rewritten using substitutions for $\tilde{w}$ at the free surface and the bottom. For z=$\varsigma(x, y, t)$ we have

$$\tilde{w} = \frac{d\varsigma}{dt} = \frac{\partial \varsigma}{\partial t} + \tilde{u}\frac{\partial \varsigma}{\partial x} + \tilde{v}\frac{\partial \varsigma}{\partial y}.$$

For z= $-$ $h(x, y)$ we have

$$\tilde{w} = -\tilde{u}\frac{\partial h}{\partial x} - \tilde{v}\frac{\partial h}{\partial y}.$$

We use also the Leibnitz integration rule

$$\int_{-h}^{\varsigma} \frac{\partial \tilde{u}}{\partial x} dz = \frac{\partial}{\partial x} \int_{-h}^{\varsigma} \tilde{u} dz - \tilde{u} \frac{\partial \varsigma}{\partial x} - \tilde{u} \frac{\partial h}{\partial x},$$

$$\int_{-h}^{\varsigma} \frac{\partial \tilde{v}}{\partial y} dz = \frac{\partial}{\partial y} \int_{-h}^{\varsigma} \tilde{v} dz - \tilde{v} \frac{\partial \varsigma}{\partial y} - \tilde{v} \frac{\partial h}{\partial y}.$$

Using all these derivations we obtain the following system of equations which is called the three dimensional shallow water equations

$$\frac{\partial \varsigma}{\partial t} + \frac{\partial}{\partial x} \int_{-h}^{\varsigma} \tilde{u} dz + \frac{\partial}{\partial y} \int_{-h}^{\varsigma} \tilde{v} dz, \tag{13.6a}$$

$$\frac{\partial \tilde{u}}{\partial t} + \tilde{u} \frac{\partial \tilde{u}}{\partial x} + \tilde{v} \frac{\partial \tilde{u}}{\partial y} + \tilde{w} \frac{\partial \tilde{u}}{\partial z} - l_C \tilde{v} = -g \frac{\partial \varsigma}{\partial x} + k_z \frac{\partial^2 \tilde{u}}{\partial z^2}, \tag{13.6b}$$

$$\frac{\partial \tilde{v}}{\partial t} + \tilde{u} \frac{\partial \tilde{v}}{\partial x} + \tilde{v} \frac{\partial \tilde{v}}{\partial y} + \tilde{w} \frac{\partial \tilde{v}}{\partial z} + l_C \tilde{u} = -g \frac{\partial \varsigma}{\partial y} + k_z \frac{\partial^2 \tilde{v}}{\partial z^2}, \tag{13.6c}$$

$$\frac{\partial \tilde{u}}{\partial x} + \frac{\partial \tilde{v}}{\partial y} + \frac{\partial \tilde{w}}{\partial z} = 0. \tag{13.6d}$$

This system of equations is solved with the following boundary and initial conditions

$$\tilde{u} n_x + \tilde{v} n_y = \tilde{u}_n \quad \text{on } \Gamma_l \tag{13.7a}$$

$$k_z \frac{\partial \tilde{u}}{\partial z} = \lambda_b \tilde{u} \sqrt{\tilde{u}^2 + \tilde{v}^2} \quad \text{on the bottom } z = -h(x, y) \tag{13.7b}$$

$$k_z \frac{\partial \tilde{v}}{\partial z} = \lambda_b \tilde{v} \sqrt{\tilde{u}^2 + \tilde{v}^2} \quad \text{on the bottom } z = -h(x, y) \tag{13.7c}$$

$$k_z \frac{\partial \tilde{u}}{\partial z} = \lambda_W W_x \sqrt{W_x^2 + W_y^2} \quad \text{on the free surface } z = \varsigma(x, y, t) \tag{13.7d}$$

$$k_z \frac{\partial \tilde{v}}{\partial z} = \lambda_W W_y \sqrt{W_x^2 + W_y^2} \quad \text{on the free surface} z = \varsigma(x, y, t) \tag{13.7e}$$

$$\varsigma(x, y, 0) = \varsigma_0(x, y), \tilde{u}(x, y, z, 0) = \tilde{u}_0(x, y, z), \tilde{v}(x, y, z, 0) = \tilde{v}_0(x, y, z),$$
$$\tilde{w}(x, y, z, 0) = \tilde{w}_0(x, y, z). \tag{13.7f}$$

Here n_x and n_y are the components of the external normal to the lateral boundary Γ_l, $\tilde{u}_n$ is a given function, λ_b is the coefficient of the bottom friction, λ_W is the coefficient of the wind stress friction, W_x and W_y are the components of the wind velocity.

The problem (13.6), (13.7) is used in simulation of 3D flows in natural water bodies.

13.2 Two-dimensional shallow water equations

Further simplification of the system (13.6) can be obtained by integrating the equations (13.6b) and (13.6c) from $-h$ to ς along the vertical axis. As a result we have the following

$$\frac{\partial \varsigma}{\partial t} + \frac{\partial Hu}{\partial x} + \frac{\partial Hv}{\partial y}, \tag{13.8a}$$

$$\frac{\partial u}{\partial t} + u\frac{\partial u}{\partial x} + v\frac{\partial u}{\partial y} - l_C v = -g\frac{\partial \varsigma}{\partial x} - \lambda_b u\sqrt{u^2+v^2} - \lambda_W W_x\sqrt{W_x^2+W_y^2}, \tag{13.8b}$$

$$\frac{\partial v}{\partial t} + u\frac{\partial v}{\partial x} + v\frac{\partial v}{\partial y} + l_C u = -g\frac{\partial \varsigma}{\partial y} - \lambda_b v\sqrt{u^2+v^2} - \lambda_W W_x\sqrt{W_x^2+W_y^2}. \tag{13.8c}$$

Here $H = h + \varsigma$ and

$$Hu = \int_{-h}^{\varsigma} \tilde{u}dz, \quad Hv = \int_{-h}^{\varsigma} \tilde{v}dz \ .$$

13.3 Model of wind-induced circulation in shallow water

13.3.1 Problem formulation

We consider the model of currents in shallow water body, described by simplified shallow water equations

$$\frac{\partial u}{\partial t} - l_C v = -g\frac{\partial \varsigma}{\partial x} - \frac{r}{h}u + \frac{\tau_x}{h},$$

$$\frac{\partial v}{\partial t} + l_C u = -g\frac{\partial \varsigma}{\partial y} - \frac{r}{h}v + \frac{\tau_y}{h},$$

$$\frac{\partial}{\partial x}(hu) + \frac{\partial}{\partial y}(hv) = 0 \ .$$

Here u and v are the components of the averaged velocity vector, $\varsigma(x,y,t)$ is the free surface level, $h(x,y)$ is the depth, τ_x and τ_y are the components of the frictional stress along the axes x and y, respectively, l_C is the Coriolis

parameter, equal to $l_C{=}2\omega\sin\theta$, where ω is the Earth's angular velocity, θ is the latitude, g is the acceleration due to gravity, $r{=}C_f\sqrt{u^2{+}v^2}$, C_f is the bottom friction coefficient.

The condition on the boundary is

$$u_n = un_x + vn_y = 0,$$

where n_x and n_y are the components of the external normal to the boundary.

Introduce the integral stream function

$$hu = \frac{\partial\Psi}{\partial y}, \quad hv = -\frac{\partial\Psi}{\partial x}$$

and obtain an equation which we will solve in the simply connected domain Ω with the boundary b.

$$\frac{\partial}{\partial t}[\frac{\partial}{\partial x}(\frac{1}{h}\frac{\partial\Psi}{\partial x}) + \frac{\partial}{\partial y}(\frac{1}{h}\frac{\partial\Psi}{\partial y})] + \frac{\partial}{\partial y}(\frac{l_C}{h}\frac{\partial\Psi}{\partial x}) - \frac{\partial}{\partial x}(\frac{l_C}{h}\frac{\partial\Psi}{\partial y})$$
$$+\frac{\partial}{\partial x}(\frac{r}{h}\frac{\partial\Psi}{\partial x}) + \frac{\partial}{\partial y}(\frac{r}{h}\frac{\partial\Psi}{\partial y}) = \frac{\partial}{\partial y}(\frac{\tau_x}{h}) - \frac{\partial}{\partial x}(\frac{\tau_y}{h}). \qquad (13.9)$$

The initial and boundary conditions are written in the form

$$\Psi\,|_b{=}\,0, \quad \Psi\,|_{t=0}{=}\,\Psi_0(x,y). \qquad (13.10)$$

We assign the components of the frictional stress of the wind by means of formula

$$\tau_x = C_W W_x\sqrt{W_x + W_y}, \quad \tau_y = C_W W_y\sqrt{W_x + W_y},$$

where W_x ï W_y are the components of the wind velocity, C_W is a coefficient.

The implicit scheme was used to approximate (13.9) with respect to time. The resulting elliptic equation for the integral stream function on the upper time level is solved by the upstream finite element method described in the previous section.

The input data were the values of the water body depth at nodes of a square grid and the wind velocity. These values were interpolated to the adaptive grid at each iteration using bilinear interpolation formulae.

The wind circulation was modelled with the following parameter values: $C_f{=}2.6\cdot10^{-3}$, $C_W{=}3.1\cdot10^{-6}$, $g{=}9.8\,m/s^2$.

13.3.2 Results of computations

In all the computations, block-structured grids were constructed by the variational barrier method. Finite difference method cannot be applied here, because this method does not guarantee the construction of convex grids.

Result of computations presented for the Mojaiskii reservoir (Figs.13.1-13.6) show that grid generation method with condensation and orthogonalization near the boundary based on the functional of the energy density increases the accuracy of computations.

Another example of the simulation of the wind currents in the Piltun and Chayvo bays is presented in Figs.13.7-13.10.

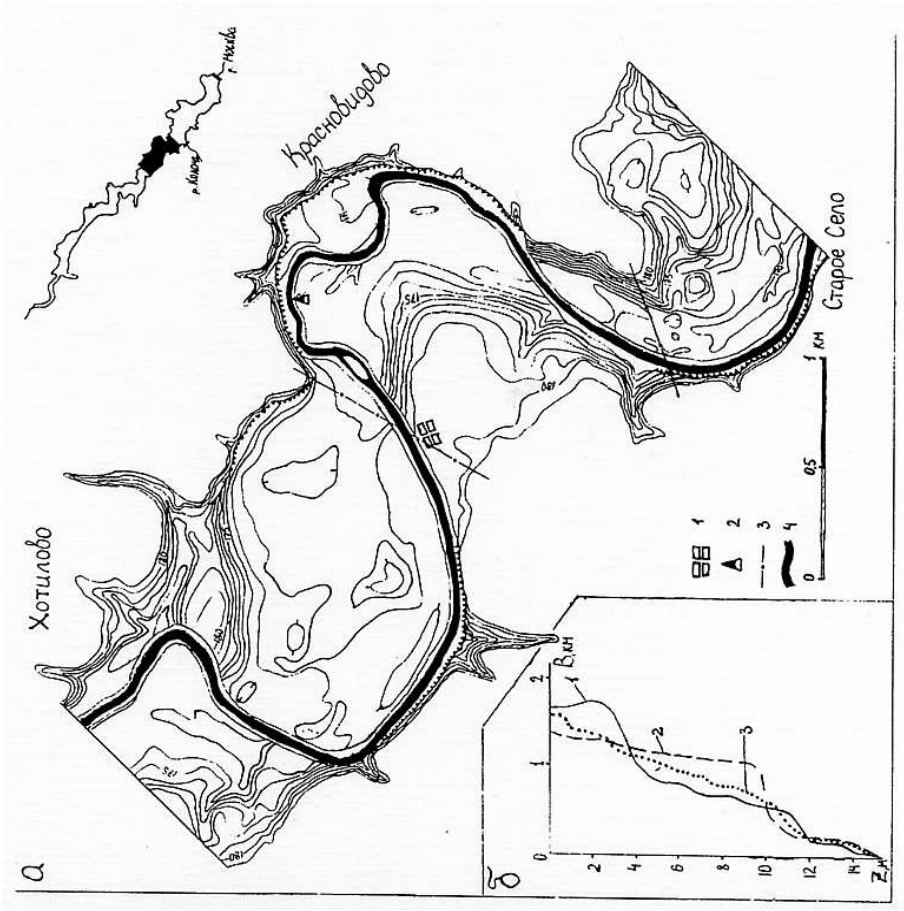

Fig. 13.1:

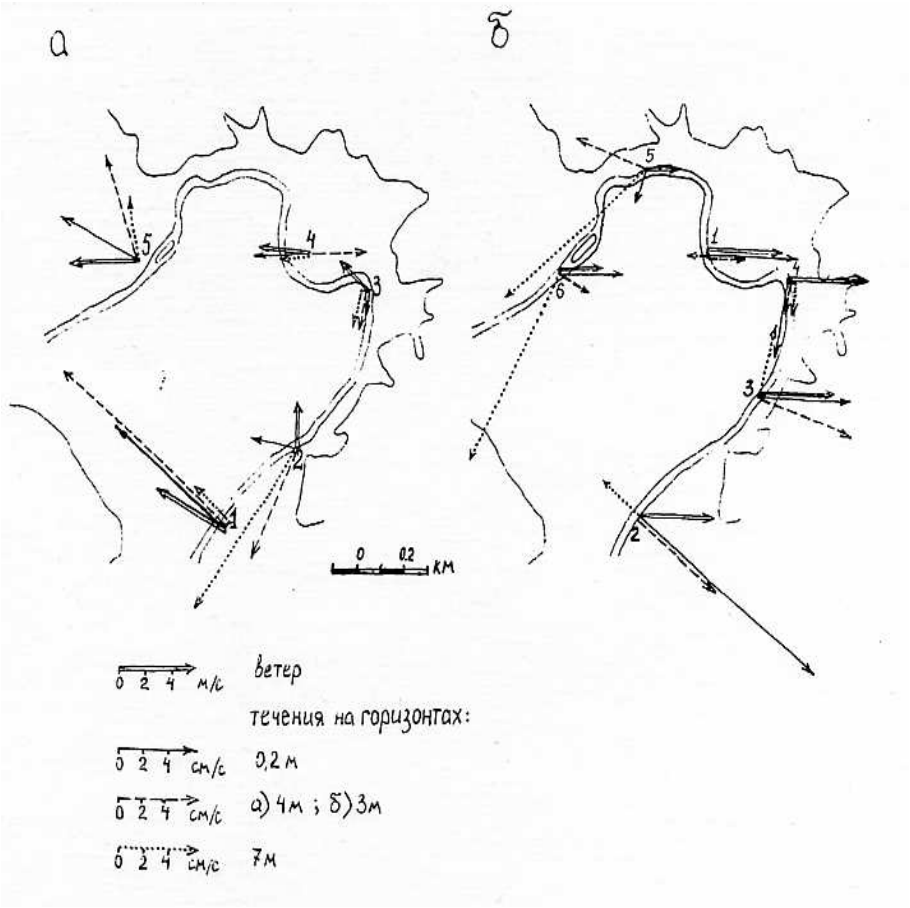
а
б
0 02 KM
0 2 4 м/с
ветер
течения на горизонтах:
0 2 4 см/с
0,2 м
0 2 4 см/с
а) 4м ; б) 3м
0 2 4 см/с
7м

Fig. 13.2:

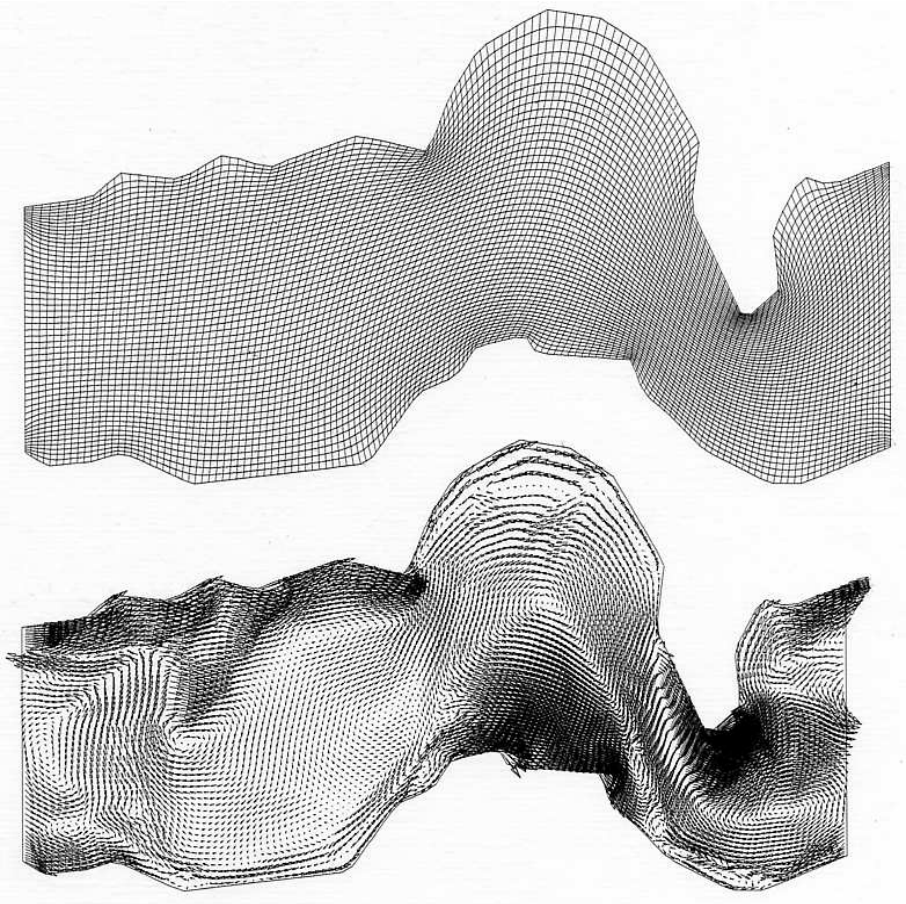

Fig. 13.3:

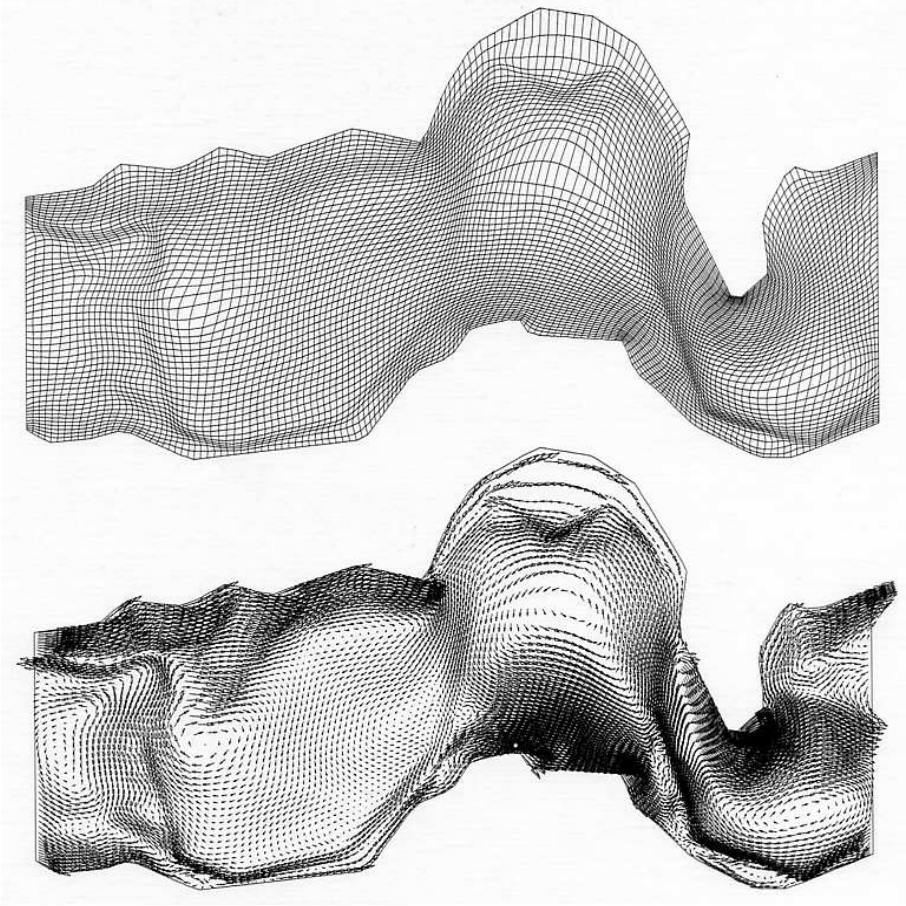

Fig. 13.4:

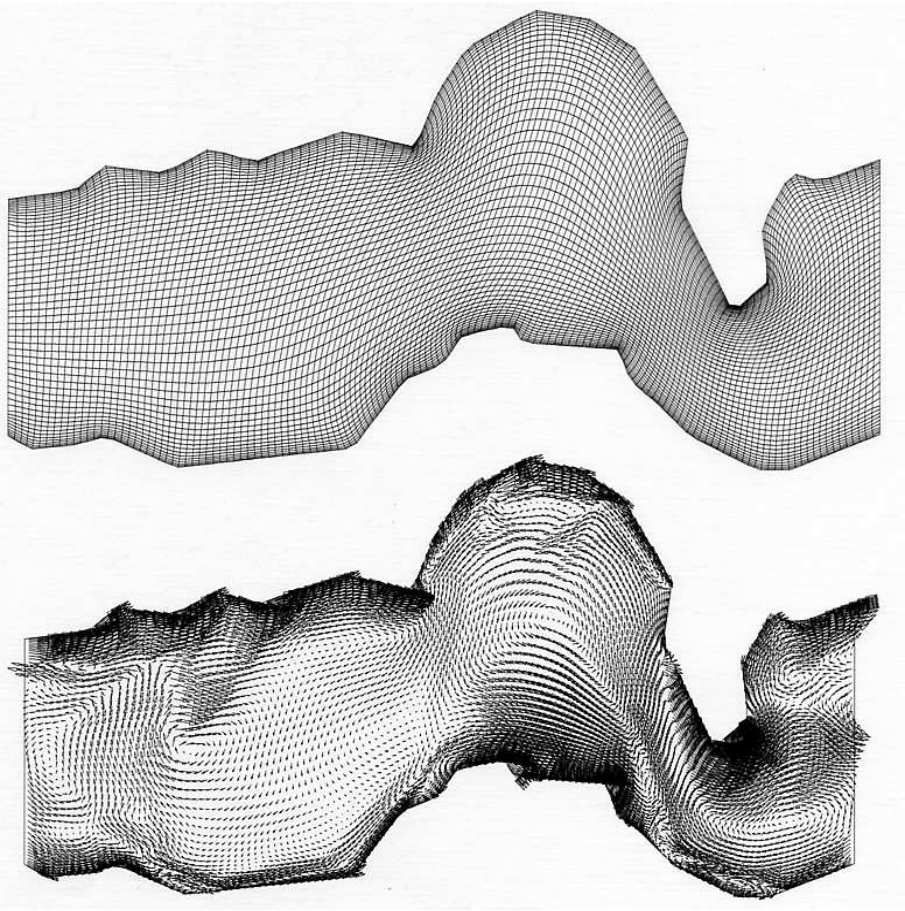

Fig. 13.5:

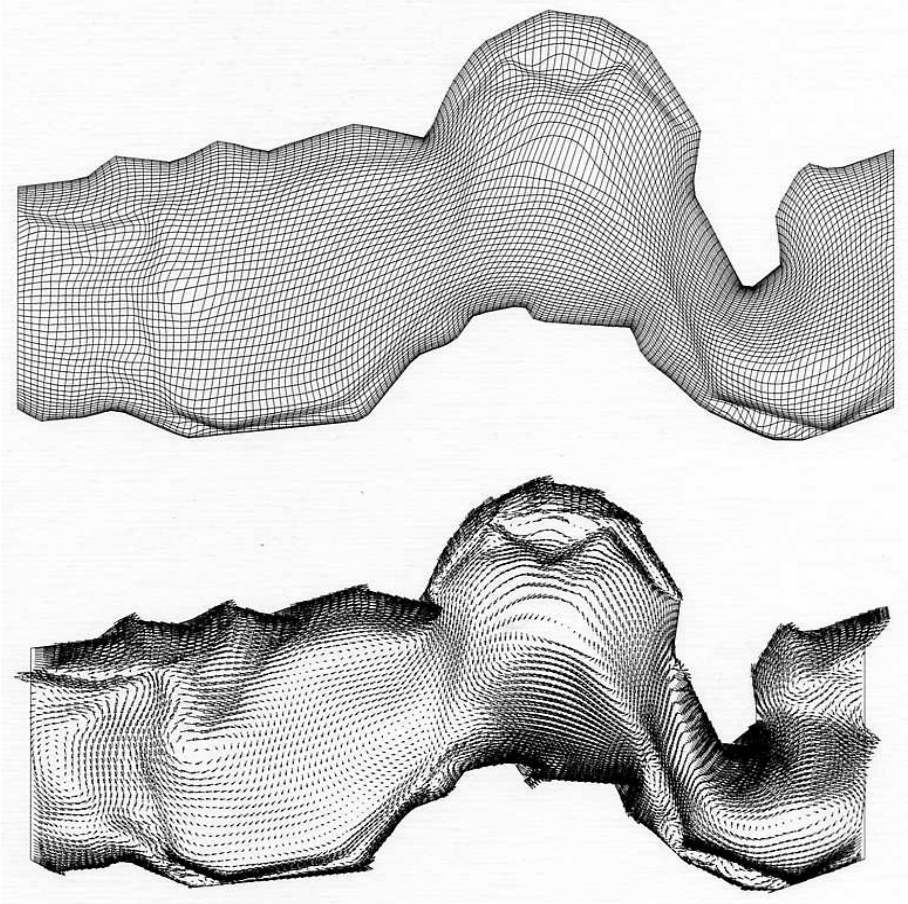

Fig. 13.6:

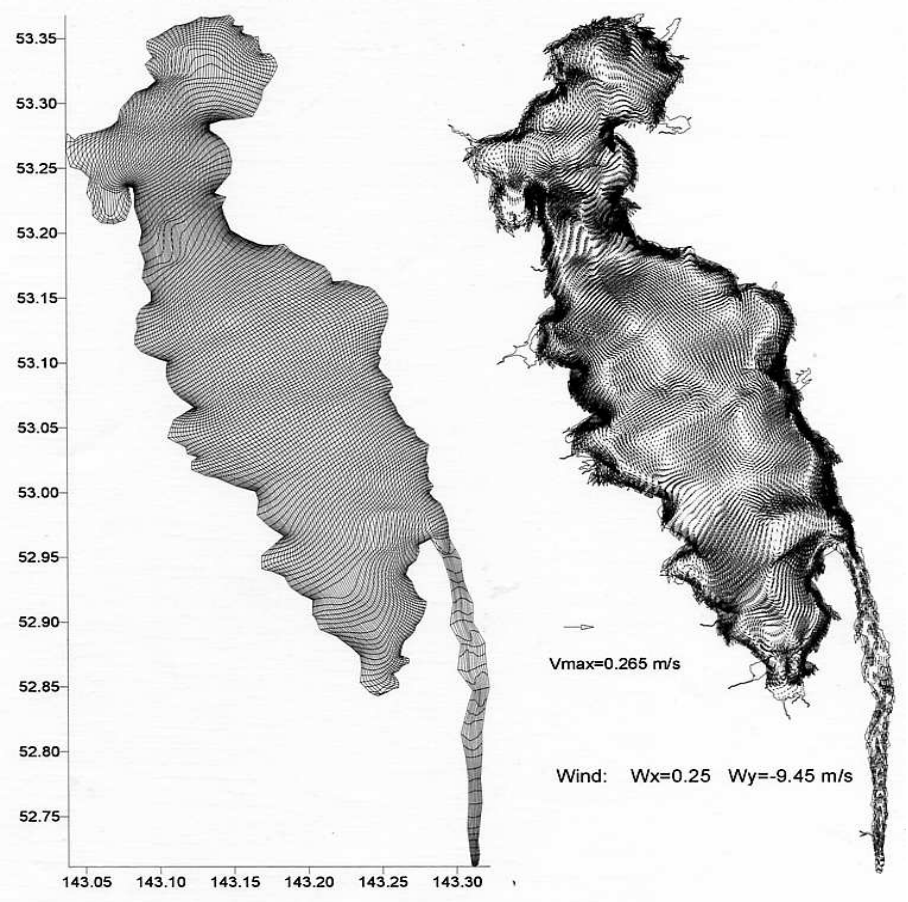
53.35
53.30
53.25
53.20
53.15
53.10
53.05
53.00
52.95
52.90
52.85
52.80
52.75
143.05
143.10
143.15
143.20
143.25
143.30
Vmax=0.265 m/s
Wind: Wx=0.25 Wy=-9.45 m/s

Fig. 13.7:

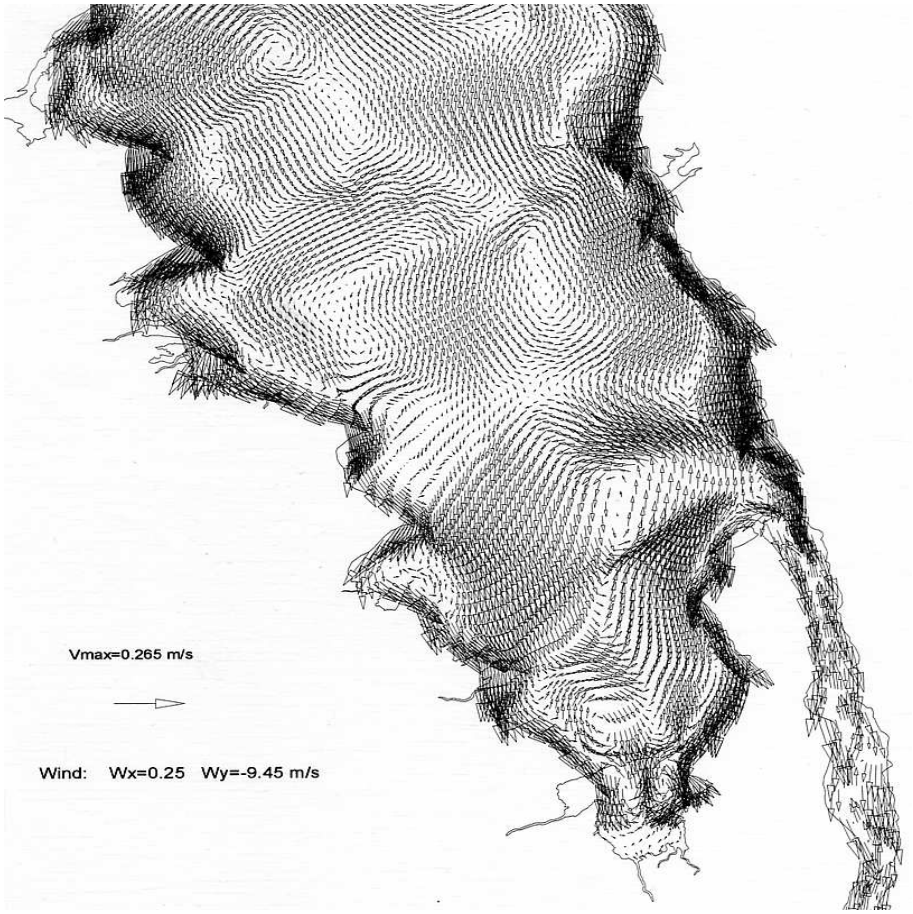

Fig. 13.8:

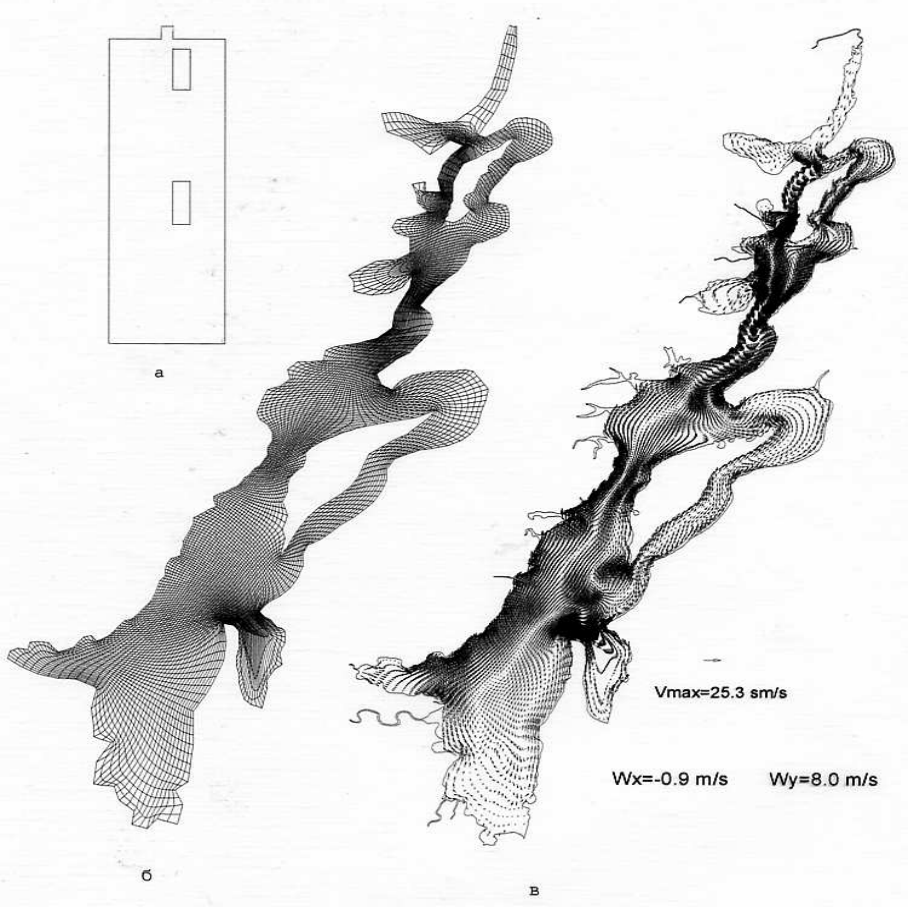

Fig. 13.9:

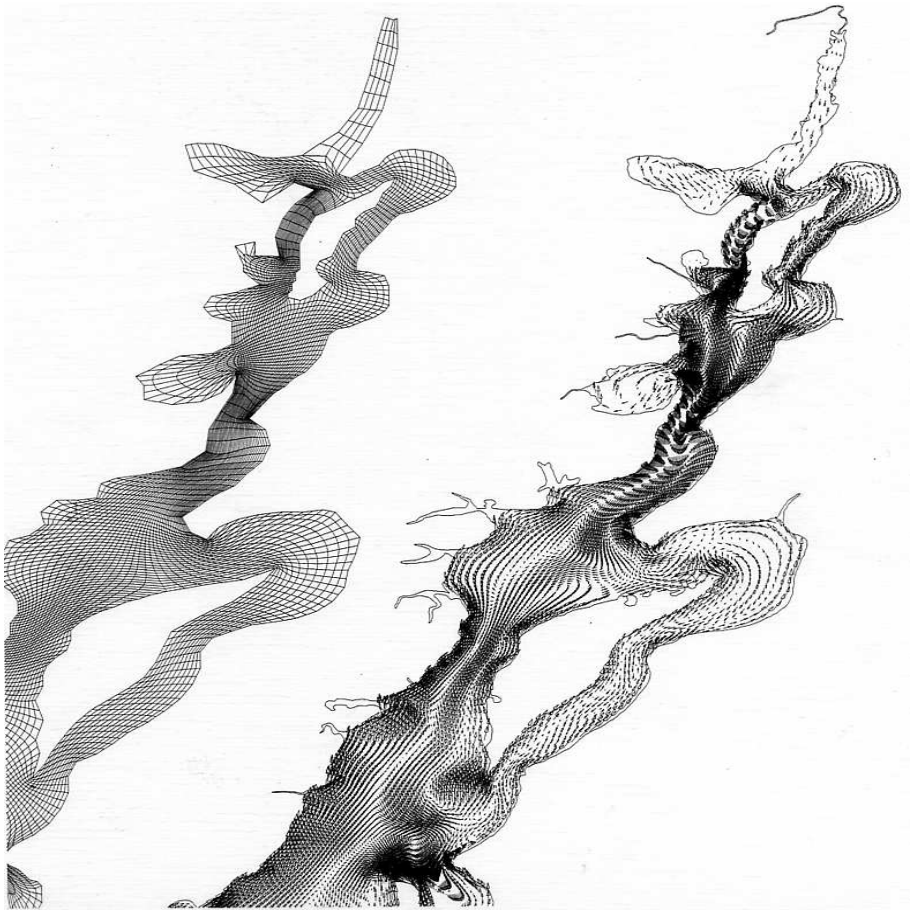

Fig. 13.10:

Chapter 14

Moving grids in simulation of free surface flow

In many approaches to numerical solution of free-surface problems, the physical domain is transformed onto a computational domain (usually a rectangle) through the change of variables involving the vertical coordinate only. However, this approach cannot be applied in certain cases, as in the presence of steep gradients of free surface level.

For this reason a technique for constructing curvilinear coordinate system, guaranteeing invertibility at the continuous level and unfolded grid generation at the discrete level is applied.

To simulate the flow through the overfall dam with discharge controlled by hosting the gate, the model, based on the Euler equations, is applied. The numerical method contains barrier method for grid generation and splitting technique for the numerical solution of equations, describing the physical process.

14.1 Problem formulation and choice of mathematical model

The principal goal of this study is to construct a mathematical model that can predict the overfall dam discharge ratings that correspond to various gate openings and various head water heights. These ratings represent the dam underflow and overflow discharge rates $Q_u(H_{in})$ and $Q_o(H_{in})$ as functions of the head water height H_{in} and various gate openings. For Rublevskii Dam the ratings cannot be derived from measurements, because just a few

regimes (data points) can be observed during a calendar year and not all of them can be quantified.

Rublevskii Dam, across the Moscow River (in operation since 1931), is a two-span overfall dam. Each 30m span is equipped with roller gates. The gates were designed and manufactured by the MAN Group company.

The roller gate is designed as a gate with downward leaf attached to the headwater side of the roller and with runoff over its crest. The mass of each gate is 62 tonnes as specified by the manufacture.

The roller is the hollow cylinder with a circular cross section of diameter 3.1m, covered with steel of thickness varying from 9.6mm at the gate posts to 13.6mm in the middle of a span.

The downward leaf has a curved surface with a curvature radius of 2.946m. The leaf is covered with 9.7mm steel sheeting.

The gate is rolled along cog rails inclined at an angle 70 degrees. The rails are fixed in grooves in the end posts and engaged with the socket bands attached to the roller ends. Each gate is hosted by the socket chain being pulled in at one end. The chain runs along a guide fixed to the gate on the headwater side. The lower end of the chain is attached to a support, and its upper end bears against a hoist gear. The geometric characteristics of the Rublevskii Dam (Fig.14.1) we used to prescribe the geometry of the mathematical model. The bottom profile was prescribed according to the Rublevskii Dam detailed drawings.

Fig.14.2*a* shows the computational domain corresponding to the dam cross section, including the roller gate as a portion of its boundary. The domain has two geometries. The first one corresponds to a hoisted roller, which is rotated so that each a point on its surface is displaced by a length equal to its elevation. This design feature was confirmed by measurements. Note that the roller opening is measured along the vertical direction. The right and left boundaries of the computational domain are located 15 and 10m from the roller axis, respectively. Fig.14.2*b* shows the computational domain corresponding to the lowest position of the roller. The initial position of the free surface (a surface profile is a line in 2D case) is also shown for both geometries in Fig.14.2.

Let us discuss the physics of the flow in some detail. The runoff current interacts with the underflow. As a result, a region of aerated turbulent flow develops on the tail water side, which corresponds to a complex water-air two-phase motion. However, tailwater turbulence has a little effect on the underflow discharge rate and no effect on the runoff, because disturbances

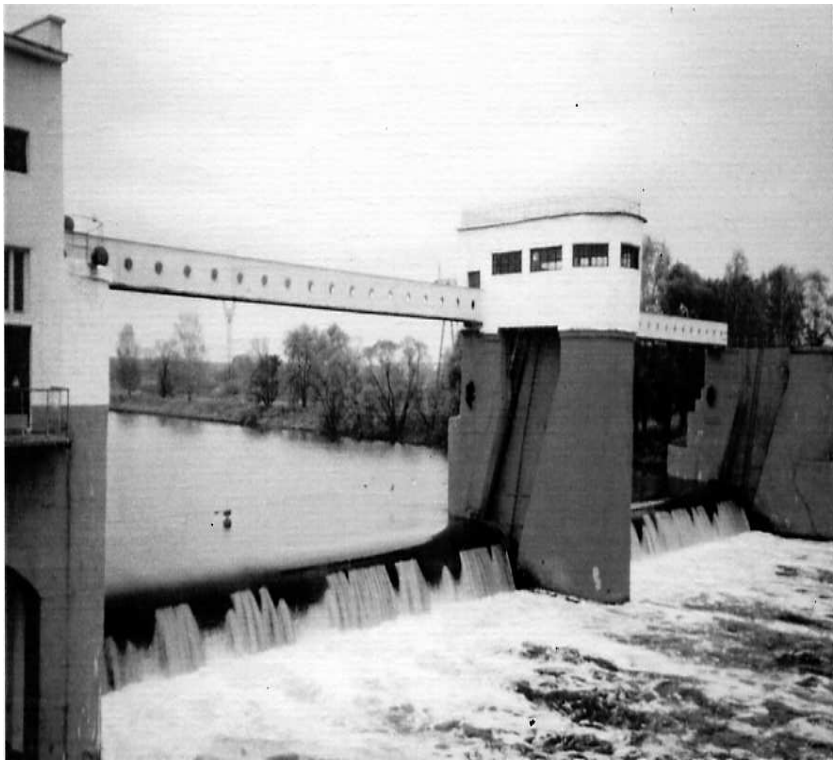

Fig. 14.1:

cannot propagate upstream the supercritical flow. Moreover, a standard dam is designed so as to minimize the effect of turbulence on the total discharge rate; otherwise, flow oscillations may prematurely wear out the roller gate.

Let us estimate the Reynolds number $Re = UL/\nu$ and the Froude number $Fr = U/\sqrt{gH}$, where U is the reference velocity, L is the reference horizontal length, H is the reference depth, $\mu = 10^{-6}m^2/s$ is the kinematic viscosity, and g is the gravitational acceleration. Using the fact that U and H vary from $U = 0.1m/s$ and $H = 5m$ at the inlet boundary to $U = 2m/s$ and $H = 0.1m$ at the roller, and assuming the horizontal reference length

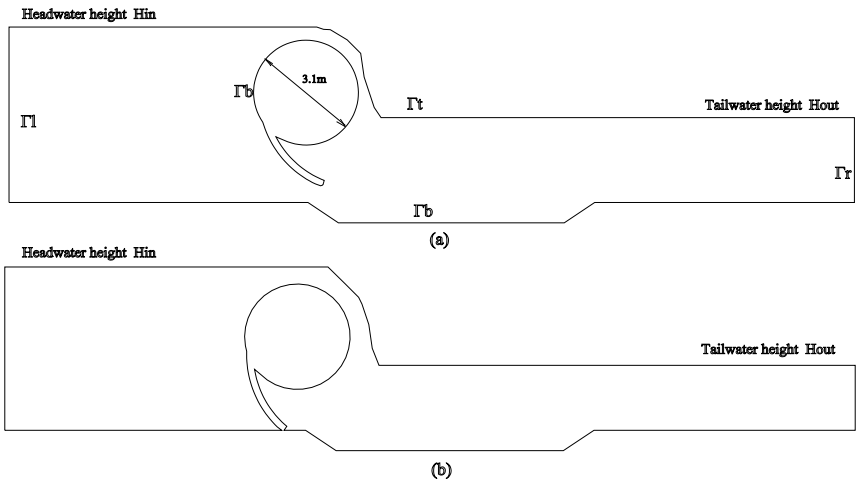

Fig. 14.2:

$L = 5m$, one finds that the Reynolds number varies from $5{\cdot}10^5$ to 10^7 with the Froude number varies from 0.014 to 2.

The choice of a mathematical model is based on the following considerations.

1. The shallow water approximation cannot be used because the flow involves substantial vertical accelerations.

2. The flow through the dam is approximately uniform spanwise, which makes it possible to restrict considerations to 2D formulation.

3. Preliminary estimates show that viscosity can be neglected.

4. Tailwater aeration can be neglected.

5. The problem must include determination of the free surface geometry, which controls the overflow velocity distribution.

14.2 Mathematical formulation of problem

A 2D unsteady free surface inviscid incompressible flow is considered in a coordinate system with horizontal x-axis pointing downstream and y-axis pointing upwards.

In a domain Ω with boundary Γ a solution is sought to the Euler equations for the inviscid incompressible flow.

$$\frac{\partial u}{\partial t} + u\frac{\partial u}{\partial x} + v\frac{\partial u}{\partial y} = -\frac{1}{\rho}\frac{\partial p}{\partial x}, \tag{14.1a}$$

$$\frac{\partial v}{\partial t} + u\frac{\partial v}{\partial x} + v\frac{\partial v}{\partial y} = -\frac{1}{\rho}\frac{\partial p}{\partial y} - g, \tag{14.1b}$$

$$\frac{\partial u}{\partial x} + \frac{\partial v}{\partial y} = 0\ . \tag{14.1c}$$

Here,u and v are flow velocity components, $\rho = 10^3 kg/m^3$, $g = 9.81 m/s^3$ is the gravitational acceleration due to gravity and p is pressure.

The domain Ω can be either simply connected or doubly connected (when the rollers are in hoisted position). Its boundary $\Gamma = \Gamma_l + \Gamma_r + \Gamma_t + \Gamma_b$. Here Γ_b represents the bottom and the roller surface where the following impermeability conditions are set

$$u_n = un_x + vn_y = 0, \quad \text{on } \Gamma_b\ . \tag{14.2a}$$

where n_x and n_y are the components of the outward normal to the boundary.

Γ_l and Γ_r are left and right boundaries, defined as $x = x_l$ and $x = x_r$.

The free surface Γ_t is defined by means of two functions $x_s(s,t)$ and $y_s(s,t)$, where s is the length along the boundary, t is time.

Boundary conditions:

Water flows into the domain across the boundary Γ_l, where a boundary condition for pressure is set and a free-surface level is prescribed

$$\frac{\partial p}{\partial n} = 0, \quad y(0,t) = y_l(t) \quad \text{on} \quad \Gamma_l\ . \tag{14.2b}$$

Condition (14.2b) is used when the convective terms in Eqs. (14.1a, b) are negligible on Γ_l. Otherwise, additional boundary conditions must be set; for example, both velocity components can be prescribed on Γ_l.

Water flows out of the domain across the boundary Γ_r, where a single boundary condition for pressure is sufficient

$$\frac{\partial p}{\partial n} = 0 \qquad \text{on} \quad \Gamma_r\ . \tag{14.2c}$$

Two boundary conditions are set on the free surface Γ_t: a kinematic one and a dynamic one. The kinematic condition is derived from the continuity

equation written for the free surface, reflecting the fact that a fluid particle initially located at the surface cannot move from it at subsequent moments

$$u_n = un_x + vn_y = \frac{\partial x_s}{\partial t} n_x + \frac{\partial y_s}{\partial t} n_y \qquad \text{on} \quad \Gamma_t \ . \tag{14.2d}$$

The dynamics condition implies that the water and air pressure are equal at the phase boundary (i.e. on the free surface)

$$p = P_a \qquad \text{on} \quad \Gamma_t \ . \tag{14.2e}$$

where P_a is the atmospheric pressure.

Since the flow may separate from the roller, condition (14.2a) is supplemented by a condition for pressure analogous to (14.2e)

$$p = P_a \quad \text{if} \quad p < P_a \qquad \text{on} \quad \Gamma_r \ . \tag{14.2f}$$

When the flow separates, part of the boundary adjoining the roller becomes free and begins to move with a certain velocity. However this condition is used in unconstrained form, serious difficulties may arise from the instability of a free-falling jet. For this reason, condition (14.2e) is set on a stationary boundary (roller surface). As a consequence, the mass conservation law is violated, and the tailwater discharge rate is overpredicted. However, numerical results show that this does not lead to significant error in discharge rating.

Initial conditions are

$$u(x, y, 0) = u_0(x, y), \quad v(x, y, 0) = v_0(x, y) \quad \text{at } t = 0 \quad \text{in } \Omega \ . \tag{14.3}$$

The problem is to find the functions

$$u(x, y, t), \quad v(x, y, t), \quad p(x, y, t) \ ,$$

satisfying equations (14.1) and the initial and boundary conditions (14.2) and (14.3).

14.3 Splitting technique

The splitting technique with respect to physical processes used to solve Eqs.(14.1) is designed as follows. Suppose that all flow variables are known

at the time level t_n. Then, the unknown values at $t_{n+1}=t_n+\tau$ are calculated using the following stages.

Stage 1:

$$\frac{\tilde{u}-u^n}{\tau} = -u^n\frac{\partial u^n}{\partial x} - v^n\frac{\partial u^n}{\partial y} \ , \tag{14.4a}$$

$$\frac{\tilde{v}-v^n}{\tau} = -u^n\frac{\partial v^n}{\partial x} - v^n\frac{\partial v^n}{\partial y} - g \ , \tag{14.4b}$$

Stage 2:

$$\frac{\tau}{\rho}\left(\frac{\partial^2 p^{n+1}}{\partial x^2} + \frac{\partial^2 p^{n+1}}{\partial y^2}\right) = \frac{\partial \tilde{u}}{\partial x} + \frac{\partial \tilde{v}}{\partial y} \ , \tag{14.5}$$

Stage 3:

$$u^{n+1} = \tilde{u} - \frac{\tau}{\rho}\frac{\partial p^{n+1}}{\partial x} \ , \tag{14.6a}$$

$$v^{n+1} = \tilde{v} - \frac{\tau}{\rho}\frac{\partial p^{n+1}}{\partial y} \ , \tag{14.6b}$$

The physical meaning of this procedure is the following. At stage 1 the intermediate values $\tilde{u}$ and $\tilde{v}$ of the velocity components are computed. In general, they do not satisfy the continuity equation (14.1*c*). At stage 2 the pressure is calculated by solving the Poisson equation. The resulting pressure is used at stage 3 to correct the velocity so that the continuity equation is satisfied by the velocity components at the next time step.

14.4 Choice of grid and representation of unknown variables

The computations were performed on a moving curvilinear grid constructed for given coordinates of the boundary grid points at every time step. The iterative variational barrier method (see Chapter 4) is used for grid generation.

The choice of approximation of unknown variables is extremely important for constructing a stable algorithm. The velocity components u and v are treated as constant inside every cell of the moving grid at every time level as that of in Godunov's scheme [57]. The pressure p is decomposed over the basis functions of the finite element method with

quadrilateral isoparametric elements, and the values of pressure may be interpreted as computed at the nodes. This makes the free-surface condition for pressure easier to use as a boundary condition of the first kind, whereas the conditions set on the bottom, roller, and fluid boundary are treated as boundary conditions of the second kind (except for the region of jet separation at the roller, where a condition of the first kind for pressure is set).

14.5 Computation of free boundary

Let us now discuss the computation of the boundary. If the values of flow variables are assumed to remain invariant during underlying time step, then it is sufficient to calculate the velocities of boundary grid nodes in order to determine a new location of the free surface. The velocities of boundary nodes are calculated in terms of flow velocities on the cell edges located on the free surface. Since velocity components are constant inside every cell, the velocity component along the normal to the boundary is readily calculated by projecting the velocity vector of the boundary cell onto the outward normal to the boundary edge. Thus, a normal velocity component is obtained for every edge of the open polygon representing the free surface. The velocity of a vertex in the polygon is calculated as the half-sum of the velocities of the edges adjoining the vertex on its left and right. At the right boundary point, the projection of the normal velocity onto the vertical axis is used. The location of the left boundary point is prescribed by the boundary condition (14.2*b*). The known values of the time step and node velocity are used to calculate new coordinates of the free-surface points.

However, this procedure may result in spurious oscillation of the free surface, which can be suppressed by applying various smoothing methods. In the present study a procedure, analogous to that of in [57] is employed. It can be explained as follows. The initial distribution of grid nodes over the free surface is stored and subsequently used at every time step. Once new coordinates of the boundary nodes have been computed as described above, the distances between grid nodes in the resulting open polygon are not equal to that of on the initial free surface. For this reason, the coordinates of boundary nodes are updated so as to define the distance between grid nodes equal to their counterparts at the initial moment. This procedure, on one hand, prevents the the occurrence of very short edges or degeneration

of boundary cells and, on the other hand, stabilizes the free-surface motion.

Another difficulty arising in the free-surface problem is associated with wave breakdown. This term refers to a nonuniquely defined free surface, and special measures must be taken to continue the computation. In the method used in the present study, wave breakdown is eliminated by using the following constraint. The angle made by each edge of the open polygon with x-axis is calculated when a new location of the free surface is computed. If the resulting angle is close to or greater than $\pi/2$, then the right endpoint of the edge is shifted so as to obtain a prescribed angle. In the present modeling the limiting angle is prescribed by the condition that its cosine is 0.01.

14.6 Numerical method for stage 1

At stage 1 of the splitting scheme, the two transport equations in (14.4) are solved for intermediate values $\tilde{u}$ and $\tilde{v}$ of the velocity components. At this stage, a grid for the new time step is already constructed, and new values of the velocity components at the cell centers are sought at the $(n+1)$th time step. The grid node coordinates at time t_n and t_{n+1} and the values of velocity components at t_n are used as input data.

At $t=0$ the free-surface geometry and velocity field must be given. If zero velocities are defined, the grid may degenerate at the roller crest. For this reason initial velocities are calculated by solving the equation for streamfunction. Boundary conditions include impermeability conditions on the bottom and free surface and uniform velocities distributions at the inlet and outlet boundaries. The ratio of the underflow and runoff discharge rate is set at 2/1 in the case of a hoisted roller.

Equations (14.4) are computed with the first-order explicit Godunove-type scheme, see the monograph [57]. Its implementation on a moving mesh includes calculation of the normal and tangential velocity components at every itercell face by solving one-dimensional Riemann problem for the nonlinear transport equation. These quantities are determined so as to take into account motion of the cell edge. The calculation formulas and stability condition can be found in [57].

As a result the velocity components are calculated at the cell centers at time t^{n+1}. The remaining calculation stages are performed on the new grid.

Note that running time can be reduced by using the following technique. Equations (14.4) can be solved within two steps. First, new values of the velocity components are calculated on the grid constructed at time t^{n+1} by applying an interpolation procedure where the transport equations are solved with velocity equal to the reversed cell-edge velocity. Then, Eqs.(14.4) are solved on the stationary mesh corresponding to the next time level. Advantages of this technique is that we use nodes motion at the separate stage. Since the flow velocity is much higher than the cell-edge velocities, therefore, at the stage of solving Eqs. (14.4) we can perform several "internal"time steps, that allows for increasing the time step and reducing the total running time. The main part of time is spent on solving the Poisson equation for the pressure at the stage 2 of the splitting scheme.

14.7 Method for solving Poisson equation at stage 2

To solve the equation (14.5) we use the finite element method with quadrilateral isoparametric elements (for detail description see [71] and Chapter 11 of the present book). The problem is formulated in a generalized form. The corresponding integrals are approximated by quadrature formulae, where the nodes coincide with the grid nodes. As a result a regular approximation, corresponding to a finite-difference scheme on nine-point stencil, is obtained to the operator of the problem on the curvilinear mesh. The matrix elements are obtained in the course of matrix inversion. An integral of the right-hand part of the Poisson equation is replaced by the integral over the cell, consisting of quadrilaterals resulting from the partition of the grid cells adjoining the current grid point by the segments that join the midpoints of their opposite sides, see Fig.11.1. This integral is replaced by the contour integral as that of in the finite volume method.

The resulting set of linear equations is solved using a block overrelaxation method [71]. The pressure from the preceding time level is used as an initial guess. Iterations are terminated if maximal pressure change at a node is less than one million of the highest pressure. This approach may lead to substantial computational cost, which can be reduced by weakening the accuracy requirement for a solution of the pressure equation.

14.8 Calculation of velocity components at stage 3

The velocity components u^{n+1} and v^{n+1} are calculated via the standard formulae of the finite element method. Recall, that since the pressure is defined at the grid nodes, the pressure derivatives in (14.6) can be calculated at any point inside a cell.

The velocity components at $t{=}t_{n+1}$ are obtained via (14.6) at the cell center. The cell center is defined by the bilinear mapping with parameters $\xi{=}\eta{=}0.5$.

The continuity equation (14.1c) written for u^{n+1} and v^{n+1} (which are the constant within the cell) can be interpreted only in the weak sense, i.e. as a system of integral identities. It would be interesting to analyze alternative formulae for calculating the velocity components.

14.9 Results of computations

The above model can be applied to any flow regime, except for flows with the surface level located at less than 10 cm above the roller. In this case there arises the problem on providing grid nondegeneracy, because the free-surface oscillation amplitude associated relaxation to a steady or quasi-steady regime frequently exceeds 10 cm.

All computations were performed with constant time step equal 0.0025 s in the case of the finest grid and 0.01 s to the coarsest grid.

Fig.14.3 shows the flow velocities for two regimes with hoisted rollers. The flow regime, corresponding to a discharge rate of 550 m^3/s and a headwater height of 127.54 m, is illustrated by the grid and flow velocity map shown in Figs.14.3a and 14.3b, respectively. The variation of the free-surface height is weak here, and the elevation head (9 cm) is consistent with that of obtained in measurements.

Fig.14.4 shows a grid fragment and the corresponding flow field obtained by computing only the runoff flow for a free-surface height of 50 cm above the rollers. It is clear that a certain free-surface geometry develops, determining the discharge rate. The separation point is located at a distance of about 1/3 of the roller diameter from the roller crest. An attached hydraulic jump is clearly seen on the right of the free-falling jet.

Table 14.1 shows the discharge rating obtained in serial computations for headwater heights corresponding to free-surface heights above the roller crest varying from 15 to 50 cm (also shown for convenience).

Now consider the results of computations designed to obtain the discharge rating for various gate openings in Rublevskii Dam. These results are shown in table 14.2. The results of measurements are shown in parentheses to demonstrate good agreement between predictions and measurements.

Figs.14.5a and 14.5b show, respectively, the grid and flow-field velocity map for a headwater height of 50 cm above the roller and a gate opening of 40 cm. Figs. 14.5c and 14.5d show the grid and flow-field velocity map for a headwater height above the roller equal to 20 cm. The graphs demonstrate the difference in runoff-underflow interaction between the two flow regimes.

Figs.14.6 shows a fragment of the computational domain with results obtained on a finer grid for a gate opening of 35 cm. For comparison, Fig.14.7 illustrates the case of gate opening equal to 50 cm. It is clear that the basic difference between Figs.14.6 and 14.7 lies in virtual absence of runoff-underflow interaction for the gate opening of 50 cm, due to an underflow discharge substantially exceeding runoff. At the same time the free-surface geometry in Fig.14.6 is somewhat different from that of shown in Fig.14.7 while the tailwater height relative to the roller is substantially higher in the latter case, which is obvious from a comparison of Figs.14.6 and 14.7.

Table 14.1.

Headwater height, m	h (cm)	Q_n m^3/s
128.54	15	7
128.59	20	11
128.64	25	15
128.69	30	20
128.74	35	26
128.79	40	32
128.84	45	38
128.89	50	44.6

Table 14.2.

Headwater height, m	h, sm	$Q_b\ m^3/s$	$Q_t\ m^3/s$	Q_b+$Q_t\ m^3/s$
				Gate opening A=0.1 m
128.69	20	39	10	49
128.79	30	40	21	61
128.89	40	40.5	32	72.5
128.99	50	41	45	86
				Gate opening A=0.15 m
128.74	20	59	11	70
128.84	30	60	21	81
128.94	40	61	33	94
129.04	50	62	45	107
				Gate opening A=0.2 m
128.79	20	78	11	89
128.89	30	79.5	22	101.5
128.99	40	81	33	114
129.01	42	83	37 (40)	120 (124)
129.09	50	84	46	130
				Gate opening A=0.3 m
128.89	20	122	10	132
128.99	30	122.5	19	141.5
129.09	40	123	33	156
129.17	48	124	48	172 (165)
129.19	50	125	50	176
				Gate opening A=0.35 m
128.94	20	151	10	161
129.04	30	152	19	171
129.14	40	158	35	194
129.21	47	162	45	207 (210)
129.24	50	164	48	212
				Gate opening A=0.4 m
128.99	20	185	11	197
129.09	30	188	19	207
129.19	40	189	33	222
129.29	50	192	48	240
				Gate opening A=0.45 m
129.04	20	216	9.5	225.5
129.14	30	219	20	239
129.24	40	224	33	257
129.28	44	226	36 (31)	262 (265)
129.34	50	228	49	269
				Gate opening A=0.5 m
129.09	20	252	13	265
129.19	30	255	26	281
129.29	40	258	32	290
129.39	50	261	49	310

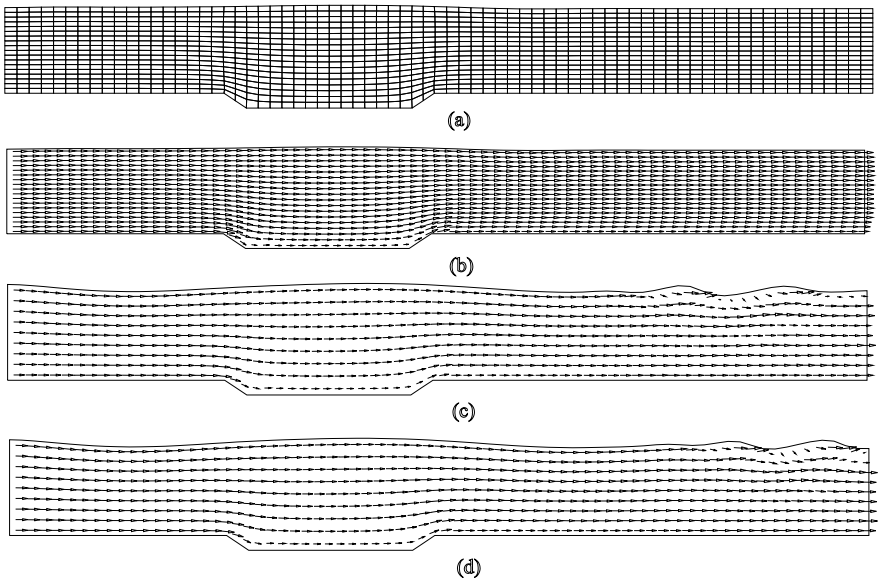

Fig. 14.3:

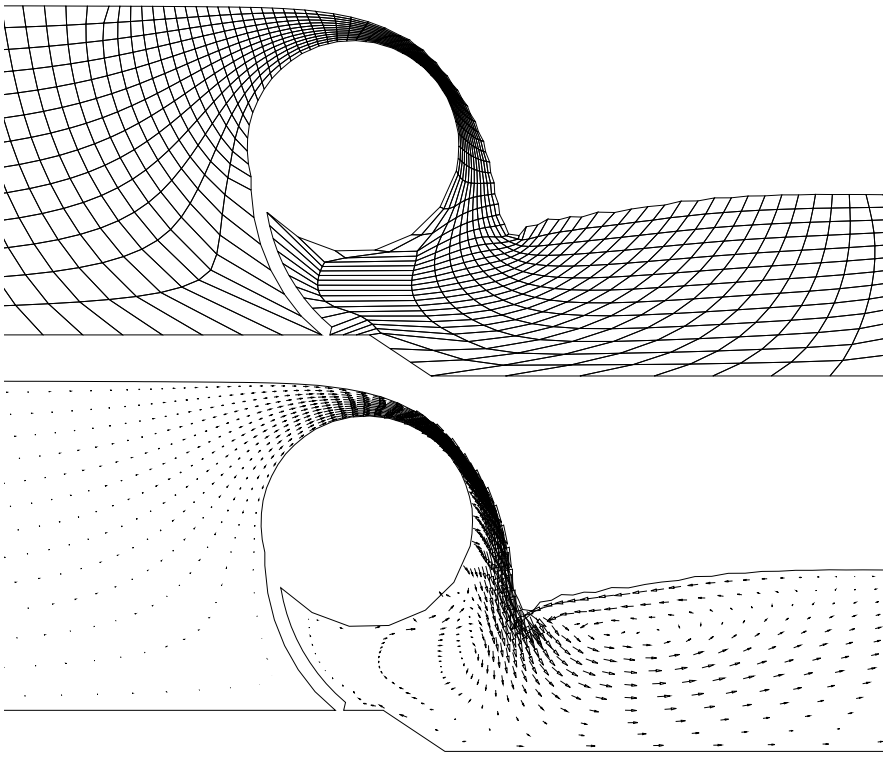

Fig. 14.4:

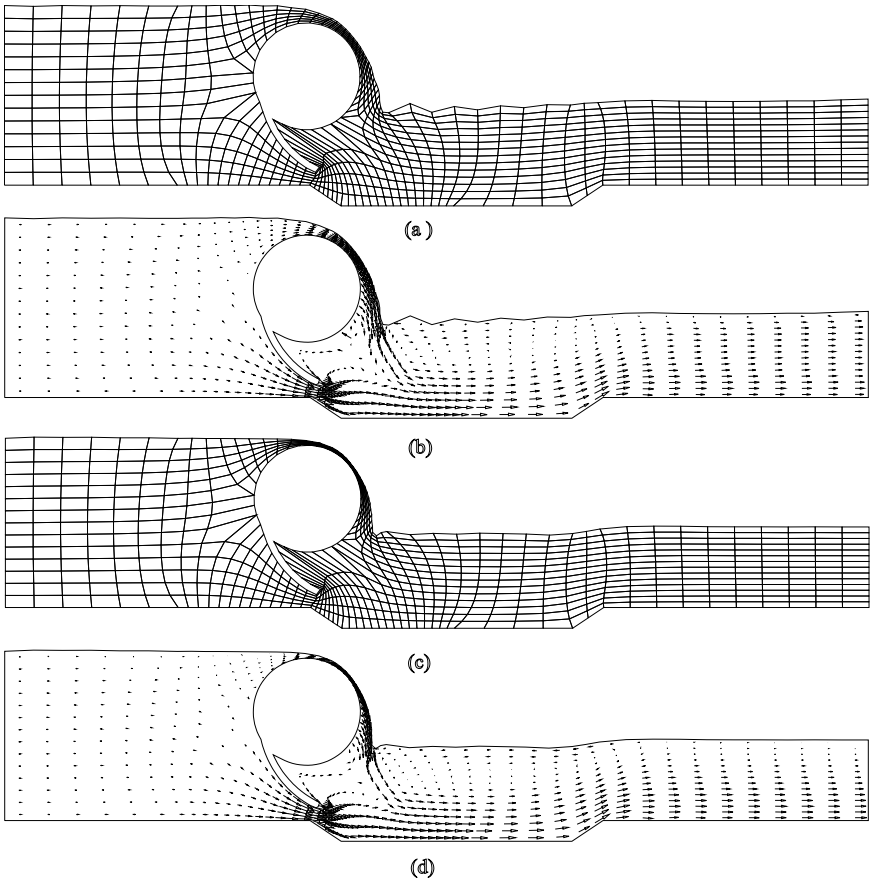

Fig. 14.5:

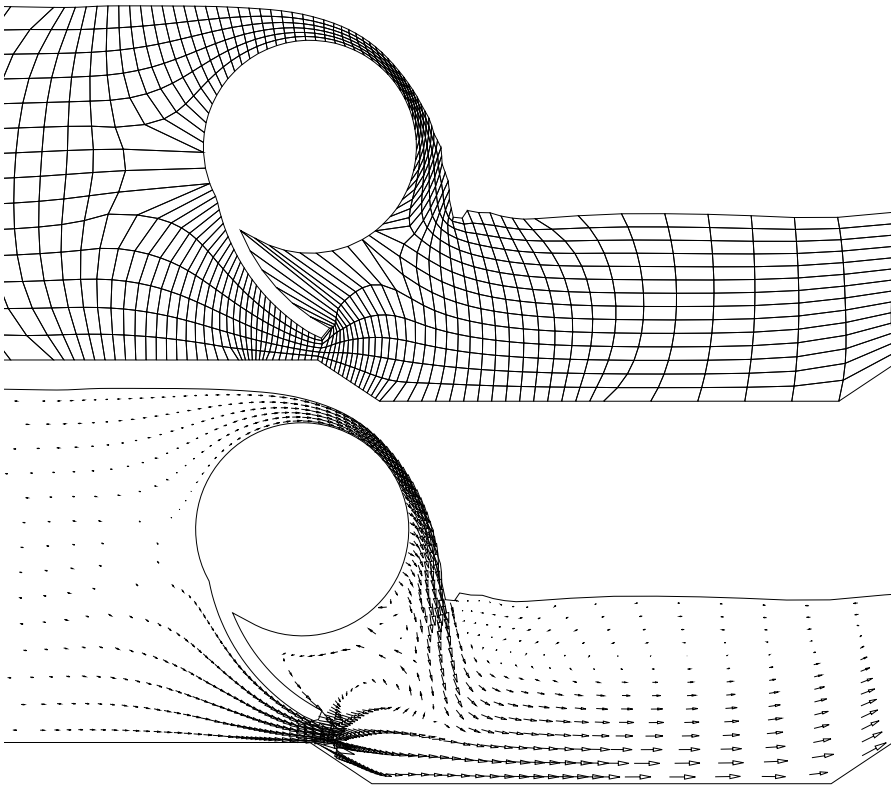

Fig. 14.6:

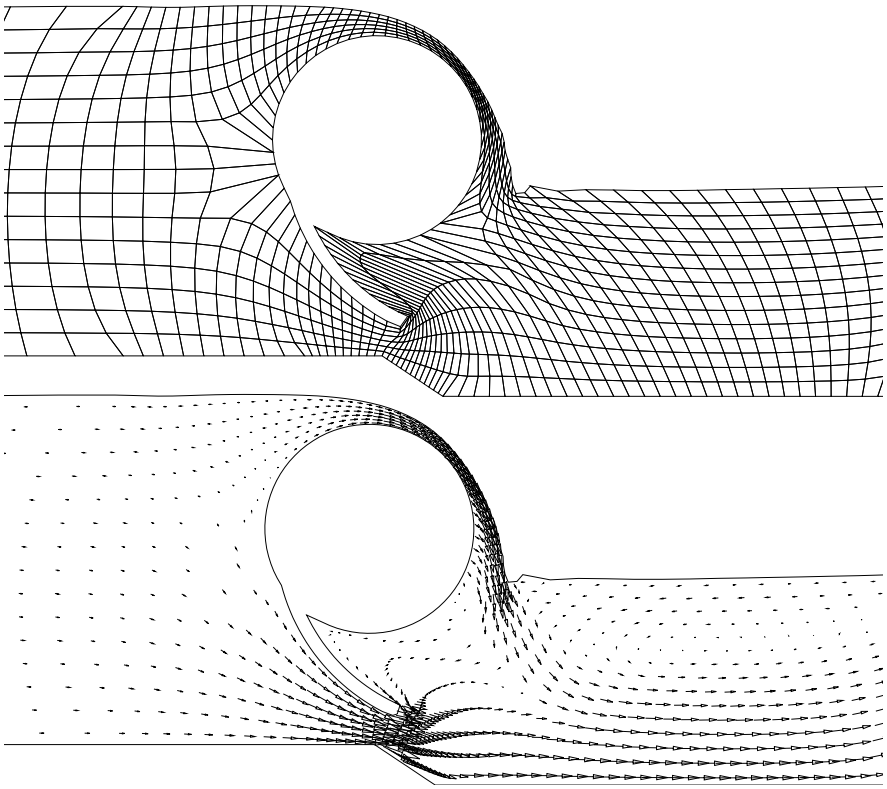

Fig. 14.7:

Appendix. Boundary nodes redistribution[1]

There are several ways to redistribute the grid nodes along the boundary $\partial\Omega$ of the domain Ω during adaptation. The simplest one is a fixed position of every point on $\partial\Omega$, referred to as "fixed position". When moving the interior nodes towards a discontinuity, some instability in mesh generation and, consequently, in the flow problem solution near the points where the discontinuity joins $\partial\Omega$ can arise. In the next method the boundary nodes are treated as interior and the vectors of shift are projected onto $\partial\Omega$ [79]; we call it "unconstrained minimization". This way can be used only if the discontinuity is nearly orthogonal to $\partial\Omega$. If not, then, when condensing, the boundary nodes overlap, adjacent cells degenerate, and modeling breaks. The next method consists of using the 1-D functional (2.9), referred to as "1-D minimization". It is more robust than the two methods discussed above and can usually be used at adaptation. However, as it has been shown in [6, 9], the 1-D and 2-D functionals are inconsistent. By this reason the parameters of adaptation c_a and τ should be selected separately. It requires additional work and is particularly cumbersome when modeling unsteady flow problems. Sometimes we get undesirable displacement of the boundary nodes up to their overlap.

Constrained minimization

It is required that we perform redistribution of the interior and boundary nodes consistently. In the suggested method we perform constrained minimization of the discrete functional (5.19) under constraints defining $\partial\Omega$, referred to as "constrained minimization". We minimize the functional

[1] Written by B. Azarenok

[6]

$$\tilde{I}^h = \sum_{i=1}^{i_{\max}} \sum_{k=1}^{4} \frac{1}{4} [F_k]_i + \sum_{l \in \mathcal{L}} \lambda_l G_l = I^h + \sum_{l \in \mathcal{L}} \lambda_l G_l, \tag{A.1}$$

where the constraints $G_l{=}G(x_l, y_l){=}0$ define $\partial\Omega$, λ_l are the Lagrange multipliers, and $\mathcal{L}$ is the set of the boundary nodes. Since the function $G(x, y)$ is assumed piecewise differentiable, the functional $\tilde{I}^h$ holds the infinite barrier on the boundary of the set of convex grids as I^h does if $f \in C^1$. Note that we use the adapted function $c_a f$ instead of f (as it was applied in section 5.2.2), where c_a is the coefficient of adaptation.

If the set of convex grids is not empty, the system of algebraic equations has at least one solution that is the convex mesh

$$R_x = \frac{\partial I^h}{\partial x_i} + \lambda_i \frac{\partial G_i}{\partial x_i} = 0, \quad R_y = \frac{\partial I^h}{\partial y_i} + \lambda_i \frac{\partial G_i}{\partial y_i} = 0, \quad G_i = 0. \tag{A.2}$$

Here $\lambda_i{=}0$ if $i{\notin}\mathcal{L}$ and constraints are defined for the boundary nodes $i \in \mathcal{L}$.

Consider the method of minimizing the functional (A.1) assuming the grid to be convex at the lth step of the iterative procedure. We use the quasi-Newton procedure to find the coordinates x_i^{l+1}, y_i^{l+1} of the ith node from the system (A.2)

$$\begin{aligned}
\tau R_x + \frac{\partial R_x}{\partial x_i}(x_i^{l+1} - x_i^l) + \frac{\partial R_x}{\partial y_i}(y_i^{l+1} - y_i^l) + \frac{\partial R_x}{\partial \lambda_i}(\lambda_i^{l+1} - \lambda_i^l){=}0,\\
\tau R_y + \frac{\partial R_y}{\partial x_i}(x_i^{l+1} - x_i^l) + \frac{\partial R_y}{\partial y_i}(y_i^{l+1} - y_i^l) + \frac{\partial R_y}{\partial \lambda_i}(\lambda_i^{l+1} - \lambda_i^l){=}0,\\
\tau G_i + \frac{\partial G_i}{\partial x_i}(x_i^{l+1} - x_i^l) + \frac{\partial G_i}{\partial y_i}(y_i^{l+1} - y_i^l){=}0,
\end{aligned} \tag{A.3}$$

where

$$\frac{\partial R_x}{\partial x_i} = \frac{\partial^2 I^h}{\partial x_i^2} + \lambda_i \frac{\partial^2 G_i}{\partial x_i^2}, \quad \frac{\partial R_x}{\partial y_i} = \frac{\partial^2 I^h}{\partial x_i \partial y_i} + \lambda_i \frac{\partial^2 G_i}{\partial x_i \partial y_i}, \quad \frac{\partial R_x}{\partial \lambda_i} = \frac{\partial G_i}{\partial x_i},$$
$$\frac{\partial R_y}{\partial x_i} = \frac{\partial^2 I^h}{\partial x_i \partial y_i} + \lambda_i \frac{\partial^2 G_i}{\partial x_i \partial y_i}, \quad \frac{\partial R_y}{\partial y_i} = \frac{\partial^2 I^h}{\partial y_i^2} + \lambda_i \frac{\partial^2 G_i}{\partial y_i^2}, \quad \frac{\partial R_y}{\partial \lambda_i} = \frac{\partial G_i}{\partial y_i}.$$

Resolving the last equation of (A.3) about $y_i^{l+1}{-}y_i^l$ and substituting it in the two remaining equations, we get the system

$$\begin{pmatrix} a_{11} & a_{12} \\ a_{21} & a_{22} \end{pmatrix} \begin{pmatrix} x_i^{l+1} - x_i^l \\ \lambda_i^{l+1} - \lambda_i^l \end{pmatrix} = \begin{pmatrix} a_{13} \\ a_{23} \end{pmatrix},$$

where

$$a_{11} = \frac{\partial R_x}{\partial x_i} - \frac{\partial R_x}{\partial y_i}\frac{\partial G_i}{\partial x_i}\Big/\frac{\partial G_i}{\partial y_i}, \quad a_{12} = \frac{\partial G_i}{\partial x_i},$$
$$a_{13} = \tau\left[\frac{\partial R_x}{\partial y_i}G_i\Big/\frac{\partial G_i}{\partial y_i} - R_x\right],$$
$$a_{21} = \frac{\partial R_y}{\partial x_i} - \frac{\partial R_y}{\partial y_i}\frac{\partial G_i}{\partial x_i}\Big/\frac{\partial G_i}{\partial y_i}, \quad a_{22} = \frac{\partial G_i}{\partial y_i},$$
$$a_{23} = \tau\left[\frac{\partial R_y}{\partial y_i}G_i\Big/\frac{\partial G_i}{\partial y_i} - R_y\right].$$

Denoting $\triangle = a_{11}a_{22} - a_{12}a_{21}$, $\triangle_1 = a_{13}a_{22} - a_{23}a_{12}$, $\triangle_2 = a_{11}a_{23} - a_{21}a_{13}$ (since $G_i = 0$, the terms a_{13}, a_{23} are simplified), we obtain

$$x_i^{l+1} = x_i^l + \triangle_1/\triangle, \quad \lambda_i^{l+1} = \lambda_i^l + \triangle_2/\triangle, \tag{A.4}$$

and y_i^{l+1} is determined from the third equation of (A.3). If the constraints are resolved about y in the form $G(x,y)=y-g(x)=0$, then

$$\frac{\partial G_i}{\partial x_i} = -\frac{\partial g_i}{\partial x_i}, \quad \frac{\partial G_i}{\partial y_i} = 1,$$

and above formulas are simplified. Constraints can be resolved about x in the form $G(x,y)=x-\tilde{g}(y)=0$ and then (here it is better to resolve the third equation of (A.3) about $x_i^{l+1}-x_i^l$)

$$\frac{\partial G_i}{\partial x_i} = 1, \quad \frac{\partial G_i}{\partial y_i} = -\frac{\partial \tilde{g}_i}{\partial y_i}.$$

These two forms of $G(x,y)$ can substitute for each other. For example, on the part of $\partial\Omega$ that is nearly parallel to the axis x the boundary should be defined in the form $y=g(x)$, and where $\partial\Omega$ is nearly parallel to the axis y it should be defined as $x=\tilde{g}(y)$.

If $\partial\Omega$ is given by parametric functions $x=x(t)$, $y=y(t)$ or tabular values $(x,y)_i$, the following algorithm can be used. When calculating the coordinates of the ith node, in the interval (x_{i-1}, x_{i+1}) we construct an interpolating parabola $t=t(x)$ using the values in three nodes $i-1, i, i+1$. From (A.4) we compute an intermediate value $\tilde{x}_i^{l+1}$, further from the interpolation formula we determine $t_i=t(\tilde{x}_i^{l+1})$ and final values x_i^{l+1}, y_i^{l+1} from the parametric formulas.

Another way of redistributing the nodes along $\partial\Omega$, given as parametric functions or by tabular values, employs a constrained minimization of the functional in parametric form and is based on solving the following system of algebraic equations, referred to as "parametric minimization",

$$R_t = R_x \frac{\partial x_i}{\partial t_i} + R_y \frac{\partial y_i}{\partial t_i} = 0,$$

via the quasi-Newton procedure

$$\tau R_t + \frac{\partial R_t}{\partial t_i} (t_i^{l+1} - t_i^l) = 0. \tag{A.5}$$

Here

$$\frac{\partial R_t}{\partial t_i} = \frac{\partial R_x}{\partial x_i} \left(\frac{\partial x_i}{\partial t_i} \right)^2 + \frac{\partial R_y}{\partial y_i} \left(\frac{\partial y_i}{\partial t_i} \right)^2 + \left(\frac{\partial R_x}{\partial y_i} + \frac{\partial R_y}{\partial x_i} \right) \frac{\partial x_i}{\partial t_i} \frac{\partial y_i}{\partial t_i} +$$
$$R_x \frac{\partial^2 x_i}{\partial t_i^2} + R_y \frac{\partial^2 y_i}{\partial t_i^2}, \qquad R_x = \frac{\partial I^h}{\partial x_i}, \quad R_y = \frac{\partial I^h}{\partial y_i}.$$

For the analytical control functions constrained and parametric minimization give similar results. Real-world 2-D flow computations have shown it is better to perform adaptation along the boundary using constrained minimization (A.3), (A.4) since the procedure (A.5) does not always ensure consistent redistribution of the nodes in Ω and on $\partial\Omega$.

The use of the constrained minimization without adaptation (i.e. when f=*const*) means that we seek the conformal mapping $x(\xi,\eta), y(\xi,\eta)$ of the parametric square onto the domain Ω with an additional parameter, so-called conformal modulus.

Note that constrained minimization can be also used to the boundary nodes redistribution when we use the functional with two metrics, considered in Chapter 9.

Examples of modeling

We demonstrate a simple test illustrating the inconsistency of redistributing the boundary and interior nodes when using various methods of boundary nodes redistribution described above and vice versa, i.e., their consistency when using another.

The 50×50 adaptive mesh is generated in the unit square $0<x,y<1$ when the control function is defined to be

$$f(x,y)=\begin{cases}1 & \text{if} \quad y<0.5,\\ 0 & \text{if} \quad y\geq 0.5.\end{cases}$$

Fragments of the adapted meshes in the vicinity of the discontinuity are presented in Fig. A.1. In the first case the coefficient c_a=0.1; see Fig. A.1(a)–(c). When we apply fixed position and 1-D minimization methods of redistributing the boundary nodes (see Fig. A.1(a)–(b)), the horizontal grid lines are not parallel and in the case of the other 3 methods they are parallel. In the next case the coefficient c_a=0.15; see Fig. A.1(d)–(f). To the fixed position method the coordinate lines become more bent; see Fig. A.1(d). Using 1-D minimization leads the boundary nodes to overlap (see Fig. A.1(e)), i.e., the mesh to fold. This happens due to the inconsistency of the nodes' redistribution in Ω and on $\partial\Omega$ despite the fact that 1-D and 2-D algorithms separately provide unfolded grid generation, see [6, 9]. In this test unconstrained minimization gives the same result as constrained and parametric minimization due to the discontinuity is orthogonal to $\partial\Omega$ and here the horizontal lines almost merge near the discontinuity and remain parallel, keeping the mesh unfolded; see Fig. A.1(f).

In the next example the discontinuity is not orthogonal to $\partial\Omega$. The control function is defined as

$$f(x,y)=\begin{cases}1 & \text{if} \quad y>5x-2,\\ 0 & \text{if} \quad y\leq 5x-2.\end{cases}$$

Fragments of the adapted meshes near the top boundary are presented in Fig. A.2. Here using unconstrained and 1-D minimization leads the boundary nodes to overlap in several tenths of mesh iterations (see Fig. A.2(a)–(b)). Constrained and parametric minimization maintain an unfolded mesh; see Fig. A.2(c).

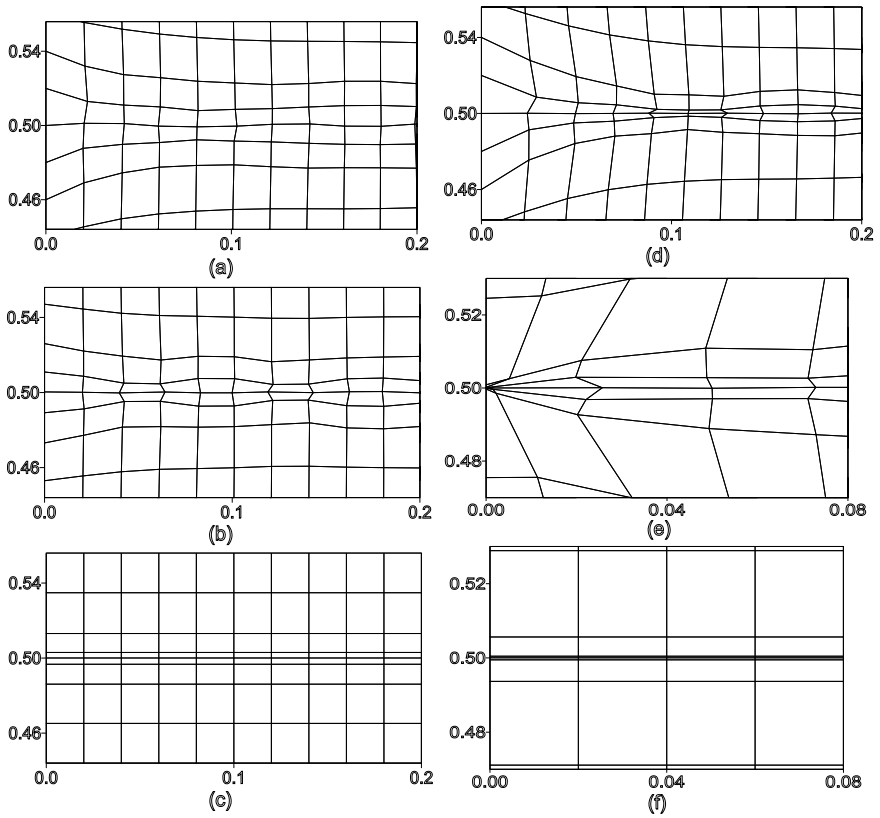

Fig. A.1: Fragment of adapted mesh. The boundary nodes are redistributed using fixed position (a), (d), 1-D minimization (b), (e), and unconstrained or constrained or parametric minimization (c), (f). Coefficient c_a=0.1 in cases (a)–(c) and c_a=0.15 in cases (d)–(f); iterative parameter τ=0.15.

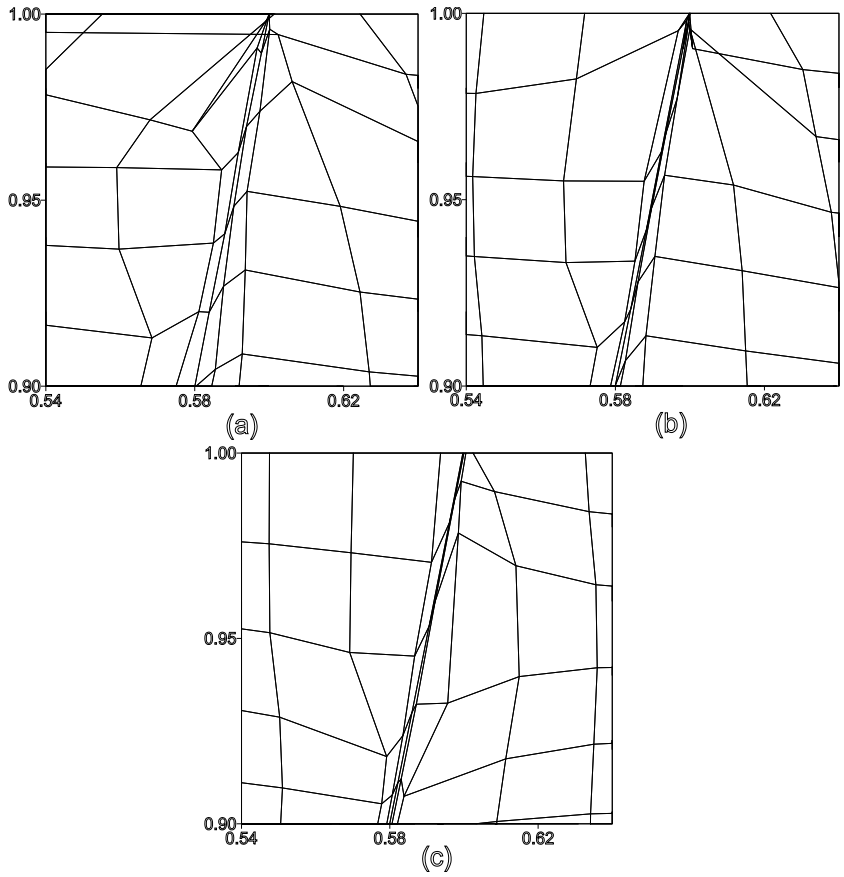

Fig. A.2: Fragment of adapted mesh. The boundary nodes are redistributed using unconstrained (a), 1-D (b), and constrained or parametric minimization (c) methods. Coefficient c_a=0.3; iterative parameter τ=0.1.

Bibliography

[1] D.A. Anderson, M.M. Ray, The use of solution adaptive grids in solving partial differential equations. Appl. Math. and Comp. 10-11 (1982) 317–338.

[2] D.A. Anderson, Equidistribution schemes, Poisson generators, and adaptive grids. Appl. Math. Comput. 24(3) (1987) 211–227.

[3] D.A. Anderson, Grid cell volume control with an adaptive grid generator. Appl. Math. Comput. 35(3) (1990) 209–217.

[4] B.N. Azarenok, S.A. Ivanenko, Application of adaptive grids in numerical analysis of time-dependent problems in gas dynamics. Comput. Maths. Math. Phys. 40(9) (2000) 1330–1349.

[5] B.N. Azarenok, S.A. Ivanenko, Application of moving adaptive grids for numerical solution of nonstationary problems in gas dynamics. Intern. J. for Numer. Meth. in Fluids. 39(1) (2002) 1–22.

[6] B.N. Azarenok, Variational barrier method of adaptive grid generation in hyperbolic problems of gas dynamics. SIAM J. Numer. Anal. 40(2) (2002) 651–682.

[7] Azarenok B.N., Ivanenko S.A., and Tang T. Adaptive mesh redistribution method based on Godunov's scheme. Comm. Math. Sci. 1(1) (2003) 152–179.

[8] B.N. Azarenok, Computation of explosion on an adaptive moving grid. Computational Mathematics and Mathematical Physics. 43(6) (2003) 880–888.

[9] B.N. Azarenok, Application of the variational barrier methods in hyperbolic gas dynamics problems. Computational Mathematics and Mathematical Physics, 43(7) (2003) 1025–1047.

[10] B.N. Azarenok, A variational hexahedral grid generator with control metric. J. Comp. Phys. 218(2006) 720–747.

[11] B.N. Azarenok, Generation of structured difference grids in two-dimensional nonconvex domains using mappings. Comput. Math. Math. Phys. 49(5) (2009) 797–809.

[12] I. Babuska, W.C. Rheinbold A-posteriory error estimates for the finite element method. Internat. J. Numer. Meth. Eng. 12(1978) 1597–1615.

[13] I. Babuska, A. Miller, The post-processing approach in the finite element method. Part 1: Calculation of displacements, stresses, and other higher derivatives of the displacements. Internat. J. Numer. Meth. Engng. 20: 1085-1109; Part 2: The calculation stress intencity factors. 20(1984) 1111–1129.

[14] T.J. Baker Developments and trends in three-dimensional mesh generation. Appl. Numer. Math. 5(4) (1989) 275–304.

[15] T.J. Baker, Delaunay-Voronoi methods, in: J.F. Thompson, B.K. Soni, N.PWeatherill (Eds.), in: Handbook of Grid Generation, CRC Press, Boca Raton, Fl, 1999 (Chapter 16).

[16] N.S. Bakhvalov, On optimization of methods for solving boundary value problems with boundary layers. USSR Comput. Maths. Math. Phys. 9(4) (1969) 841–859.

[17] V.V. Belikov, Numrical complex "TRIANArids geneator of triangular finite elements in arbitrary planar domains. USSR GOSFAP. PO007705.

[18] P.P. Belinskii, S.K. Godunov, Yu.B. Ivanov, I.K. Yanenko, The use of a class of quasiconformal mappings to construct difference grids in domains with curvilinear boundaries. USSR Comput. Maths. Math. Phys. 15(6) (1975) 131–139.

[19] J.B. Bell, G.R. Shubin, An adaptive grid finite difference method for concervative laws. J. Comp. Phys. 1983. 52 (1983) 569–591.

[20] M.G. Berger, J. Oliger, Adaptive mesh refinement for hyperbolic partial differential equations. J. Comp. Phys. 53(3): 484-512. 1984.

[21] Blacker T.D. Paving: A New Approach To Automated Quadrilateral Mesh Generation. International Journal For Numerical Methods in Engineering, Num 32, 811-847. 1991.

[22] Blacker T.D. and Meyers R.J. Seams and Wedges in Plastering: A 3D Hexahedral Mesh Generation Algorithm. Engineering with Computers, Vol 2, Num 9, 83-93. 1993.

[23] Bobilev N.A., Ivanenko S.A. and Ismailov I.G. Several remarks on homeomorphic mappings. Mathematical notes, 60(4): 593-596. 1996.

[24] Boender E. Reliable Delaunay-based mesh generation and mesh improvement. Communications in Numerical Methods in Engineering. 10: 773-783. 1994.

[25] De Boor C. Good approximation by splines with variable knots II. Conference on numerical solution of differential equations. Lecture Notes in Mathematics. N 363. Berlin. Springer-Verlag. 1973. pp. 12-20.

[26] Brackbill J.U. and Saltzman J.S. Adaptive zoning for singular problems in two dimensions. J. Comput. Phys., Vol.46(3): 342-368. 1982.

[27] Brackbill J.U., Kothe D.B., and Ruppel H.L. FLIP: a low-dissipation, particle-in-cell method for fluid flow. Comput. Phys. Commun., Vol. 48, No 1, 25-38. 1988.

[28] Brackbill J.U. An adaptive grid with directional control. J. Comp. Phys. 108(1): 38-50. 1993.

[29] Carey G.F. Computational grids: generation, adaptation, and solution strategies. Taylor & Francis. 1997.

[30] Carey G.F. and Dinh H.T. Grading function and mesh redistribution. SIAM J. Numer. Anal. 22(3): 1028-1040. 1985.

[31] Mathematical aspects of numerical grid generation. Ed. Castillo J.E. Philadelphia. SIAM. 1991.

[32] Charakhch'yan A.A. Almost conservative difference schemes to equations of gas dynamics. Comput. Maths. Math. Phys. 33(11): 1681-1692. 1993.

[33] Charakhch'yan A.A. Compound difference schemes for time-dependent equations on non-uniform meshes. Communic. in Numeric. Methods in Engineering, Vol. 10, No. 2, 93-110.

[34] Charakhch'yan A.A. and Ivanenko S.A. A variational form of the Winslow grid generator. J. Comp. Phys, 136(2): 385-398. 1997.

[35] Dannenhoffer J.D. A comparison of two adaptive grid techniques. Numer. Grid Generat. Comput. Fluid Mech. 88. Mumbles. 1988. P.319-328.

[36] Dar'in N.A. and Mazhukin V.I. On one approach in adaptive grid generation for time-dependent problems. Comput. Maths. Math. Phys. 28(3): 454-460. 1988.

[37] Dvinsky A.S. Adaptive grid generation from harmonic maps on Riemanian manifolds. J. Comp. Phys. 95(3): 450-476. 1991.

[38] Delaunay B., Sur la sphère vide. Bull. Acad. Science USSR VII: Class Sci. Mat. Nat. 6: 793-800. 1934.

[39] Degtyarev L.M. and Ivanova T.S. Method of adaptive grids in one-dimensional time-dependent convection-diffusion problems. Differ. Uravn. 29(7): 1179-1192. 1993.

[40] Diaz A.R., Kikuchi N., and Taylor J.E. A method of grid optimization for finite element method. Comp. Meth. Appl. Mech. Engng. 41: 29-45. 1983.

[41] Dompierre J., Labbe P., Guibault F. and Camarero R. Proposals of Banchmarks for 3D Unstructured Tetrahedral Mesh Optimization. In Proceedings of the 7th International Meshing RoundTable'98, pp.459-478, 1998.

[42] Dwyer H.A., Smooke M.D., and Kee R.J. Adaptive gridding for finite difference solution to heat and mass transfer problems. Appl. Math. and Comput. V. 10/11, 339-356. 1982.

[43] J.E.Eells and J.H.Sampson, Harmonic mappings of Riemannian manifolds. Amer. J. Math. 86, 1, 109-160, 1964.

[44] J.E.Eells and L.Lemair, Another report on harmonic maps. Bulletin of the London Mathematical Society. 20(86): 387-524, 1988.

[45] Eiseman P.R. Adaptive grid generation. Comput. Methods in Appl. Mech. and Engineering, Vol. 64, 321-376. 1987.

[46] Emel'yanov K.V. Using optimal difference grids in solving problems with singular distribution. USSR Comput. Maths. Math. Phys. 34(6): 36-943. 1994.

[47] F.T.Farrell and L.E.Jones, Topological rigidity for compact nonpositively curved manifolds. Proc. Sympos. Pure Math. 54 (Amer. Math. Soc., Providence, RI, 1993) 229-274.

[48] F.T.Farrell and L.E.Jones, Some non-homeomorphic harmonic homotopy equivalences. Bull. London Math. Soc. Vol. 28, pp.177-182, 1996.

[49] Frey W.H. and Field D.H. Mesh relaxation: A new Technique for Improving Triangulations, International Journal For Numerical Methods in Engineering, Vol 31, 1121-1133. 1991.

[50] F.B.Fuller, Harmonic mappings. Proc.Nat.Acad.Sci., USA, Vol.40, 987-991, 1954.

[51] George P.L. Automatic mesh generation. Application to finite element methods. Chichester, John Wiley & Sons Ltd. 1991. 333 p.

[52] George P.L., Borouchaki H. Delaunay triangulation and meshing. Application to finite elements/ Paris. Hermes. 1998. 413 p.

[53] S. K. Godunov. Finite difference method for numerical computation of discontinous solution of the equations of fluid dynamics. Matematicheskii Sbornik, 47:271, 1959. translated from Russian by I. Bohachevsky.

[54] S. K. Godunov: Reminiscences about Difference Schemes. Journal of Computational Physics, Vol. 153, No. 1, Jul 1999, pp. 6-25.

[55] S.K. Godunov and G.P. Prokopov, On computation of conformal transformations and construction of difference meshes. USSR Comput. Maths. Math. Phys. 5(5): 1031–1059. 1967.

[56] S.K.Godunov and G.P.Prokopov, The use of moving meshes in gas-dynamics calculations. USSR Comput. Maths. Math. Phys. 12(2): 182-191. 1972.

[57] S.K. Godunov (Ed.), A.V. Zabrodin, M.Ya. Ivanov, A.N. Kraiko, and G.P. Prokopov, Numerical Solution of Multi-Dimensional Problems in Gas Dynamics, *Nauka Press* (Moscow, 1976); (French translation: Résolution Numérique des Problémes Multidimensionnels de la Dynamique des Gaz, *Mir*, Moscou, 1979.)

[58] Godunov S.K., Zhukov V.T., and Feodoritova O.V. An Algorithm for Construction of Quasi–isometric Grids in Curvilinear Quadrangular Regions. In: Proceedings of the 16th Int. Conf. on Numerical Methods in Fluid Dynamics, Arcachon, France, July 6-10, pp.49-54, 1998.

[59] Golias N.A. and Tsiboukis T.D. An Approach to Refining Three-Dimensional Tetrahedral Meshes Based on Delauney Transformations. International Journal for Numerical Methods in Engineering, Vol 37, 793-812. 1994.

[60] Grebennikov A.I. On choice of nodes at approximation of function by splines. USSR Comput. Maths. Math. Phys. 16(1): 219-223. 1976.

[61] R.Hamilton, Harmonic maps of manifolds with boundary. Lecture Notes in Math. Vol.471, 165 p., 1975.

[62] , in: J.F. Thompson, B.K. Soni, N.PWeatherill (Eds.), in: Handbook of Grid Generation, CRC Press, Boca Raton, Fl, 1999 Handbook of Grid Generation. Eds. J.F.Thompson, B.K.Soni and N.P.Weatherill, CRC Press, Boca Raton, Fl., 1999.

[63] P.Hartman, On homotopic harmonic maps. Canad. J. Math. Vol.19, 673-687, 1967.

[64] Hagmeijer R. Grid adaptation based on modified anisotropic diffusion equations formulated in the parametric domain. J. Comput. Phys., 115, 169-183. 1994.

[65] Ivanenko S.A. Construction of curvilinear grids and their using in finite element method for solving equations of shallow water. CCAS, 1985, 36 p. (in Russian).

[66] Ivanenko S.A. and Charakhch'yan A.A. Algorithm of construction grids of convex quadrilaterals. Dokl. of USSR Acad. of Scien. 295(2): 280-283.

[67] Ivanenko S.A. and Charakhch'yan A.A. Curvilinear grids of convex quadrilaterals. USSR Comput. Maths. Math. Phys. 28(2): 126-133. 1988.

[68] Ivanenko S.A. Generation of non-degenerate meshes. USSR Comput. Maths. Math. Phys. 28(5): 141-146. 1988.

[69] Ivanenko S.A. Frows calculations in reservoirs on curvilinear meshes. CCAS, 1991, 36 p. (in Russian).

[70] Ivanenko S.A. Adaptive grids and grids on surfaces. Comp. Maths. Math. Phys, Vol. 33, No. 9, 1179-1193. 1993

[71] Ivanenko S.A. Adaptive curvilinear grids in the finite element method. Comput. Maths. Math. Phys. 35(9): 1071-1087. 1995.

[72] Ivanenko S.A. Adaptive - harmonic grid generation and its application for numerical solution of the problems with boundary and interior layers. Comput. Maths. Math. Phys. 35(10): 1203-1220. 1995.

[73] Ivanenko S.A. Adaptive-harmonic grid generation. Moscow, CCAS, 1997, 182 p. (in Russian).

[74] S.A. Ivanenko Harmonic mappings, in: J.F. Thompson, B.K. Soni, N.PWeatherill (Eds.), in: Handbook of Grid Generation, CRC Press, Boca Raton, Fl, 1999 (Chapter 8).

[75] Ivanenko S.A. Control of cell shape in the construction of a grid. (Russian) Zh. Vychisl. Mat. Mat. Fiz. 40, 2000, no. 11, 1662–1684; translation in Comput. Math. Math. Phys. 40, 2000, no. 11, 1596–1616

[76] Ivanenko S.A. and Muratova G.V. Adaptive grid shallow water modeling. Appl. Numer. Maths. 32(4): 447-482. 2000.

[77] Ivanenko S.A. Existence of equations describing the classes of nondegenerate curvilinear coordinates in arbitrary domains, Comput. Maths. Math. Phys. 42(1): 43-48, 2002.

[78] Jaquotte O.-P. A mechanical model for a new grid generation method in computational fluid dynamics. Comp. Math. and Appl. Mech. Enging. 66: 323-338. 1988.

[79] Jacquotte O-P. Grid optimization methods for quality improvement and adaptation, in: J.F. Thompson, B.K. Soni, N.PWeatherill (Eds.), in: Handbook of Grid Generation, CRC Press, Boca Raton, Fl, 1999 (Chapter 33).

[80] Jiang B.N. and Carey G.F. Adaptive refinement for least squares finite elements with element-by-element congugate gradient solution. Int. J. Numer. Meth. Eng. V.24. N 3 P. 569-580. 1987.

[81] Joest J. and Shoen R. On the existence of harmonic diffeomorphisms between surfaces. Invent. Math., 66, 353-359, 1982.

[82] Kennon S.R. and Dulikravich G.S. Composite computational grid generation using optimization. In: Proceedings of the Conference on Numerical Grid Generation in Computational Fluid Dynamics, edited by. J.Hauser and C.Taylor, Pinaridge, Swansea, U.K. 217-225. 1986.

[83] Kennon S.R. and Anderson D.A. Unstructured grid adaption for non-convex domains. In: Proceedings of the Conference on Numerical Grid Generation in Computational Fluid Mechanics, London U.K., 1988, edited by S.Sengupta, J.Hansen, P.R. Eiseman and J.F.Thompson, Pineridge press, Swansea U.K., 599-609.

[84] Khamayseh A. and Mastin C.W. Surface grid generation based on elliptic PDE models. Appl. Math. Comput. 65, No. 1-3, 253-264. 1994.

[85] P. Knabner, S. Korotov, G. Summ, Conditions for the invertibility of the isoparametric mapping for hexahedral finite elements, Finite Elements in Analysis and Design, 40 (2) (2003) 159–172.

[86] P. Knupp, On the invertibility of the isoparametric map, Comp. Meth. in Appl. Mech. and Engng. 78 (1990) 313–329.

[87] Knupp P., Steinberg S. Fundamentals of grid generation/ Boca Raton. CRC Press. 1993. 286 p.

[88] Knupp P.M. Matrix Norms and the Condition Number. A General Framework to Improve Mesh Quality via Node-Movement. In: Proceedings of 8th International Meshing Roundtable, South Lake Tahoe, CA, USA, pp. 13-22, 1999.

[89] Knupp P., Margolin L. and Shashkov M. Reference Jacobian optimization-based rezone strategies for arbitrary Lagrangian Eulerian methods, J. Comput. Phys., 176: 93-128. 2002.

[90] Levi H. On the non-vanishing of the Jacobian in cirtain one-to-one mappings. Bull. Amer. Math. Soc. 42, 689-692, 1936.

[91] Liseikin V.D. Construction of structured grids on n - dimensional surfaces. USSR Comput. Maths. Math. Phys. 31(11): 1670-1683. 1991.

[92] Liseikin V.D. Technology of constructing 3D grids in problems of aerohydrodynamics (review). Topics of nuclear science and technolody. Ser. Mathematical modelling of physical processes. 1991, Issue 3: 31-45. (in Russian).

[93] Liseikin V.D. On some interpretations of a smoothness functional used in constructing regular and adaptive grids. Russ. J. Numer. Anal. Modelling. 8(6): 507-518. 1993.

[94] Liseikin V.D. Grid Generation Methods. New York. Springer-Verlag. 1999.

[95] Liu A. and Joe B., Relationship Between Tetrahedron Shape Measures, Bit, 34, pp.268-287, 1994.

[96] Loehner R. and Parikh P. Generation of three-dimensional unstructured grids by the advancing-front method. Int. J. Numer. Methods Fluids 8, No. 10, 1135-1149. 1988.

[97] Meshcheryakov Yu.P. and Shapeev V.P. Some geometrical methods of consructing defference grids in domains with curvilinear boundaries. Chisl. Metody Mechaniki Sploshnoy Sredy. Novosibirsk, 9(2): 91-1032. 1978 [in Russian].

[98] Muller K. and Muller R.N. Moving finite elements I. SIAM J. Numer. Anal. 18(6): 1019-1032. 1981.

[99] Muller K. and Muller R.N. Moving finite elements I. SIAM J. Numer. Anal. 18(6): 1033-1057. 1981.

[100] Nakahashi K. and Deiwert G.S. Three-dimensional adaptive grid method. AIAA paper 85-0486. 1985.

[101] Oden J.T., Demkowicz L., Strouboulis T., and Devlow P. Adaptive methods for problems in solid and fluid mechanics. in: Accuracy Estimates and Adaptive Refinements in Finite Element Computations (ed. I.Babuska et al.). John Willey & Sons Ltd., 1986, pp. 249-280.

[102] Pardhanani A. and Carey G.F. Optimization of computational grids. Numer. Methods Partial Differ. Equations 4, No. 2, 95-117. 1988.

[103] Pearce D. Optimized grid generation with geometry definition decoupled. AIAA Paper. 1990.

[104] Pereyra V. and Sewell E.G. Mesh selection for discrete solutions of boundary value problems in ordinary differential equations. Numer. Math. 23(3): 261-268. 1975.

[105] Pyke J. Grid adaptive algorithms for the solution of Euler equations on irregular grids. J. Comp. Phys. V. 71. N 1. P. 194-223. 1987.

[106] Prokopov G.P. Construction of orthogonal difference grids using conformal mapping. Prepint of Keldysh Institute for Applied Mathematics of USSR Academy of Science. N 45, 1970. (in Russian).

[107] Prokopov G.P. On construction of difference grids, close to orthogonal, in domains with curvilinear boundaries. Prepint of Keldysh Institute for Applied Mathematics of USSR Academy of Science. N 17, 1974. (in Russian).

[108] Prokopov G.P. Some general questions of grid generation algorithms. Prepint of Keldysh Institute for Applied Mathematics of USSR Academy of Science. N 4, 1987. (in Russian).

[109] Prokopov G.P. On comparison of algorithms and codes of constructing two-dimensional regular grids. Prepint of Keldysh Institute for Applied Mathematics of USSR Academy of Science. N 4, 1987. (in Russian).

[110] Prokopov G.P. About the comparative analysis of algorithms and programs for regular two dimensional grid generation. Topics of Nuclear Science and Technolody. Ser. Mathematical modelling of physical processes. 1993, Issue 1: 7-12. (in Russian).

[111] Prokopov G.P. Universal variational functionals for 2D grid generation. Prepint of Keldysh Institute for Applied Mathematics of Russian Academy of Science. N 1(2001), 36 p. (in Russian).

[112] Rank E. and Babushka I. An expert system for the optimal mesh design in hp-version of the finite element method. Int. J. Numer. Meth. Eng. V. 24. N 11. P. 2087-2106. 1987.

[113] Roache P.J. and Steinberg S. A new approach to grid generation using a variational formulation. In: Proc. AIAA 7-th CFD conference, Cincinnati, 1985,360-370.

[114] R.D. Russel, J. Christiansen, Adaptive mesh selection strategies for solving boundary value problems. SIAM J. Numer. Anal. 15(1) (1978) 59–80.

[115] G. Ryskin, L.G. Leal, Orthogonal mapping. J. Comp. Phys. 50(1) (1983) 71–100.

[116] Zh.M. Sakhabutdinov, G.A. Petrov, S.V. Maiburova, Costruction and optimization 3D curvilinear meshes. Topics of nuclear science and technolody. Ser. Mathematical modelling of physical processes. Issue 1 (1993) 9–18 (in Russian).

[117] J. Saltzman, Variational methods for generating meshes on surfaces. J. Comput. Phys. 63(1986) 1–19.

[118] J.T. Sampson, Some properties and applications of harmonic mappings. Ann. Ecole Norm. Suo. 11(1978) 211–228.

[119] T.I. Serezhnikova, A.F. Sidorov, O.V. Ushakova, On one method of construction of optimal curvilinear grids and its applications. Sov. J. Numer. Anal. Math. Modelling. 4(2). (1989) 137–155 (in Russian).

[120] T.I. Shabashova, On consructing optimal curvilinear grids in 3D domains. Chisl. Metody Mechaniki Sploshnoy Sredy. Novosibirsk, 17(1) (1981) 144–155 (in Russian).

[121] Yu.D. Shevelev, Spatial problems of numerical aerohydrodynamics. Moscow, Nauka, 1986 (in Russian).

[122] M.H. Shih, Yu T., B.K. Soni, Interactive grid generation and NURBS applications. Appl. Math. Comput. 65(1-3) (1994) 279–294.

[123] O.S. Shirokovskaya, Notes to paper by Fidorov A.F. "On one algorithm for computing optimal difference grids", USSR Comput. Maths. Math. Phys. 9(2) (1969) 468–469.

[124] R. Shoen, S.T. Yau, On univalent harmonic maps between surfaces. Invent. Math. 44 (1978) 265–278.

[125] A.F. Sidorov, On one algorithm for computing optimal difference grids. Proc. Steklov. Math. Institute. 24 (1966) 147–151.

[126] A.F. Sidorov, T.I. Shabashova, On a method of constructing optimal grids in multidimensional domains. Chisl. Metody Mechaniki Sploshnoy Sredy. Novosibirsk, 12 (1981) 106–123 (in Russian).

[127] A.F. Sidorov, O.V. Ushakova, On a method of constructing optimal adaptive grids and it applications. Chisl. Metody Mechaniki Sploshnoy Sredy. Novosibirsk, 16(5) (1981) 101-115 (in Russian).

[128] A.F. Sidorov, O.B. Khairullina, O.V. Ushakova, Variational methods of construction of optimal grids, in: J.F. Thompson, B.K. Soni, N.PWeatherill (Eds.), in: Handbook of Grid Generation, CRC Press, Boca Raton, Fl, 1999 (Chapter 36).

[129] I.D. Sofronov, V.V. Rasskazova, L.V. Nesterenko, Irregular grids in methods of computing unsteady problems of gas dynamics. Topics of Nuclear Science and Technolody. Ser. Numer. Mathem. and Informatics. Issue 1: (1994) 131–183. (in Russian).

[130] A.M. Sorokin, Structured and unstructured grid generation - an evolutionary approach, in:Numerical grid generation in computational fluid dynamics and related fields, Swansea, Wales, 6th-8th April, 1994.

[131] S.P. Spekreijse, Elliptic grid generation based on laplace equations and algebraic transformations. J. Comp. Phys. 118(1995) 28–61.

[132] S.P. Spekreijse, Elliptic generation systems, in: J.F. Thompson, B.K. Soni, N.PWeatherill (Eds.), in: Handbook of Grid Generation, CRC Press, Boca Raton, Fl, 1999 (Chapter 4).

[133] J.L. Steger, D.S. Chaussee, Generation of Body-fitted Coordinates Using Hyperbolic Partial Differential Equations, SIAM J. Sci. Statist. Comput. 1(1980) 431–437.

[134] R. Arina, S. Tarditi, Orthogonal block structured surface grids in: M.J. Baines (ed.) et al.: Numerical methods for fluid dynamics 4. Proceedings of the conference held at Reading University, United Kingdom, April 1992. Oxford: Clarendon Press (1993) 293–300.

[135] S. Steinberg, P. Roache, Anomalies in grid generation in curves. J.Comp.Phys. 91(1990) 255–277.

[136] S. Steinberg, P. Roache, Variational curve and surface grid generation. J. Comput. Phys. 100(1) (1992) 163–178.

[137] G. Strang, G.J. Fix An Analysis of the Finite Element Method. Englewood Cliffs, N.J., Prentice-Hall Inc. 1973.

[138] T. Takagi, K. Miki, B.C.J. Chen, U.T. Sha, Numerical generation of boundary-fitted curvilinear coordinate systems for arbitrary curved surfaces. J. Comp. Phys. 58(1985) 67–79.

[139] P.D. Thomas, Composite three dimensional grids generated by elliptic systems. AIAA Journal, 20(9) (1982) 1195–1202.

[140] J.F. Thompson, F.C. Thames, C.W. Mastin, Automatic numerical generation of body-fitted curvilinear coordinate system for field containing any number of arbitrary two-dimensional bodies. J. Comp. Phys. 15(3) (1974) 299–319.

[141] J.F. Thompson, Z.U.A. Warsi, C.W. Mastin, Boundary-fitted coordinate systems for numerical solution of partial differential equations. J. Comp. Phys. 47(2) (1982) 1–108.

[142] J.F. Thompson, Grid generation techniques in computational fluid dynamics. AIAA Journal. 22(11) (1984) 1505–1523.

[143] J.F. Thompson, Z.U.A. Warsi, C.W. Mastin, Numerical Grid Generation. North-Holland, N.Y. etc. 1985.

[144] Y. Tu, J.F. Thompson, Three-dimensional solution - adaptive grid generation on composite configurations. AIAA Journal, 29(12) (1991) 2025–2026.

[145] A.N. Tikhonov, A.D. Gorbunov, Error estimates to Runge-Kutta methods and choice of optimal grids. USSR Comput. Maths. Math. Phys. 4(2): 232-242. 1964.

[146] J.G. Tiniko-Ruiz, P. Barrera-Sanchez, Area Functionals in Plane Grid Generation. In: Proceedings of the 6th International Conference on Numerical Grid Generation in Computational Field Simulation, University of Greenwich, July 6-9, (1998) 293–302.

[147] A.I. Tolstykh, On grid nodes condensing when solving and application of high-order schemes at numerical study of viscous gas flow. USSR Comput. Maths. Math. Phys. 18(1) (1978) 902–914.

[148] O.V. Ushakova, Theorem of existence and uniqueness of solution in boundary value problem of 1D optimal adaptive grids. Modeling in Mekhanics. Novosibirsk. 3(2) (1989) 134–141 (in Russian).

[149] O.V. Ushakova, Conditions of nondegeneracy of three-dimensional cells. A formula of a volume of cells, SIAM J. Sci. Comp. 23(4) (2001) 1273–1289.

[150] O.V. Ushakova, Conditions of nondegeneracy for different types of grids, in: O.V. Ushakova (Ed.), Advances in Grid Generation, Nova Science Publishers, New York, 2005 (Chapter 9).

[151] O.V. Ushakova, Classification of hexahedral cells, Comp. Math. Math. Phys. 48 (8) (2008) 1327-1348.

[152] P.N. Vabishchevich, Composite adaptive meshes in problems of mathematical physics. USSR Comput. Maths. Math. Phys. 29(6) (1989) 902–914.

[153] S.A. Vavasis, A Bernstein-Bézier sufficient condition for invertibility of polynomial mapping functions, See http://www.arxiv.org, cs.NA/0308021 (2003).

[154] M.G. Voronoi, Nouvelles applications des paramètres continus à la thèorie des formes quadratiques. J. Reine u. Angew. Math. 134 (1908) 198–287.

[155] Z.U.A. Warsi, W.N. Tuarn, Surface mesh generation using elliptic equations. Numer. grid generation in computational fluid dynamics. UK, Pineridge Press, (1986) 95–110.

[156] Z.U.A. Warsi, Numerical grid generation in arbitrary surfaces through a second-order differential-geometric model. J. Comput. Phys. 64 (1986) 82–96.

[157] A.B. White Jr. On selection of equidistributing meshes for two-point boundary-value problems. SIAM J. Numer. Anal. 16(3) (1979) 472–502.

[158] A.B. White Jr. On the numerical solution of initial/boundary value problems in one space dimension. SIAM J. Numer. Anal. 19(4) (1982) 683–697

[159] A.M. Winslow, Numerical solution of quasilinear Poisson equation in nonuniform triangle mesh. J. Comput. Phys. 1(2) (1966) 149–172.

[160] A.M. Winslow, Adaptive mesh zoning by the equipotential method. UCID-19062, Lawrence Livermore National Laboratories, University of California. 1981.

[161] N.N. Yanenko, N.T. Danaev, V.D. Liseikin, On a variational method for generating grids. Chisl. Metody Mechaniki Sploshnoy Sredy. Novosibirsk, 8(4) (1977) 157–163. (in Russian).